Dielectric Relaxation of Polysiloxanes and Kerr Effect of p-Phenylene Vinylene Oligomers

Andrew Arthur Goodwin

Doctor of Philosophy

THE UNIVERSITY OF ASTON IN BIRMINGHAM

July 1987

The University of Aston in Birmingham

Dielectric Relaxation of Polysiloxanes and Kerr Effect of p-Phenylene Vinylene Oligomers

A thesis submitted for the degree of Doctor of Philosophy
by
Andrew Arthur Goodwin
1987

SUMMARY

The dielectric relaxation behaviour of a series of cyclic and linear poly(dimethyl siloxanes) with $\bar{n}_n$ in the range 28 to 99 has been studied, as a function of temperature (142.0K-157.5K) and frequency (12-10^5Hz). Activation energies for the α-relaxation process, Davidson-Cole empirical distribution factors, β, and mean-square dipole moments per repeat unit, $<\mu^2>$, have been calculated. Differences in values of ΔH_{act} reflected restricted dipolar rotation for the cyclic structures, compared to the linear structures, over the range of molecular weights studied.

The dielectric relaxation behaviour of a series of linear oligomers of methyl phenyl siloxane, with n in the range 4 to 10, a series of linear fractions of poly(methyl phenyl siloxane), with $\bar{n}_n$ in the range 31 to ~1370, and a cyclic oligomer of methyl phenyl siloxane, with n=10, has been studied as a function of temperature (155.5K-264.0K) and frequency (12-10^5Hz). Activation energies for the α-relaxation process, Davidson-Cole and Cole-Cole empirical distribution factors, β and α, respectively, and mean-square dipole moments per repeat unit have been calculated. The reduced flexibility of short methyl phenyl siloxane chains, compared to dimethyl siloxane chains, was apparent from a comparison of dipole moment ratios.

The dielectric relaxation behaviour of poly(methyl hydrogen siloxane) and poly(n-hexyl methyl siloxane) has been studied as a function of temperature and frequency.

A polysiloxane liquid crystal has been synthesised and its dielectric relaxation behaviour has been studied, as a function of temperature and frequency, in the liquid crystalline phase and below T_g.

Poly(p-phenylene vinylene) and related oligomers have been synthesised and characterised by a variety of experimental techniques. The Kerr effect of two oligomeric fractions, in solution in PPG 2025, has been measured. The electrical conductivities of the undoped and I_2-doped polymer and oligomers have been measured.

Keywords: dielectric relaxation, polysiloxanes, polymer liquid crystals, poly(p-phenylene vinylene), Kerr effect.

ACKNOWLEDGEMENTS

I am grateful to my supervisor, Dr. M. S. Beevers, for his encouragement, intellectual involvement and guidance throughout this work. I would also like to thank him for writing the computer programs.

I would like to thank the staff of the mechanical and glassblowing workshops for the construction of numerous pieces of apparatus used in this study. My thanks are also extended to the technical staff of this department. I would also like to express my appreciation to my colleagues for some useful discussions.

Finally, I am indebted to the University of Aston for providing financial support during the period 1983-1986.

CONTENTS

page

CHAPTER 1 INTRODUCTION 21

CHAPTER 2 DIELECTRIC THEORY

2.01 Dielectrics in Static Fields 36
2.02 Dielectric Relaxation-Single Relaxation Behaviour 40
2.03 Multiple Relaxation Behaviour 45
2.04 Temperature and Dielectric Relaxation 50
2.05 Dielectric Relaxation in Polymers 51

CHAPTER 3 EXPERIMENTAL METHODS

3.01 Introduction 52
3.02 Dielectric Apparatus for the Measurement of C_p and Tanδ at Various Frequencies 53
3.03 Dielectric Cells 53
3.04 Temperature Control in the Range 203K-298K 56
3.05 Measurement of Electrical Capacitance and Dissipation Factor in the Range 203K-298K 56
3.06 Apparatus for Temperature Control Below 203K 58
3.07 Measurement of Electrical Capacitance and Dissipation Factor Below 203K 58
3.08 Measurement of Stray Capacitances 60
3.09 Apparatus for Parallel Resistance Measurement 61
3.10 Resistance Cell Design 61

page

3.11 Measurement of Parallel Resistance at Room Temperature 61

3.12 Volume Resistivity and Volume Conductivity 61

3.13 Dielectric Apparatus for Measurement of Static Dielectric Permittivity 63

3.14 Measurement of Static Dielectric Permittivity 63

3.15 Kerr Effect Apparatus 65

3.16 Large Sample Volume Kerr Cell 67

3.17 Measurement of Absolute Kerr Constants 67

3.18 Measurement of Relative Kerr Constants 71

CHAPTER 4 MATERIALS

4.01 Introduction 72

4.02 Poly(dimethyl siloxanes) 72

4.03 Poly(methyl phenyl siloxanes) 72

4.04 A Synthetic Route to a Polymer Liquid Crystal 73

4.05 Stage 1- Synthesis of Mesogenic Group 73

4.06 Synthesis of 4-Allyloxybenzoic Acid 73

4.07 Synthesis of 4-Allyloxybenzoyl chloride 75

4.08 Synthesis of [4(Allyloxy)benzoyl]4-methoxyphenyl 75

4.09 Stage 2- Attachment of the Mesogenic Group to a Polymer Backbone 76

4.10 Differential Scanning Calorimetry 78

4.11 Synthesis of Poly(n-hexyl methyl siloxane) 81

page

4.12 Gel Permeation Chromatography 81

4.13 Synthesis and Characterisation of Poly(p-phenylene vinylene) 81

4.14 Separation of Oligomers of PPV 87

4.15 Infra-Red Spectroscopy 89

4.16 Elemental Analysis 89

4.17 Gel Permeation Chromatography 91

4.18 Ultra-Violet Spectroscopy 91

4.19 Solid State Nuclear Magnetic Resonance Spectroscopy 95

CHAPTER 5 DIELECTRIC RESULTS

5.01 Dielectric Properties of Cyclic and Linear Poly(dimethyl siloxanes)(PDMS) 97

5.02 The Dielectric Loss Results 97

5.03 Measurement of the Dielectric Relaxation Activation Energy 108

5.04 Cole-Cole Plots 108

5.05 Dielectric Properties of Oligomers of Methyl Phenyl Siloxane (MPS) and Poly(methyl phenyl siloxane) (PMPS) 140

5.06 The Dielectric Loss Results 140

5.07 Dielectric Relaxation Activation Energy 141

5.08 Cole-Cole Plots 141

page

5.09 Dielectric Properties of Poly(methyl hydrogen siloxane)[PMHS], Poly(n-hexyl methyl siloxane) and a Polysiloxane Liquid Crystal 184

5.10 The Dielectric Loss Results 184

5.11 Dielectric Relaxation Activation Energy 189

5.12 Cole-Cole Plots 189

CHAPTER 6 DISCUSSION OF DIELECTRIC RESULTS

6.01 Introduction 202

6.02 Dielectric Relaxation Activation Energies of Cyclic and Linear Poly(dimethyl siloxanes) 202

6.03 Davidson-Cole Analysis of Dielectric Data Obtained for Cyclic and Linear Poly(dimethyl siloxanes) 205

6.04 Mean-Square Dipole Moments of Cyclic and Linear Poly(dimethyl siloxanes) 207

6.05 Dielectric Relaxation Energies of Linear Oligomers of Methyl Phenyl Siloxane, Linear Fractions of Poly(methyl phenyl siloxane) and a Cyclic Oligomer of Methyl Phenyl Siloxane 213

6.06 Davidson-Cole Analysis of Linear Oligomers of Methyl Phenyl Siloxane, Linear Fractions of Poly(methyl phenyl siloxane) and a Cyclic Oligomer of Methyl Phenyl Siloxane 216

page

6.07 Experimental Mean-Square Dipole Moments of Linear Oligomers of Methyl Phenyl Siloxane, Linear Fractions of Poly(methyl phenyl siloxane) and a Cyclic Oligomer of Methyl Phenyl Siloxane 218

6.08 Dielectric Relaxation Activation Energies of Poly(methyl hydrogen siloxane), Poly(n-hexyl methyl siloxane) and a Polymer Liquid Crystal 222

6.09 Cole-Cole Plots 223

6.10 Experimental Mean-Square Dipole Moments for Poly(methyl hydrogen siloxane) and Poly(n-hexyl methyl siloxane) 225

CHAPTER 7 KERR EFFECT THEORY AND RESULTS

7.01 Historical Development of the Kerr Effect 226

7.02 Theoretical Interpretation 227

7.03 Solution Molar Kerr Constants 230

7.04 Solution Molar Kerr Constants at Infinite Dilution 231

7.05 Calculation of Theoretical Molar Kerr Constants using Bond Polarisabilities and Dipole Moments 233

7.06 Molecular Kerr Constants of p-Tolaldehyde 235

7.07 Dipole Moment of p-Tolaldehyde 238

7.08 Molecular Kerr Constants of F1 and F2 240

page

7.09 Theoretical Molecular Kerr Constants of p-Tolaldehyde, F1 and F2 242

7.10 Electrical Conductivity Results 247

CHAPTER 8 CONCLUSIONS AND SUGGESTIONS FOR FUTURE WORK 250

APPENDIX 1 COMPUTER PROGRAMS

Program 1 Davidson-Cole analysis 256

Program 2 Calculation of mean-square dipole moments 266

Program 3 Calculation of molar Kerr constants 269

APPENDIX 2 EXPERIMENTAL DATA 272

LIST OF REFERENCES 275

TABLES

Table no.		page
(6-1)	Davidson-Cole empirical distribution factor, β, for cyclic and linear poly(dimethyl siloxanes)	206
(6-2)	Experimental mean-square dipole moments per repeat unit, at 148K, for cyclic and linear poly(dimethyl siloxanes)	208
(6-3)	Davidson-Cole empirical distribution factor, β, for linear oligomers of methyl phenyl siloxane, linear fractions of poly(methyl phenyl siloxane) and a cyclic oligomer of methyl phenyl siloxane	217
(6-4)	Experimental mean-square dipole moments for linear oligomers of methyl phenyl siloxane, linear fractions of poly(methyl phenyl siloxane) and a cyclic oligomer of methyl phenyl siloxane	219
(7-1)	Values of ${}_sK_1$ for 1,4-dioxan and PPG 2025, at 298K, and ${}_mK_2$ for p-tolaldehyde, at 298K	239
(7-2)	Values of ${}_sK_2$ and ${}_mK_2$ for F1 and F2 in PPG 2025, at 333K	243
(7-3)	Bond and group polarisability tensors and permanent dipole vectors used in theoretical Kerr constant calculations	244

Table no. page

(7-4) Theoretical and experimental values of the molecular Kerr constant for p-tolaldehyde, F1 and F2 245

(7-5) Electrical conductivities of doped and undoped oligomers of phenylene vinylene and poly(phenylene vinylene) 248

FIGURES

Figure no. page

(2-1) Argand diagram of the complex current-voltage relationship 42

(2-2) Debye dielectric dispersion curves 44

(2-3) Cole-Cole plots 46

(3-1) Dielectric cells 'A' and 'B' 55

(3-2) The 'Minus Seventy' Thermostat Bath 57

(3-3) Apparatus for temperature control below 203K 59

(3-4) Stainless steel resistance cell 62

(3-5) Apparatus for measurement of static dielectric permittivity 64

(3-6) Kerr effect apparatus 66

(3-7) Typical optical pulses 68

(3-8) Large sample volume Kerr cell 69

(4-1) Synthesis of a polymer liquid crystal 74

(4-2) Infra-red spectrum of [4-(allyloxy)benzoyl]4-methoxyphenyl 77

(4-3) Infra-red spectra of polysiloxane liquid crystal reaction mixture 79

(4-4) Differential scanning calorimetry curves of a polysiloxane liquid crystal 80

(4-5) Infra-red spectra of poly(n-hexyl methyl siloxane) reaction mixture 82

(4-6) Gel permeation chromatograph of poly(methyl hydrogen siloxane) 83

(4-7) Gel permeation chromatograph of a polysiloxane liquid crystal 84

(4-8) Gel permeation chromatograph of poly(n-hexyl methyl siloxane) 85

(4-9) Molecular distillation apparatus 88

(4-10) Infra-red spectrum of poly(p-phenylene vinylene) 90

(4-11) Gel permeation chromatograph of p-tolaldehyde, F1 and F2 92

Figure no. page

(4-12) Plot of elution volume against log molecular weight for p-tolaldehyde, F1 and F2 93

(4-13) Ultra-violet spectra of F1, F2 and P1 94

(4-14) Solid state ^{13}C NMR spectrum of poly(p-phenylene vinylene) 96

(5-1) Frequency dependence of $C_p\tan\delta/C_p\tan\delta_{(max)}$ for cyclic PDMS with $\bar{n}_n$=28 at various temperatures. 98

(5-2) Frequency dependence of $C_p\tan\delta/C_p\tan\delta_{(max)}$ for cyclic PDMS with $\bar{n}_n$=35 at various temperatures. 99

(5-3) Frequency dependence of $C_p\tan\delta/C_p\tan\delta_{(max)}$ for cyclic PDMS with $\bar{n}_n$=50 at various temperatures. 100

(5-4) Frequency dependence of $C_p\tan\delta/C_p\tan\delta_{(max)}$ for cyclic PDMS with $\bar{n}_n$=66 at various temperatures. 101

(5-5) Frequency dependence of $C_p\tan\delta/C_p\tan\delta_{(max)}$ for cyclic PDMS with $\bar{n}_n$=99 at various temperatures. 102

(5-6) Frequency dependence of $C_p\tan\delta/C_p\tan\delta_{(max)}$ for linear PDMS with $\bar{n}_n$=28 at various temperatures. 103

(5-7) Frequency dependence of $C_p\tan\delta/C_p\tan\delta_{(max)}$ for linear PDMS with $\bar{n}_n$=34 at various temperatures. 104

(5-8) Frequency dependence of $C_p\tan\delta/C_p\tan\delta_{(max)}$ for linear PDMS with $\bar{n}_n$=57 at various temperatures. 105

(5-9) Frequency dependence of $C_p\tan\delta/C_p\tan\delta_{(max)}$ for linear PDMS with $\bar{n}_n$=72 at various temperatures. 106

Figure no. page

(5-10) Frequency dependence of $C_p\tan\delta/C_p\tan\delta_{(max)}$ for linear PDMS with $\bar{n}_n$=86 at various temperatures. 107

(5-11) Log(f_{max}/Hz) against T^{-1}(K) for cyclic PDMS with $\bar{n}_n$=28 109

(5-12) Log(f_{max}/Hz) against T^{-1}(K) for cyclic PDMS with $\bar{n}_n$=35 110

(5-13) Log(f_{max}/Hz) against T^{-1}(K) for cyclic PDMS with $\bar{n}_n$=50 111

(5-14) Log(f_{max}/Hz) against T^{-1}(K) for cyclic PDMS with $\bar{n}_n$=66 112

(5-15) Log(f_{max}/Hz) against T^{-1}(K) for cyclic PDMS with $\bar{n}_n$=99 113

(5-16) Log(f_{max}/Hz) against T^{-1}(K) for linear PDMS with $\bar{n}_n$=28 114

(5-17) Log(f_{max}/Hz) against T^{-1}(K) for linear PDMS with $\bar{n}_n$=34 115

(5-18) Log(f_{max}/Hz) against T^{-1}(K) for linear PDMS with $\bar{n}_n$=57 116

(5-19) Log(f_{max}/Hz) against T^{-1}(K) for linear PDMS with $\bar{n}_n$=72 117

(5-20) Log(f_{max}/Hz) against T^{-1}(K) for linear PDMS with $\bar{n}_n$=86 118

(5-21) Cole-Cole plots for cyclic PDMS with $\bar{n}_n$=28 at various temperatures 119

(5-22) Cole-Cole plots for cyclic PDMS with $\bar{n}_n$=28 at various temperatures 120

(5-23) Cole-Cole plots for cyclic PDMS with $\bar{n}_n$=35 at various temperatures 121

(5-24) Cole-Cole plots for cyclic PDMS with $\bar{n}_n$=35 at various temperatures 122

(5-25) Cole-Cole plots for cyclic PDMS with $\bar{n}_n$=50 at various temperatures 123

(5-26) Cole-Cole plots for cyclic PDMS with $\bar{n}_n$=50 at various temperatures 124

(5-27) Cole-Cole plots for cyclic PDMS with $\bar{n}_n$=66 at various temperatures 125

Figure no. page

(5-28) Cole-Cole plots for cyclic PDMS with $\bar{n}_n$=66 at various temperatures 126

(5-29) Cole-Cole plots for cyclic PDMS with $\bar{n}_n$=99 at various temperatures 127

(5-30) Cole-Cole plots for cyclic PDMS with $\bar{n}_n$=99 at various temperatures 128

(5-31) Cole-Cole plots for linear PDMS with $\bar{n}_n$=28 at various temperatures 129

(5-32) Cole-Cole plots for linear PDMS with$\bar{n}_n$=28 at various temperatures 130

(5-33) Cole-Cole plots for linear PDMS with $\bar{n}_n$=34 at various temperatures 131

(5-34) Cole-Cole plots for linear PDMS with $\bar{n}_n$=34 at various temperatures 132

(5-35) Cole-Cole plots for linear PDMS with $\bar{n}_n$=57 at various temperatures 133

(5-36) Cole-Cole plots for linear PDMS with $\bar{n}_n$=57 at various temperatures 134

(5-37) Cole-Cole plots for linear PDMS with $\bar{n}_n$=72 at various temperatures 135

(5-38) Cole-Cole plots for linear PDMS with $\bar{n}_n$=72 at various temperatures 136

(5-39) Cole-Cole plots for linear PDMS with $\bar{n}_n$=86 at various temperatures 137

(5-40) Cole-Cole plots for linear PDMS with $\bar{n}_n$=86at various temperatures 138

(5-41) Frequency dependence of $C_p\tan\delta/C_p\tan\delta_{(max)}$ for linear MPS with n=4 at various temperatures. 142

Figure no. page

(5-42) Frequency dependence of $C_p\tan\delta/C_p\tan\delta_{(max)}$ for linear MPS with n=6 at various temperatures. 143

(5-43) Frequency dependence of $C_p\tan\delta/C_p\tan\delta_{(max)}$ for linear MPS with n=8 at various temperatures. 144

(5-44) Frequency dependence of $C_p\tan\delta/C_p\tan\delta_{(max)}$ for linear MPS with n=10 at various temperatures. 145

(5-45) Frequency dependence of $C_p\tan\delta/C_p\tan\delta_{(max)}$ for linear PMPS with $\bar{n}_n$=31 at various temperatures. 146

(5-46) Frequency dependence of $C_p\tan\delta/C_p\tan\delta_{(max)}$ for linear PMPS with $\bar{n}_n$=50.5 at various temperatures. 147

(5-47) Frequency dependence of $C_p\tan\delta/C_p\tan\delta_{(max)}$ for linear PMPS with $\bar{n}_n$=82 at various temperatures. 148

(5-48) Frequency dependence of $C_p\tan\delta/C_p\tan\delta_{(max)}$ for linear PMPS with $\bar{n}_n$=153 at various temperatures. 149

(5-49) Frequency dependence of $C_p\tan\delta/C_p\tan\delta_{(max)}$ for linear PMPS with $\bar{n}_n$=284 at various temperatures. 150

(5-50) Frequency dependence of $C_p\tan\delta/C_p\tan\delta_{(max)}$ for linear PMPS with $\bar{n}_n$~1370 at various temperatures. 151

(5-51) Frequency dependence of $C_p\tan\delta/C_p\tan\delta_{(max)}$for cyclic MPS with n=10 at various temperatures. 152

(5-52) Log(f_{max}/Hz) against T^{-1}(K) for linear oligomers of methyl phenyl siloxane 153

(5-53) Log(f_{max}/Hz) against T^{-1}(K) for linear PMPS with $\bar{n}_n$=31 154

(5-54) Log(f_{max}/Hz) against T^{-1}(K) for linear PMPS with $\bar{n}_n$=50.5 155

Figure no. page

(5-55) Log(f_{max}/Hz) against T^{-1}(K) for linear PMPS with $\bar{n}_n$=82 156

(5-56) Log(f_{max}/Hz) against T^{-1}(K) for linear PMPS with $\bar{n}_n$=153 157

(5-57) Log(f_{max}/Hz) against T^{-1}(K) for linear PMPS with $\bar{n}_n$=284 158

(5-58) Log(f_{max}/Hz) against T^{-1}(K) for linear PMPS with $\bar{n}_n$~1370 159

(5-59) Log(f_{max}/Hz) against T^{-1}(K) for a cyclic oligomer of methyl phenyl siloxane with n=10 160

(5-60) Cole-Cole plots for a linear oligomer of methyl phenyl siloxane with n=4 at various temperatures 161

(5-61) Cole-Cole plots for a linear oligomer of methyl phenyl siloxane with n=4 at various temperatures 162

(5-62) Cole-Cole plots for a linear oligomer of methyl phenyl siloxane with n=6 at various temperatures 163

(5-63) Cole-Cole plots for a linear oligomer of methyl phenyl siloxane with n=6 at various temperatures 164

(5-64) Cole-Cole plots for a linear oligomer of methyl phenyl siloxane with n=8 at various temperatures 165

(5-65) Cole-Cole plots for a linear oligomer of methyl phenyl siloxane with n=8 at various temperatures 166

(5-66) Cole-Cole plots for a linear oligomer of methyl phenyl siloxane with n=10 at various temperatures 167

(5-67) Cole-Cole plots for a linear oligomer of methyl phenyl siloxane with n=10 at various temperatures 168

(5-68) Cole-Cole plots for linear PMPS with $\bar{n}_n$=31 at various temperatures 169

(5-69) Cole-Cole plots for linear PMPS with $\bar{n}_n$=31 at various temperatures 170

(5-70) Cole-Cole plots for linear PMPS with $\bar{n}_n$=50.5 at various temperatures 171

Figure no. page

(5-71) Cole-Cole plots for linear PMPS with $\bar{n}_n$=50.5 at various temperatures 172

(5-72) Cole-Cole plots for linear PMPS with $\bar{n}_n$=82 at various temperatures 173

(5-73) Cole-Cole plots for linear PMPS with $\bar{n}_n$=82 at various temperatures 174

(5-74) Cole-Cole plots for linear PMPS with $\bar{n}_n$=153 at various temperatures 175

(5-75) Cole-Cole plots for linear PMPS with $\bar{n}_n$=153 at various temperatures 176

(5-76) Cole-Cole plots for linear PMPS with $\bar{n}_n$=284 at various temperatures 177

(5-77) Cole-Cole plots for linear PMPS with $\bar{n}_n$=284 at various temperatures 178

(5-78) Cole-Cole plots for linear PMPS with $\bar{n}_n$~1370 at various temperatures 179

(5-79) Cole-Cole plots for linear PMPS with $\bar{n}_n$~1370 at various temperatures 180

(5-80) Cole-Cole plots for a cyclic oligomer of MPS with n=10 at various temperatures 181

(5-81) Cole-Cole plots for a cyclic oligomer of MPS with n=10 at various temperatures 182

(5-82) Frequency dependence of $C_p\tan\delta/C_p\tan\delta_{(max)}$ for linear PMHS at various temperatures. 185

(5-83) Frequency dependence of $C_p\tan\delta/C_p\tan\delta_{(max)}$ for linear poly(n-hexyl methyl siloxane) at various temperatures. 186

Figure no. page

(5-84) Frequency dependence of $C_p\tan\delta/C_p\tan\delta_{(max)}$ for a side-chain polymer liquid crystal in the liquid crystalline phase at various temperatures. 187

(5-85) Frequency dependence of $C_p\tan\delta/C_p\tan\delta_{(max)}$ for a side-chain polymer liquid crystal below T_g at various temperatures. 188

(5-86) Log(f_{max}/Hz) against T^{-1}(K) for poly(methyl hydrogen siloxane) and poly(n-hexyl methyl siloxane) 190

(5-87) Log(f_{max}/Hz) against T^{-1}(K) for a polysiloxane liquid crystal in the liquid crystalline phase and below T_g 191

(5-88) Cole-Cole plots for linear poly(methyl hydrogen siloxane) at various temperatures 192

(5-89) Cole-Cole plots for linear poly(methyl hydrogen siloxane) at various temperatures 193

(5-90) Cole-Cole plots for linear poly(n-hexyl methyl siloxane) at various temperatures 194

(5-91) Cole-Cole plots for linear poly(n-hexyl methyl siloxane) at various temperatures 195

(5-92) Cole-Cole plots for a polysiloxane liquid crystal in the liquid crystalline phase at various temperatures 198

(5-93) Cole-Cole plots for a polysiloxane liquid crystal in the liquid crystalline phase at various temperatures 199

(5-94) Cole-Cole plots for a polysiloxane liquid crystal below T_g at various temperatures 200

(5-95) Cole-Cole plots for a polysiloxane liquid crystal below T_g at various temperatures 201

(6-1) Average dielectric relaxation activation energies for cyclic and linear poly(dimethyl siloxanes) 202

(6-2) Experimental mean-square dipole moments, $<\mu^2>$, for cyclic poly(dimethyl siloxanes) 209

Figure no. page

(6-3) Experimental mean-square dipole moments, $<\mu^2>$, for linear poly(dimethyl siloxanes) 210

(6-4) Dipole moment ratio, $<\mu^2>/nm^2$, for cyclic and linear poly(dimethyl siloxanes) 212

(6-5) Average dielectric relaxation activation energies for linear methyl phenyl siloxanes and for a cyclic methyl phenyl siloxane 214

(6-6) Dipole moment ratio, $<\mu^2>/nm^2$, for linear methyl phenyl siloxanes and for linear dimethyl siloxanes 221

(7-1) Molecular polarisability ellipsoid 228

(7-2) B_{12} against ω_2 and ε_{12} against ω_2 for solutions of p-tolaldehyde in 1,4-dioxan at 298K 236

(7-3) B_{12} against ω_2 and ε_{12} against ω_2 for solutions of p-tolaldehyde in PPG 2025 at 298K 237

(7-4) B_{12} against ω_2 for solutions of F1 and F2 in PPG 2025 at 333K 241

CHAPTER 1

INTRODUCTION

Polymers as Insulators.

Dielectric data provide valuable information on the nature of molecular motion in polymers[1]. For efficient utilisation of electrical insulating materials in electrical apparatus, devices and cables, knowledge of the dielectric loss behaviour of materials under specific operating conditions is required. Significant dielectric losses may not only represent unecessary signal loss but may also lead to failure due to thermal instability[2].

The voltages applied to electrical devices can range from a millivolt or less to more than 750kV. Electronic applications can require frequencies as high as 100GHz. Electrical power losses are important at these high voltages and frequencies.

Thus, the a.c. characteristics of insulating materials are often of direct functional importance. For instance, cable insulation should have minimum capacitance (a low dielectric constant) with the lowest possible dielectric loss. This is desirable so as to minimise the dissipation of the signal power to heat within the dielectric material itself. On the other hand, capacitors require an insulation system of the highest capacitance in minimum space, eg; plastic films with a high dielectric constant.

As well as voltage and frequency, mechanical stress, time, temperature, moisture and other contaminents may also affect the electrical behaviour of insulating materials. These factors interact in a complex fashion. For example, water vapour can cause the formation of microscopic clusters in the dielectric material which increases the loss through a mechanism of interaction between the conductivity of the water droplets and the dielectric permittivity of the insulator. This phenomenon is known as the Maxwell-Wagner effect.

Under high electrical gradients, complications arise from space charge and other non-linear effects, with the result that the dielectric loss behaviour cannot be readily predicted as a function of the electric field.

The nature of molecular motion in polymers is not only important from an engineering point of view, but it is also of interest at a more fundamental level, namely in the physical and chemical characterisation of rigid-chain and flexible-chain polymers. The dynamic behaviour of bulk polymers and polymers in solution has been widely studied using a variety of experimental techniques.

Nuclear Magnetic Resonance.

NMR experiments provide a powerful tool for the study of molecular motion and re-orientation in any material possessing nuclear magnetic dipoles. A characteristic quality of nuclear magnetic relaxation is the short range of the interaction. Consequently, magnetic relaxation is a probe of molecular motion on a local scale. The orientation of nuclear magnets are usually only loosely coupled to molecular orientation or position. Thus, the spin-lattice relaxation time, T_1, is usually much longer than the molecular correlation time, τ_c.

The variation of T_1 with molecular weight has been observed for many polymers in solution[3]. It is generally found that, above a fairly low 'critical' molecular weight, the relaxation times are independent of chain length. Below this 'critical' molecular weight the relaxation times increase with decreasing molecular weight, indicating that motions of the polymer chain as a whole have become sufficiently rapid to influence the relaxation. For poly(dimethyl siloxane) the 'critical' degree of polymerisation has been shown to be < 400[4]. The variation of ^1H T_1 over a wide range of concentration for poly(dimethyl siloxane) in C_2Cl_4 has been shown to be consistent with very short-range segmental motions involving 2-3 monomer units[4].

For solutions of poly(dimethyl siloxane) in C_2Cl_4 it has been observed that ^1H T_2, unlike T_1, is a decreasing function of molecular weight above a certain concentration[4]. The rate of decrease increases with concentration.

It has been suggested that the different behaviour of T_1 and T_2 arises from the contribution of slower, long range motions to the expression for T_2. These motions are hindered by an increase in macroscopic viscosity and by an increase in chain entanglements to a greater extent than segmental motions.

The complementary nature of dielectric relaxation and magnetic relaxation has been emphasised in a number of studies. A magnetic relaxation study of a series of poly(fluorostyrenes) by Matsuo and co-workers[5] showed that rotation of the phenyl group accounts for the observed dielectric relaxation, but has little effect on spin relaxation. The authors suggest that a comparison of the time scales of backbone motions, observed by a variety of experiments, is dependent upon an understanding of the nature of the contributing motions. McCall[6] has shown that main chain and side chain motions in polymers, some of which are dielectrically inactive, are amenable to study by magnetic relaxation.

<u>Kerr Effect.</u>

Another technique which has been shown to be complementary to dielectric studies is that of the Kerr effect. The sensitivity of the Kerr effect to variations in molecular geometry and environment has made it a useful tool for studying the conformations of molecules. Electro-optic measurements provide a general approach for the determination of structural characteristics through the derivation of bond and group polarisabilities[7].

An early theory of the Kerr effect for flexible polymers did not express the Kerr constant in terms of clearly defined bond parameters, but was based on the idea of mutually independent orientation of freely jointed chain segments, each segment comprising a small number of bonds in sequence along the chain[8]. The conclusion was that the Kerr constant for a flexible polymer was independent of molecular weight. This theory was supported by a Kerr effect study carried out by Champion and co-workers[9] on solutions of polystyrene, in CCl_4, in the molecular weight range 1×10^5-35×10^5. The authors found good agreement between experimental values of the Kerr constant and theoretical ones calculated using the "segmental" theory of the Kerr effect, with the assumption that the dipole moment of polystyrene acts in a direction perpendicular to the segment. In addition, the experimental specific Kerr constant was found to be nearly independent of molecular weight.

Later theories of the Kerr effect for flexible polymers related the Kerr constant to clearly defined bond parameters. In support of these theories, Tonelli and co-workers carried out theoretical Kerr constant calculations, based on the rotational isomeric state model of Flory and co-workers and the additivity of bond polarisability tensors and dipole moment vectors, for a series of poly(oxyethylene glycols)[10], a series of oligomers of vinyl chloride and poly(vinyl chloride)[11]. They compared the theoretical results with the corresponding experimental values of ${}_mK/x$ where ${}_mK$ is the molar Kerr constant and x is the number of repeat units. For a poly(oxyethylene glycol) with x=320, the authors found good agreement between experimental and theoretical values of ${}_mK/x$. Good agreement was also found between experimental and theoretical values of ${}_mK/x$ for oligomers of vinyl chloride and a fraction of PVC with x=672.

In addition to Kerr effect studies carried out under steady state conditions, the dynamical response of polymers to pulsed electric fields and the dispersion of the Kerr effect in a.c. fields has also been observed. Studies of this kind permit the calculation of the birefringence relaxation time and related parameters. Also, using these techniques, it is possible to observe the helix-coil or rigid rod-coil transformation which is a molecular weight dependent property of certain polymers and biopolymers[12]. A study of poly(n-butyl isocyanate), in the molecular weight range 2×10^4-3×10^5, has been carried out by Jennings and co-workers[13], using pulsed electric fields and a.c. fields at intermediate frequencies in order to observe such a transformation. It was found that at low molecular weights the PBIC molecules behaved as rigid rods whereas, at molecular weights above 5×10^4, the PBIC molecules became flexible. This study also provided information concerning the disposition of the dipole moment within the molecule and the chain configuration.

Kerr constants for solutions of rigid-chain polymers are typically 10^2-10^3 times higher than Kerr constants measured for solutions of flexible polymers[14]. The dispersion of the Kerr effect at intermediate frequencies is a characteristic property of rigid-chain polymers. Experiments carried out on solutions of flexible polymers with moderate viscosities show that, at frequencies up to 10^7Hz, no dispersion of the Kerr effect is observed. For solutions of rigid-chain polymers dispersion of the Kerr effect decreases almost to zero at higher frequencies. This has been interpretated in terms of the rotation of permanent dipoles, the anisotropy of dielectric polarisabilty being negligible. The shift of dispersion curves towards higher frequencies with decreasing molecular weight, i.e. shorter relaxation times, has been taken as proof that the molecular motion responsible for the Kerr effect of rigid-chain polymers is rotation of the whole molecule.

With regard to experiments carried out in the time domain, no single experimental technique is able to unequivocally establish the mechanism for the relaxation of a particular molecular probe since each technique will provide information on only a part of the total time dependent orientation distribution function. Interpretations concerning detailed mechanisms for relaxation in amorphous and crystalline polymers should be made using the results of as many complementary experiments as possible[15,16].

Cyclic Polymers.

Although cyclic macromolecules such as cyclic DNA and cyclic polypeptides are known to occur in nature, and have been studied, investigations into synthetic cyclic macromolecules have, until recently, usually been concerned with oligomeric species.

During the past decade, however, sharp fractions of cyclic PDMS molecules, containing hundreds of skeletal bonds, have been synthesised by ring-chain equilibration reactions and fractionated using preparative g.p.c[17]. This has permitted comparitive studies of the physical and chemical properties of cyclic and linear polymers to be made.

The bulk properties and dilute solution properties of cyclic and linear fractions of PDMS have been studied and compared. It is found that there are distinct differences in the equilibrium properties of low molecular weight cyclics and linears. These differences tend to reflect the configurational restrictions and reduced flexibility of the cyclic molecules. It has been shown that, at high molecular weights, refractive index[18], density[18], ^{29}Si n.m.r. chemical shift[19] and T_g[20] have equal limiting values for both cyclic and linear PDMS. The critical chain lengths above which Gaussian limiting ratios of properties are attained vary greatly. For radii of gyration it is at $\bar{n}_n \sim 25$[21], for diffusion coefficients it is at $\bar{n}_n \sim 15$[22] and for bulk viscosities it is at $\bar{n}_n = 400$[23].

Dielectric Properties of Polysiloxanes.

The electrical, as well as the physical and chemical, properties of polysiloxanes were studied by a few workers during the 1940's and the 1950's[24-29]. These materials had unusual properties and were deemed potentially useful as liquid dielectrics because of their low dissipation factors at high temperature or high frequency. Later on, more detailed experimental and theoretical studies of the static dielectric properties of polysiloxanes were published. In these studies the polarisations, dipole moments and dipole moment ratios of the materials received some attention[30-33].

Beevers and co-workers[34] found that, for $n<20$, the dipole moment ratio, at 298K, for cyclic PDMS is lower than the dipole moment ratio for a corresponding linear PDMS. Once again, this is an indication of the configurational restrictions present in small PDMS rings. At high molecular weights the dipole moment ratio had equal limiting values for cyclic and linear PDMS.

Following the wider availabilty of commercial instruments, some dielectric relaxation studies of linear polysiloxanes were undertaken. The α-relaxations of poly(dimethyl siloxane) and poly(methylphenyl siloxane) were investigated in the audio frequency region and at lower frequencies, around the glass transition temperature[35-39]. It was observed that the dielectric behaviour of PDMS was complicated by the onset of crystallisation as the temperature was slowly lowered. To investigate this behaviour further, Adachi and co-workers[38] measured the dielectric loss of a linear PDMS sample of high molecular weight that had been annealed at 195K to induce crystallisation. They compared this data with loss data obtained from the same sample that had been rapidly quenched to low temperatures to reduce crystallisation. Measurable differences in the dielectric behaviour of the two samples were found. The crystallised sample exhibited a lower magnitude of the dielectric dispersion, a higher dielectric relaxation activation energy at 160K and a significant broadening of the loss curves. This behaviour was interpretated in terms of crystallites restricting the motions of adjacent dipolar segments situated in amorphous regions. Baird and co-workers[37] reported that the loss curves of crystallised PDMS were broader on the low frequency side, this behaviour being typical of crystalline organic polymers.

In addition, the effects of a variety of polar and non-polar plasticisers on the dielectric relaxation behaviour of siloxane polymers has been studied[40-41].

Although the dielectric relaxation properties of high molecular weight linear PDMS have been investigated, as outlined above, as far as the author is aware, this is the first comparitive study of the dielectric relaxation properties of a series of cyclic PDMS fractions and a series of linear PDMS fractions possessing intermediate molecular weights.

Side-Chain Liquid Crystalline Polymers.

Thermotropic liquid crystalline polymers belong to a relatively new class of liquid crystalline compounds. The interest in this field is accounted for by the possibility of creating polymeric systems which combine the properties of low molecular weight liquid crystals with the properties of high molecular weight polymers, making it possible to produce films, fibres and coatings with novel features. The synthesis, structure and properties of these compounds have been extensively studied[42-43].

Even though liquid crystalline phases are characterised by long range orientational order, it does not extend over the whole sample. Published values of the local order parameter, denoted by S, tend to vary widely depending upon the polymer system, the mesophase structure and the temperature. It has been demonstrated, by n.m.r.[44] and e.s.r.[45], that, for a nematic poly(acrylate) with phenyl benzoate side groups, decoupling of the side groups from the main chain is not complete. In addition, the length of the flexible spacer has been shown to have little effect on the value of S[42]. On a macroscopic scale the unit vector S_d, which describes the the local preferred direction of the mesogenic side groups, is randomly distributed.

Extensive molecular motions occur in the mesophase of liquid crystals. In the last few years such motions have been studied by dielectric relaxation spectroscopy, a method which has proved to be a useful tool in investigating the dynamic behaviour of low molecular weight and polymer liquid crystals[46].

Kresse and co-workers[47-49] were the first group to study the dielectric properties of unorientated acrylate and methacrylate liquid crystal polymers having alkylcyanobiphenyl units in the side chain. They observed a broad dielectric absorption in the liquid crystal phase, which they termed the δ-process. They assigned this absorption to a re-orientation of the CN dipoles (i.e. the mesogenic groups) around the polymer backbone. The groups of Zentel[50] and Kresse[51] also identified the same relaxation process in a series of unorientated liquid crystal poly(acrylates) and poly(methylacrylates) having aromatic ester groups in the side chain. They concluded that a second observed relaxation process, (the α-process), was associated with the glass transition of the polymer.

Later on, the dielectric properties of partially and fully aligned liquid crystal polymers were studied by various workers. Haase and co-workers[52-54], for fully orientated poly(acrylate) and poly(siloxane) liquid crystals possessing cyanobiphenyl and aromatic ester units in the side chain, were able to measure values of ε'' and ε' with the long axes of the mesogenic groups parallel and perpendicular to the measuring electric field. A Cole-Cole analysis of the dielectric data obtained with the long axes of the mesogenic groups parallel to the measuring electric field (i.e. the process with the main component in $\varepsilon_{||}$), namely the δ-process mentioned above, suggested that this process was characterised by a narrow distribution of relaxation times. A similar analysis of the dielectric data obtained with the long axes of the mesogenic groups perpendicular to the measuring electric field, (i.e. the process with the main component in $\varepsilon_{\perp}$), suggested that this absorption was composed of a number of relaxation processes, each process being characterised by a broad distribution of relaxation times.

Williams and co-workers[55-62] have conducted an extensive experimental and theoretical study of the dielectric relaxation behaviour of liquid crystalline siloxane polymers possessing aromatic ester units in the side chain, in the unaligned, partially aligned and fully aligned homeotropic states.

For unaligned samples, in the liquid crystal phase, the dielectric absorption was found to consist of two broad components. To conform to earlier nomenclature, these processes were labelled δ and α (in order of ascending frequency). The δ process was assigned to motions of the longitudinal component, $\mu_{||}$, of the dipole moment of the side groups, while the α-process was assigned to motions of the transverse component, $\mu_{\perp}$, of the dipole moment of the side groups. The broadness of the longitudinal absorption, compared to the corresponding absorption in a low molecular weight liquid crystal, reflected the co-operative nature of dielectric relaxation in the polymeric materials, in part due to the influence of the main chain on the behaviour of the side chains. The apparent activation energy for an unaligned sample, in the liquid crystalline phase, was found to be 183 kJ mol^{-1}, while, in the isotropic state, the apparent activation energy was found to be 138 kJ mol^{-1}.

The materials were aligned by heating into the isotropic region, applying an a.c. voltage, and then cooling slowly into the liquid crystalline phase. Different degrees of director alignment were possible, depending upon the temperature, magnitude and frequency of the applied field. There was a marked change in the dielectric behaviour of the materials on going from the unaligned state to the fully aligned state. The main features of this change were a three-fold enhancement of the δ process and a diminution of the α process. It was also noted that the loss curve describing the δ process was slightly broader than that for a single relaxation time process, but narrower than the loss curves observed for amorphous or crystalline polymers.

Thus, Williams and co-workers were able to demonstrate that the dielectric properties of these materials could be altered by subjecting them to differing thermal/electrical aligning treatments.

Coles and co-workers[63] have also suggested that dielectric relaxation is a convenient non-optical means of determining the order parameter S and also for estimating the degree of director alignment, S_d, in partially aligned materials.

The speed of response of polymer liquid crystals to a.c. fields is slow in comparison to low molecular weight crystals and prevents their use in active displays. However, because they are able to retain their alignment almost indefinitely (in the liquid crystal phase as well as below T_g[64]), they have potential for storing optical information imparted by a laser beam[65].

Polymers as Conductors.

Polymers with conjugated π-electron backbones, such as polyacetylene, polyphenylene, polypyrrole and others, exhibit properties which allow them to be oxidised and reduced more easily than conventional polymers. Charge transfer agents (dopants), for example I_2, AsF_5 and H_2SO_4, effect this oxidation or reduction and in doing so convert an insulating polymer into a conducting polymer with near metallic conductivity in many cases. The problems lie in attempting to combine the processability and other attractive properties of polymers with the electronic properties of metals or semi-conductors.

The doping of conjugated polymers generates higher conductivities, compared to the undoped polymer, primarily by increasing the charge carrier concentration. This is accomplished by oxidation or reduction with electron acceptors or donors, respectively. Since, in some cases, the dopant constitutes as much as 50% by weight of the conducting polymer, a more appropriate description would be 'charge transfer complex'. Doping is usually accomplished by direct exposure of the polymer to a charge transfer agent in the gas or solution phase, or by electrochemical methods.

In an attempt to understand the nature of electrical conductivity in these materials different theoretical treatments have been applied to various conjugated polymers. Much of the theoretical work on doped polymers has concentrated on the charged defects formed in the polymer chain. Although the mechanism of charge carrier transport in doped conjugated polymers has not been fully established, Hall effect measurements carried out on several compositions of conducting polymers confirm that electrical transport in doped polymers occurs predominately via the organic material.

Gourley and co-workers[66] measured the electrical conductivity of a series of poly(phenylene vinylene) pellets prepared by a variety of synthetic methods and doped with AsF_5. The number of repeat units of the samples varied between 1 and 11. They found that the limiting conductivities of these materials were insensitive to molecular weight, double bond configuration and the type of end group present. They attributed this behaviour to further polymerisation and isomerisation of the samples upon doping with AsF_5 which, they suggested, produced the same chain extended, cross linked and doped materials.

As an improvment over earlier studies of the electrical properties of low molecular weight PPV powders, the groups of Karasz[67-68] and Murase[69-71] have developed a synthetic method for producing high molecular weight PPV films. This is based upon the synthesis of of a soluble, polymeric precursor which can be cast into film form and subsequently converted by thermal or chemical means into PPV. The precursor film can be stretched to high extent during the thermal treatment which results in high molecular orientation and increased conductivity upon doping. The film exhibits anisotropy of conductivity, with conductivity increasing parallel to the drawing axis and remaining approximately constant perpendicular to the drawing axis. Karasz and co-workers and Murase and co-workers have measured electrical conductivities of 500 $(\Omega cm)^{-1}$ and 2780 $(\Omega cm)^{-1}$, respectively, for stretched films of PPV doped with AsF_5. Moreover, Karasz and co-workers have reported that limiting conductivity was reached at an average conjugation length of six repeats units[72].

Conducting polymers have already been shown to have potential for applications in rechargeable batteries, electro-optic devices and sensors[73-76].

CHAPTER 2.

DIELECTRIC THEORY.

Introduction.

In this chapter a theoretical basis will be provided for the interpretation of the dielectric data acquired for the polymer samples.

2.01: Dielectrics in Static Electric Fields.

For a parallel plate capacitor having surface charge density q, on its opposite plates of area A, and separation d, then the resultant field E_o, in vacuo, is;

$$E_o = 4\pi q \qquad (2\text{-}01)$$

The potential difference, V_o, developed across the capacitor is given by the product $E_o d$. Accordingly, the capacitance C_o of the system is defined as;

$$C_o = Aq/V_o \qquad (2\text{-}02)$$

$$= Q/V_o \qquad (2\text{-}03)$$

where Q is the charge on the capacitor.

Insertion of a dielectric material between the plates of the capacitor lowers the voltage, V_o, to a value V_i, with the result that the capacitance of the parallel plate system is augmented to a value C, given by;

$$C = Q/V_i \qquad (2\text{-}04)$$

This effect has been described traditionally by introducing the static permittivity, or dielectric constant, ε, which is defined as;

$$\varepsilon = C/C_o \qquad (2\text{-}05)$$

The dielectric constant varies from one substance to another and it is strongly dependent upon molecular structure. Its value is particularly affected by any polarity within the molecules.

For a gaseous system Debye[77] (1929) derived the relationship between the static dielectric constant, ε_o, and the dipole moment μ;

$$(\varepsilon_o-1)/(\varepsilon_o-2) = 4\pi N[\alpha_e + \mu^2/kT]/3 \qquad (2\text{-}06)$$

where N is the number of molecules per unit volume, α_e is the electronic distortion polarisation of the molecule, k is the Boltzmann constant and T is the absolute temperature. Equation (2-06) is only valid when applied to experimental data obtained on low density polar gases and very dilute solutions containing polar molecules.

Onsager[78] (1936) was the first to extend the Debye equation to dielectrics comprised of a condensed phase of polar molecules. He accomplished this by introducing the concept of a reaction field effect. By considering a rigid point dipole at the centre of a sphere in a dielectric continuum of static dielectric constant, ε_o, he showed that the effective dipole moment μ_i, of a molecule in the liquid state is;

$$\mu_i = [(\varepsilon_\infty + 2)/3]\frac{(2\varepsilon_0 + 1)}{(2\varepsilon_0 + \varepsilon_\infty)}\mu \qquad (2\text{-}07)$$

where ε_∞ is the optical value of the dielectric constant, and μ is the dipole moment of the molecule as defined by the Debye equation, where the interaction effects of the neighbouring molecules are neglected. Under the effect of the reaction field, the average orientation of the molecules under an applied electric field becomes;

$$\overline{\cos\theta} = \frac{3\varepsilon_0}{(2\varepsilon_0 + 1)}[\mu E/3kT] \qquad (2\text{-}08)$$

(for a random orientation of dipoles the average value of $\overline{\cos\theta} = 0$, whereas, for orientation of all the dipoles in the direction of the field $\overline{\cos\theta} = 1$)

which leads to the final form of the Onsager equation;

$$\mu_i^2 = \frac{27kT(2\varepsilon_0 + \varepsilon_\infty)(\varepsilon_0 - \varepsilon_\infty)}{12\pi N\ (\varepsilon_0)\ \ (\varepsilon_\infty + 2)^2} \qquad (2\text{-}09)$$

The Onsager equation was an improvement over the Debye equation and it has been applied to polymers in solution and in the undiluted state.

In a theory developed by Kirkwood[79] (1939), the short range interactions between molecules in the liquid state were dealt with by the introduction of a correlation function, g, to take account of local order.

The relationship between ε_0 and the dipole moment μ of the molecule in the liquid state was obtained as;

$$\frac{(\varepsilon_0-1)(2\varepsilon_0+1)}{(9\varepsilon_0)} = \frac{4\pi N}{3}\left[\alpha_e + \frac{g\mu^2}{3kT}\right] \qquad (2\text{-}10)$$

Frohlich[80] (1949) proposed a model that included both the short range interactions between the molecules and the resulting deformation polarisation, both of which had been neglected previously. Frohlich considered once more a sphere within a continuum of static dielectric constant ε_0, containing N dipole units per unit volume. Based on this model, Frohlich obtained the equation;

$$(\varepsilon_0-\varepsilon_\infty) = \frac{(3\varepsilon_0)}{(2\varepsilon_0+\varepsilon_\infty)}\frac{(4\pi N)}{3kT}\frac{(\varepsilon_\infty+2)^2}{9}g\mu^2 \qquad (2\text{-}11)$$

The usefulness of Frohlich´s formula is mainly restricted by our ignorance of the correlation factor g, which necessarily depends on the shapes of molecules, the disposition of the permanent dipoles within them, the anisotropy of polarisability and the presence of charge distributions of higher orders of symmetry.

2.02: Dielectric Relaxation - Single Relaxation Behaviour

At low electric field gradients, when a dielectric is subjected to an external electric field, its electrical response will depend upon a number of parameters, such as the frequency of the applied field, the temperature and the molecular structure of the dielectric substance. Under some conditions, no measureable phase difference between the dielectric displacement, D, and voltage gradient, E, vectors will occur, and , consequently, the ratio D/E will be defined by a constant equal to the real value of the dielectric constant, ε'. On the other hand, if under a given set of a.c. conditions a phase angle difference, δ, arises between the D and E vectors, then the former and latter must be expressed as;

$$D_o \exp\ [i(\omega t-\delta)] \qquad (2\text{-}12)$$

and;

$$E_o \exp\ [i\omega t] \qquad (2\text{-}13)$$

respectively,so that;

$$D_o \exp\ [i\omega t-\delta] = \varepsilon^* E_o \exp\ [i\omega t] \qquad (2\text{-}14)$$

where D_o and E_o are the amplitudes of the respective vectors, ω is the angular frequency, t is time and ε^* is the complex value of the dielectric constant defined by;

$$\varepsilon^* = \varepsilon' - i\varepsilon'' \qquad (2\text{-}15)$$

where ε'' is the imaginary part of the dielectric constant and is referred to as the dielectric loss factor and $i = \sqrt{-1}$.

An Argand diagram of the complex current-voltage relationship is shown in Figure (2-1). In the absence of loss mechanisms, the current leads the voltage by 90°. When a loss process interferes, a phase lag is introduced because of the inability of the dipoles to follow immediately the changes of direction of the field. The resulting phase angle is less than 90°, and the difference between the actual phase angle and 90° is denoted by δ.

The two dielectric constants, ε' and ε'', are linked by the relation;

$$\frac{\varepsilon''}{\varepsilon'} = \tan\delta \qquad (2\text{–}16)$$

where $\tan\delta$ is the dissipation factor. The physical meaning of the quantity $\tan\delta$ is;

$$\tan\delta = \frac{\varepsilon''}{\varepsilon'} = \frac{\text{energy dissipated per cycle}}{\text{energy stored per cycle}}$$

where ε'' and ε' are experimentally observable quantities that may be used to characterise the dielectric dispersion over a wide range of frequency and temperature.

The frequency dependence of ε'' and ε' was first described by Debye[77] (1929). His treatment rested on two essential premises; (i) exponential approach to equilibrium, and; (ii) the principle of superposition. For a single relaxation process he showed that;

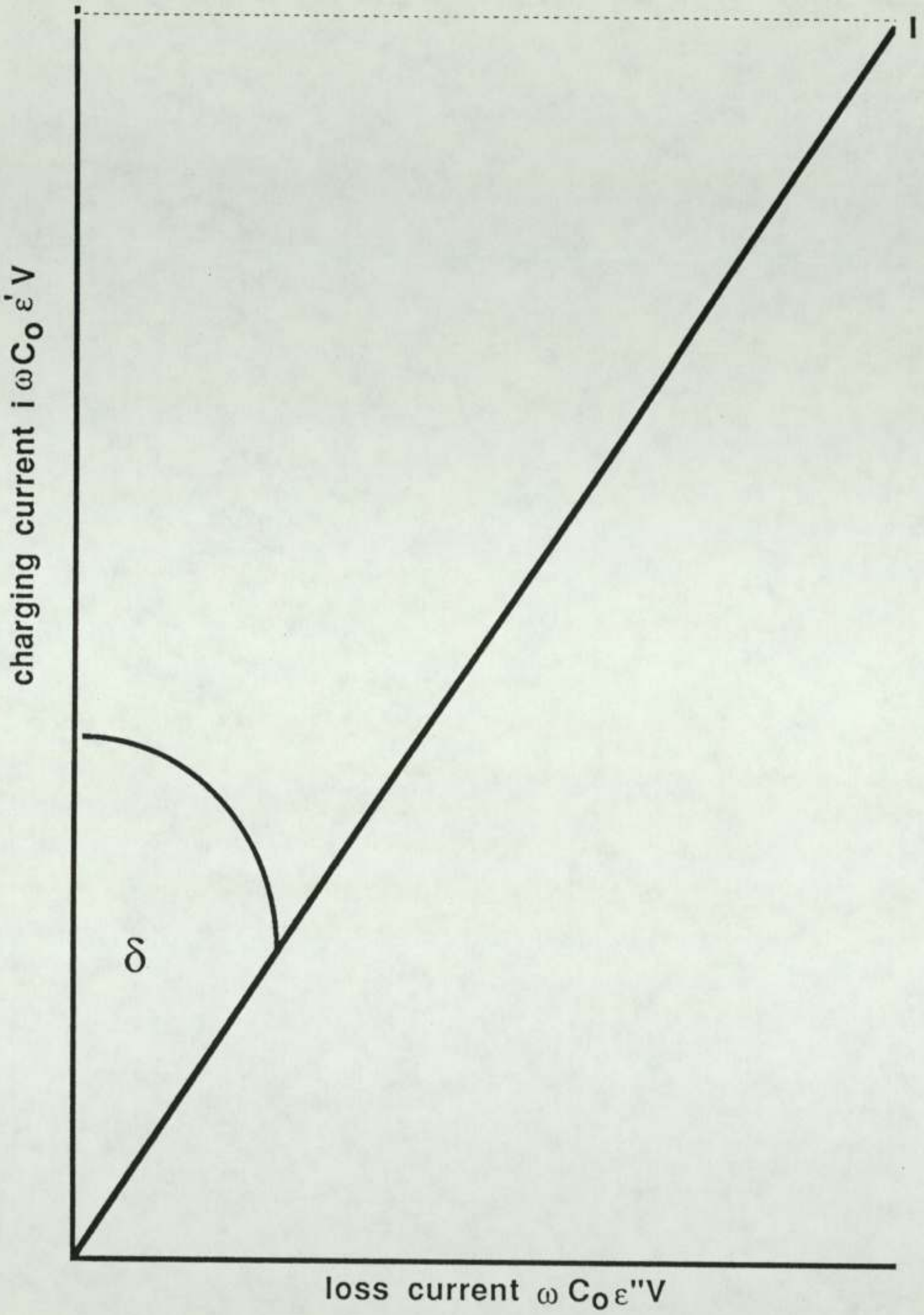

Figure (2-1) Argand diagram of complex current-voltage relationship

$$\varepsilon^* = \varepsilon_\infty + \frac{(\varepsilon_0 - \varepsilon_\infty)}{(1+i\omega\tau)} \qquad (2\text{-}17)$$

Equating real and imaginary parts gives;

$$\varepsilon'(\omega) = \varepsilon_\infty + \frac{(\varepsilon_0 - \varepsilon_\infty)}{(1+\omega^2\tau^2)} \qquad (2\text{-}18)$$

and;

$$\varepsilon''(\omega) = \frac{(\varepsilon_0 - \varepsilon_\infty)\omega\tau}{(1+\omega^2\tau^2)} \qquad (2\text{-}19)$$

where ε_∞ is the high frequency permittivity, ε_0 is the static permittivity, ω is the angular frequency and τ is the relaxation time for the process. The plots of ε' and ε'' versus log ω are depicted in Figure (2-2). It can be seen that ε'' attains a maximum at $\omega = 1/\tau$ or $f = 1/2\pi\tau$, where f is the frequency of the electric field in Hz. At this frequency, the maximum value of ε'' becomes equal to;

$$\varepsilon''_{(max)} = \frac{(\varepsilon_0 - \varepsilon_\infty)}{2} \qquad (2\text{-}20)$$

and ε' assumes the value;

$$\varepsilon' = \frac{(\varepsilon_0 + \varepsilon_\infty)}{2} \qquad (2\text{-}21)$$

Also, from (2-16), (2-18) and (2-19), we have;

$$\tan\delta = \frac{(\varepsilon_0 - \varepsilon_\infty)\omega\tau}{\varepsilon_0 + \varepsilon_\infty\,\omega^2\tau^2} \qquad (2\text{-}22)$$

the maximum of $\tan\delta$, when $d(\tan\delta)/d\omega = 0$, occurs at a frequency;

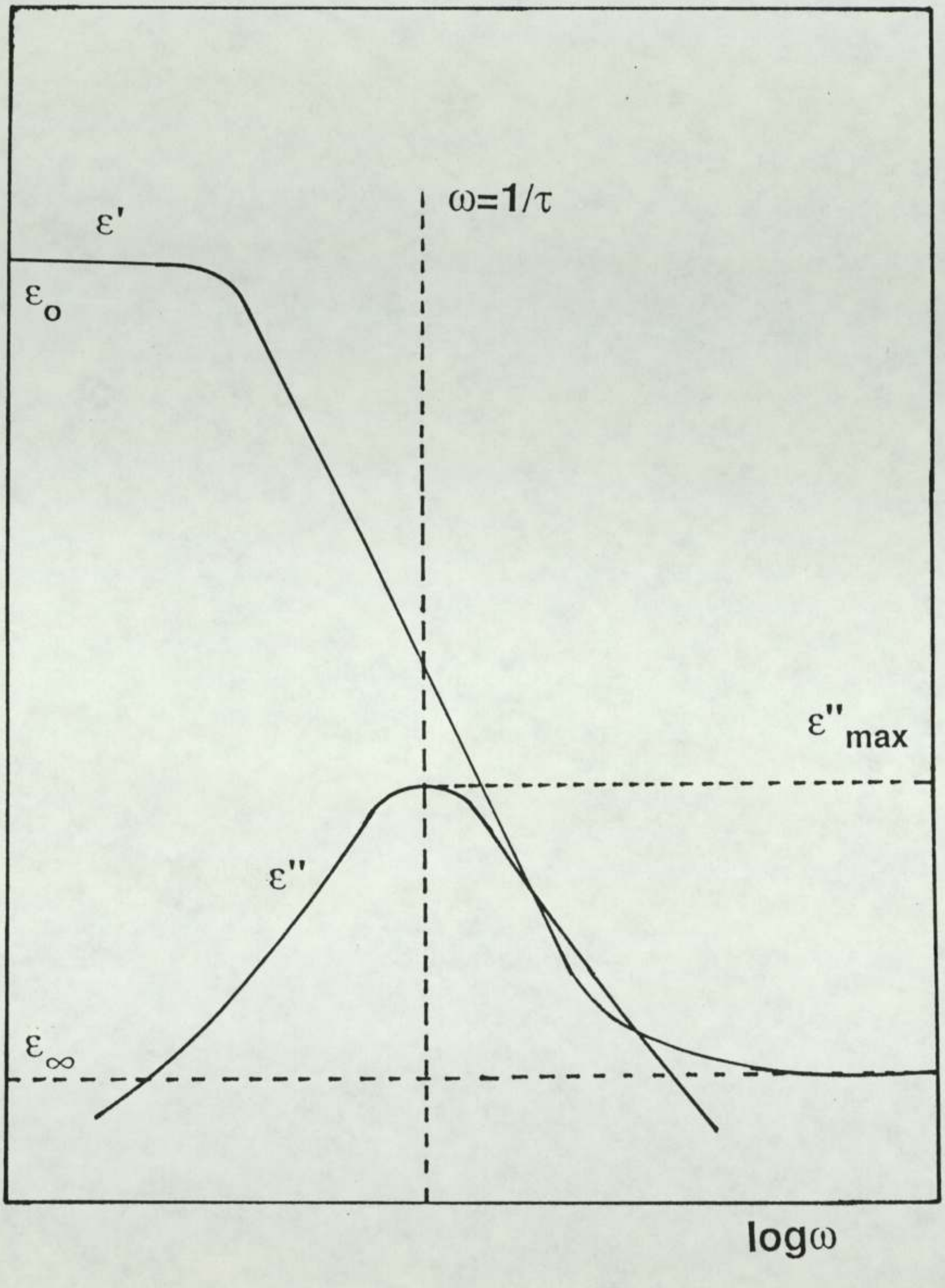

(Figure (2-2) Debye dielectric dispersion curves

$$\omega = 1/[\tau\,(\varepsilon_0/\varepsilon_\infty)^{1/2}] \qquad (2\text{-}23)$$

attaining a value equal to;

$$\tan\delta = \frac{(\varepsilon_0 - \varepsilon_\infty)}{2(\varepsilon_0\varepsilon_\infty)^{1/2}} \qquad (2\text{-}24)$$

The maximum of tanδ is seen not to be coincident with that of ε". The displacement of the tanδ peak depends upon the difference between the ε_0 and ε_∞ values.

The dependence of ε" on ε' may be used to test how well the Debye model fits a real case. Eliminating the parameter ωτ between equation (2-18) and (2-19) gives;

$$[\varepsilon' - (\varepsilon_0 + \varepsilon_\infty)/2] + \varepsilon''^2 = [(\varepsilon_0 - \varepsilon_\infty)/2]^2 \qquad (2\text{-}25)$$

This is the equation of a circle, centre $[(\varepsilon_0 + \varepsilon_\infty)/2, 0]$, radius $(\varepsilon_0 - \varepsilon_\infty)/2$, so that a plot of ε" against ε' should give a semicircle, as shown in Figure (2-3(a)). Experimental results for many polar liquids give excellent agreement with theoretical curve.

2.03: Multiple Relaxation Behaviour.

Relaxations observed in polymers show broader dispersion curves and lower loss maxima than those predicted by the Debye model. This led Cole and Cole[81] (1941) to suggest the following semi-empirical equation for dielectric relaxation in polymers;

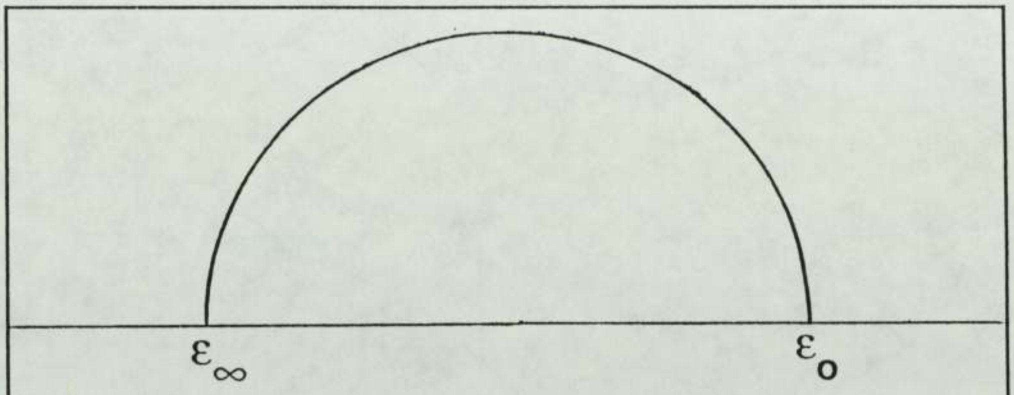

(a) semi-circular Cole-Cole plot

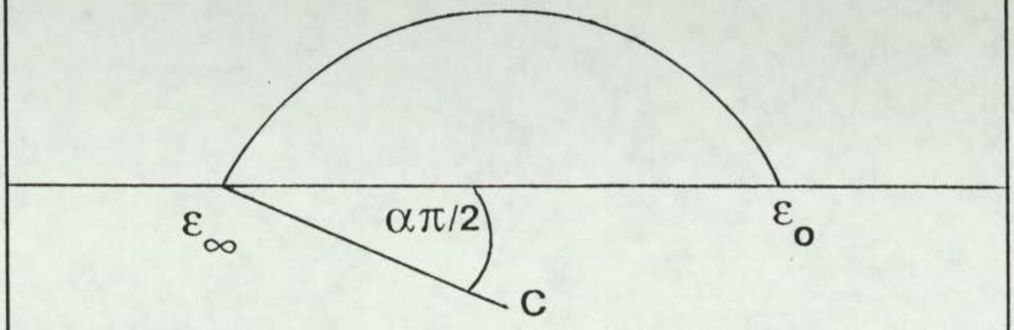

(b) Cole-Cole plot with centre situated below real axis

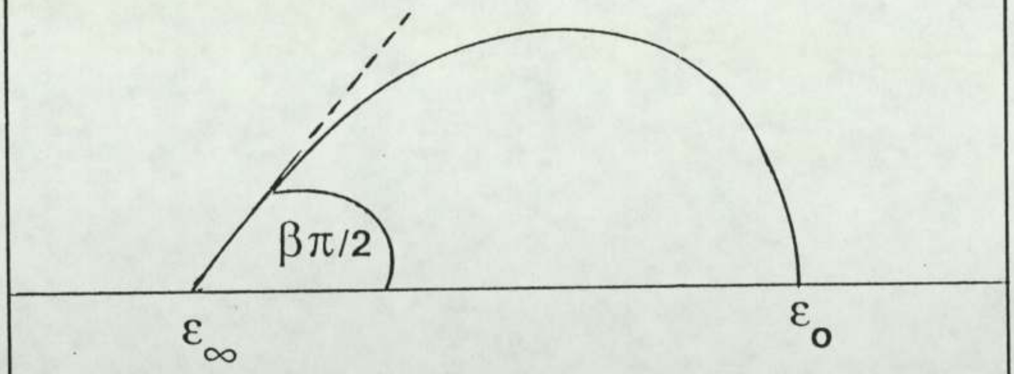

(c) Davidson-Cole plot

(Figure 2-3) Cole-Cole plots

$$\varepsilon^* = \varepsilon_\infty + \frac{(\varepsilon_0 - \varepsilon_\infty)}{1 + (i\omega\tau)^{1-\alpha}} \quad (2\text{-}26)$$

where $0 < \alpha \leq 1$, and α is an empirical quantity specifying the broadness of the distribution.

Equation (3-26) better describes a broad dispersion, and gives an ε'' versus ε' plot in which the centre of the semi-circle is depressed below the abscissa, as shown in Figure(2-3(b)). The flatter or more shallow the circular arc then the greater is the span of relaxation times associated with the relaxation process.

The centre of the circle is given by;

$$[(\varepsilon_0-\varepsilon_\infty)/2,\ -(\varepsilon_0-\varepsilon_\infty)/2 \text{ cotan } \beta\pi/2] \quad (2\text{-}27)$$

where $\beta=1-\alpha$.

The radius of the circle is given by;

$$(\varepsilon_0-\varepsilon_\infty)/2 \text{ cosec } \beta\pi/2 \quad (2\text{-}28)$$

Equation (2-26) corresponds to the superposition of a group of Debye-like relaxation processes with a range of relaxation times that are symmetrically distributed around the mean relaxation time τ. Such a spread of relaxation times is seen as a likely explanation of the broadness of the relaxation in a system of entangled polymer molecules, due to the co-operative nature of dipolar motion. Although the exact form of the distribution of relaxation times in the Cole-Cole equation is not based on any special model, the empirical parameter α is a convenient one for specifying the broadness of experimental relaxation peaks, and it has been extensively used for this purpose.

Referring to Figure (2-3(b)), the angle between the line connecting C to ε_∞ and the real axis is equal to $\alpha\pi/2$. Note that, in the case of $\alpha=0$, the locus of the Cole-Cole plot approaches the ε' axis at 90° and equation (2-26) reduces to equation (2-17), i.e., Debye.

The Cole-Cole empirical equation relates only to dispersion and absorption curves that are symmetrical about the position $\omega\tau=1$. It is often found that the dielectric loss curves have a high frequency broadening and the Cole-Cole arcs for such systems are said to be skewed. Davidson and Cole[82] (1950) attempted to fit the experimental results to the following function;

$$\varepsilon^*(\omega) = \varepsilon_\infty + (\varepsilon_0 + \varepsilon_\infty)/(1 + i\omega\tau)^\beta \qquad (2\text{-}29)$$

where β is a parameter, $0<\beta\leq1$.

Also;

$$(\varepsilon'(\omega) - \varepsilon_\infty)/(\varepsilon_0 - \varepsilon_\infty) = (\cos\phi)^\beta(\cos\beta\phi) \qquad (2\text{-}30)$$

and;

$$(\varepsilon''(\omega) - \varepsilon_\infty)/(\varepsilon_0 - \varepsilon_\infty) = (\cos\phi)^\beta(\sin\beta\phi) \qquad (2\text{-}31)$$

where $\tan\phi = \omega\tau_1$.

For maximum loss $\omega\tau_1 \neq 1$, but is given by;

$$\omega_{(max)}\tau_1 = \tan\{1/(\beta+1)(\pi/2)\} \qquad (2\text{-}32)$$

where $\omega_{(max)}$ is the angular frequency corresponding to maximum loss.

Figure (2-3(c)) shows a typical Davidson-Cole arc plot. At low frequencies the arc is circular, but at high frequencies the curve approaches the abscissa along a straight line. The angle between this line and the abscissa is $\beta\pi/2$. Note that the frequency f_1, from $\tau_1 = 1/2\pi f_1$, is lower than the one for which ε'' is a maximum and corresponds to the point on the complex plane locus for which $\theta=\beta\pi/4$. Many measurements on solutions of polymers in low molecular weight solvents often give results that are fitted by the Davidson-Cole function.

The treatment proposed by Havrilak and Negami[83] (1967) produced an equation applicable to both skewed and semi-circular arc plots. They introduced the empirical function;

$$(\varepsilon^*(\omega) - \varepsilon_\infty)/(\varepsilon_0 - \varepsilon_\infty) = [1 + (i\omega\tau)^{1-\alpha}]^{-\beta} \qquad (2\text{-}33)$$

where $0<\alpha\leq1$ and $0<\beta\leq1$.

When $\beta=1$ and $\alpha=0$ the Debye function is obtained. Havrilak and Negami applied equation (2-33) to results obtained for more than twenty polymers and found good agreement in most cases.

It is apparent from the preceding discussion that Cole-Cole plots are a very convenient graphical method for the representation of the entire dielectric properties of a chemical system. Superpositioning of Cole-Cole plots, together with a vertical displacement of curves obtained at different temperatures permits the effect of temperature on ε' and ε" to be easily ascertained. For a complete set of relaxation data, the limiting values of ε_0 and ε_∞ may be obtained from the intersection of the locus of Cole-Cole plots on the ε' axis.

It is also noted that Cook and co-workers[84] (1970) introduced a non-exponential time-domain decay function of the form;

$$\psi(t) = \exp[-(t/\tau)^{\gamma}] \qquad (2\text{-}34)$$

where $0<\gamma\leq1$.

2.04: Temperature and Dielectric Relaxation.

The concept of thermal activation over a potential energy barrier was first applied to to dielectric phenomena by Eyring[85] (1936). He showed that the rate constant for the movement of molecular dipoles between two or more possible equilibrium positions separated by a potential energy barrier was;

$$K_0 = kT/h \exp[-\Delta F/RT] \qquad (2\text{-}35)$$

where k is the Boltzmann constant, h is Planck's constant and R is the gas constant. Here ΔF is the free energy of dipolar relaxation and is defined as;

$$\Delta F = \Delta H - T\Delta S \qquad (2\text{-}36)$$

where ΔH is the activation energy of dipole relaxation and ΔS is the entropy of activation. In terms of the rate constant approach, the dipole relaxation time, τ, is, by definition, the inverse of K_0, so that we have;

$$\tau = h/kT \exp[\Delta H/RT]\exp[-\Delta S/R] \qquad (2\text{-}37)$$

or, in logarithmic form;

$$\ln\tau = \Delta H/RT - \ln T + (\ln h/k - \Delta S/R) \qquad (2\text{-}38)$$

Since the last term on the right-hand side of equation (2-38) is independent of temperature and because the contribution from the lnT term is small, a plot of $\ln\tau$ against 1/T would be expected to be a straight line. This is an example of the Arrhenius law, and, in practice it is usual to plot $\log f_{(max)}$ against 1/T to obtain a straight line graph possessing a gradient of $-\Delta H/2.303R$.

2.05: Dielectric Relaxation in Polymers.

Dielectric relaxation processes observed in polymers are generally classified into two main kinds. For amorphous polymers with flexible polar side groups the high temperature process is referred to as the α relaxation, and is attributed to the large scale conformational rearrangements of the main chains, while the low temperature process, referred to as the β relaxation, results from the motion of side groups. However even in amorphous polymers without polar side groups two relaxation processes are sometimes observed. For crystalline polymers with high degrees of crystallinity a third relaxation process, associated with the crystalline phase, is sometimes present.

CHAPTER 3

EXPERIMENTAL METHODS

3.01:Introduction.

This study is concerned with the measurement of experimentally observable quantities, using a variety of experimental techniques, to yield information concerning the static and dynamic properties of polymers. The measured quantities can conveniently be described in three separate sections. They are:

1.The parallel electrical capacitance, C_p, and the dissipation factor, $\tan\delta$. These are quantities from which can be calculated the dielectric constant, ε', and the dielectric loss factor, ε''. A considerable amount of information concerning the motion and flexibity of polymer molecules can be deduced from the temperature and frequency dependence of ε' and ε''.

2.The solution static dielectric permittivity, ε_{12}, and the experimental Kerr constant, B. These are complementary tools used in the elucidation of molecular structures.

3.The parallel resistance R_p. The measurement of electrical resistance allows an insight into the conductive properties of a compound through the inverse relationship between electrical resistivity and electrical conductivity.

The apparatus and techniques used to facilitate these measurements will be described in this chapter.

3.02: Dielectric Apparatus for the Measurement of C_p and Tanδ at Various Frenquencies.

The measurement of the electrical capacitance and the dissipation factor was carried out using a GenRad 1689 Precision RLC Digibridge connected to a dielectric cell containing the sample under test. The temperature was accurately controlled using the apparatus described below. Repeated measurements, separated by a number of days, were carried out on an oligomer of methylphenyl siloxane with n=4 and a cyclic fraction of PDMS with n=50 to test for reproducibility. It was found that, for these samples, the results were reproducible to within a few percent.(see appendix)

Electrical connections between the Digibridge and the dielectric cell were made using a four terminal, guarded GenRad 1657-9600 extender cable. The cable was slightly modified with the replacement of the "high" and "low" banana plugs by BNC plugs. The guard plug was left unchanged. The corresponding BNC sockets were mounted onto a small Tufnol sheet and the two terminal dielectric cell was connected to these sockets. Prior to the connection of the dielectric cell a zeroing procedure was carried out on the Digibridge and extender cable to compensate for stray capacitances.

3.03: Dielectric Cells.

Two dielectric cells were used in this study. Both cells were of a parallel plate capacitor construction. Diagrams of the cells are shown in Figure (3-1).

Dielectric cell A was constructed from two identical brass plates measuring 4cm. by 1cm. PTFE spacers and an epoxy based resin were used to fix a 0.25 mm gap between the plates and to seal the vertical sides of the capacitor. Electrical connections were made using stiff copper wires. The capacitor had a sample volume of approximately 0.1 cm^3 and was contained inside a glass tube. The electrical capacitance of the empty cell was approximately 25pF. This cell was used to measure the electrical capacitance and dissipation factor of a series of cyclic poly(dimethyl siloxanes), a series of linear poly(dimethyl siloxanes), a series of linear oligomers of methyl phenyl siloxane, a series of linear poly(methyl phenyl siloxanes), a linear poly(methyl hydrogen siloxane), poly(n-hexyl methyl siloxane) and a cyclic oligomer of methyl phenyl siloxane.

Dielectric cell B was constructed from two identical brass plates measuring 4 cm. by 1 cm. The plates were separated and held in position by PTFE thread seal tape, which also served to seal the vertical sides of the capacitor. Avoiding the use of an epoxy based resin to seal the cell meant that this cell, unlike cell A, could be taken apart, the polymer liquid crystal could then be applied onto the plates, and the cell could be re-assembled ready for use. This procedure was necessary because the high viscosity of the polymer liquid crystal prevented it from flowing. The cell was contained inside a glass tube and electrical connections were made using stiff copper wires. The electrical capacitance of the empty cell and the sample volume were not measured. This

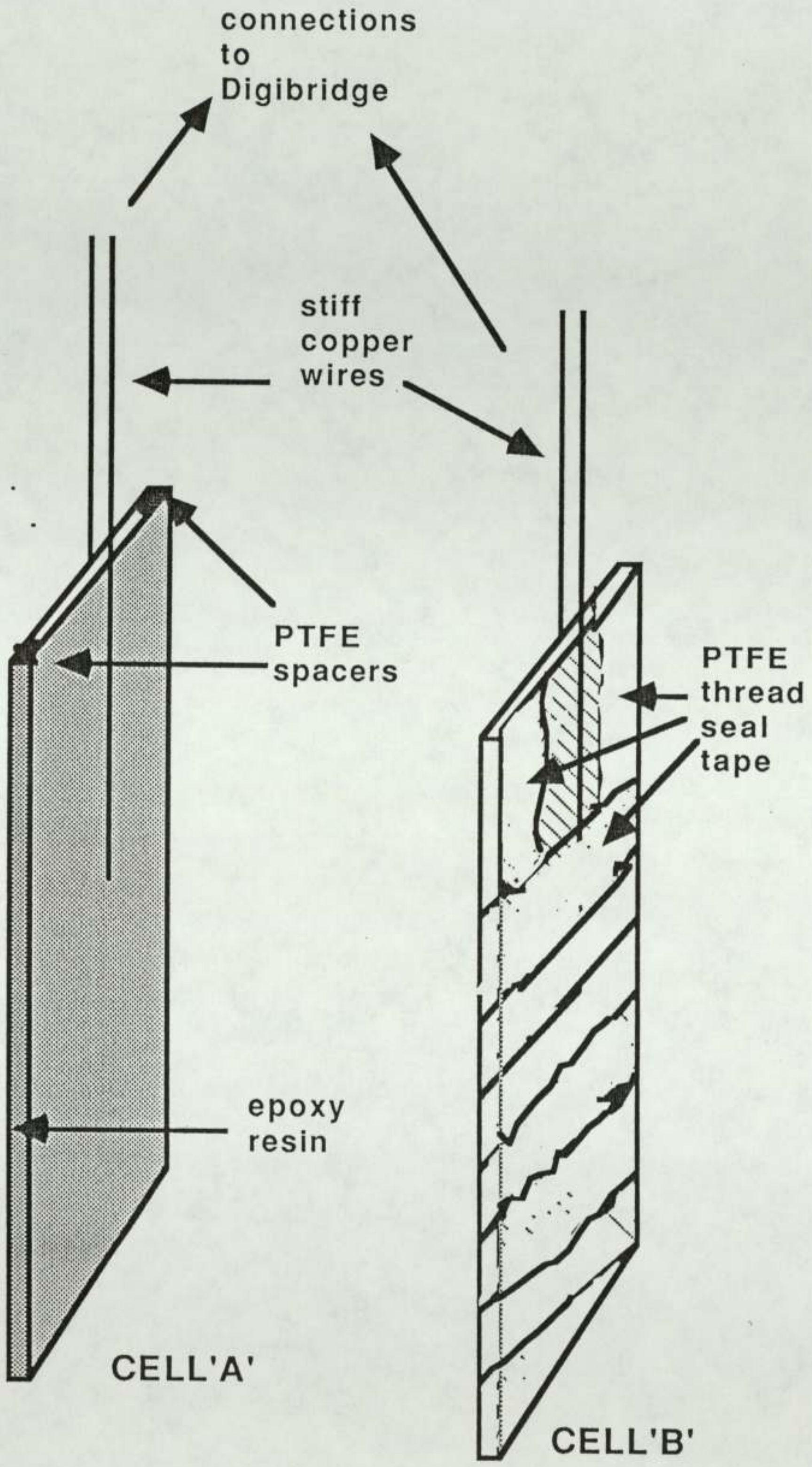

FIGURE (3-1). DIELECTRIC CELLS 'A' AND 'B'.

cell was used to measure the electrical capacitance and the dissipation factor of the polymer liquid crystal sample.

3.04: Temperature Control in the Range 203K-298K.

Temperature control in this region was required for the measurement of the dielectric relaxation of a series of linear poly(methyl phenyl siloxanes), a cyclic oligomer of methyl phenyl siloxane and a polymer liquid crystal. This was achieved using a "Minus Seventy" Thermostat Bath, Bridge Control Model (Townson and Mercer Ltd., Croydon, UK). A cross-sectional diagram of this apparatus is shown in Figure (3-2). The heat exchanger vessel was half-filled with acetone and solid CO_2. The temperature control vessel was filled with acetone. A short length of copper pipe, used to electrically shield the dielectric cell, was fixed in a vertical position to the underside of the temperature control vessel lid. A hole drilled through the lid allowed suspension of the dielectric cell into the shield. A guard socket was mounted onto the topside of the lid and electrically connected to the shield. The temperature was measured by a total immersion alcohol thermometer. The temperature control of this apparatus was ± 0.1K.

3.05: Measurement of Electrical Capacitance and Dissipation Factor in the Range 203K-298K.

The acetone in the temperature control vessel was cooled to the required temperature. A period of ten minutes was then allowed for temperature equilibration between the bath and the cell after which electrical capacitance and dissipation factor measurements were made. The average of ten measurements

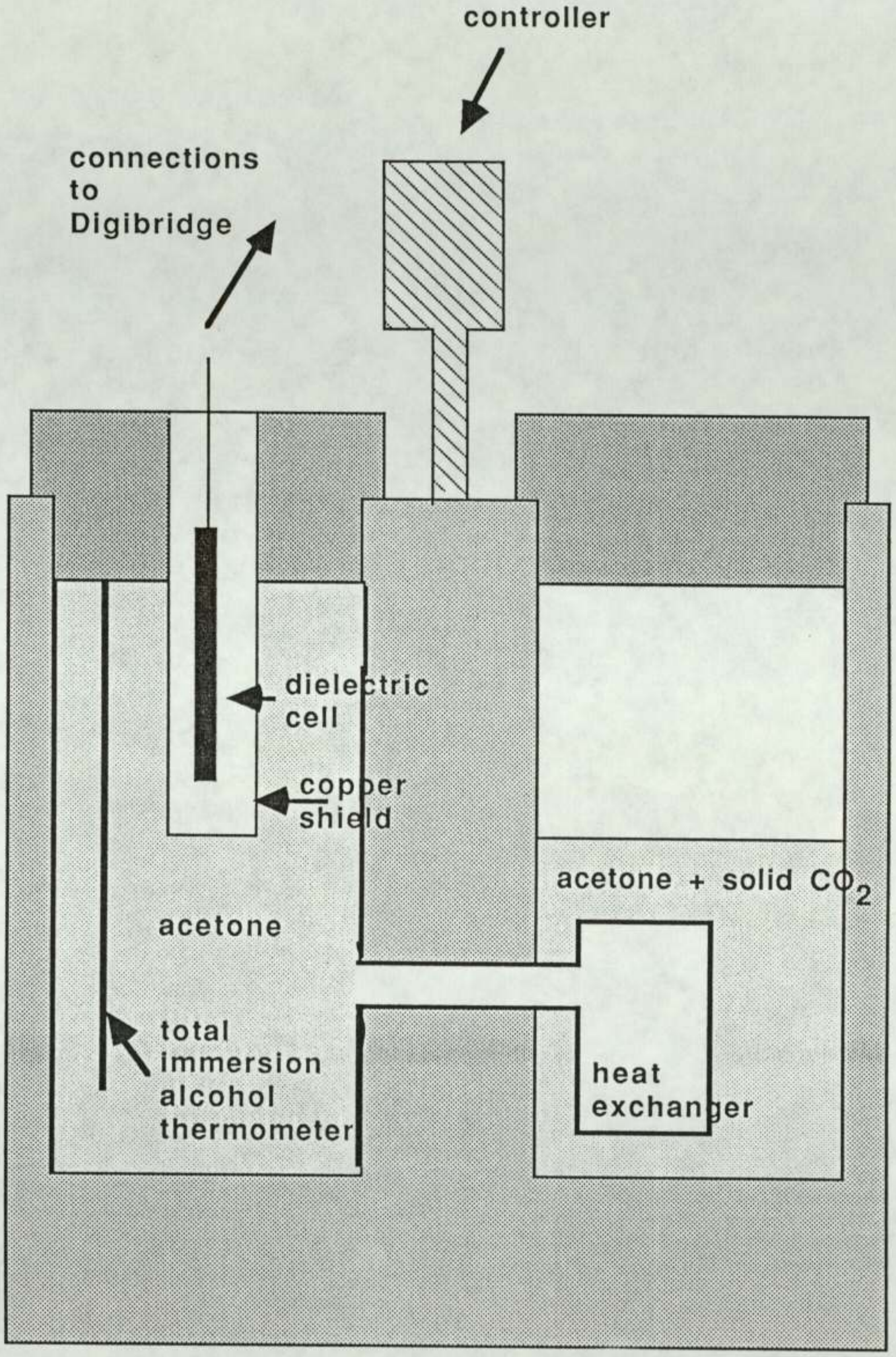

FIGURE (3-2).
CROSS-SECTIONAL DIAGRAM OF THE 'MINUS SEVENTY' BATH.

was taken at up to fifteen spot frequencies in the range 12Hz to 10^5 Hz. This procedure was repeated at five different temperatures for each sample.

3.06: Apparatus for Temperature Control Below 203K.

Temperature control in this region was required for cyclic and linear poly(dimethyl siloxane) fractions, linear oligomers of methyl phenyl siloxane, a linear poly(methyl hydrogen siloxane), and poly(n-hexyl methyl siloxane). A cross-sectional diagram of the apparatus designed for this purpose is shown in Figure (3-3). A cooling vessel was constructed using two Dewar flasks, one fitting inside the other. The gap between the Dewar flasks was filled with liquified N_2. Thirty resistors , each of resistance 820Ω, were connected in series and inserted into the inner Dewar so as to form a uniform heating "cage". Electrical connections were made between the resistors and a stabilised voltage supply (Farnell Instruments). A lid was fashioned from expanded polystyrene to provide thermal insulation. The dielectric cell was connected, using thin copper wires, to two minature bnc connectors mounted on a Tufnol board.

The temperature was measured by an iron-constantan thermocouple. The measurement junction of the thermocouple was fixed to the back of one electrode of the dielectric cell. The thermocouple emf was measured by a Keithley 616 Digital Electrometer. The temperature control of this apparatus was ± 0.25K.

3.07: Measurement of Electrical Capacitance and Dissipation Factor Below 203K.

Before enclosing the dielectric cell within the cooling vessel the sample under test was rapidly quenched below it's glass transition temperature in liquified N_2 at a rate of 50K/min. This was necessary to reduce

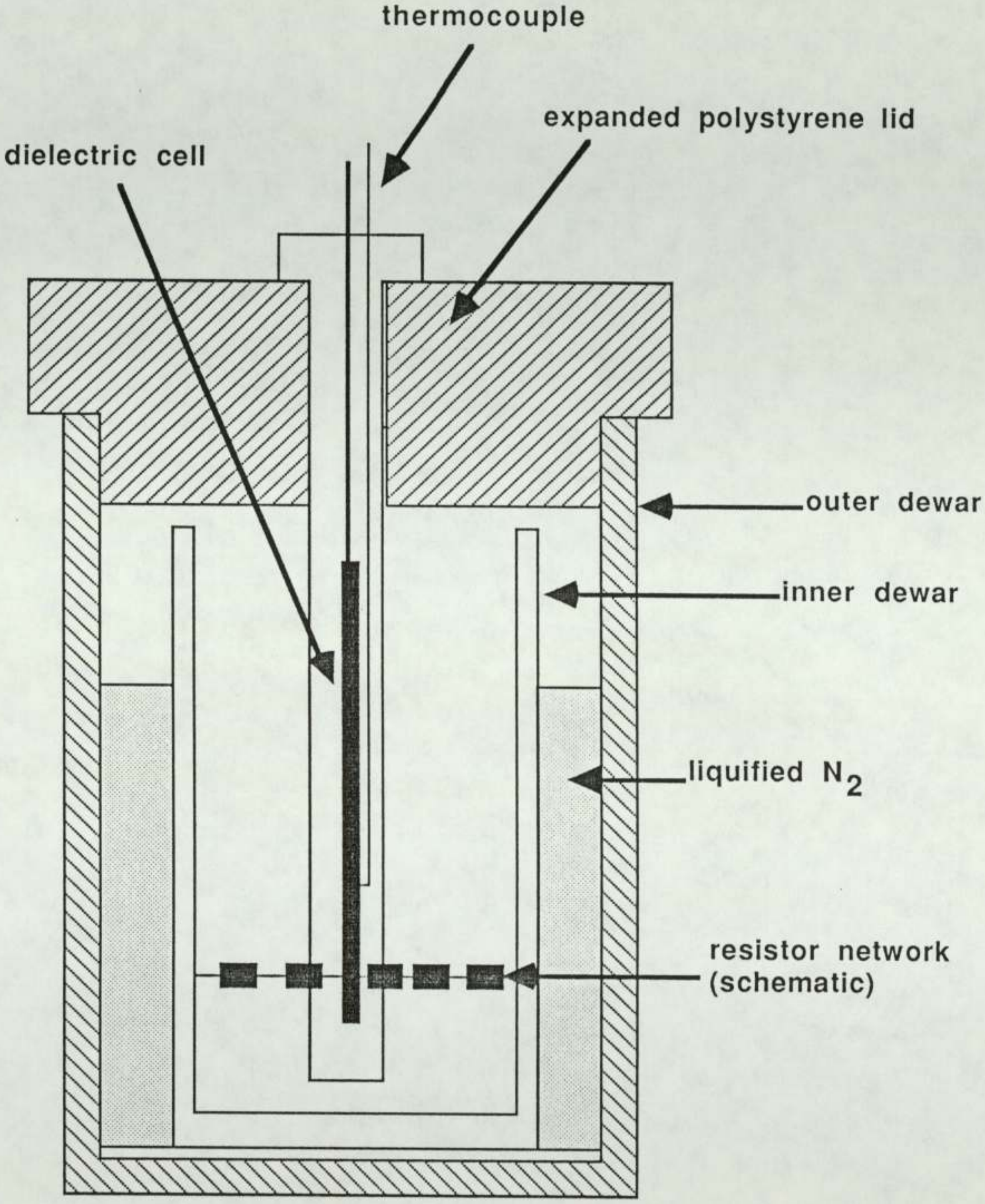

FIGURE (3-3). APPARATUS FOR TEMPERATURE CONTROL BELOW 203K.

crystallisation of the polymer. A small current , producing approximately one watt of heating in the resistor network, was then required to heat the sample. At the temperature of interest the power supply was disconnected for measurement purposes, as simultaneous operation of the Digibridge in measure mode and the power supply was not possible due to electrical interference. The average of ten measurements was taken at up to fifteen spot frequencies in the range 12Hz to10^5 Hz. This procedure was repeated at five different temperatures for each sample.

3.08: Measurement of Stray Capacitances.

It was necessary to measure the stray capacitances associated with dielectric cells A and B so as to facilitate the calculation of the dielectric constant for the polysiloxane samples.

For a real capacitor with stray capacitances, ΔC, assumed to be constant, it follows that;

$$\frac{(C_s - \Delta C)}{(C_a - \Delta C)} = \varepsilon_s \qquad (3\text{-}01)$$

where C_a and C_s are the measured capacitances of the dielectric cell when filled with air and a standard dielectric, respectively, and ε_s is the static dielectric permittivity of the standard. Solving eqn. (3-01) for ΔC gives;

$$\Delta C = \frac{(\varepsilon_s C_a - C_s)}{(\varepsilon_s - 1)} \qquad (3\text{-}02)$$

The standard dielectric used in this study was toluene ($\varepsilon_s = 2.379$ at

298K[86]). The stray capacitances were measured at 298K at various spot frequencies in the range 12Hz to 10^5Hz.

3.09: Apparatus for Parallel Resistance Measurement.

All parallel resistance measurements were made using the 1689 Digibridge previously mentioned connected to a two terminal resistance cell containing the sample under test.

The zeroing procedure and electrical connections between the Digibridge and the resistance cell were made as previously described for the electrical capacitance and dissipation factor measurements.

3.10: Resistance Cell Design.

A cross-sectional diagram of the stainless steel resistance cell is shown in Figure (3-4). The sample was contained between the central ram and the base of the cell, the central ram and the base forming the cell teminals. A PTFE spacer was used to electrically insulate both terminals. This cell was used to measure the parallel resistance of oligomers of p-phenylene vinylene and poly(p-phenylene vinylene).

3.11: Measurement of Parallel Resistance at Room Temperature.

The average of ten measurements was taken at each of thirteen spot frequencies in the range 12Hz to 10^5Hz. A pressure of $5.88 \times 10^7 Nm^{-2}$ was maintained upon the sample for the duration of the measurements. The thickness of the sample disc was measured using a travelling microscope.

3.12: Volume Resistivity and Volume Conductivity.

Volume resistivity, ρ_V, is defined as

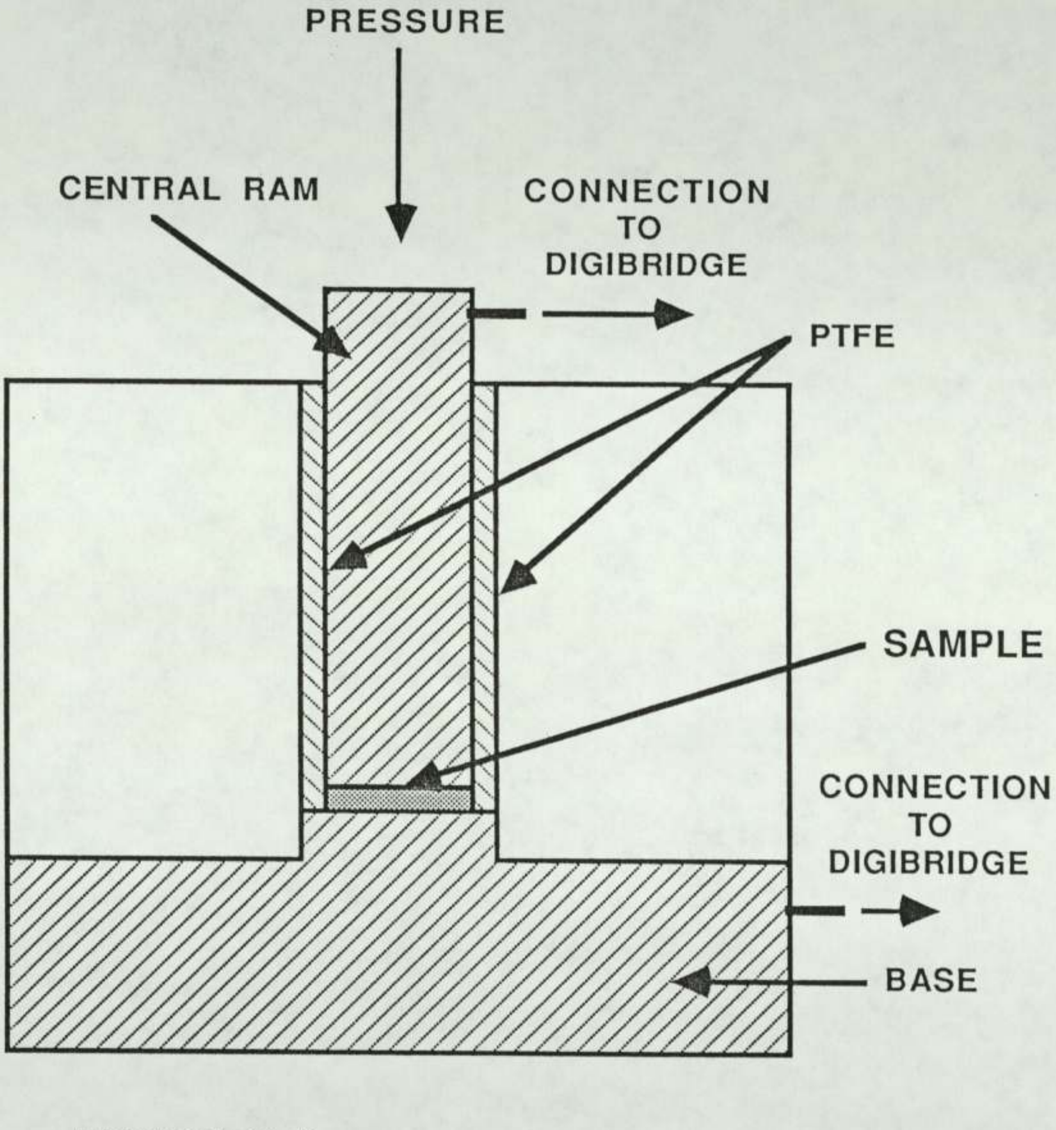

FIGURE (3-4)
STAINLESS STEEL RESISTANCE CELL

$$\rho_v = \frac{R_p A}{L} \qquad (3\text{-}03)$$

where R_p is the measured parallel resistance at 10KHz, A is the cross-sectional area of the electrodes and L is the thickness of the disc. Hence, volume conductivity, σ_v, is given by $(\rho_v)^{-1}$.

3.13: Apparatus for Measurement of Solution Static Dielectric Permittivity.

Full details concerning the construction and operation of this apparatus can be found in reference 87. This apparatus was used to measure the static dielectric permittivity of p- tolaldehyde . A diagram of the apparatus is shown in Figure (3-5).

3.14: Measurement of Static Dielectric Permittivities.

For a real capacitor with stray capacitances, ΔC, it may be shown that;

$$\frac{(C_s - \Delta C) - (C_a - \Delta C)}{(C_x - \Delta C) - (C_a - \Delta C)} = \frac{(C_s - C_a)}{(C_x - C_a)} = \frac{(\varepsilon_s - 1)}{(\varepsilon_x - 1)} \qquad (3\text{-}04)$$

where C_a, C_s, and C_x are the measured capacitances of the dielectric cell when filled with air, a standard dielectric, and the material under test, respectively, and ε_s and ε_x are the static dielectric permittivities of the standard and material under test, respectively.

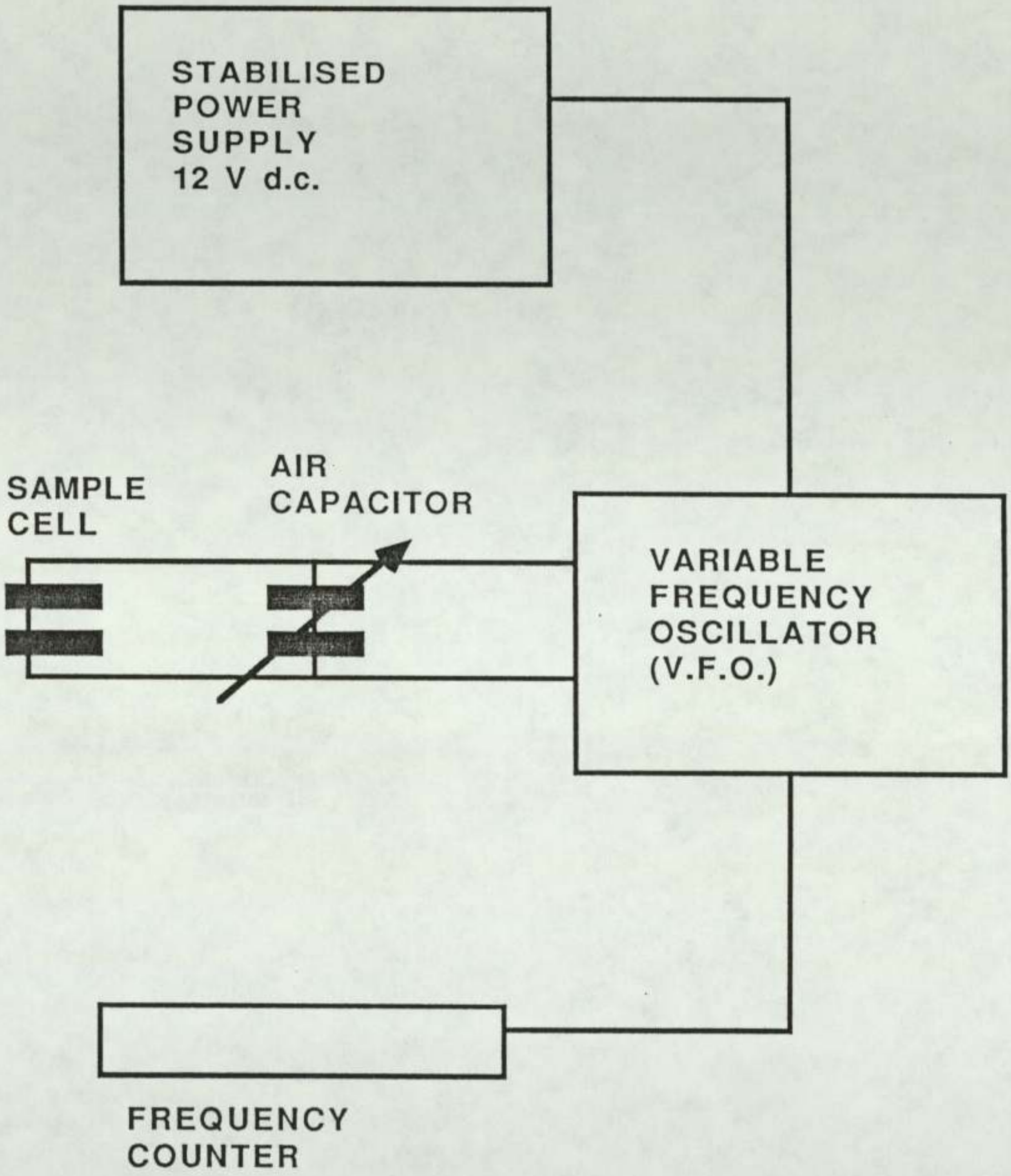

FIGURE (3-5) APPARATUS FOR MEASUREMENT OF STATIC DIELECTRIC PERMITTIVITY

Hence;

$$\varepsilon_x = 1 + \frac{(C_x - C_a)}{(C_s - C_a)} (\varepsilon_s - 1) \qquad (3\text{-}05)$$

However, since the square of the reciprocal frequency of the V.F.O. is proportional to the value of the capacitance, the respective frequency terms may be substituted into (3-05) to give;

$$\varepsilon_x = 1 + \frac{[(f_x)^{-2} - (f_a)^{-2}]}{[(f_s)^{-2} - (f_a)^{-2}]} (\varepsilon_s - 1) \qquad (3\text{-}06)$$

3.15: Kerr Effect Apparatus.

A diagram of the apparatus used to measure the electrically induced phase difference, δ, is shown in Figure (3-6). A parallel plane- polarised beam of monochromatic light is passed through the Kerr cell such that the plane of polarisation of the light is at an angle of 45^{o} relative to the direction of the applied pulsed electric field, E. In the presence of this electric field the light leaving the cell is generally elliptically polarised. After passing through a quarter wave retarder , orientated with it's principal optical axis at 45^{o} to the direction of the applied electric field , the light can be nulled by rotating the analyser. The angular difference , α, between the principal planes of the polariser and the analyser is equal to $\delta/4$ if a

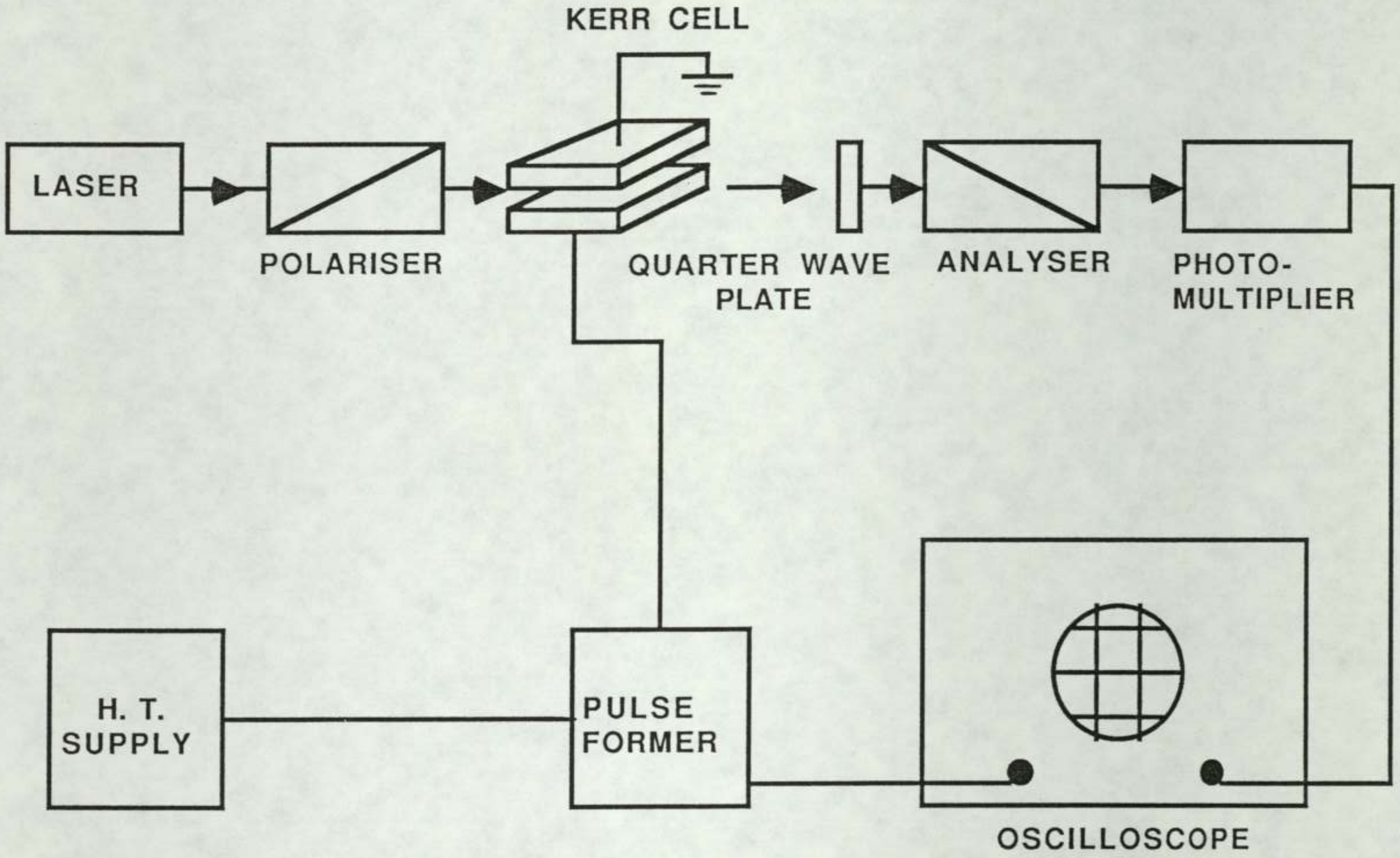

FIGURE (3-6) KERR EFFECT APPARATUS

pulsed a.c. electric field is used. Changes in the level of light were detected by a photomultiplier. The output of the photomultiplier was connected to an oscilloscope thus enabling the electrically-induced optical pulse to be displayed. A series of typical optical pulses are shown in Figure (3-7). Further details concerning the Kerr effect apparatus can be found in reference 87.

3.16: Large Sample Volume Kerr Cell.

A cross sectional diagram of the large sample volume Kerr cell is shown in Figure(3-8). The cylindrical body of the cell was made from double-walled glass, whilst the two electrodes were made from steel. The length of the electrodes was 180mm. The inter-electrode gap was 1.00mm and was set by means of four glass spacers. The electrode assembly was held in position by four springs which pressed against the inside of the cell body. The cell was closed by B19 cones , onto the smaller ends of which optical quality quartz discs were fused. The h.t. supply was connected to the electrodes using two threaded brass wires, which screwed vertically into the steel through the filling tubes. The outer cavity of the cell body served as a water jacket and the temperature of the cell was controlled by a Churchill water- pump thermostat.

3.17: Measurement of Absolute Kerr Constants.

The experimentally determined Kerr constant is defined by[88];

$$B = \frac{\delta}{2\pi L(V/d)^2} \qquad (3\text{-}07)$$

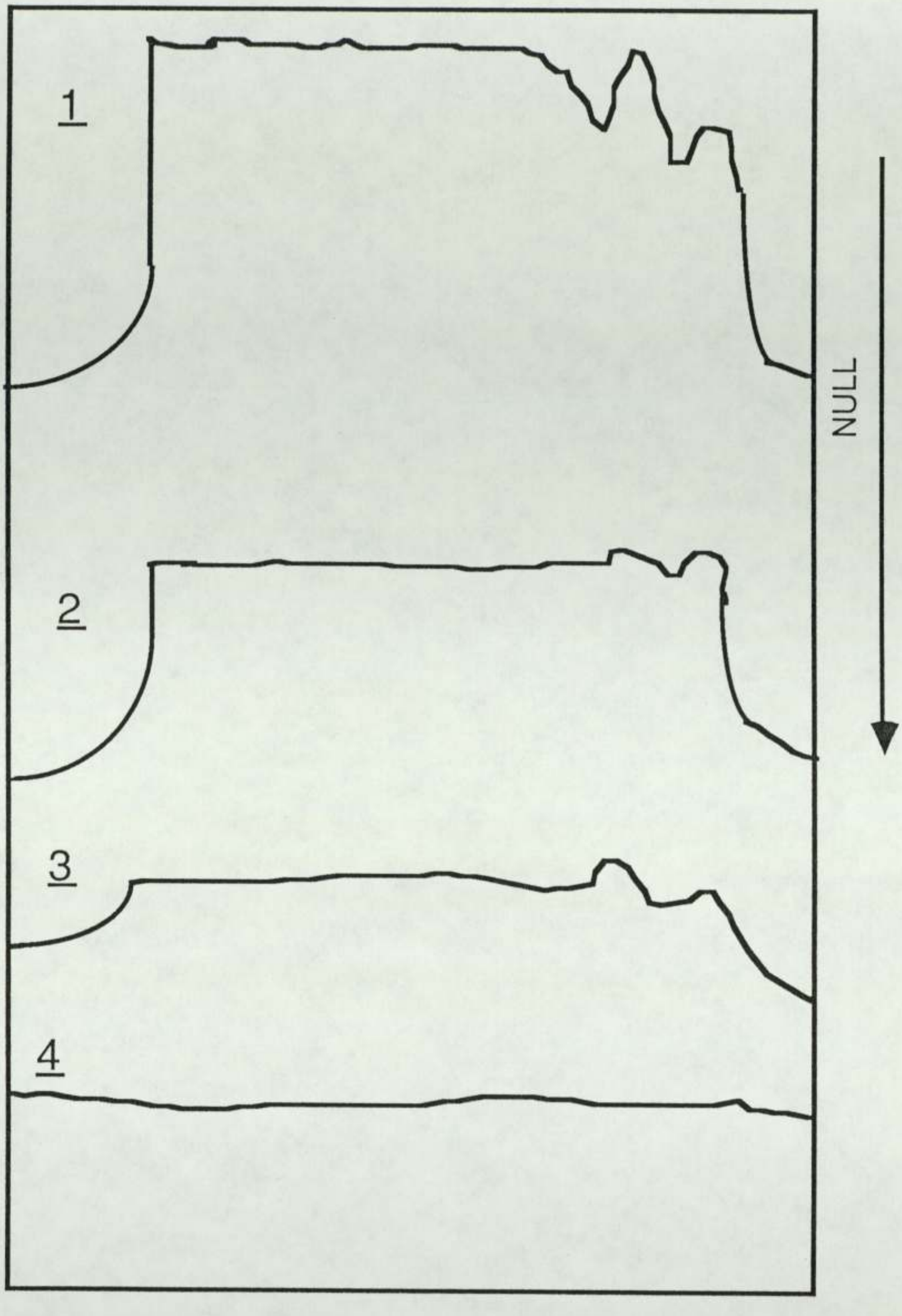

FIGURE (3-7) SCHEMATIC DIAGRAM OF TYPICAL OPTICAL PULSES

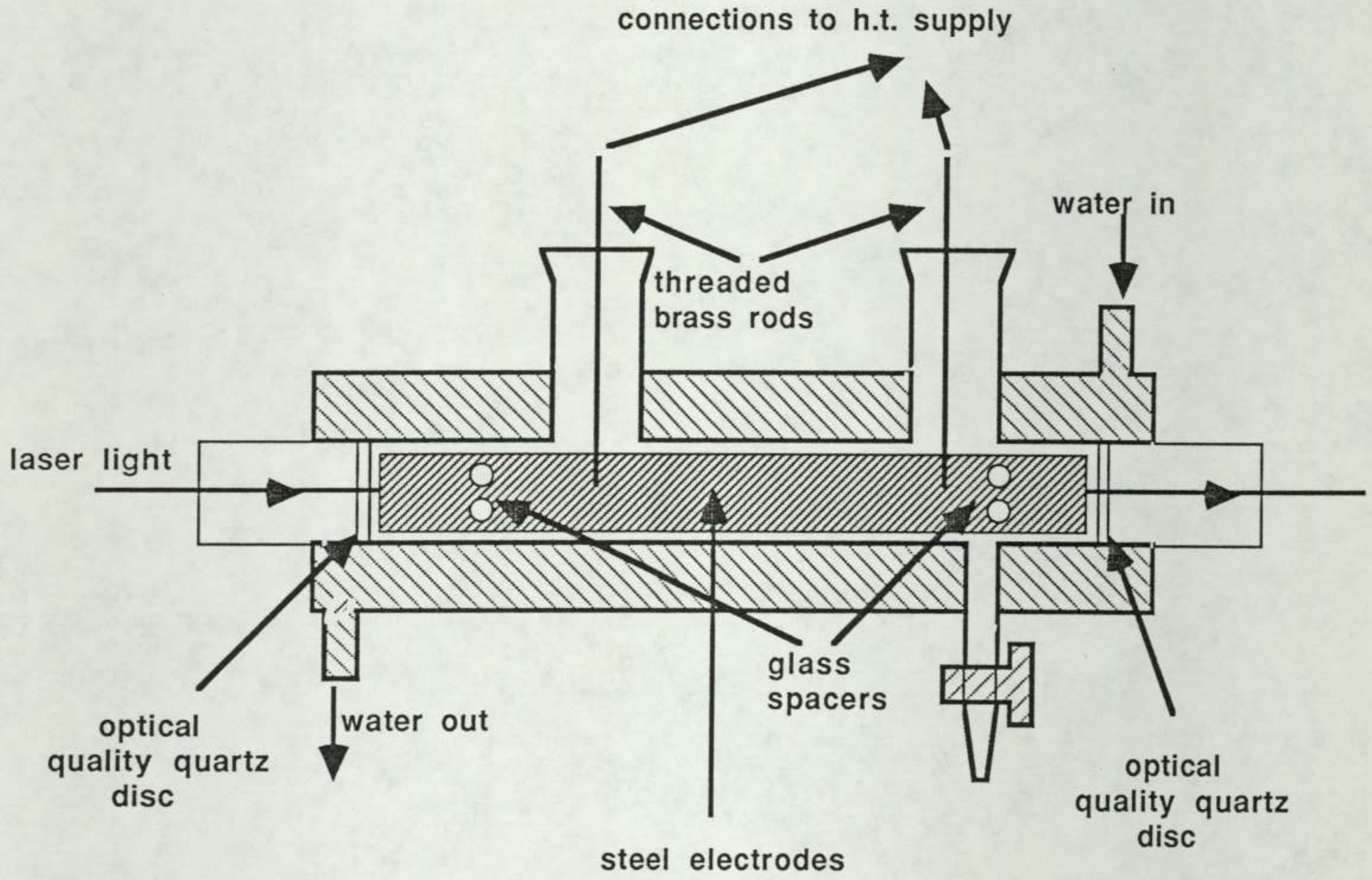

FIGURE(3-8) CROSS-SECTIONAL DIAGRAM OF LARGE SAMPLE VOLUME KERR CELL where;

δ is the electrically induced phase difference between the components of light parallel and perpendicular to the applied electric field, E, L is the optical path length between the electrodes, V is the applied voltage and d is the electrode separation.

For the pulsed electric field method of measuring the Kerr effect the rotation of the plane of polarisation, α, is related to the phase difference by;

$$\alpha = \delta/4 \qquad (3\text{-}08)$$

substituting into equation (3-07) gives;

$$\alpha = \frac{\pi L(V/d)^2 B}{2} \qquad (3\text{-}09)$$

Thus a plot of α against V^2 should give a straight line passing through the origin with a gradient equal to $(\pi LB)/2d^2$, thereby allowing the experimental value of B to be determined. If straight line plots are obtained using equation (3-09) then the Kerr law is obeyed (i.e. α is proportional to E^2).

In practice the absolute rotation, α, was not measured. Instead a directly proportional quantity, α', was obtained from an arbitarely calibrated dial. The rotation α, in degrees, is related to α' by;

$$\alpha = 0.9 \times 0.0174532\alpha'.$$

3.18: Measurement of Relative Kerr Constants.

The Kerr effect measurements in this study were not conducted by the absolute method described previously. Instead, the graph of α' against V^2 was plotted for the unknown and the gradient, m_X, found. The cell was then calibrated with a liquid of known Kerr constant, B_S. The graph of α' against V^2 for the standard liquid gave a gradient, m_S. The Kerr constant, B_X, of the unknown liquid could then simply be found using;

$$B_X = (m_X/m_S)B_S \qquad (3\text{-}10)$$

CHAPTER 4

MATERIALS

4.01:Introduction.

The materials used in this study were a combination of "gifts" from York University and compounds synthesised by the author. The synthesis and characterisation of a polymer liquid crystal, poly(n-hexyl methyl siloxane) and poly(p-phenylene vinylene) will be described in this chapter.

4.02: Poly(dimethyl siloxanes).

A series of polymer samples consisting of five linear poly(dimethyl siloxane) fractions and five cyclic poly(dimethyl siloxane) fractions were provided by Dr. J. A. Semlyen of York University. The number average number of skeletal bonds, $\bar{n}_n$, was in the range 28-99. The ratio of M_w to M_n where M_w is the weight average molecular weight and M_n is the number average molecular weight, varied between 1.03 and 1.08.

4.03: Poly(methyl phenyl siloxanes).

A series of samples consisting of four linear oligomers of methyl phenylsiloxane and six linear poly(methyl phenyl siloxane) fractions were provided by Dr. J.A. Semlyen of York University. For the oligomers the number of skeletal bonds, n, was in the range 4-10. For the polymer fractions the number average number of skeletal bonds, $\bar{n}_n$, was in the range 31 - ~1370. A cyclic oligomer, $[PhMeSiO]_5$, was also provided.

4.04: A Synthetic Route to a Polymer Liquid Crystal.

The preparative methods adopted in this study to facilitate the synthesis of a side chain polymer liquid crystal comprised a combination of methods successfully utilised by other workers[89-92].

The polymer liquid crystal was synthesised in two stages. Firstly, a mesogenic group, [4(allyloxy)benzoyl]4-methoxyphenyl, was synthesised by an esterification reaction. Secondly, the mesogenic group was attached, via a flexible alkyl spacer, as a side chain to a poly(methyl hydrogen siloxane)[PMHS] backbone by a polyhydrosilation reaction. The second stage of the synthetic route is shown in Figure (4-1).

4.05: Stage 1- Synthesis of Mesogenic Group.

Whilst the mesogenic group used in this study exhibits no mesophase of its own, it is structurally similar to many of the low molecular weight liquid crystals that have been synthesised and utilised in the production of thermotropic polymer liquid crystals[93-96].

4.06: Synthesis of 4-Allyloxybenzoic acid.

0.05 moles (6.9g) of 4-hydroxybenzoic acid (BDH), 0.05 moles (4.3cm^3) of allyl bromide (Aldrich Chem. Co. Ltd.), 0.10 moles (5.6g) of potassium hydroxide (BDH) and a small amount of potassium iodide (BDH) were dissolved in a mixture of technical grade ethanol (35cm^3) and distilled water (10cm^3). The resulting brown solution was refluxed for twelve hours after which it was diluted by the addition of of distilled water (100cm^3) and neutralised with concentrated hydrochloric acid. The resulting white precipitate was collected by suction

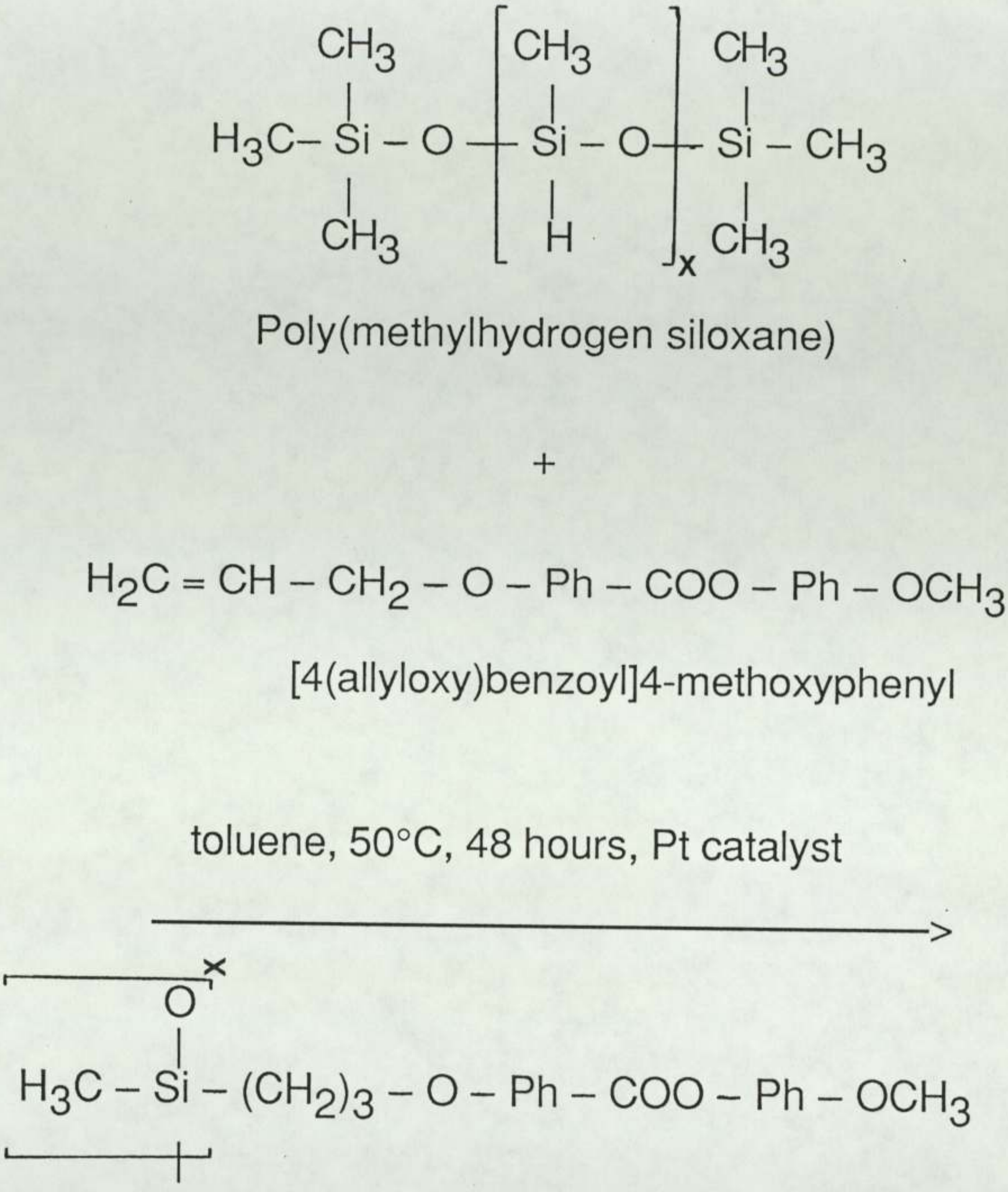

$H_3C-Si(CH_3)_2-O-[Si(CH_3)(H)-O]_x-Si(CH_3)_2-CH_3$

Poly(methylhydrogen siloxane)

+

$H_2C=CH-CH_2-O-Ph-COO-Ph-OCH_3$

[4(allyloxy)benzoyl]4-methoxyphenyl

$$\xrightarrow{\text{toluene, 50°C, 48 hours, Pt catalyst}}$$

$[-O-Si(CH_3)((CH_2)_3-O-Ph-COO-Ph-OCH_3)-]_x$

polymer liquid crystal

Figure (4-1) synthetic route to a polymer liquid crystal filtration and purified by twice recrystallising from ethanol. The reaction yielded 6.0g (67% of theoretical yield) of 4-allyloxybenzoic acid. The melting point was found to be 162°C, which is identical to the value measured by Ringsdorf and co-workers[90].

4.07: Synthesis of 4-Allyloxybenzoyl chloride.

0.05 moles (8.9g) of 4-allylyoxybenzoic acid, 0.075 moles of thionyl chloride (BDH) and two drops of freshly distilled dimethylformamide were reacted at room temperature until a clear solution remained. The solvents were removed under reduced pressure to leave the crude acid chloride as a pale yellow liquid.

4.08: Synthesis of [4(Allyloxy)benzoyl]4-methoxyphenyl.

The crude acid chloride was dissolved in 25cm^3 of dichloromethane (BDH) and the resulting solution was slowly added, in the absence of moisture, to a solution containing 0.05 moles (6.2g) of methoxyphenol (Aldrich Chem. Co. Ltd.) and 0.06 moles (6.2g) of triethylamine (BDH) in 100cm^3 of dichloromethane. The temperature was maintained below 5°C throughout the addition by use of an ice bath. Upon completion of the addition the mixture was stirred at room temperature for four hours and then refluxed for one hour. The solvent and excess triethylamine were then removed under reduced pressure and the solid thus obtained was dissolved in 100cm^3 of dichloromethane and filtered through 50cm^3 of 60-120 mesh silica gel (BDH). The silica gel was washed with an additional 100 cm^3 of dichloromethane and the filtrate and washings were combined. The solvent was removed under reduced pressure to leave the crude ester product, which was further purified by twice recrystallising from ethanol. The reaction yielded 7.1g of the aromatic ester (50% of the theoertical yield). The melting point of the ester was found to be 86°C. Previous workers have measured the melting point of this material and found it to be 89°C[89,91] and 90°C[92]. Elemental analysis gave the following results;

Calculated: C: 71.8% H: 5.6%

Found: C: 71.8% H: 5.8%

An infra red spectrum of the compound is shown in Figure (4-2). The absorption maxima at 1720cm^{-1} is characteristic of the carbonyl group in aryl esters. Absorption maxima arising from the aromatic groups are present at 1600cm^{-1} and 1420cm^{-1}

4.09: Stage 2- Attachment of the Mesogenic Group to a Polymer Backbone.

Chloroplatinic acid, $H_2PtCl_6 \cdot 6H_2O$, has for many years been the most commonly used catalyst for hydrosilations, a term used to describe the addition of an SiH bond to a C=C function. The catalyst, particularly when used in isopropanol, is commonly referred to as Speiers catalyst, in recognition of the part played by the American chemist J. L. Speier in the discovery of its usefulness and the interpretation of its action. Only a very small quantity is needed, the amount most commonly required being in the region of 10^{-5} moles of catalyst per mole of silicon hydride.

It is only recently however, that a (poly)hydrosilation reaction has been used to synthesise a side chain polysiloxane liquid crystal; Finkelmann and co-workers producing the first such examples in 1980. Since this initial success Finkelmann's work has been widely cited in the literature pertaining to polysiloxane liquid crystals. The polyhydrosilation reaction has also been investigated by Gray and co-workers at Hull university[98,99].

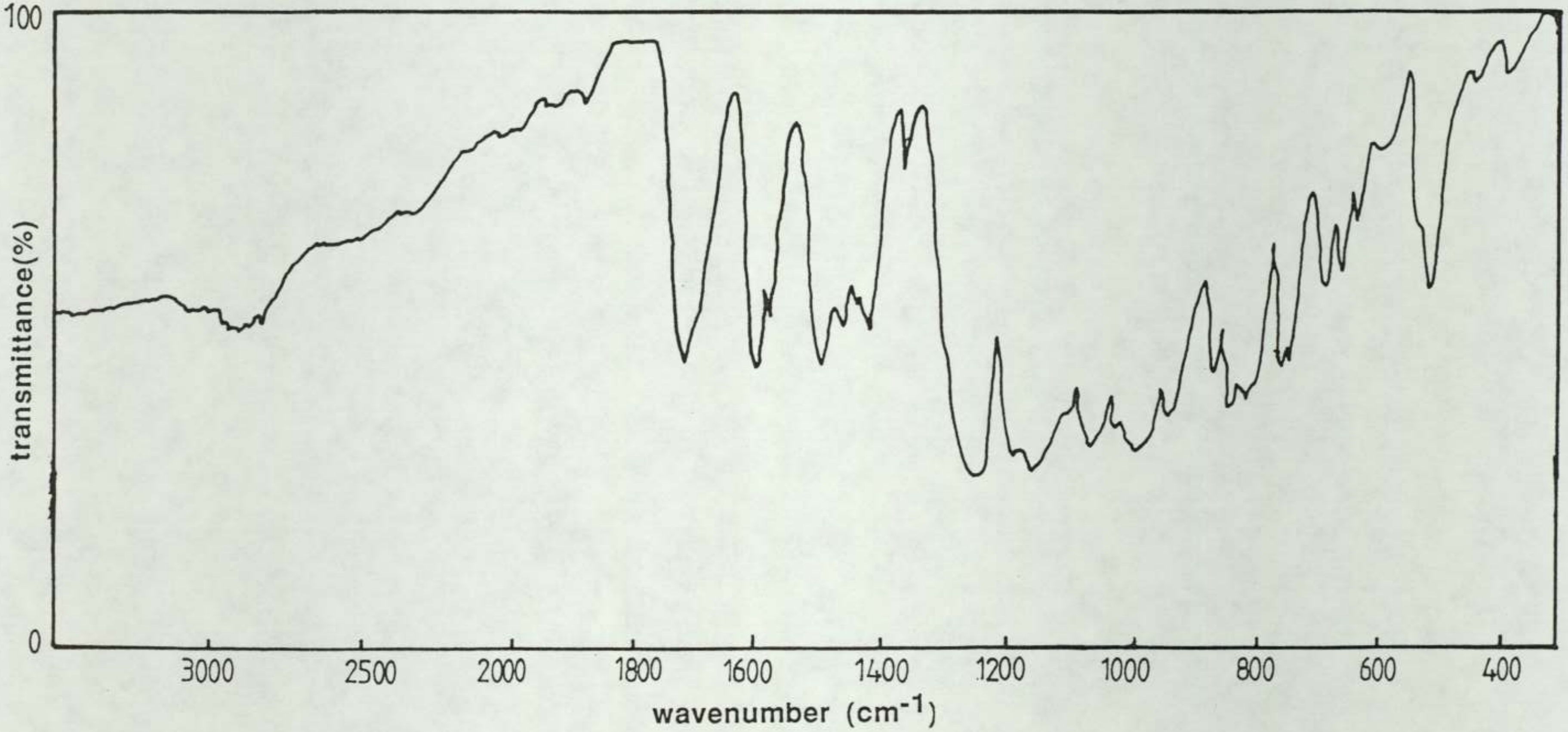

<u>Figure (4-2)</u> Infra-red spectrum of [4(allyloxy)benzoyl]4-methoxyphenyl

The polyhydrosilation method utilised in this study was as follows: 0.01 moles (2.84g) of the unsaturated compound containing the mesogenic side group and 0.008 moles (0.48g) of a poly(methyl hydrogen siloxane) [Dow Corning 1107] were added to 30cm^3 of freshly distilled toluene. Nitrogen gas was bubbled through the solution for twenty minutes after which two drops of the catalyst solution (10mg hexachloroplatinic acid (Aldrich Chem. Co. Ltd.) in 5cm^3 isopropanol (BDH)) were added. The reaction mixture was protected from moisture and heated at 50°C for 48 hours. The wet gel-like product was then twice precipitated from a small volume of methanol at room temperature.

The extent of the completion of the reaction was determined by infra red spectroscopy. This involved monitoring the peak area of the Si-H absorption, at 2140 cm^{-1}(Apfel and co-workers, in an earlier study[91], monitored the Si-H absorption at 2180 cm^{-1}), in the reaction mixture at t=0 hours and at t=48 hours. The relevant i. r. spectra are shown in Figure (4-3). From peak area measurements it was estimated that the reaction, after 48 hours, was approximately 75% complete, ie; 75% of the available Si-H bonds had reacted with a mesogenic group.

4-10: Differential Scanning Calorimetry.

DSC experiments were carried out on a Perkin Elmer DSC2 Differential Scanning Calorimeter. The resulting thermograms are shown in Figure (4-4). In addition, the clearing point of the sample was determined visually. The temperature range of the transition observed in this way agreed well with the phase transitions measured by D.S.C. These were;

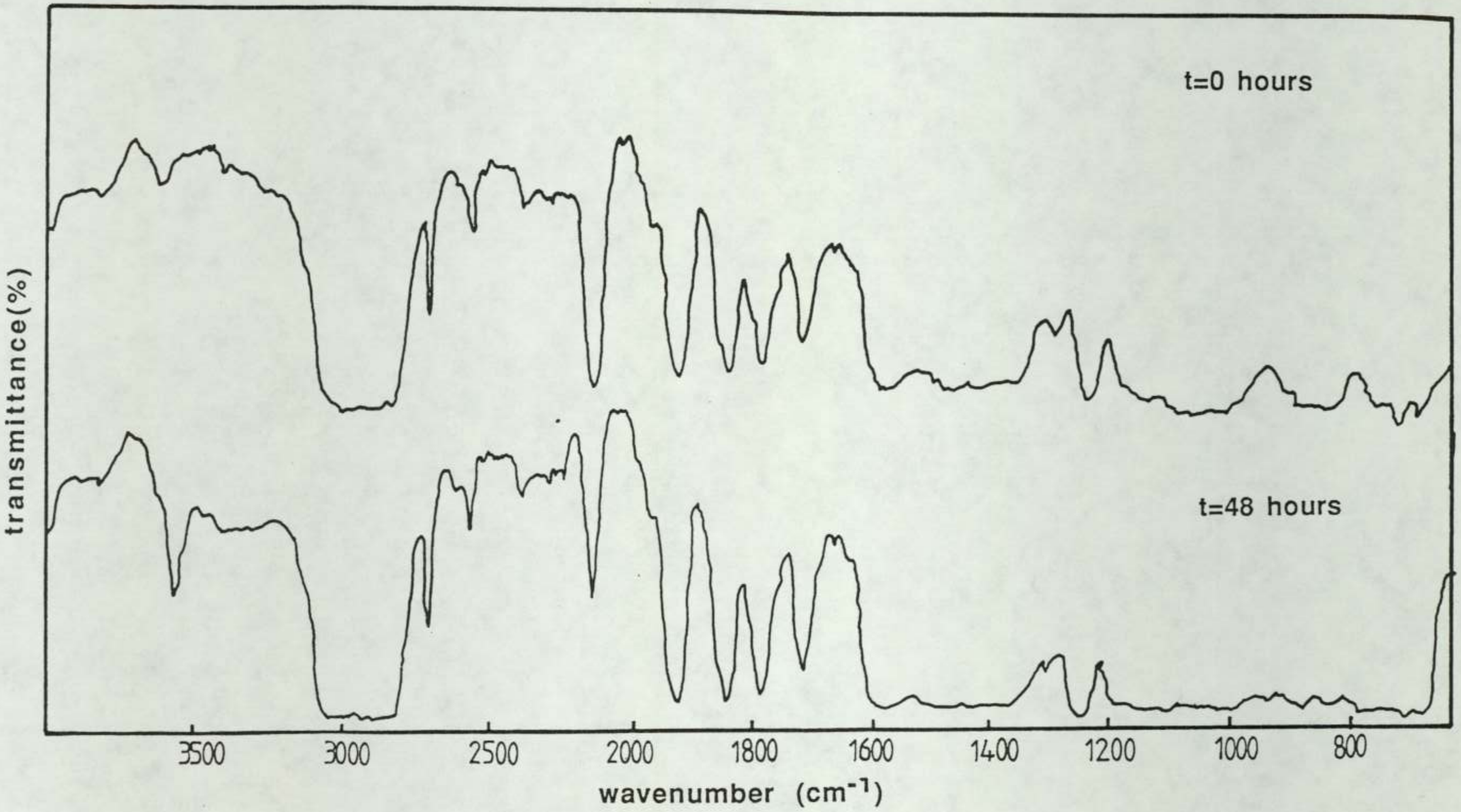

Figure (4-3) Infra-red spectra of PMHS + mesogenic group reaction mixture at t=0 hours and t=48 hours

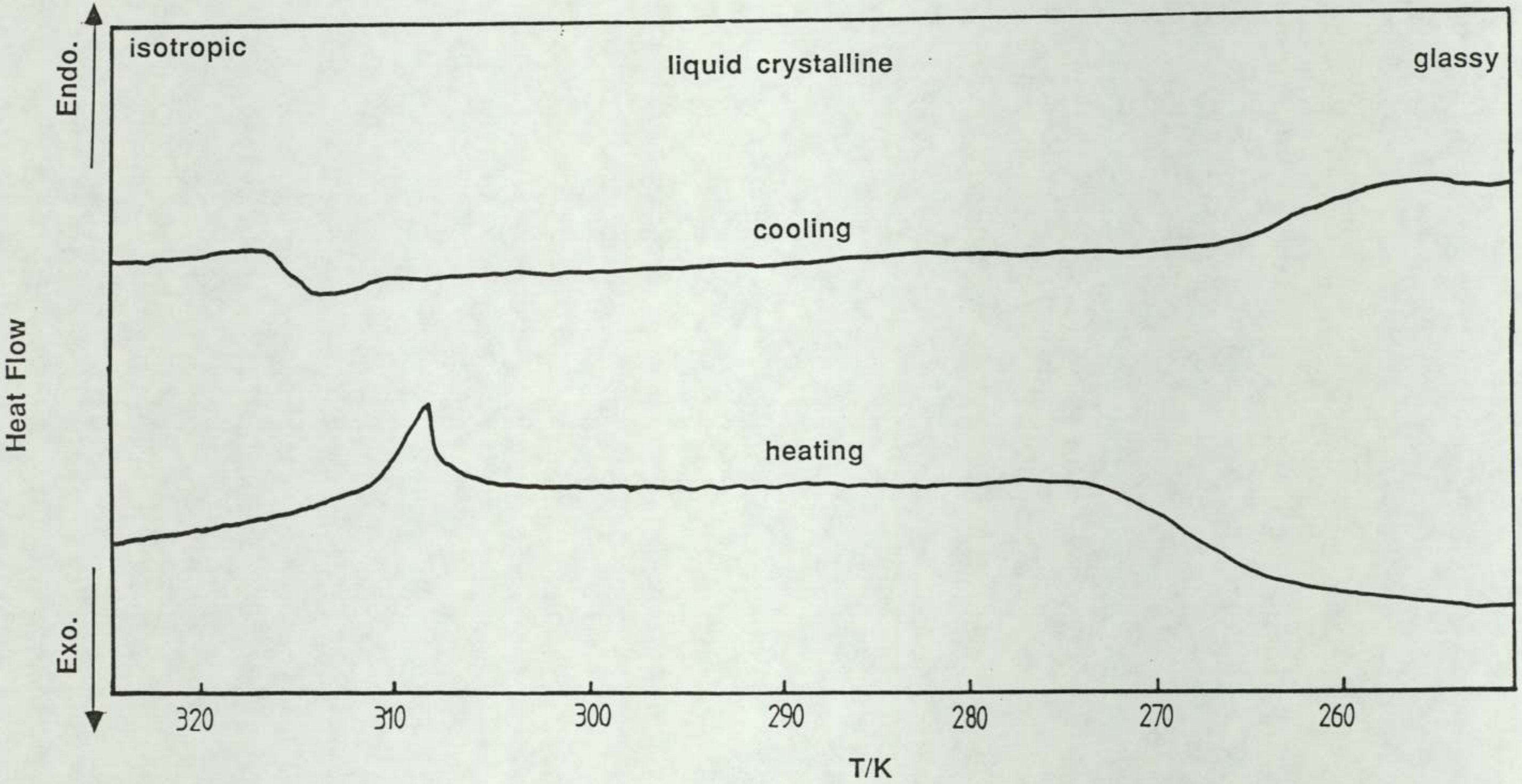

<u>Figure (4-4)</u> Differential scanning calorimetry curves for a polysiloxane liquid crystal [heating and cooling at 10K/min]

Heating: glassy–liquid crystalline; 262K-273K. LC–isotropic; 307K-312K

Cooling: isotropic–LC; 317K-313K liquid crystalline–glassy; 267K-257K

4.11: Synthesis of Poly(n-hexyl methyl siloxane).

A poly(hydrosilation reaction) reaction was carried out, under the same reaction conditions as above, using hex-1-ene in place of the mesogenic group. An analogous I.R. spectroscopy analysis indicated that, after 48 hours, the reaction was 50% complete. The relevant I.R. spectra are shown in Figure (4-5).

4-12: Gel Permeation Chromatography.

Gel permeation chromatography studies were carried out using a Perkin-Elmer Series 10 liquid chromatograph incorporating a Perkin-Elmer LC-85B spectrophotometric detector. The column was packed with Styragel and the solvent was tetrahydrofuran. The wavelength of detection was 254nm and the flow rate was 1ml/min.

G.P.C. chromatograms of the materials PMHS, the polymer liquid crystal and poly(n-hexyl methyl siloxane) are shown in Figures (4-6)-(4-8).

4-13: Synthesis and Characterisation of Poly(p-phenylene vinylene).

The first reported synthesis of poly(phenylene vinylene), general formula $C_nH_{[n-(2N-2)]}$, where n is the number of carbon atoms and N is the number of phenyl nuclei, was made by McDonald and Campbell in 1960[100]. The polymer was synthesised via the Wittig reaction. They estimated the degree of polymerisation(DP) to be 9. Hoeg and co-workers[101], in 1964, treated ω,ω-dichloro-p-xylene with sodium amide in liquid ammonia and obtained PPV with an estimated DP of 10. Ouchi[102], in 1966, claimed to have synthesised high molecular weight PPV by a Wurtz-Fittig type reaction . Rajarmann[103]

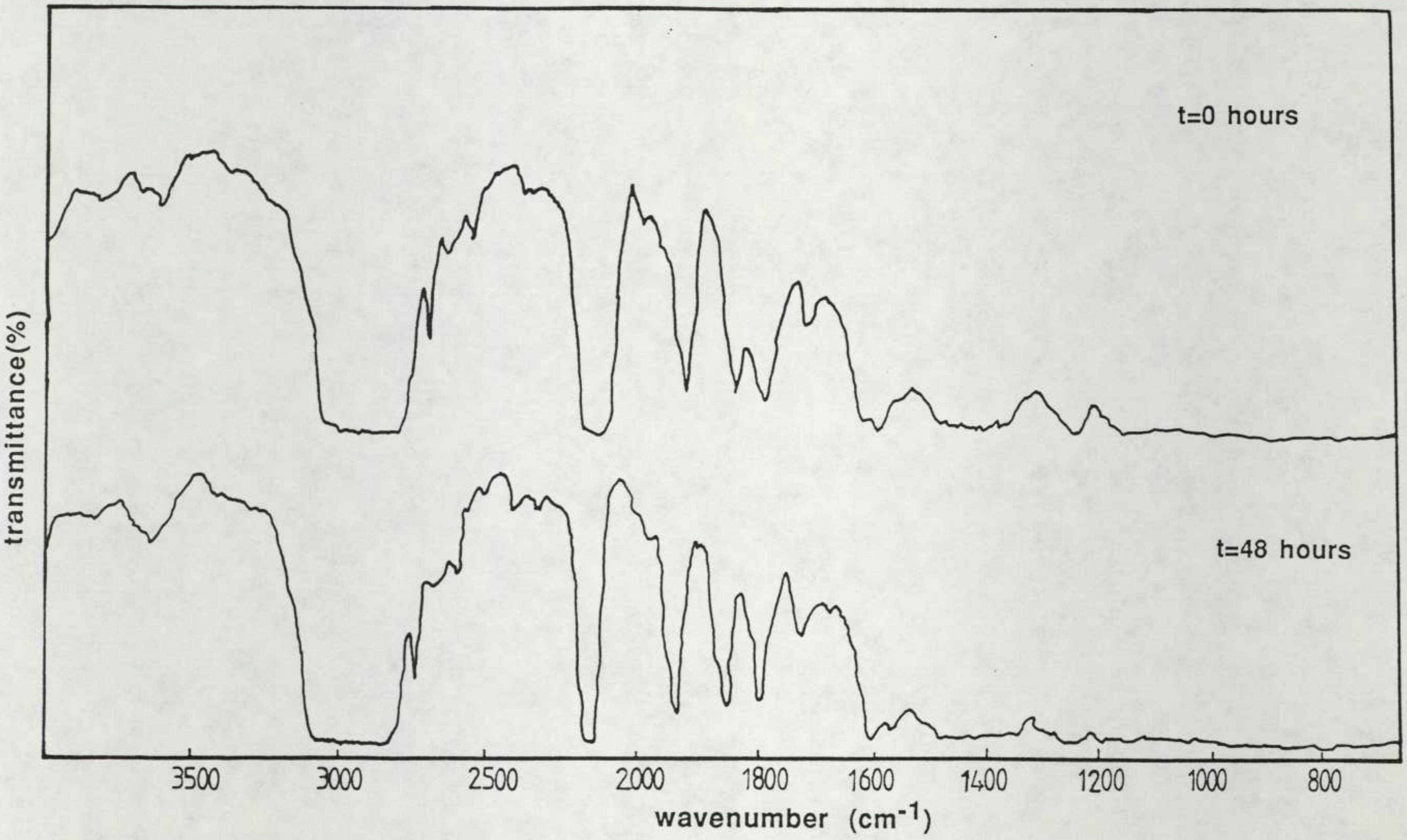

<u>Figure (4-5)</u> Infra red spectra of PMHS + hex-1-ene reaction mixture at t=0 hours and t=48 hours

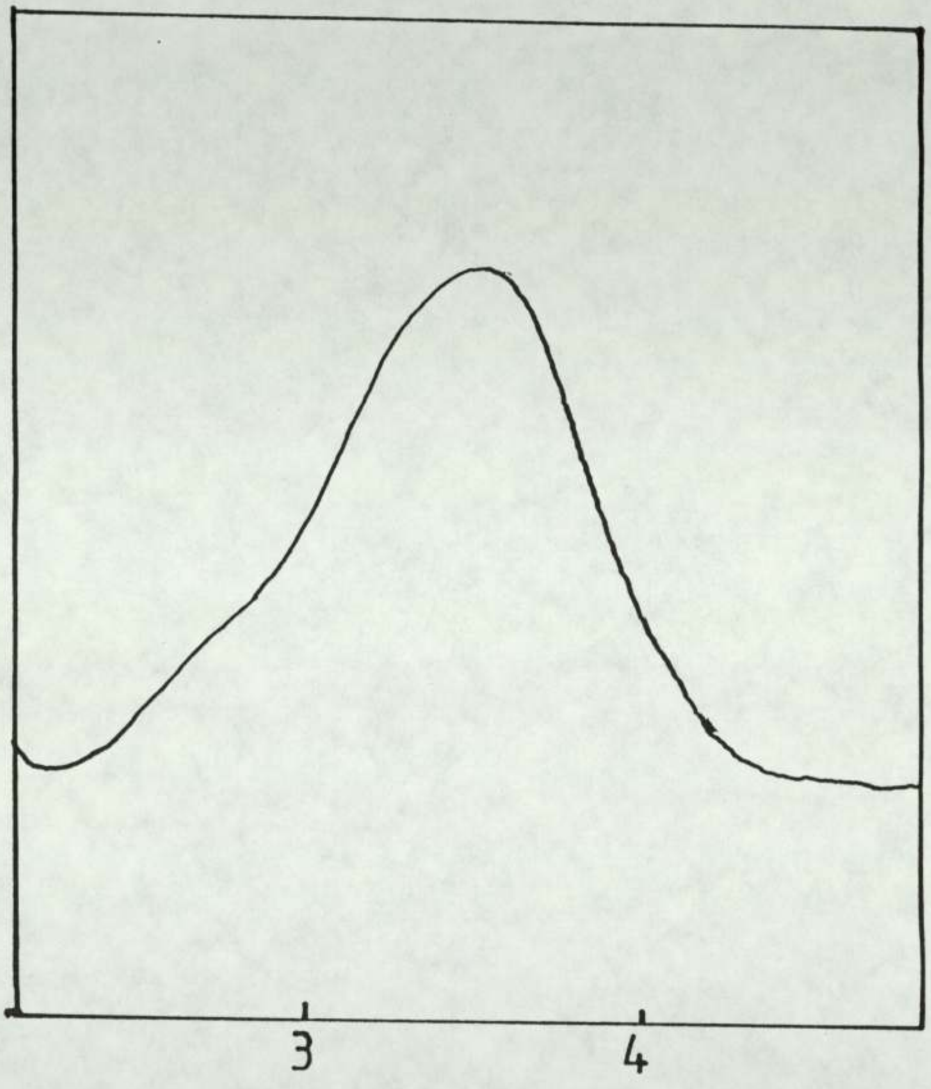

<u>Figure (4-6)</u> Gel permeation chromatograph of poly(methylhydrogen siloxane)

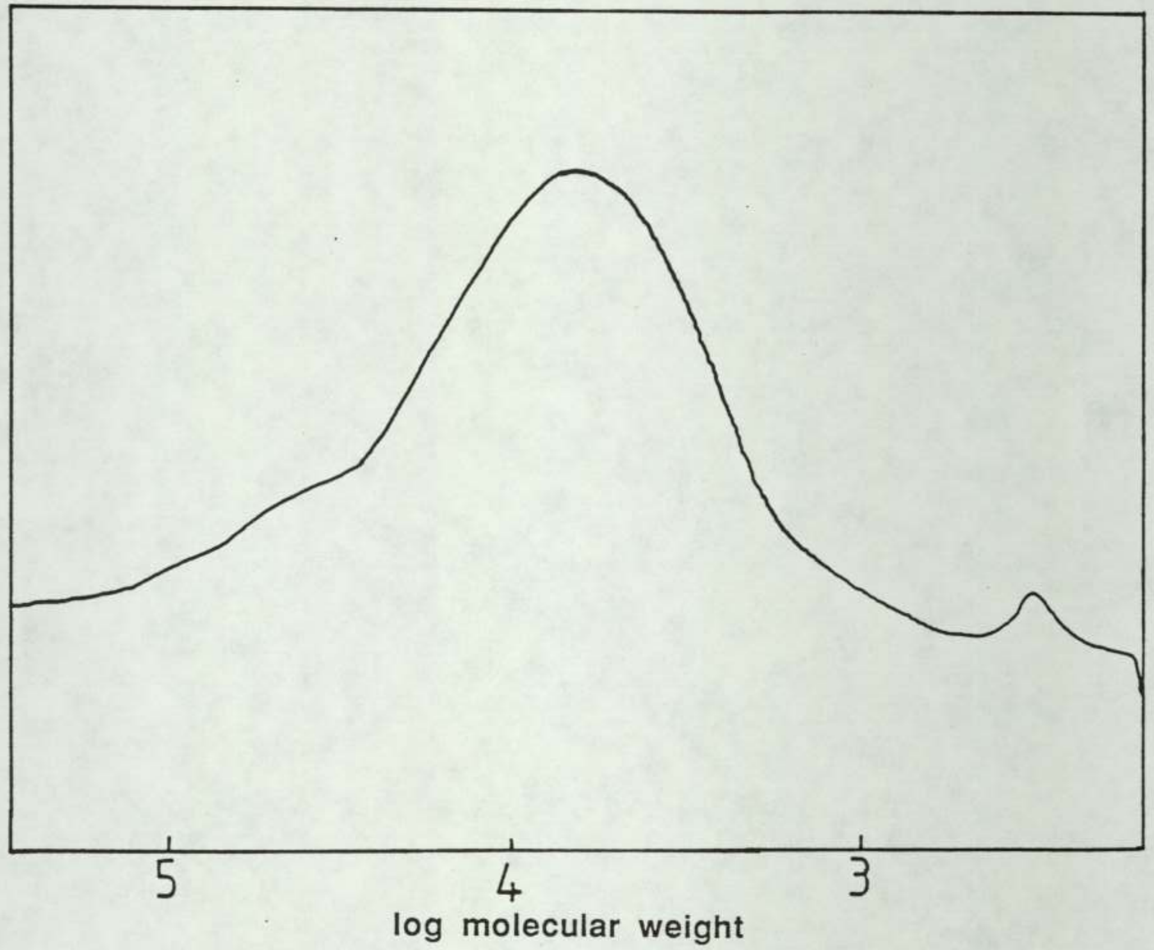

Figure (4-7) Gel permeation chromatograph of a polysiloxane liquid crystal

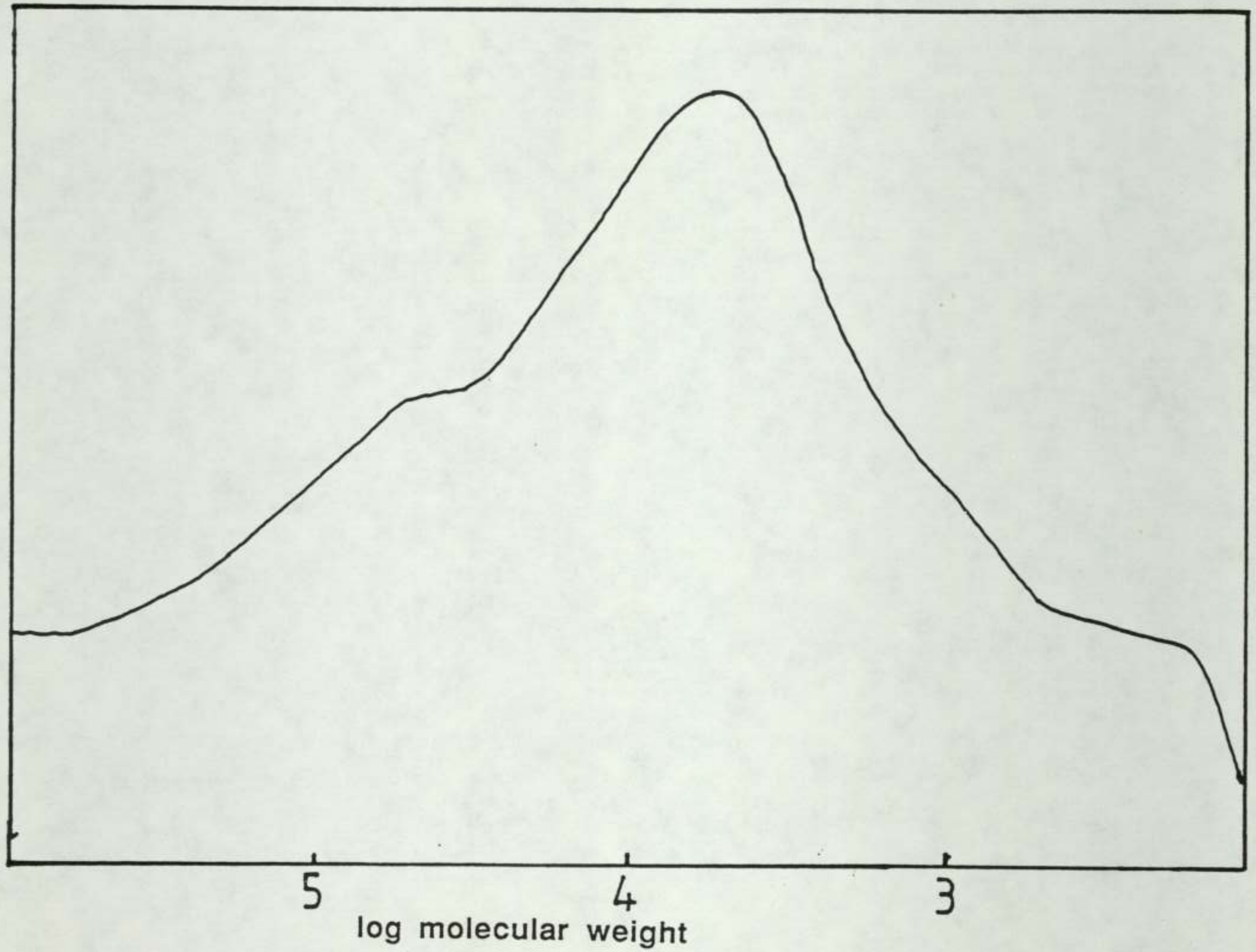

<u>Figure (4-8)</u> Gel permeation chromatograph of poly(n-hexyl methyl siloxane)

made use of a reductive coupling method, developed by MacMurray and co-workers[104], to synthesise the polymer in 1981.

In addition to the studies mentioned above, numerous other workers have been involved in synthesising PPV since 1964. The two most popular methods of preparation have been the Wittig reaction and the dehydrohalogenation of p-xylylidene dihalides[105]. A common drawback of these preparative methods is that they yield only infusible and insoluble oligomeric powders.

In 1984, the groups of Gagnon and Murase, using the methods developed by Wessling, Zimmerman[106] and Kanbe[107], starting from a water soluble precursor polymer, were able to prepare highly oriented, high molecular weight films of poly(p-phenylene vinylene).

In view of the potentially interesting electro-optical and electrical properties that may be exhibited by poly(p-phenylene vinlylene), a preparation of the polymer was undertaken for the purpose of studying such properties. The synthetic method chosen was a relatively simple condensation polymerisation using a methyl substituted aldehyde that was reported by Kossmehl and co-workers[108] in 1981. The procedure was as follows;

Potassium tert-butoxide and p-tolaldehyde were reacted in a mole ratio of 2:1, respectively, in solution in freshly distilled dimethylformamide, at 80°C for 20 hours. After this time the reaction mixture was cooled, distilled water was added, and the resulting product, a lemon-yellow powder, was collected and dried. The maximum yield achieved was ~40%. From this reaction, the expected molecular structure of the polymer is;

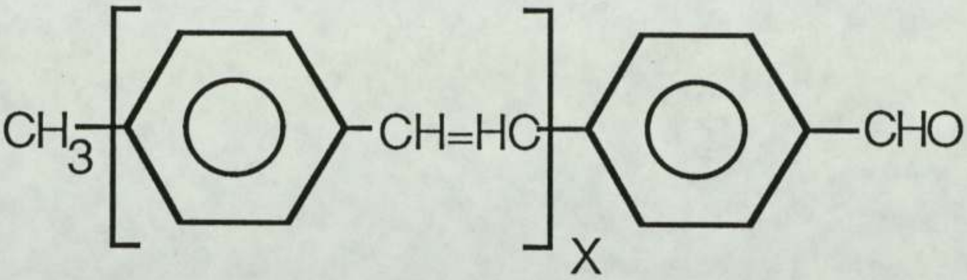

Poly(p-phenylene vinylene)

4-14: Separation of Oligomers of PPV.

The most efficient method of extracting oligomers of p-phenylene vinylene from the reaction product was found to be molecular distillation, carried out under high temperature and low pressure conditions. This was done using the apparatus shown in Figure (4-9). Two sharp fractions were obtained from the reaction product. The first fraction, (F1), pale yellow in colour, condensed onto the 'cold finger' in the temperature range 180°C-200°C. The second fraction, (F2), which was lemon yellow in colour, condensed onto the cold finger in the temperature range 300°C-320°C. Increasing the temperature steadily, over a period of hours, as high as 450°C, did not result in further fractionation. The residual polymer (P1) was coloured yellow/orange.

F1 and F2 were weakly soluble in most polar solvents, the solubility typically being <0.2%(w/v). The melting point of F1 was 165°C-167°C and the melting point of F2 was 290°C-293°C

An attempt was made to determine molecular weight using vapour pressure osmometry.The poor solubility of the polymer and oligomers prevented an accurate determination. The polymer and oligomers were characterised using

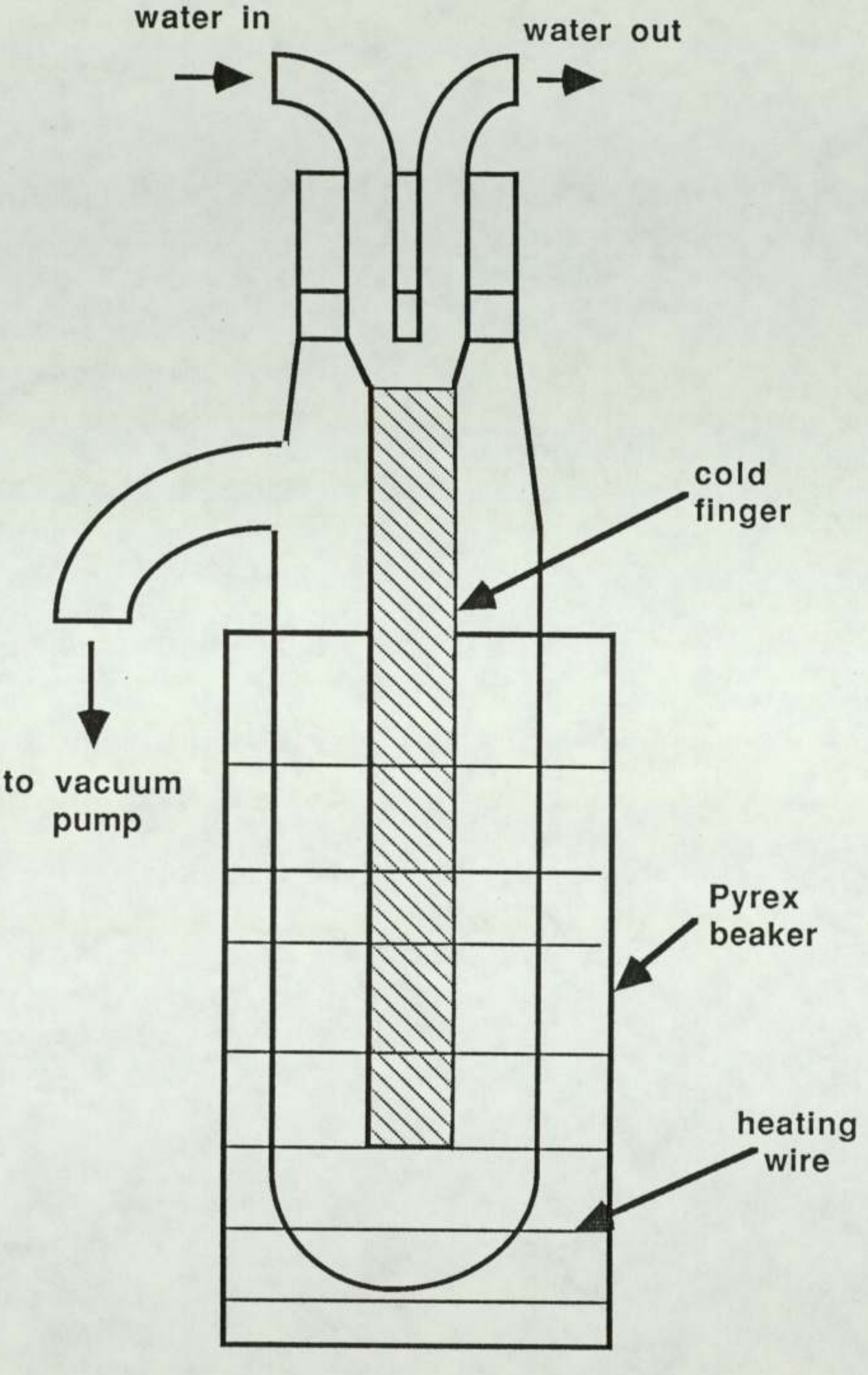

Figure (4-9) Molecular distillation apparatus

I.R. and U.V. spectroscopy, elemental analysis, gel permeation chromotography and solid state NMR.

4.15: Infra-red spectroscopy.

Infra-red spectroscopy was carried out on the reaction product, in the form of a KBr disc, using a Perkin-Elmer 599 Infra-Red Spectrophotometer. The spectrum is shown in Figure (4-10).

The spectrum exhibits absorption maxima at 820cm^{-1}(arising from para-disubstituted benzene rings), 960cm^{-1}(arising from trans-ethylenic unsaturation), 1580cm^{-1}(arising from ethylenic bonds conjugated with aromatic rings), 1680cm^{-1}(arising from aldehydic end groups) and 3000cm^{-1}(arising from methyl end groups).

4-16:Elemental Analysis.

Theoretically, the data from elemental analysis should provide infomation pertinant to the molecular weight problem. Practically, however, the disadvantage of this approach is that the values of the C/H atomic ratios for different chain lengths of poly(phenylene vinylene) are experimentally indistinguishable. The theoretical C/H atomic ratio of an oligomer of phenylene vinylene with x=1 is 1.14, while for an oligomer with x=2, the ratio is 1.19. The limiting value of the theoretical C/H atomic ratio for an infinitely long poly(phenylene vinylene) chain is 1.33.

The elemental analysis results for F1, F2 and the residual polymer(P1) are presented below;

F1:	Calculated for x=1:	C: 86.5%	H: 6.3%
	Found:	C: 84.8%	H: 6.5%

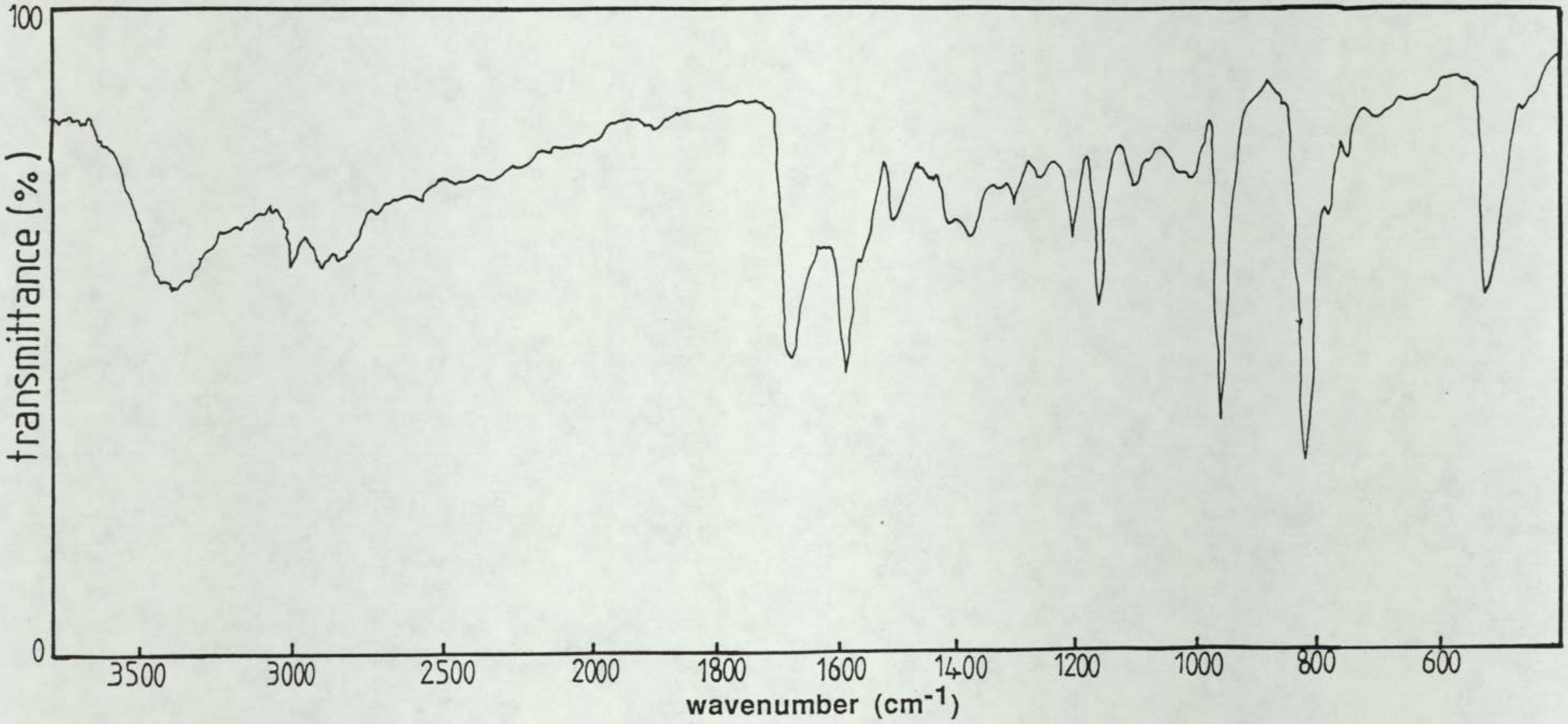

<u>Figure (4-10)</u> Infra red spectrum of poly(p-phenylene vinylene)

F2: Calculated for x=2: C: 88.9% H: 6.2%
Found: C: 87.2% H: 6.4%
Residual polymer: Found: C: 89.9% H:6.1%

The experimental C/H atomic ratios for F1, F2 and P1 are 1.09, 1.14 and 1.20, respectively.

4-17: Gel Permeation Chromotography.

Gel permeation chromotography studies were carried out using an ACS-HPLC 300 pump incorporating an ACS-HPLC Monitor 750-11 detector and a custom built glass column. The column was packed with Sephadex LH-20 and the solvent was chloroform. Detection was at 254nm and the flow rate was 2ml/min. A gel permeation chromatograph of a solution of F1, F2 and p-tolaldehyde in chloroform is shown in Figure (4-11). Individual peaks were identified from GPC studies on the single components. A plot of the logarithm of the molecular weight of F1 (assuming x=1), F2 (assuming x=2) and p-tolaldehyde is shown in Figure (4-12). Also included on the plot is a data point corresponding to the logarithm of the molecular weight for an oligomer with x=3. This peak is indicated in Figure (4-11) by an arrow.

The plot produced an approximate straight line, indicating that p-tolaldehyde, F1 andF2 belong to an homologous series of compounds.

4-18: Ultra-Violet Spectroscopy.

U.V. spectra of F1, F2 and P1 were obtained using a Pye-Unicam SP 800B. The spectra is shown in Figure (4-13). The solvent for F1 and F2 was chloroform. The P1 spectrum was obtained by a reflectance method.

Figure (4-11) Gel permeation chromatograph for F1, F2 and p-tolaldehyde in chloroform

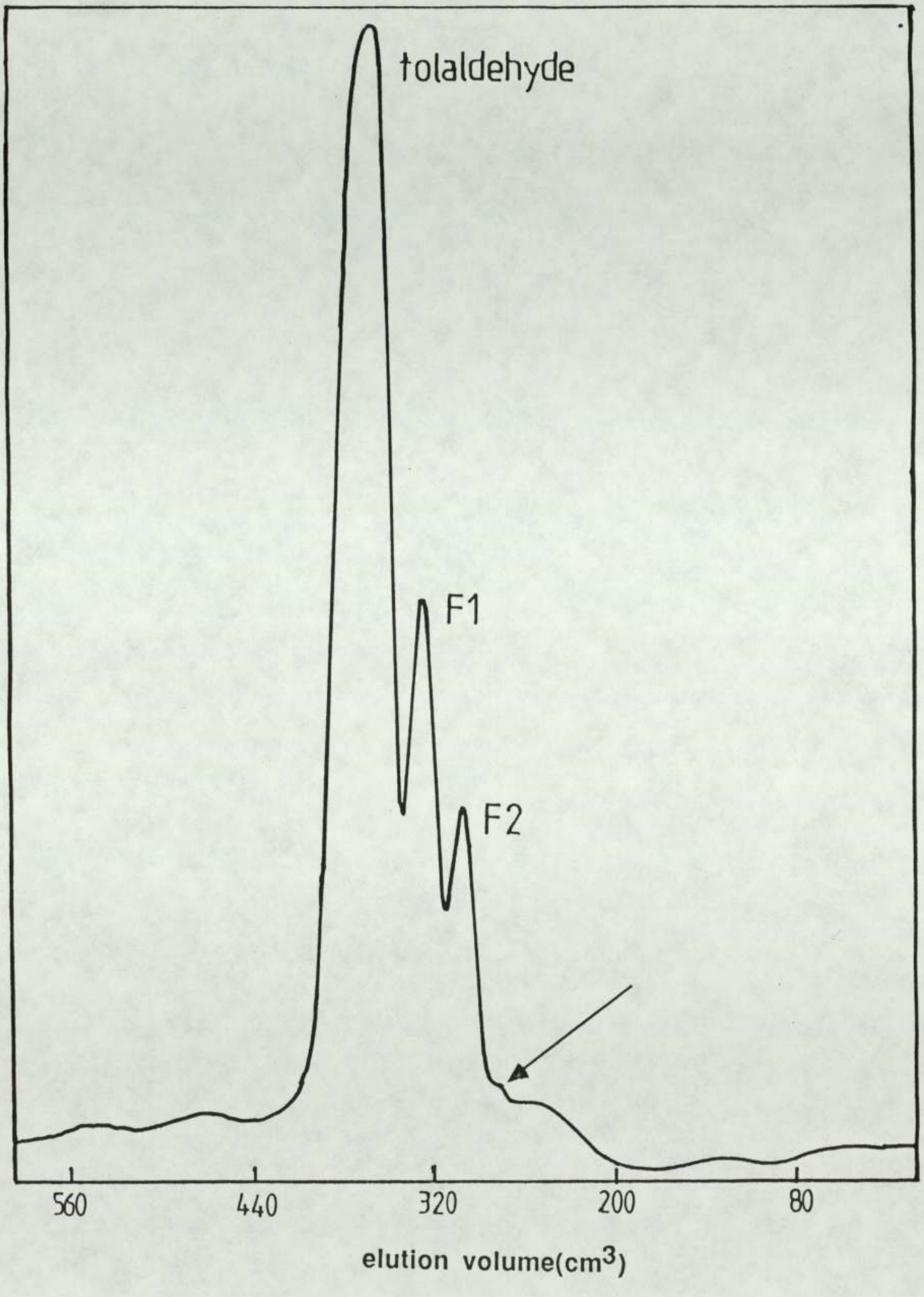

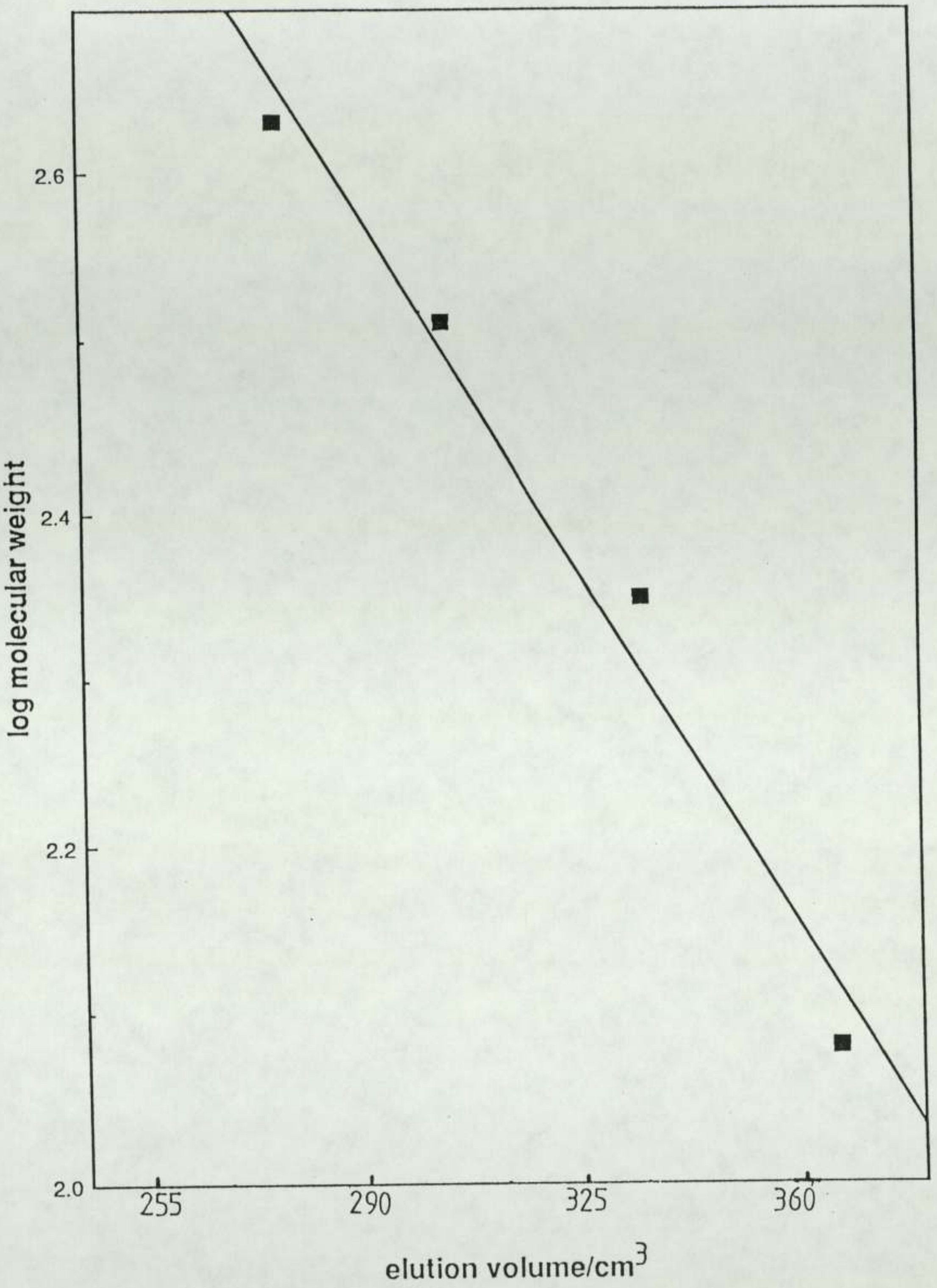

Figure (4-12) Plot of log molecular weight against elution volume for F1, F2 and p-tolaldehyde in chloroform

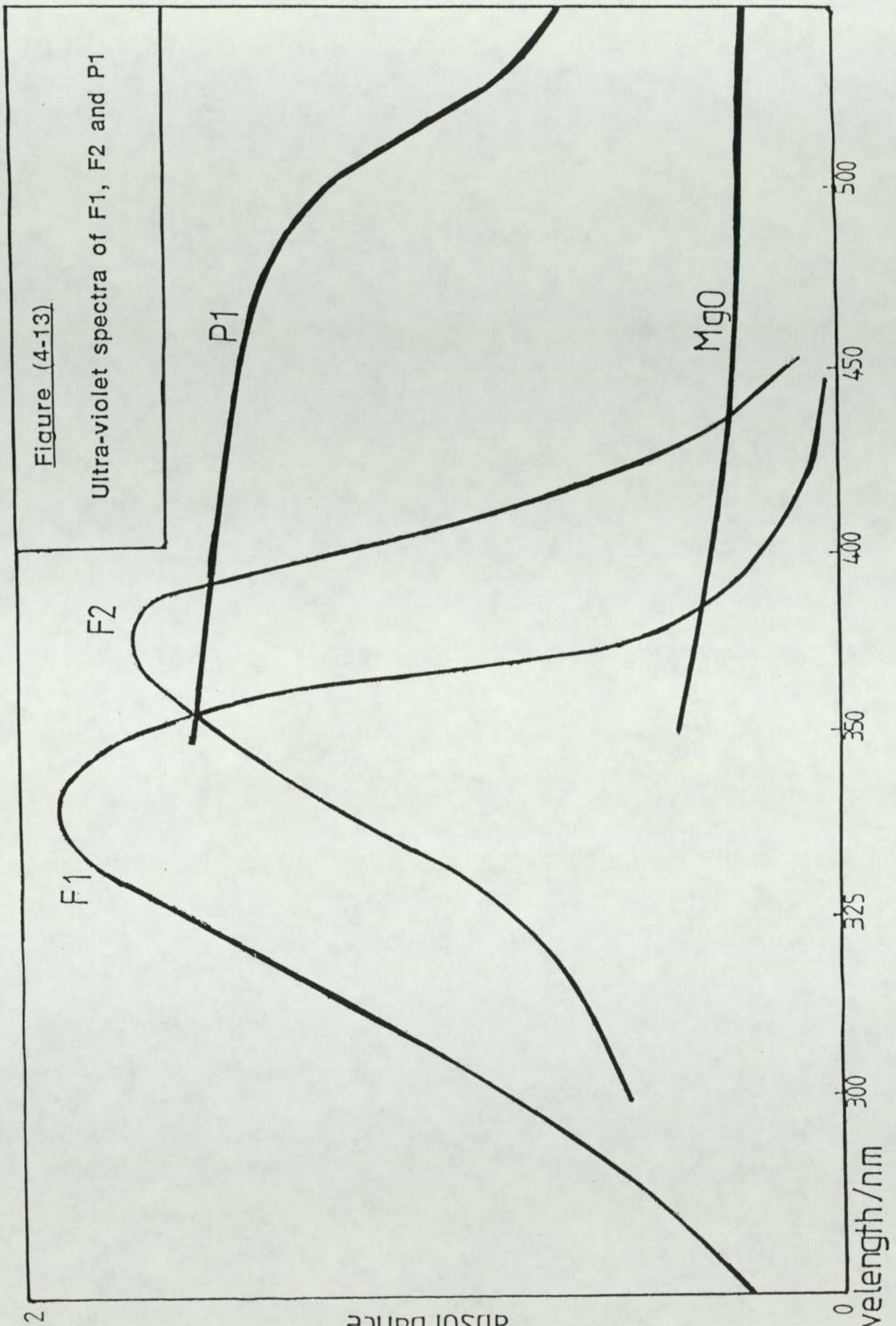

Figure (4-13)

Ultra-violet spectra of F1, F2 and P1

The position of λ_{max} for F1 is at 337nm, while for F2 λ_{max} is positioned at 375nm. The position of λ_{max} for P1 is shifted to wavelengths >450nm.

The form of the P1 spectrum conceals any discrete absorption maxima that are present. F1 and F2 would appear to consist mainly of a single component. An increase in conjugation (i.e. P1>F2>F1) would account for the shift in λ_{max} towards higher wavelengths.

4-19: Solid State Nuclear Magnetic Resonance Spectroscopy.

A solid state ^{13}C NMR spectrum of the reaction product was obtained using a Bruker AC 300 NMR spectrophotometer. The spectrum is shown in Figure (4-14). The peaks were assigned with the aid of reference 109.

Overall, the evidence presented in 4-15 to 4-19 indicates that poly(p-phenylene vinylene) has been synthesised, via a polycondensation reaction, and that F1 and F2 are low molecular weight members of an homologous series.

For the purposes of the following Kerr effect calculations requiring a knowledge of molecular weights, F1 will be assigned an x value equal to one and F2 will be assigned an x value equal to two., where x is the number of repeat units of p-phenylene vinylene.

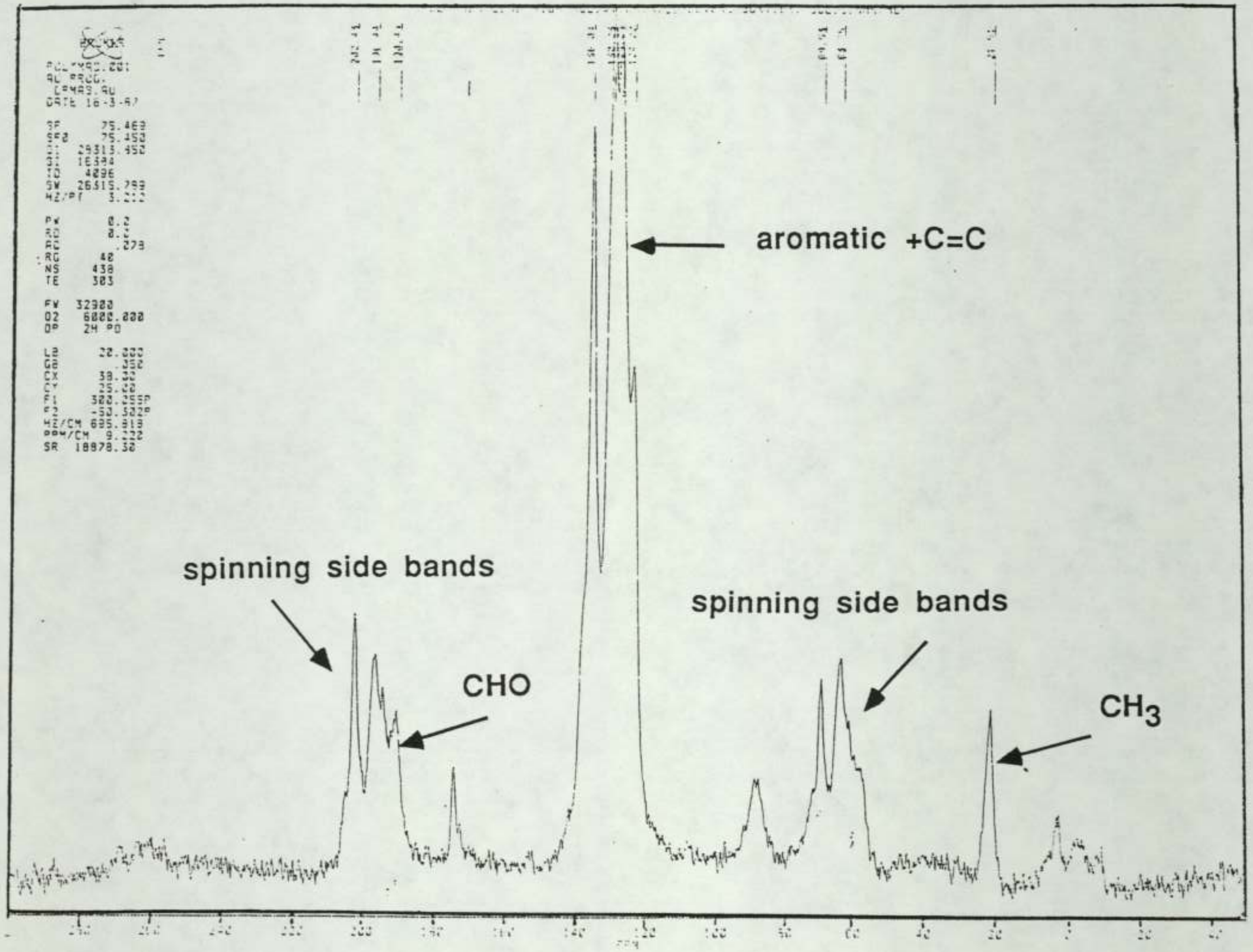

Figure (4-14) Solid state n.m.r. spectrum of P1

CHAPTER 5.

DIELECTRIC RESULTS.

5.01: Dielectric Properties of Cyclic and Linear Poly(dimethyl siloxanes)(PDMS).

The dielectric relaxation behaviour of a series of undiluted cyclic poly(dimethyl siloxanes) and a series of linear poly(dimethyl siloxanes) has been measured, as a function of temperature (142.0K-157.5K) and frequency (12-10^5Hz), using the dielectric apparatus described in Chapter 3.

5.02: The Dielectric Loss Results.

The variation of $C_p \tan\delta$, where C_p is the parallel capacitance and $\tan\delta$ is the dissipation factor, with respect to log (f/Hz), at various temperatures, is shown as a series of normalised plots, for the cyclic and linear PDMS fractions, in Figures (5-1) to (5-10).

The presence of a broad α-type relaxation process for cyclics and linears is readily discernible. The loss curves are asymmetric, showing broadening on the high frequency side which is typical of the behaviour found for the α-relaxation process in organic amorphous polymers above T_g[110]. The movement of $f_{(max)}$, which is the frequency corresponding to maximum loss, within the frequency range 12-10^5Hz, occurs over a relatively small temperature interval for both cyclic and linear fractions of PDMS, this interval not exceeding 10K. For the cyclic fractions the temperature interval is shifted approximately 6K towards higher temperatures, ie; for cyclic PDMS fractions and linear PDMS fractions of similar molecular size, the cyclics move more slowly

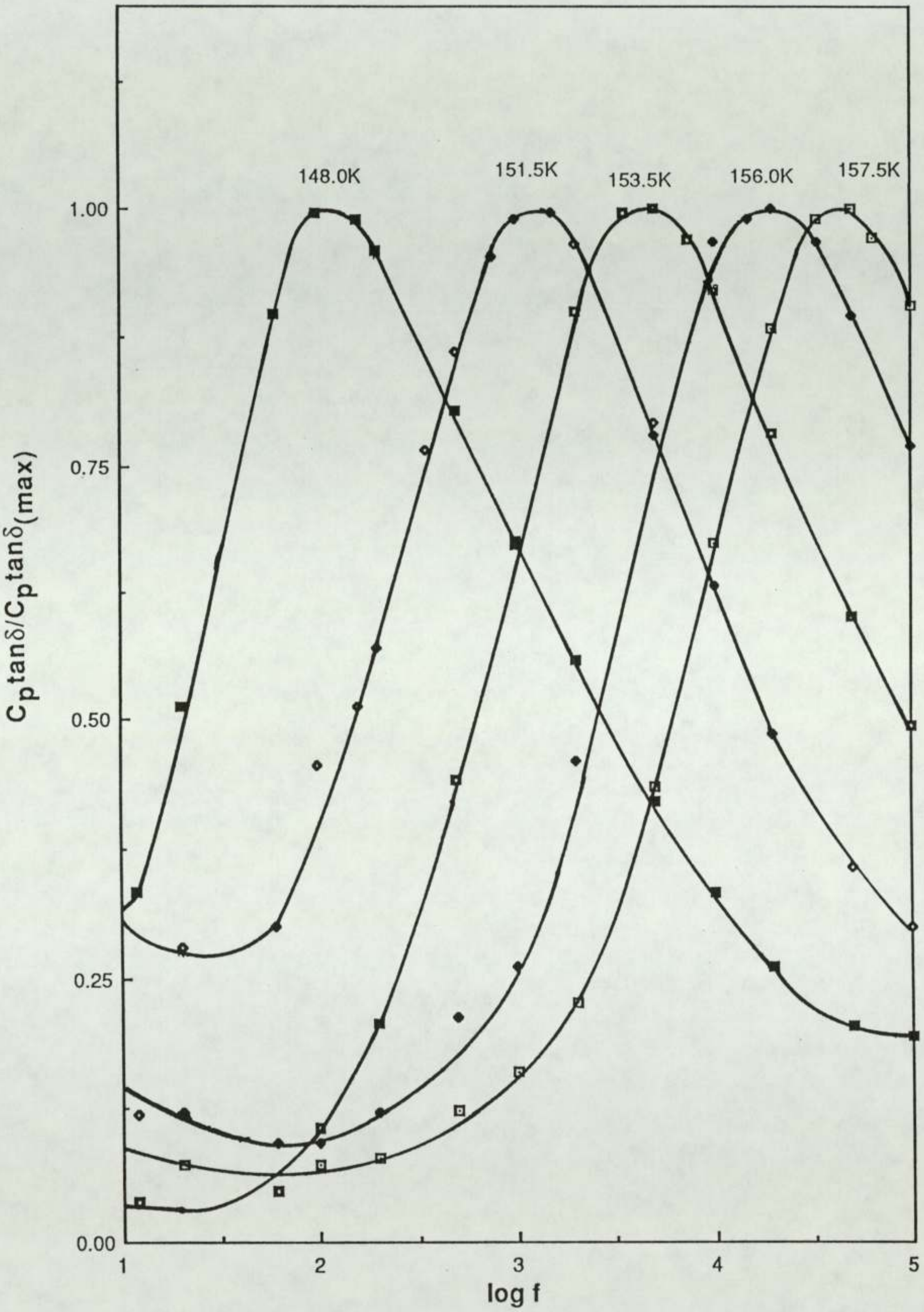

Figure (5-1). Frequency dependence of $C_p\tan\delta/C_p\tan\delta_{(max)}$ for cyclic PDMS with $\bar{n}_n$=28 at various temperatures.

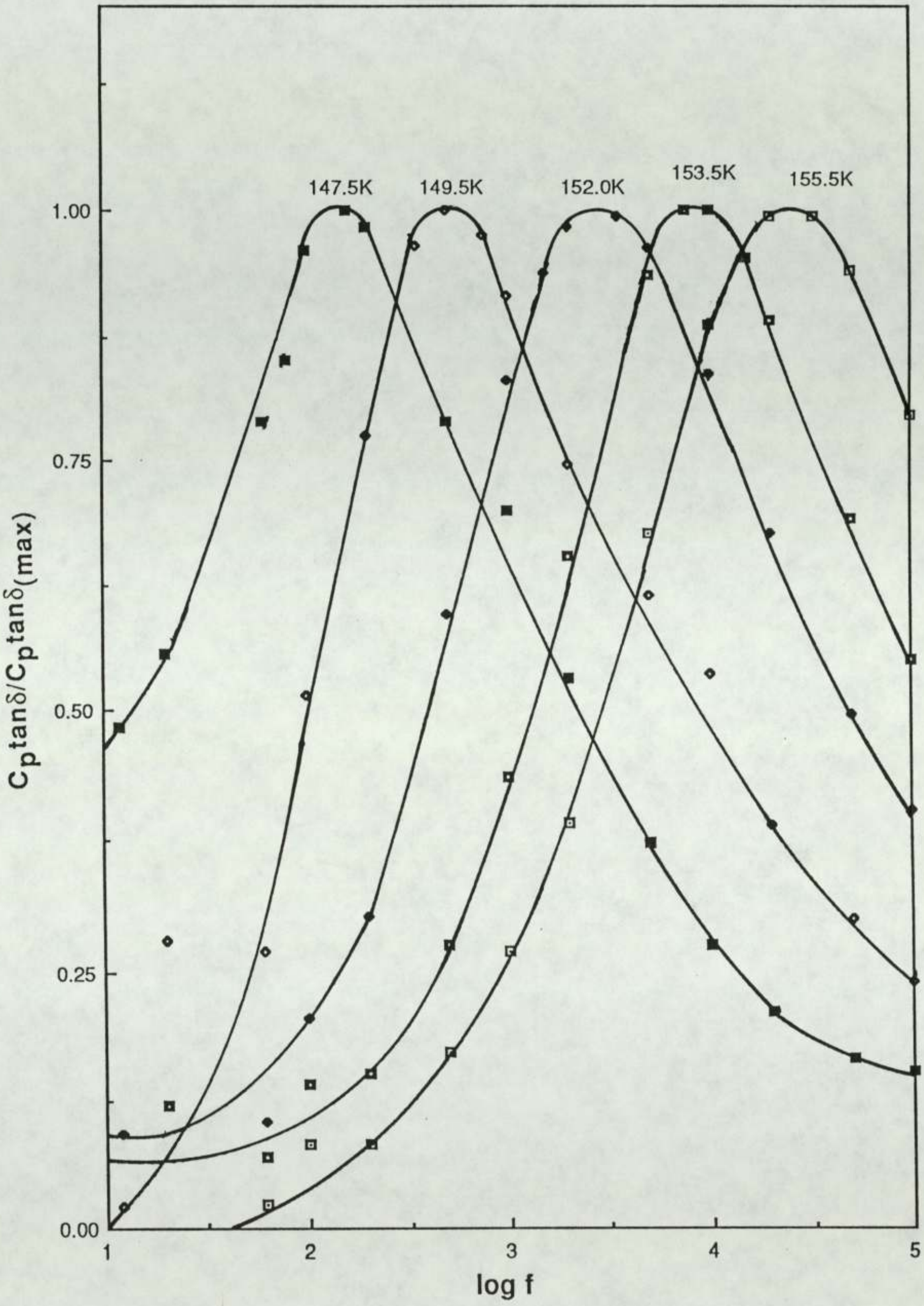

Figure (5-2). Frequency dependence of $C_p\tan\delta/C_p\tan\delta_{(max)}$ for cyclic PDMS with $\bar{n}_n$=35 at various temperatures.

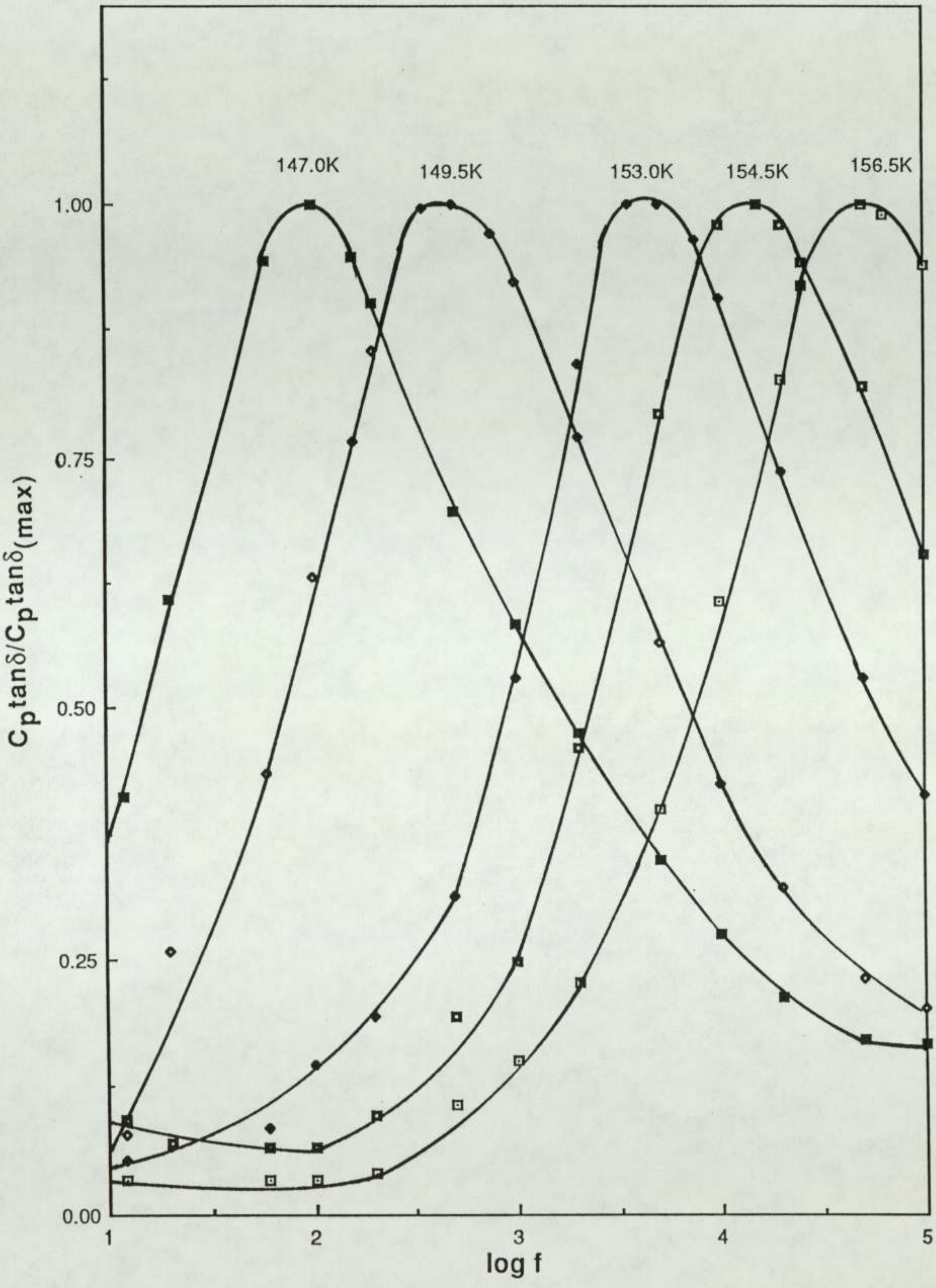

Figure (5-3). Frequency dependence of $C_p\tan\delta/C_p\tan\delta_{(max)}$ for cyclic PDMS with $\bar{n}_n$=50 at various temperatures.

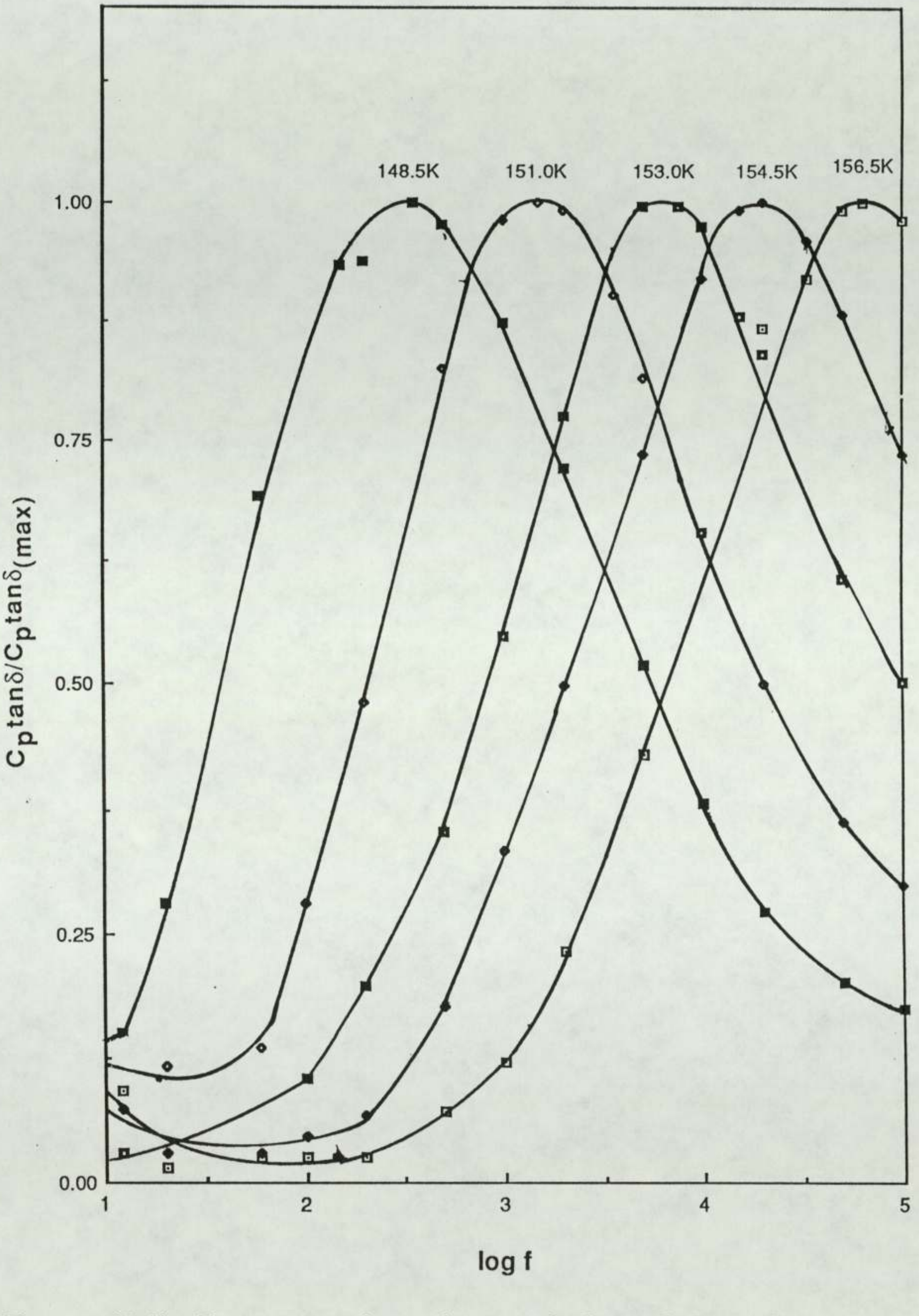

<ins>Figure (5-4)</ins>. **Frequency dependence of $C_p\tan\delta/C_p\tan\delta_{(max)}$ for cyclic PDMS with $\bar{n}_n$=66 at various temperatures.**

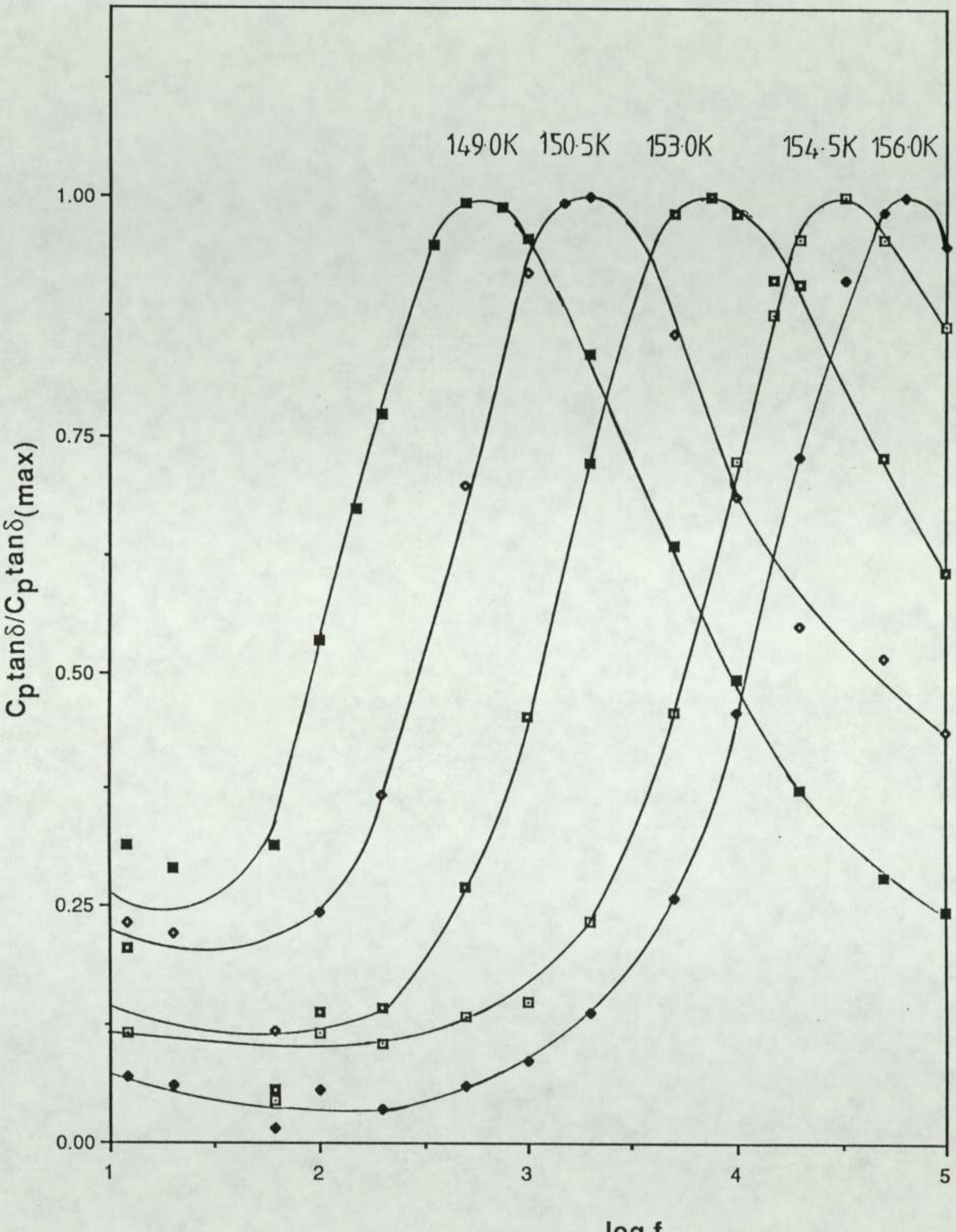

Figure (5-5). Frequency dependence of $C_p \tan\delta / C_p \tan\delta_{(max)}$ for cyclic PDMS with $\bar{n}_n$=99 at various temperatures.

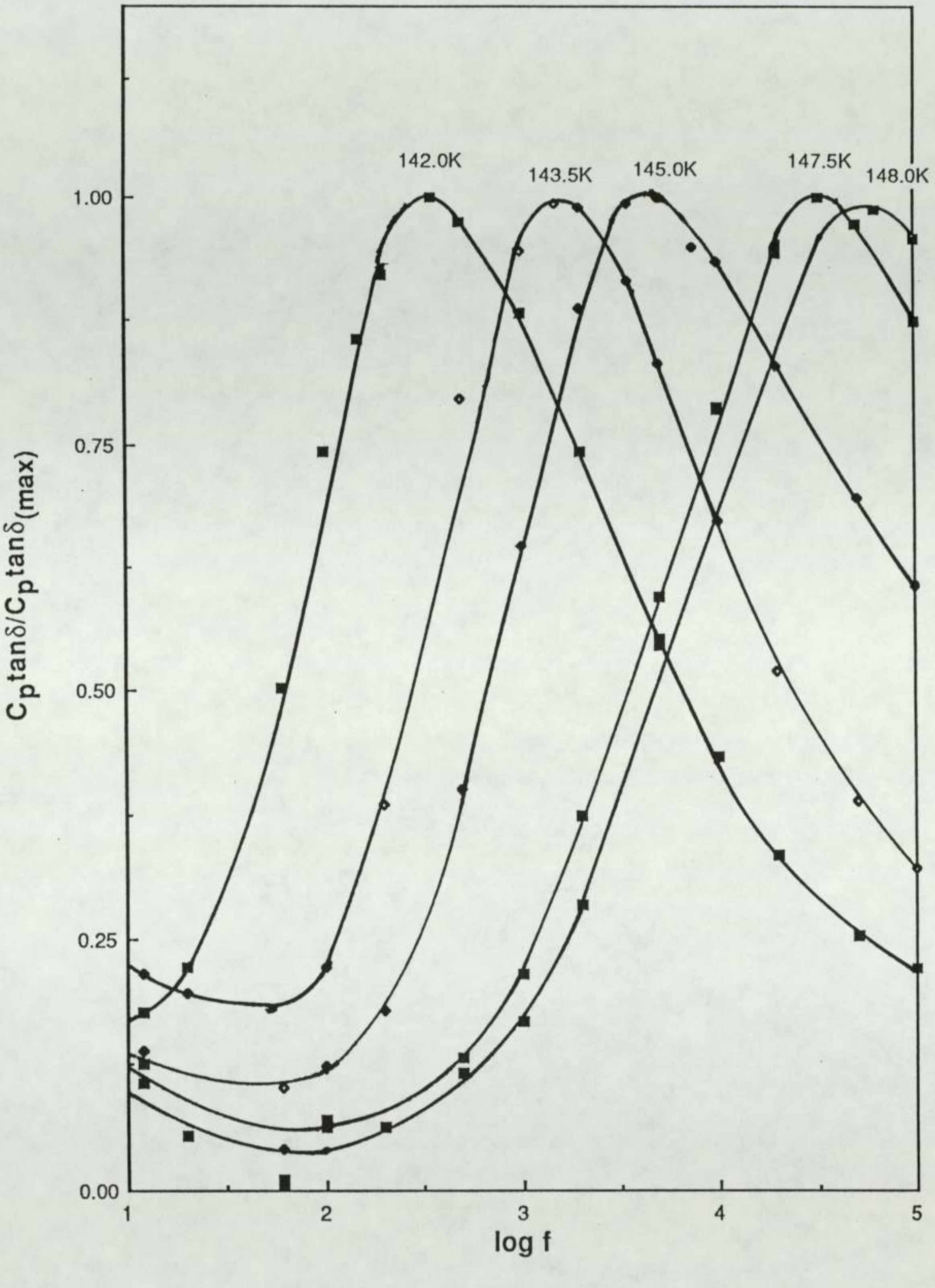

Figure (5-6). Frequency dependence of $C_p \tan\delta / C_p \tan\delta_{(max)}$ for linear PDMS with $\bar{n}_n$=28 at various temperatures.

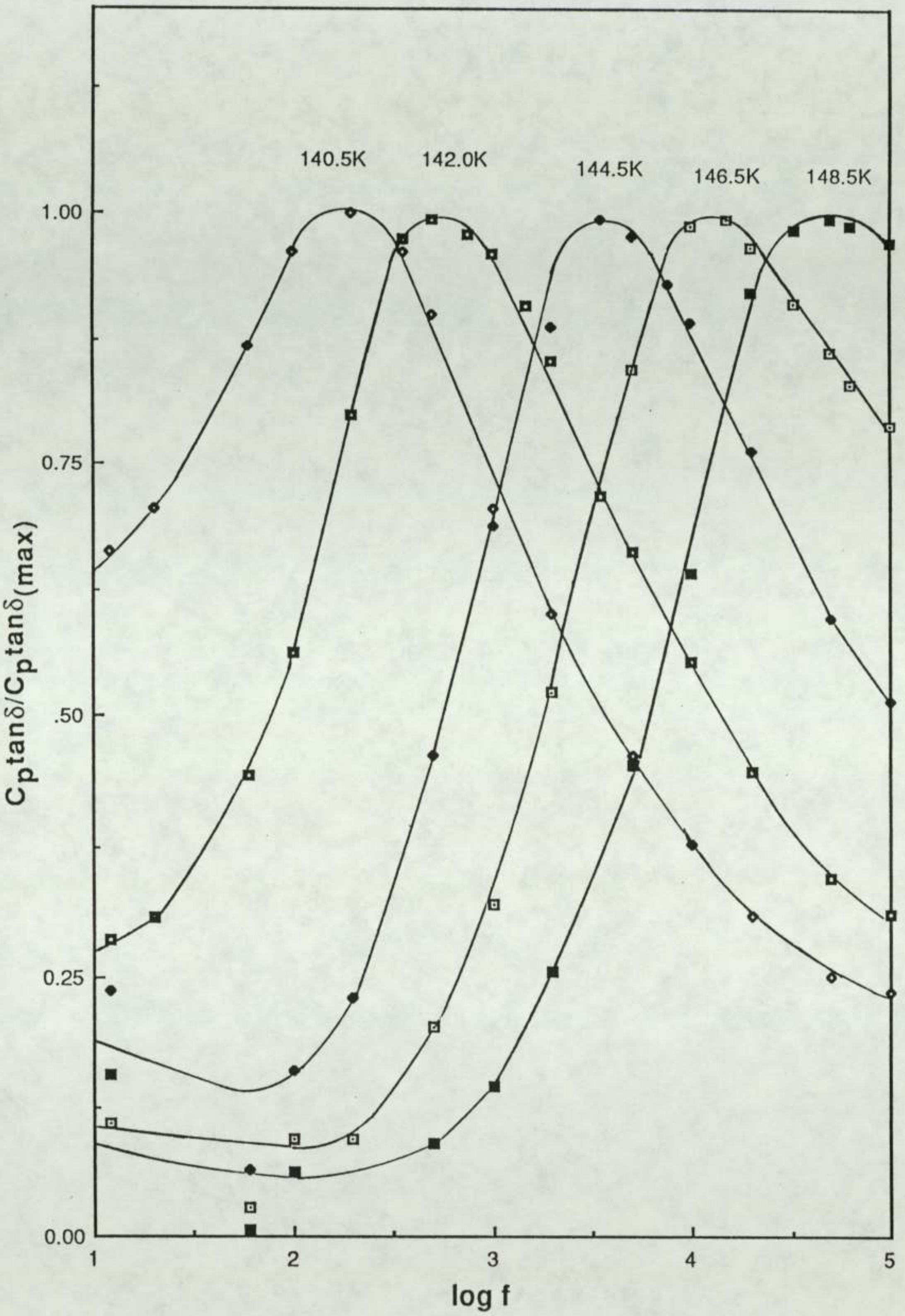

Figure (5-7). Frequency dependence of $C_p\tan\delta/C_p\tan\delta_{(max)}$ for linear PDMS with $\bar{n}_n$=34 at various temperatures.

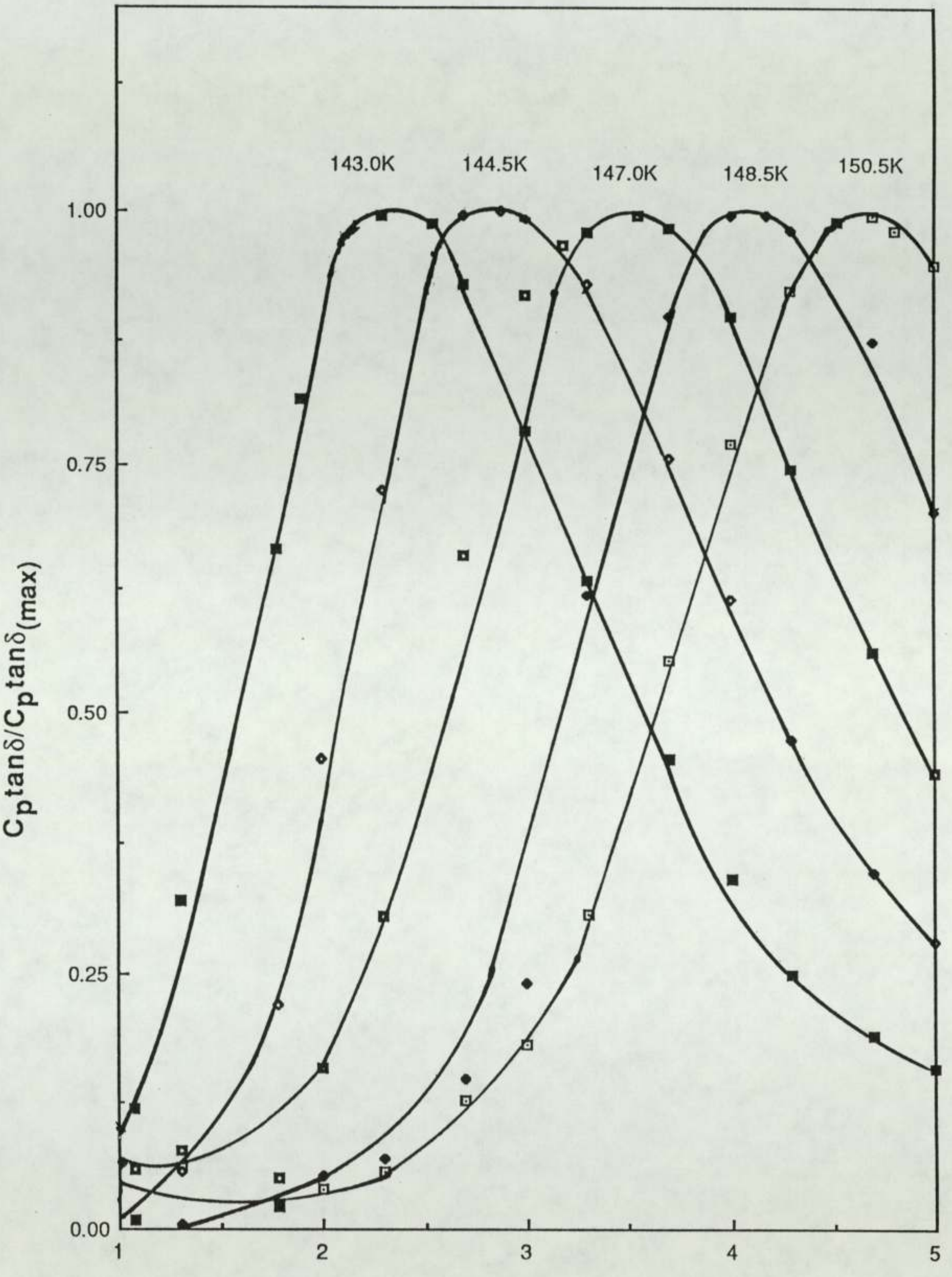

Figure (5-8). Frequency dependence of $C_p \tan\delta / C_p \tan\delta_{(max)}$ for linear PDMS with $\bar{n}_n$=57 at various temperatures.

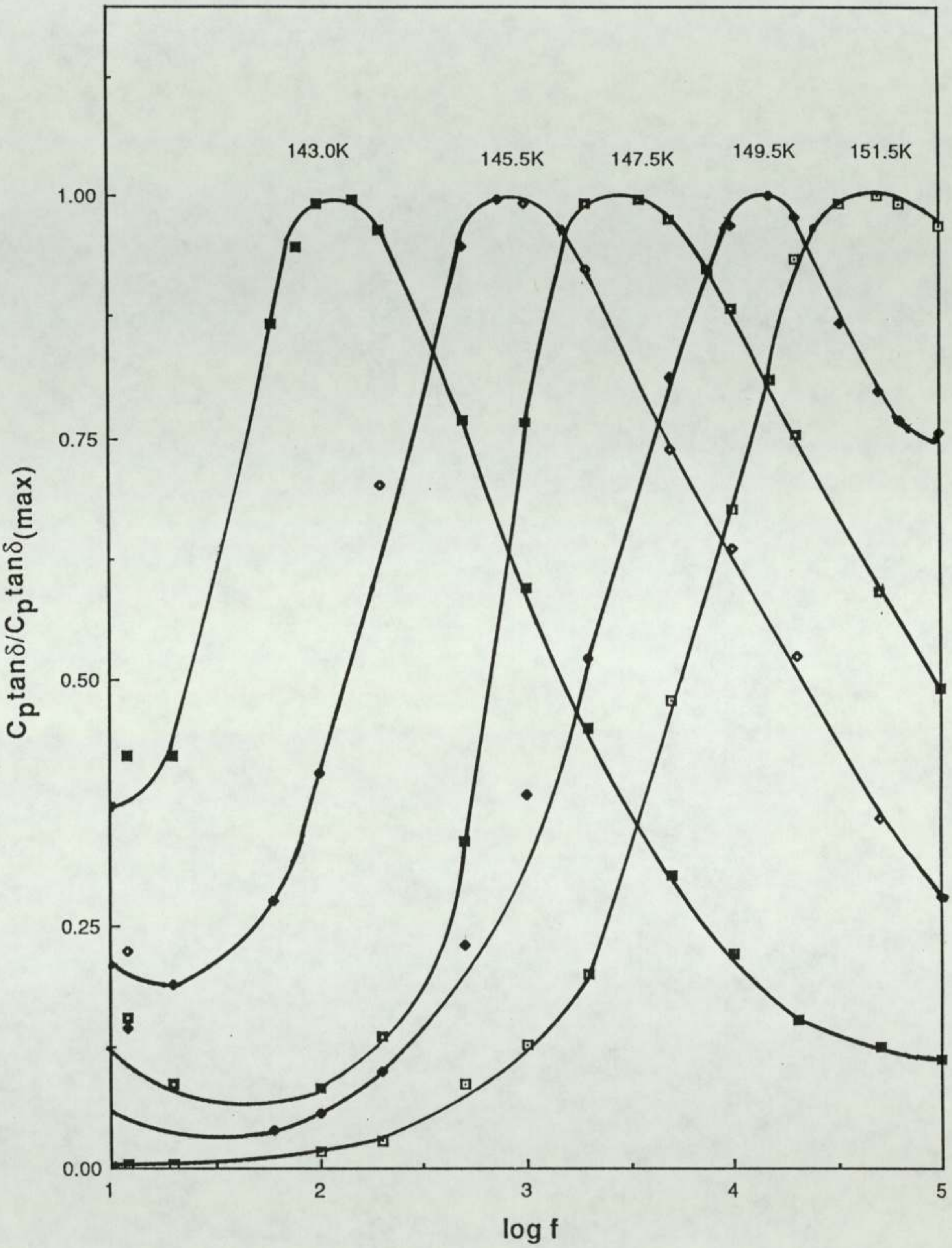

Figure (5-9). Frequency dependence of $C_p \tan\delta / C_p \tan\delta_{(max)}$ for linear PDMS with $\bar{n}_n=72$ at various temperatures.

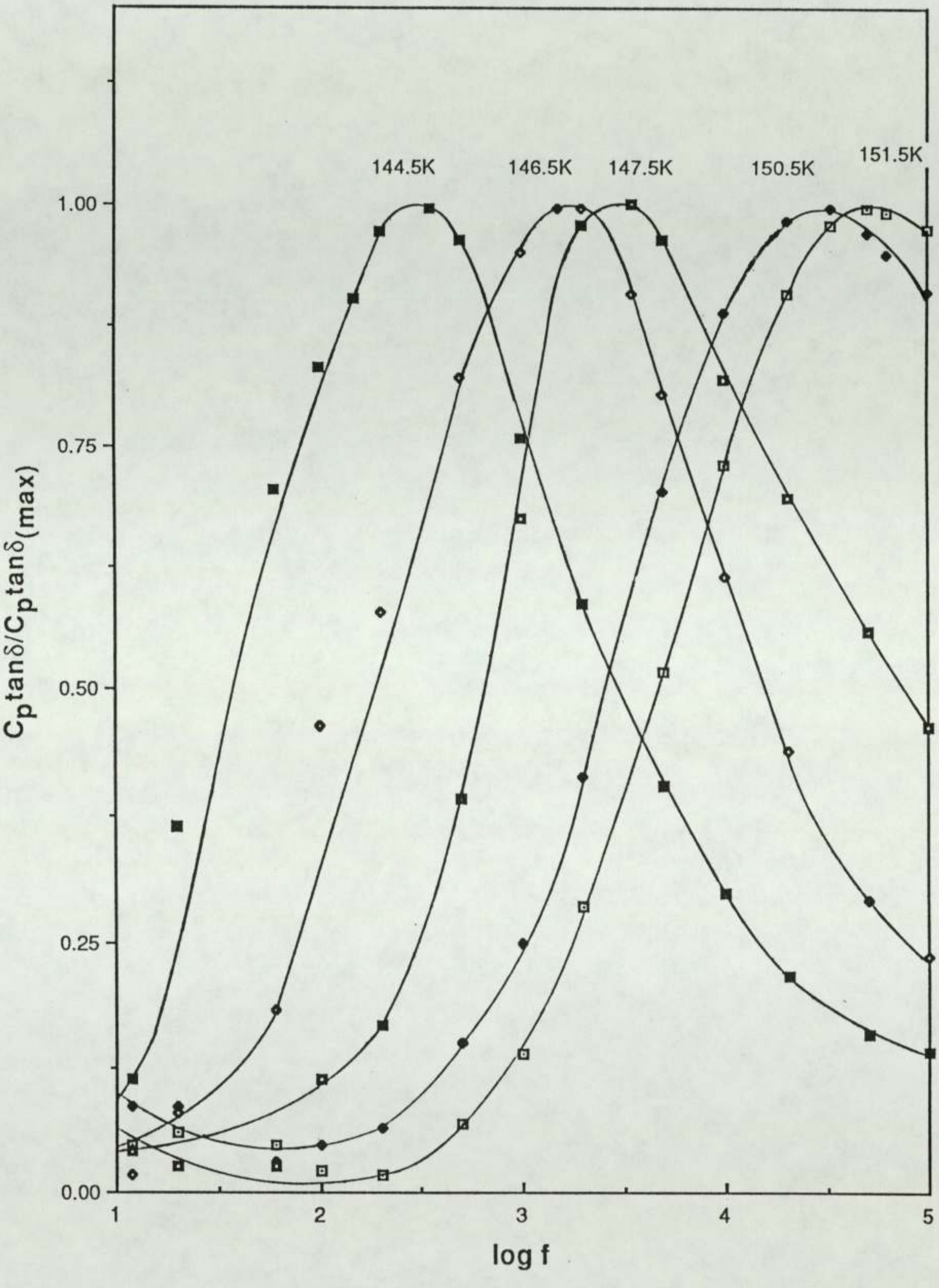

<u>Figure (5-10).</u> **Frequency dependence of $C_p \tan\delta / C_p \tan\delta_{(max)}$ for linear PDMS with $\bar{n}_n$=86 at various temperatures.**

than their linear counterparts.

The width of the loss curves at half-height is roughly two decades of frequency.

5-03: Measurement of the Dielectric Relaxation Activation Energy.

Arrhenius plots of the logarithm of the frequency corresponding to maximum dielectric loss, plotted as a function of the reciprocal of the absolute temperature, for cyclic and linear fractions of PDMS, are shown in Figures (5-11) to (5-20). All the plots are linear, within experimental error, and have a slope which is proportional to the activation energy for the dielectric relaxation process.

5-04: Cole-Cole Plots.

Cole-Cole plots of ε'' against ε' are presented in Figures (5-21) to (5-40) for cyclic and linear fractions of PDMS, at various temperatures. The values of ε'' and ε' are corrected to allow for the small contraction, ~2%, in the volume of the polymer fractions produced by cooling the samples to low temperatures. The curves are skewed-arcs, and are consistent with the empirical analysis of Davidson and Cole discussed in Chapter 3.

The limiting low frequency permittivity value, ε_0, is measured by extrapolating the circular arc onto the real axis. The limiting high frequency permittivity value, ε_∞, is estimated from the plots where the data is more complete by a linear extrapolation onto the real axis. A single ε_∞ is estimated in this way for each fraction and is assumed to be constant over the small range of temperatures at which measurements were carried out. The derivation of ε_0 and ε_∞ in this manner permits the calculation of the

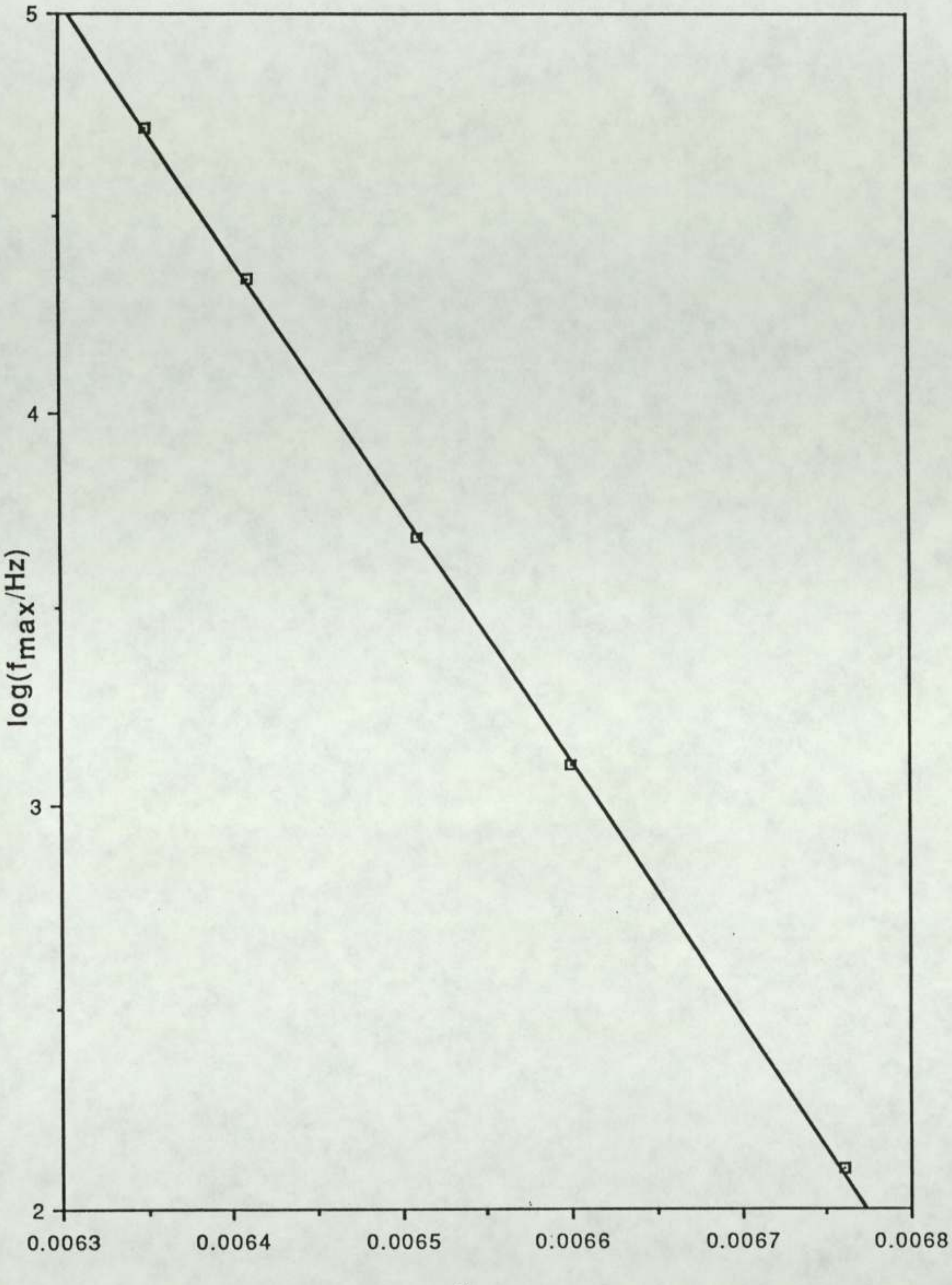

Figure (5-11) Log(f_{max}/Hz) against T^{-1}(K) for cyclic PDMS with $\bar{n}_n$=28

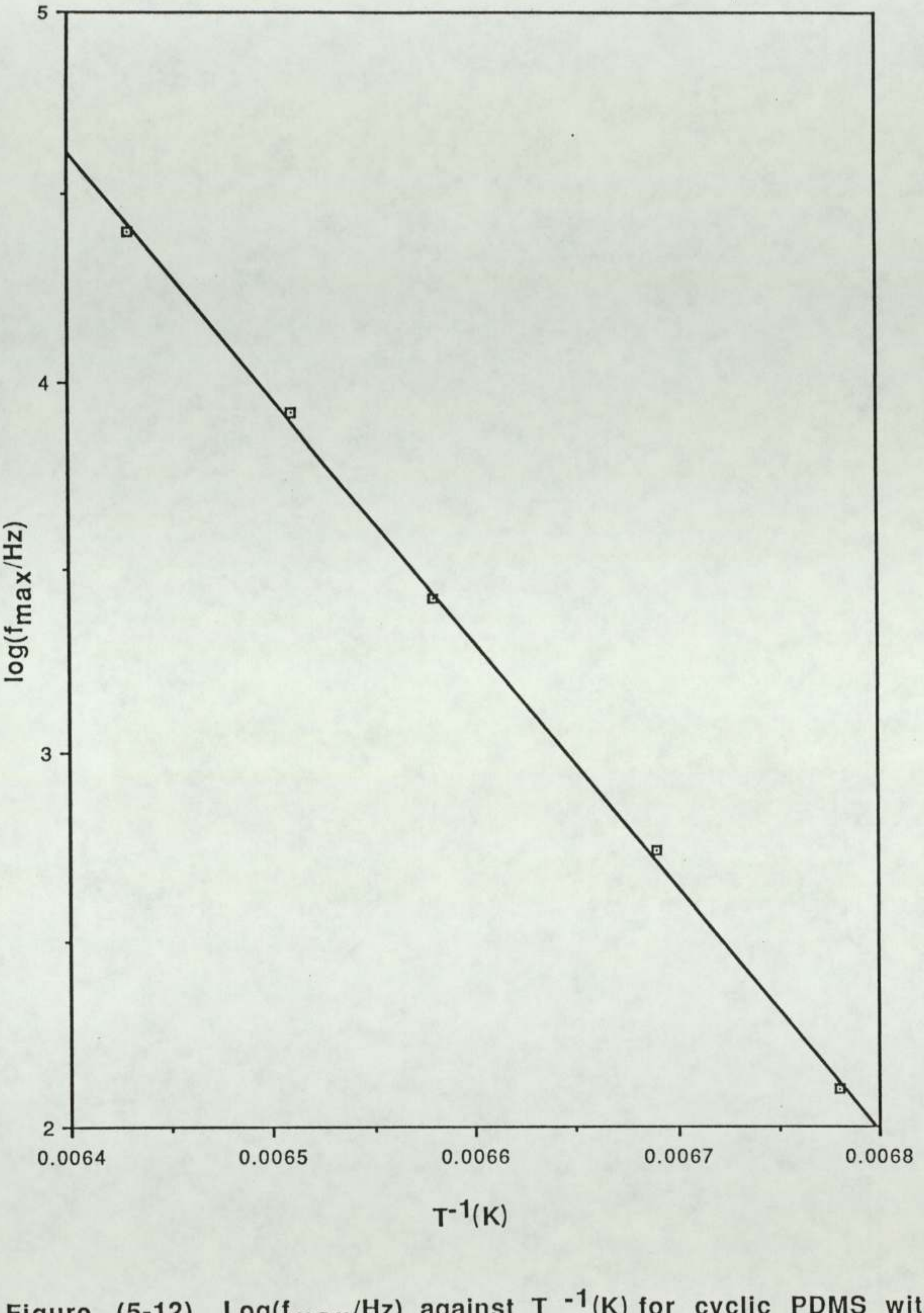

Figure (5-12) Log(f_{max}/Hz) against T^{-1}(K) for cyclic PDMS with $\bar{n}_n$=35

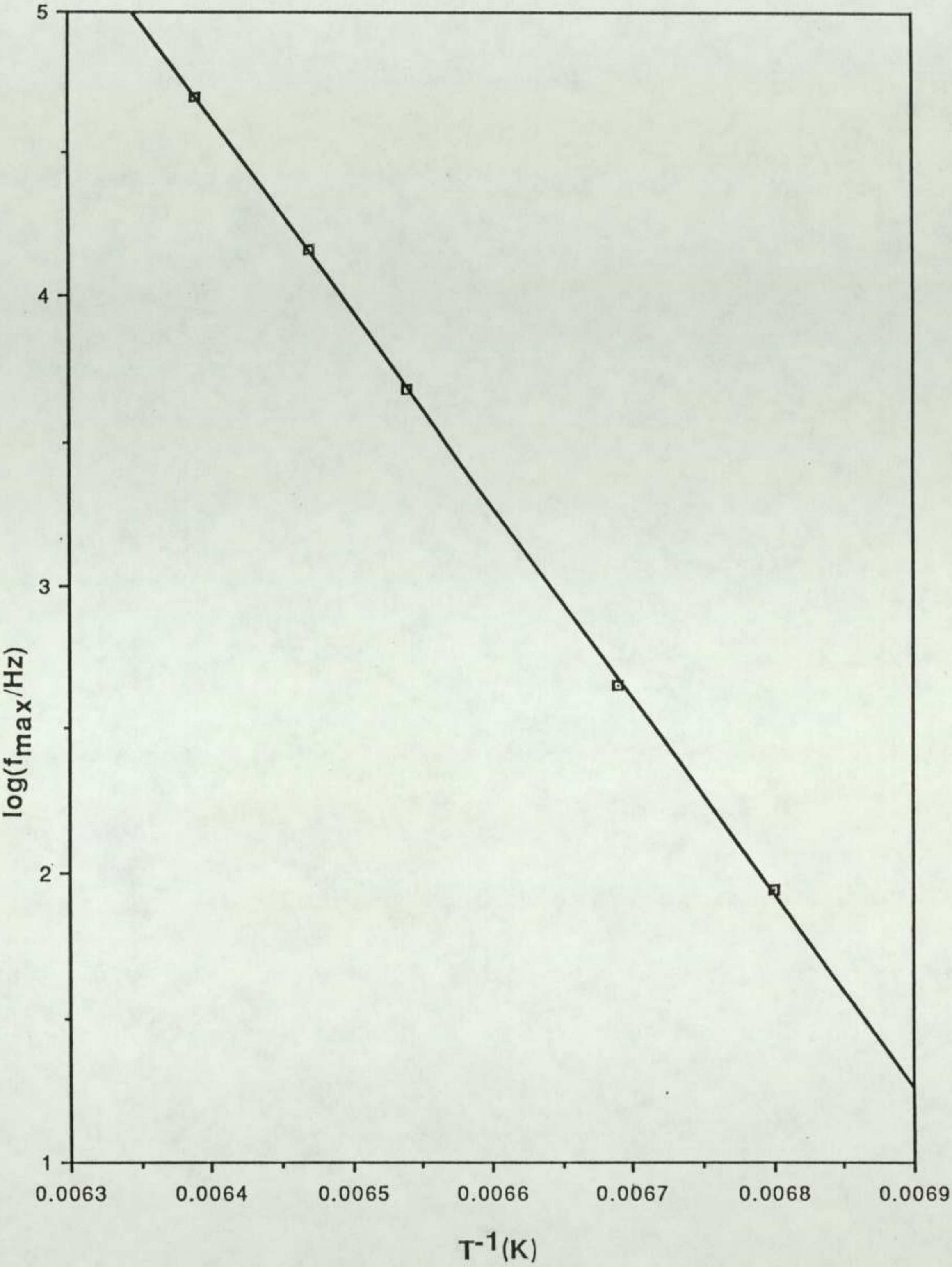

Figure (5-13) Log(f_{max}/Hz) against T^{-1}(K) for cyclic PDMS with $\bar{n}_n$=50

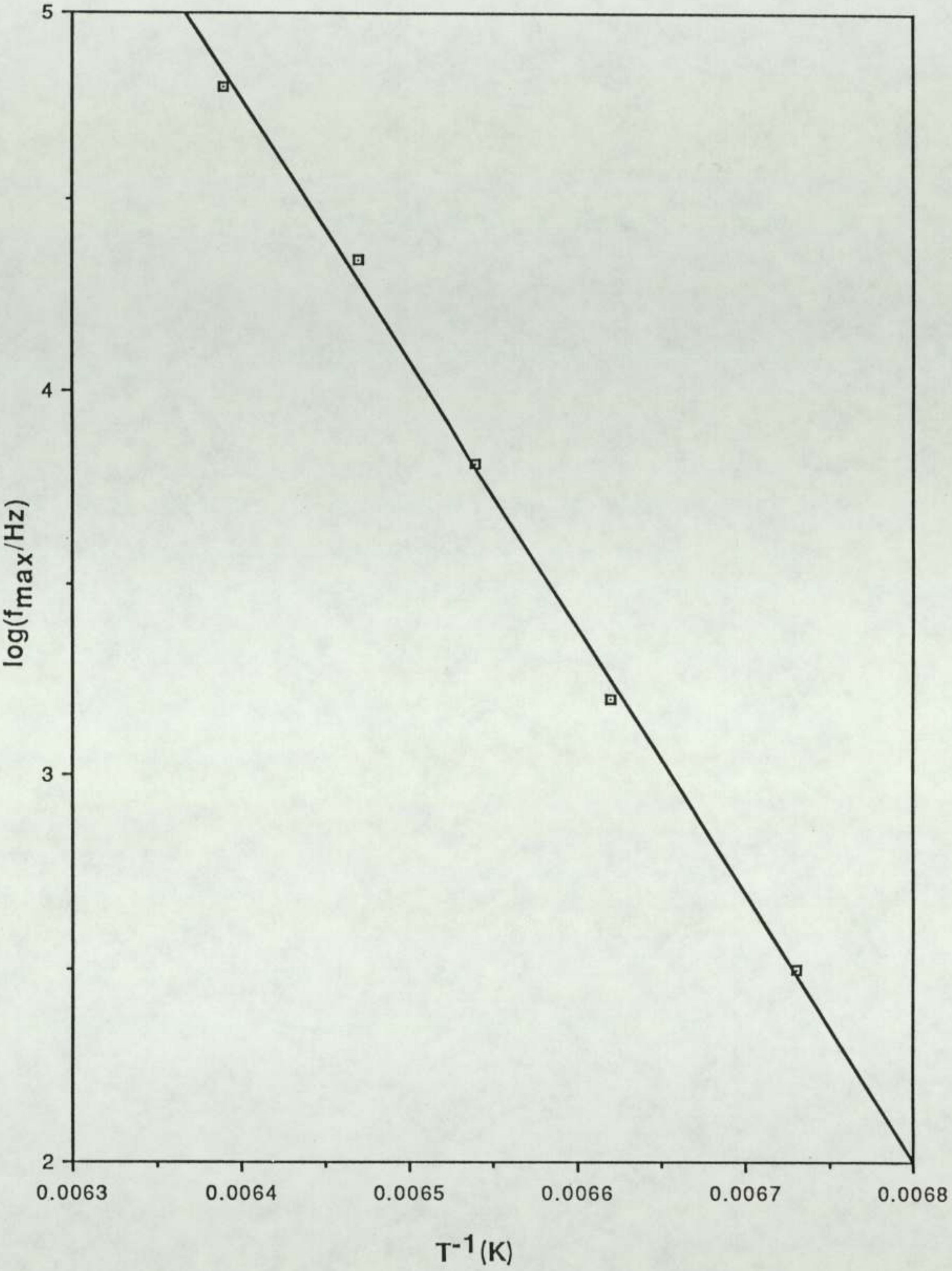

Figure (5-14) $\log(f_{max}/Hz)$ against $T^{-1}(K)$ for cyclic PDMS with $\bar{n}_n$=66

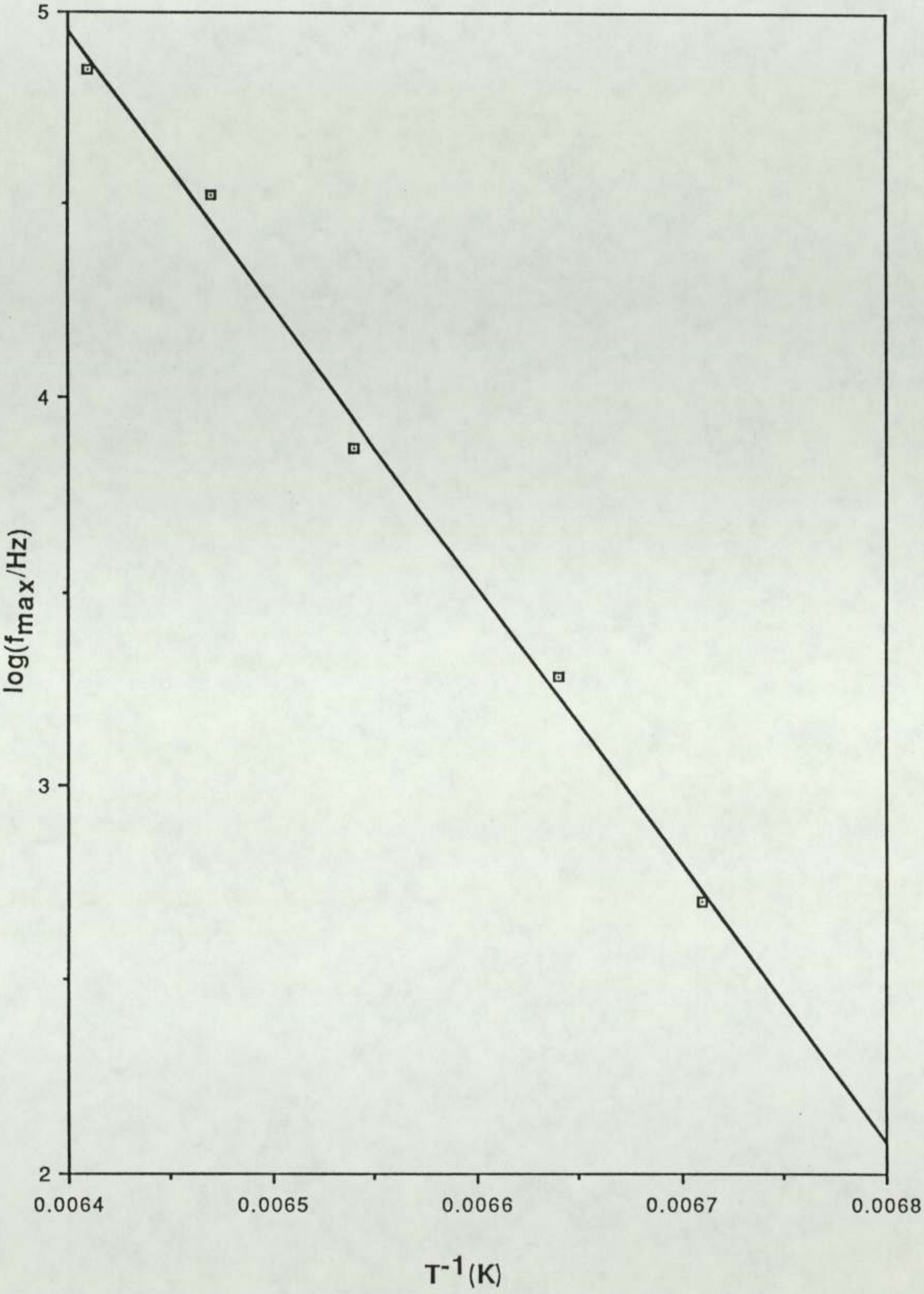

Figure (5-15) Log(f_{max}/Hz) against T^{-1}(K) for cyclic PDMS with $\bar{n}_n$=99

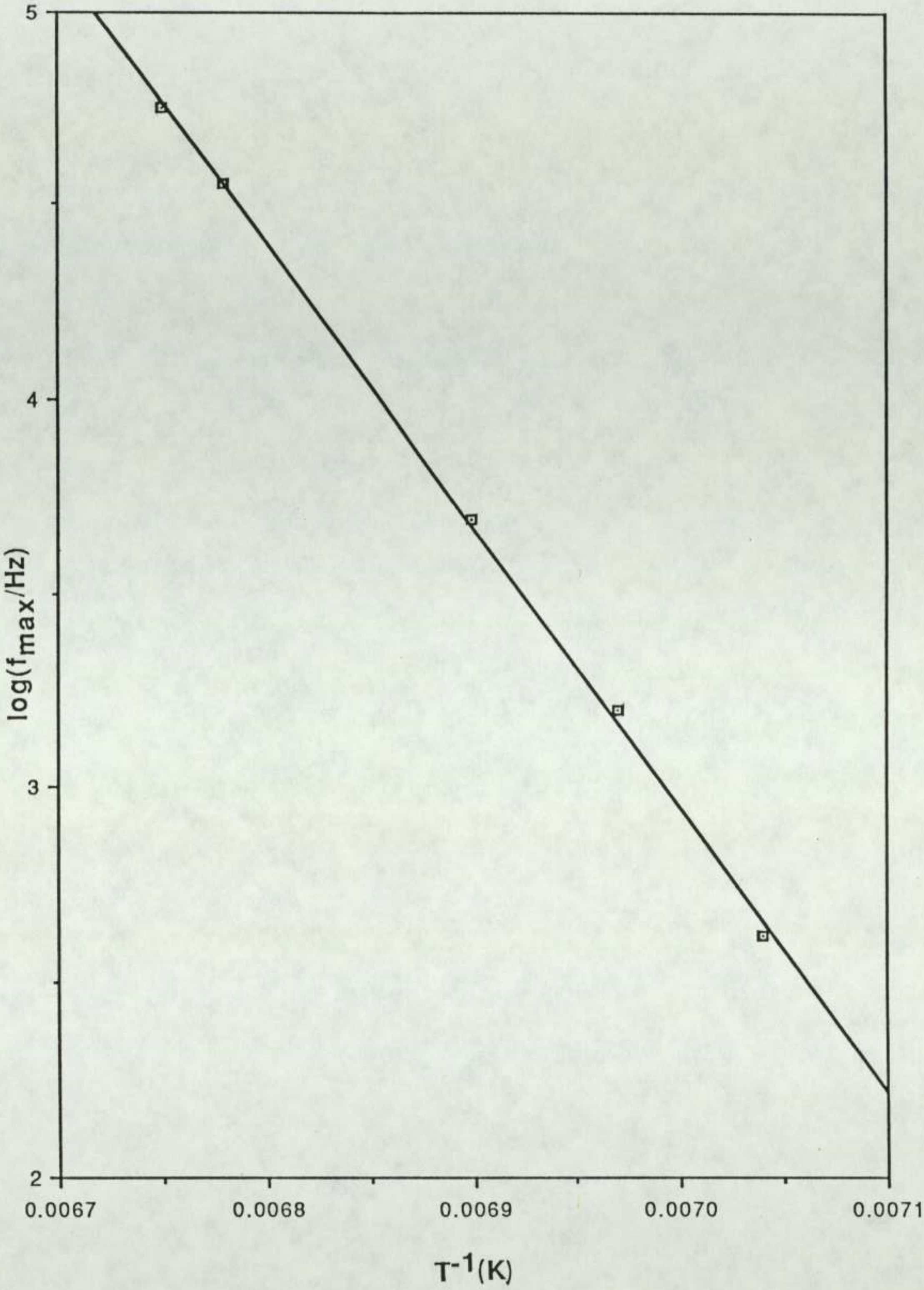

<u>Figure (5-16)</u> $\log(f_{max}/Hz)$ against $T^{-1}(K)$ for linear PDMS with $\bar{n}_n=28$

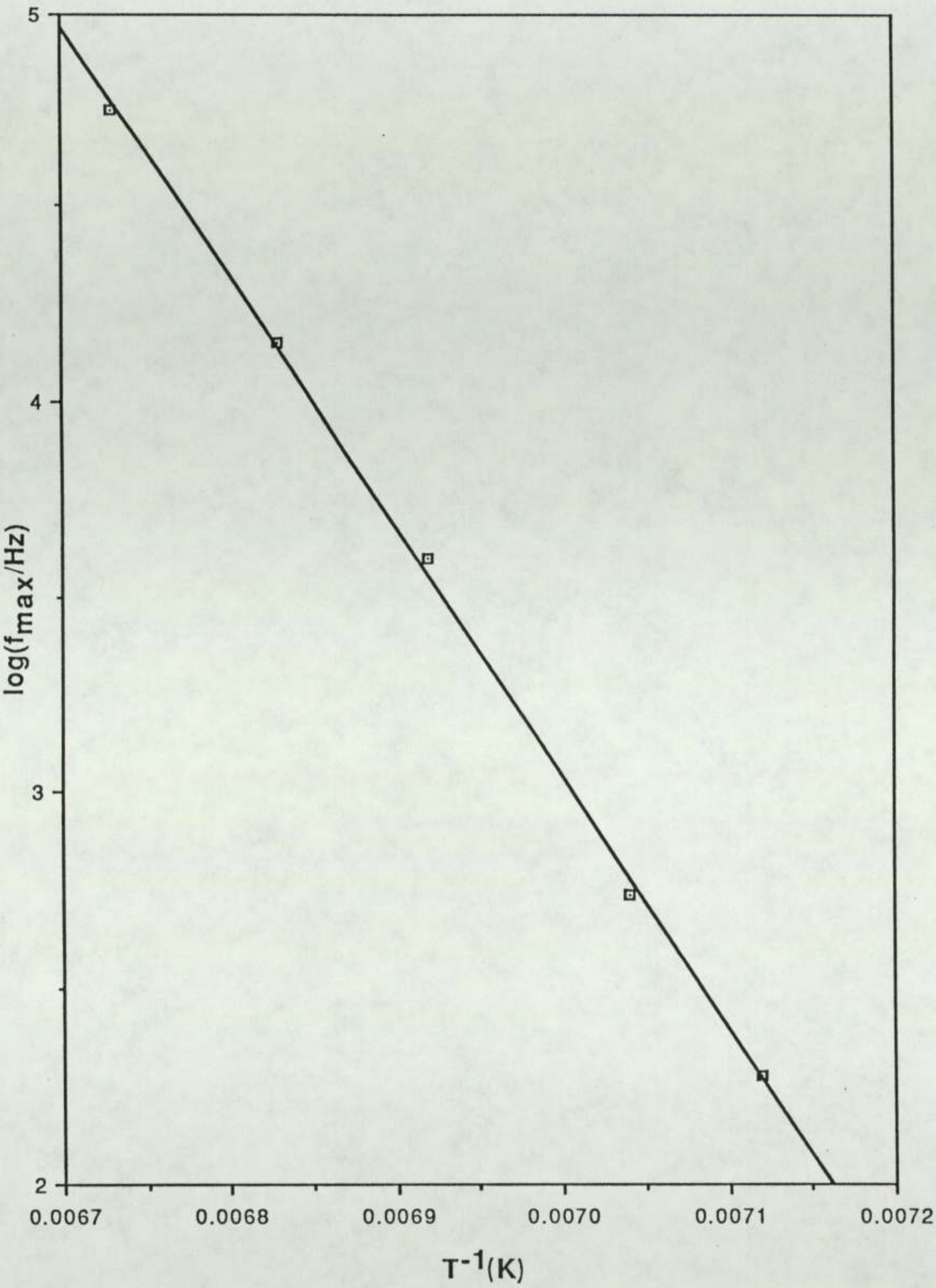

<u>Figure (5-17)</u> Log(f_{max}/Hz) against T^{-1}(K) for linear PDMS with $\bar{n}_n$=34

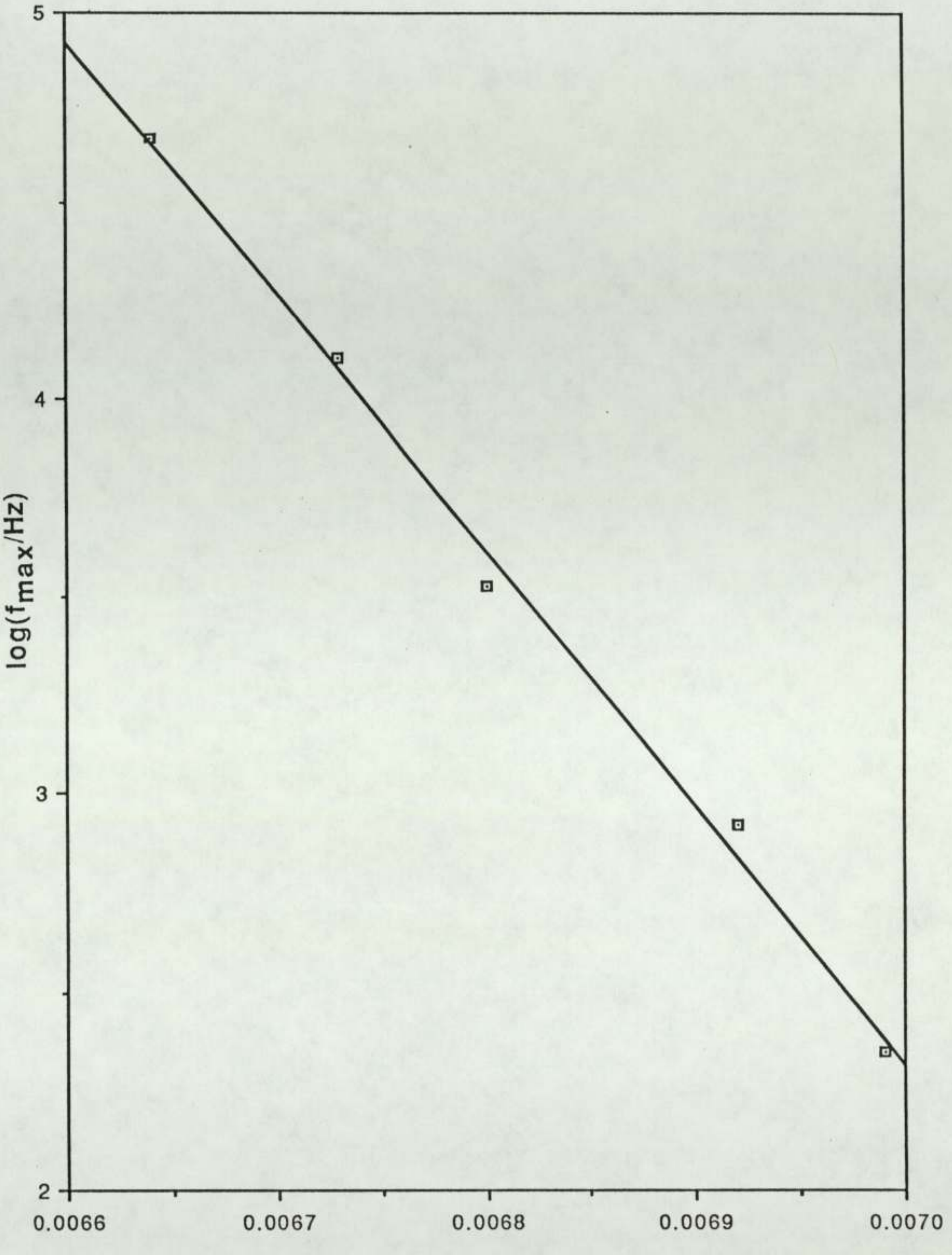

Figure (5-18) Log(f_{max}/Hz) against T^{-1}(K) for linear PDMS with $\bar{n}_n$=57

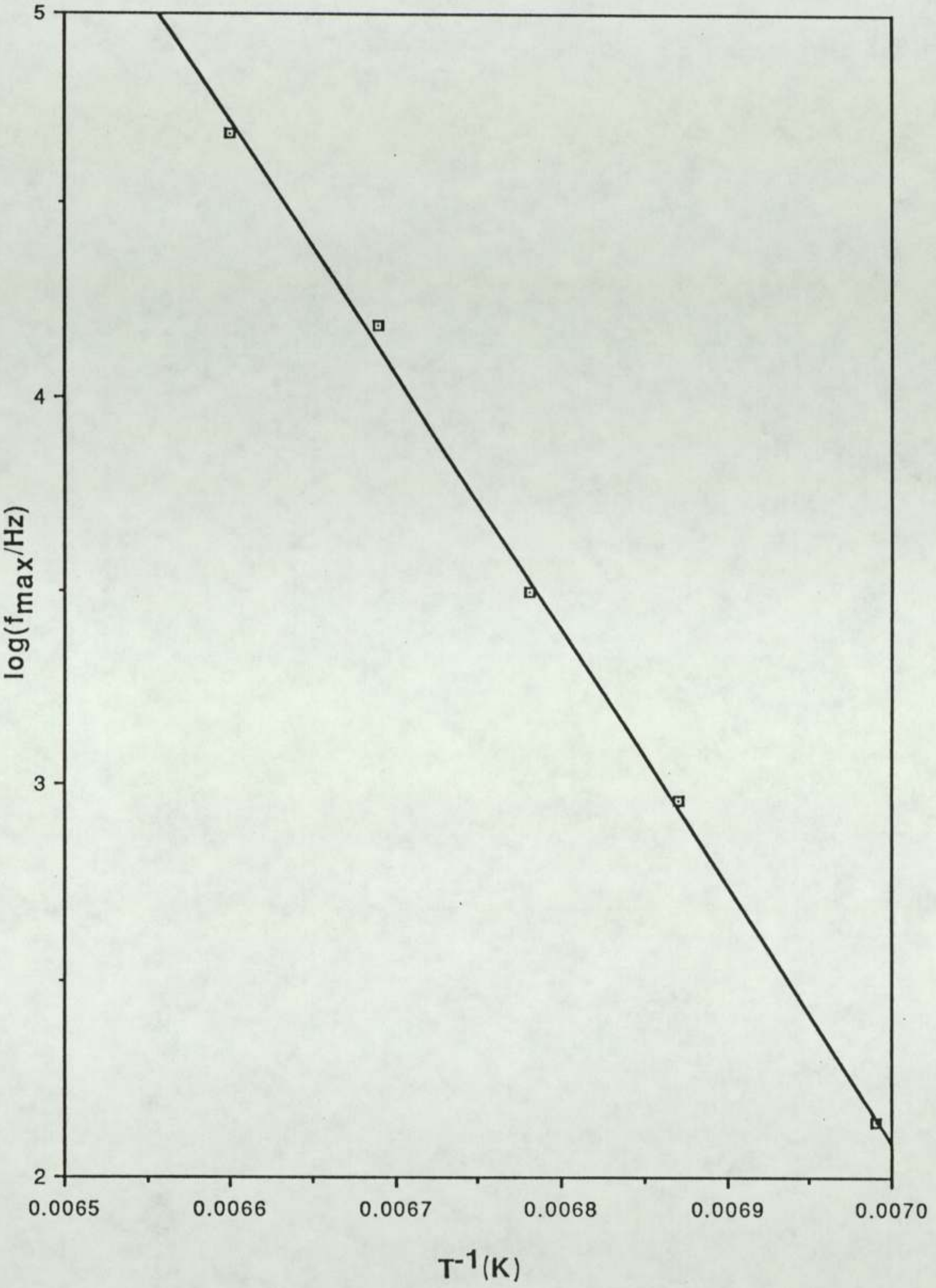

Figure (5-19) Log(f_{max}/Hz) against T^{-1}(K) for linear PDMS with $\bar{n}_n$=72

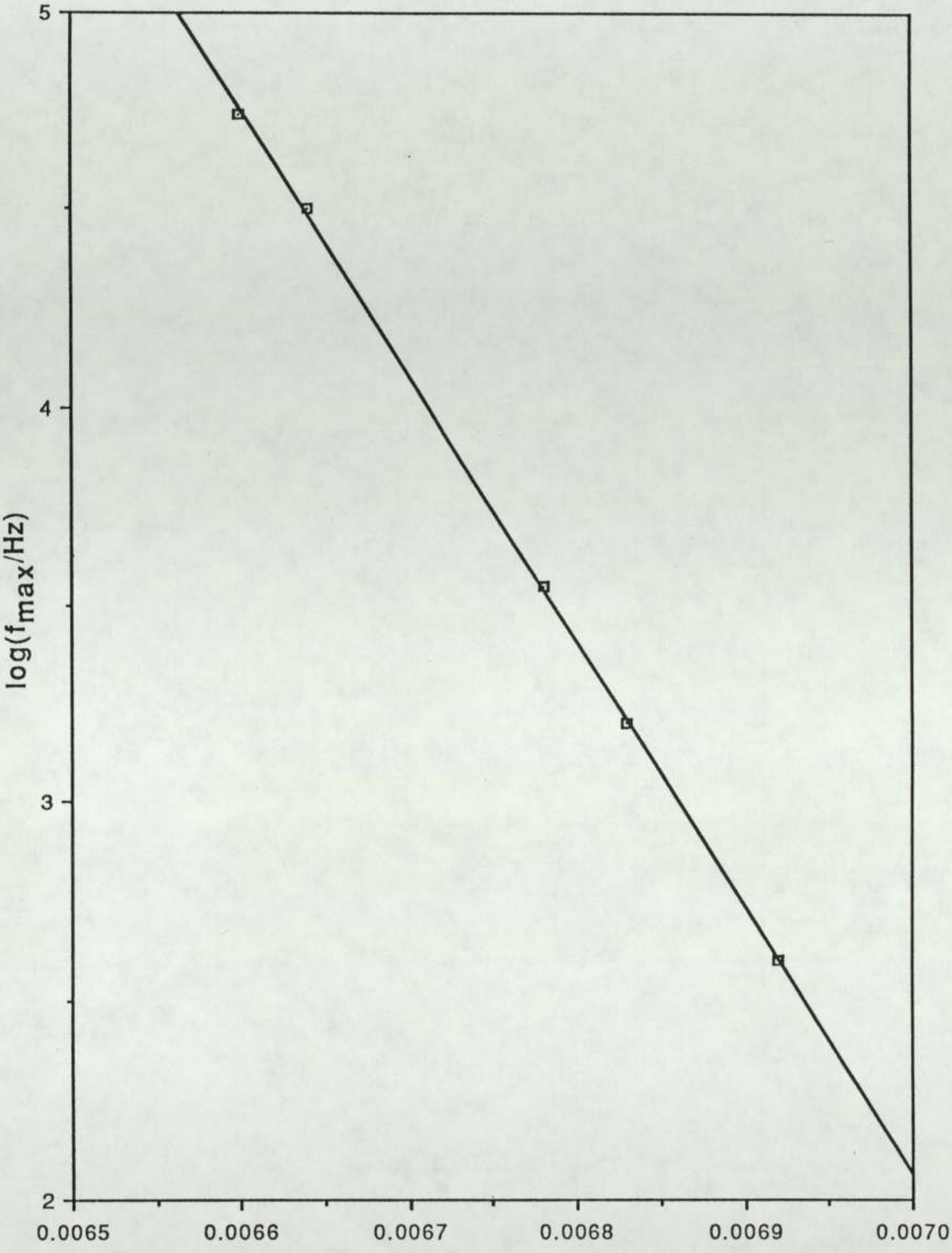

Figure (5-20) Log(f_{max}/Hz) against T^{-1}(K) for linear PDMS with $\bar{n}_n$=86

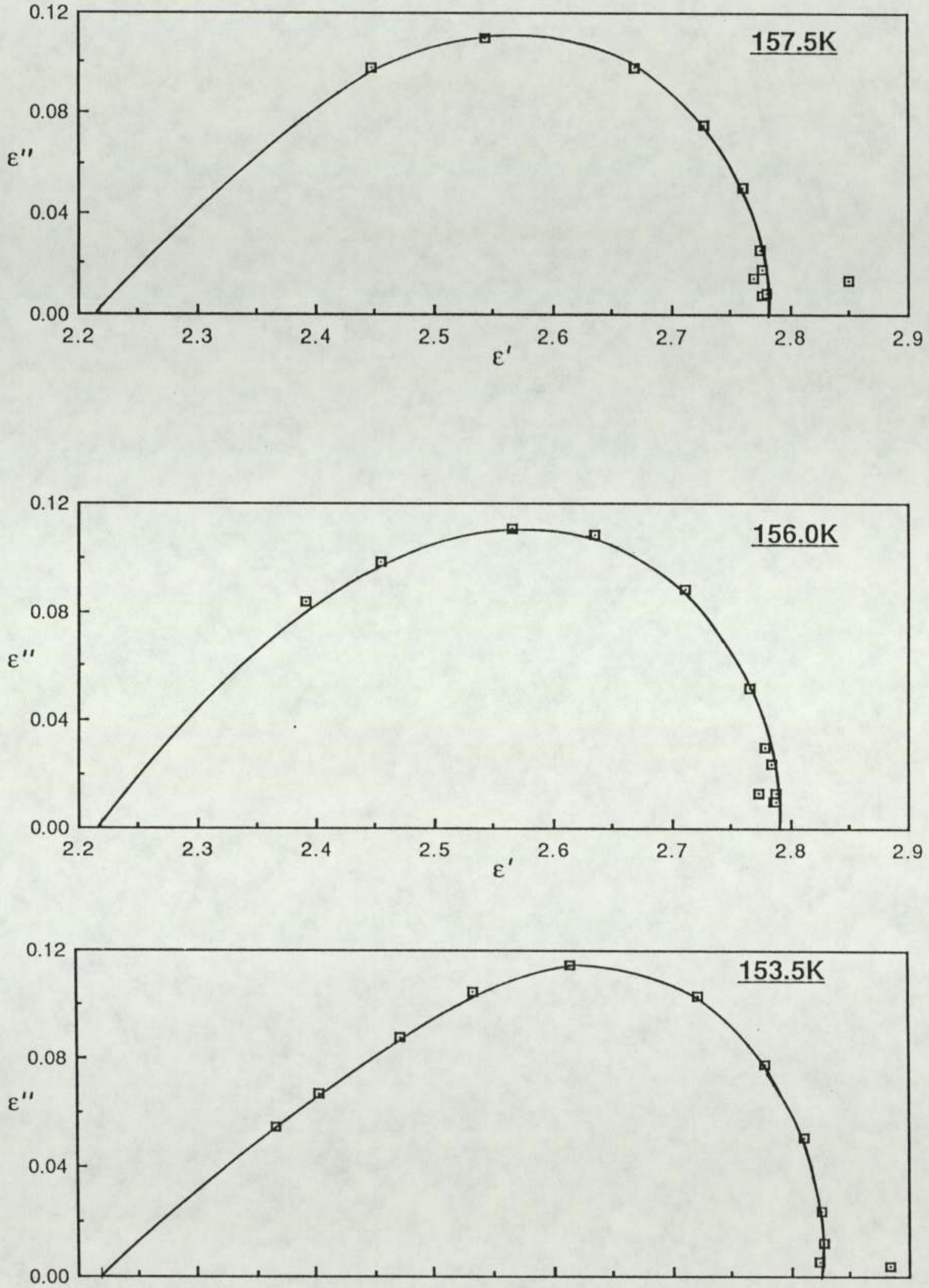

Figure (5-21) Cole-Cole plots for cyclic PDMS with $\bar{n}_n$=28 at various temperatures

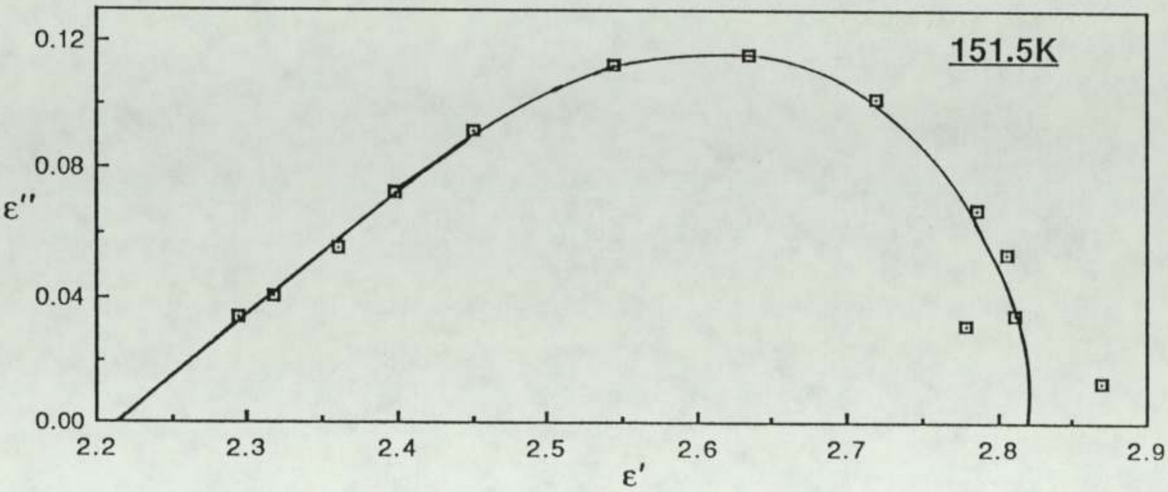

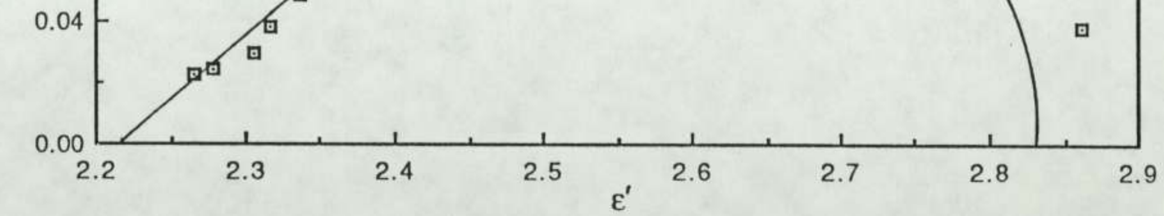

Figure (5-22) Cole-Cole plots for cyclic PDMS with $\bar{n}_n$=28 at various temperatures

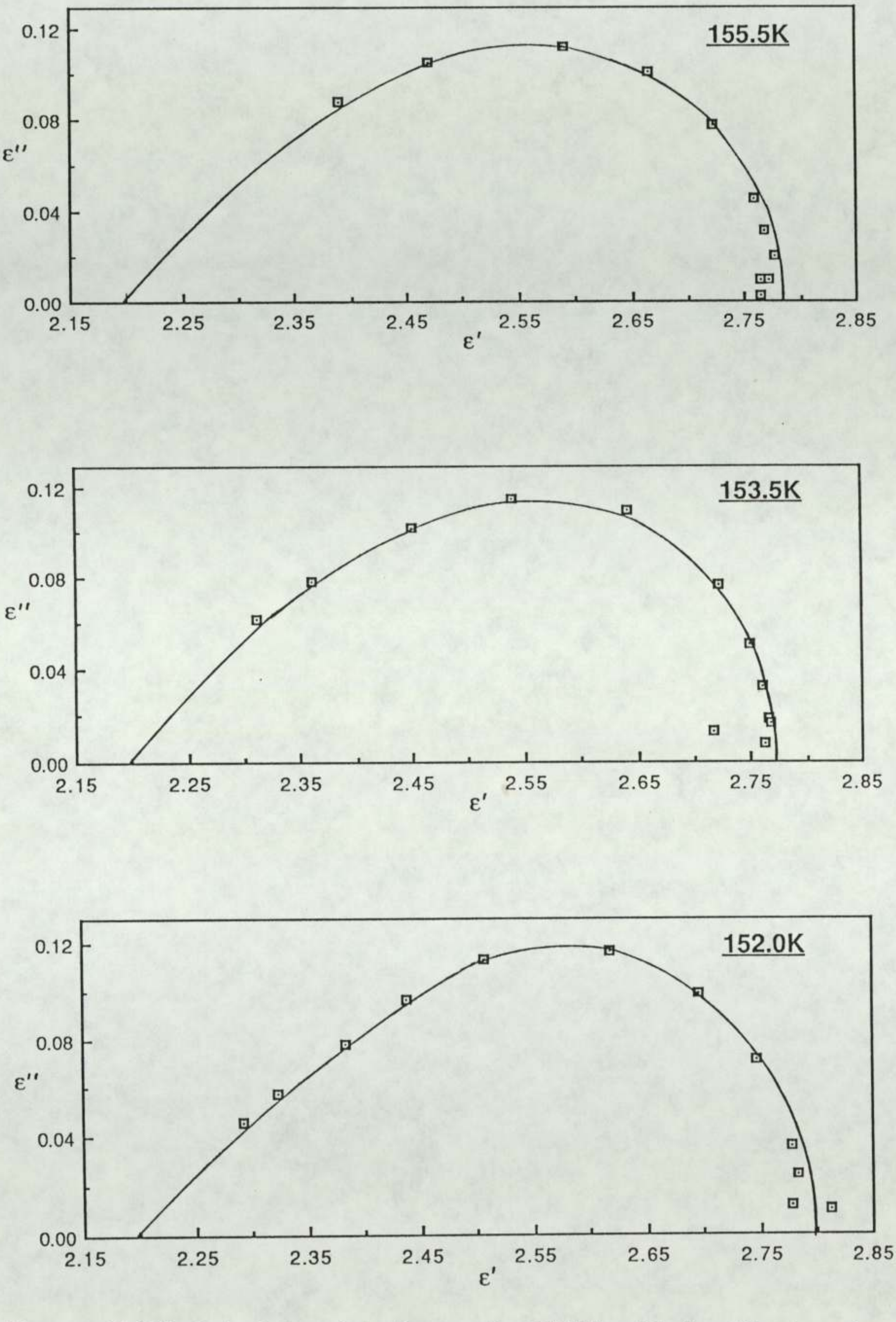

Figure (5-23) Cole-Cole plots for cyclic PDMS with $\bar{n}_n$=35 at various temperatures

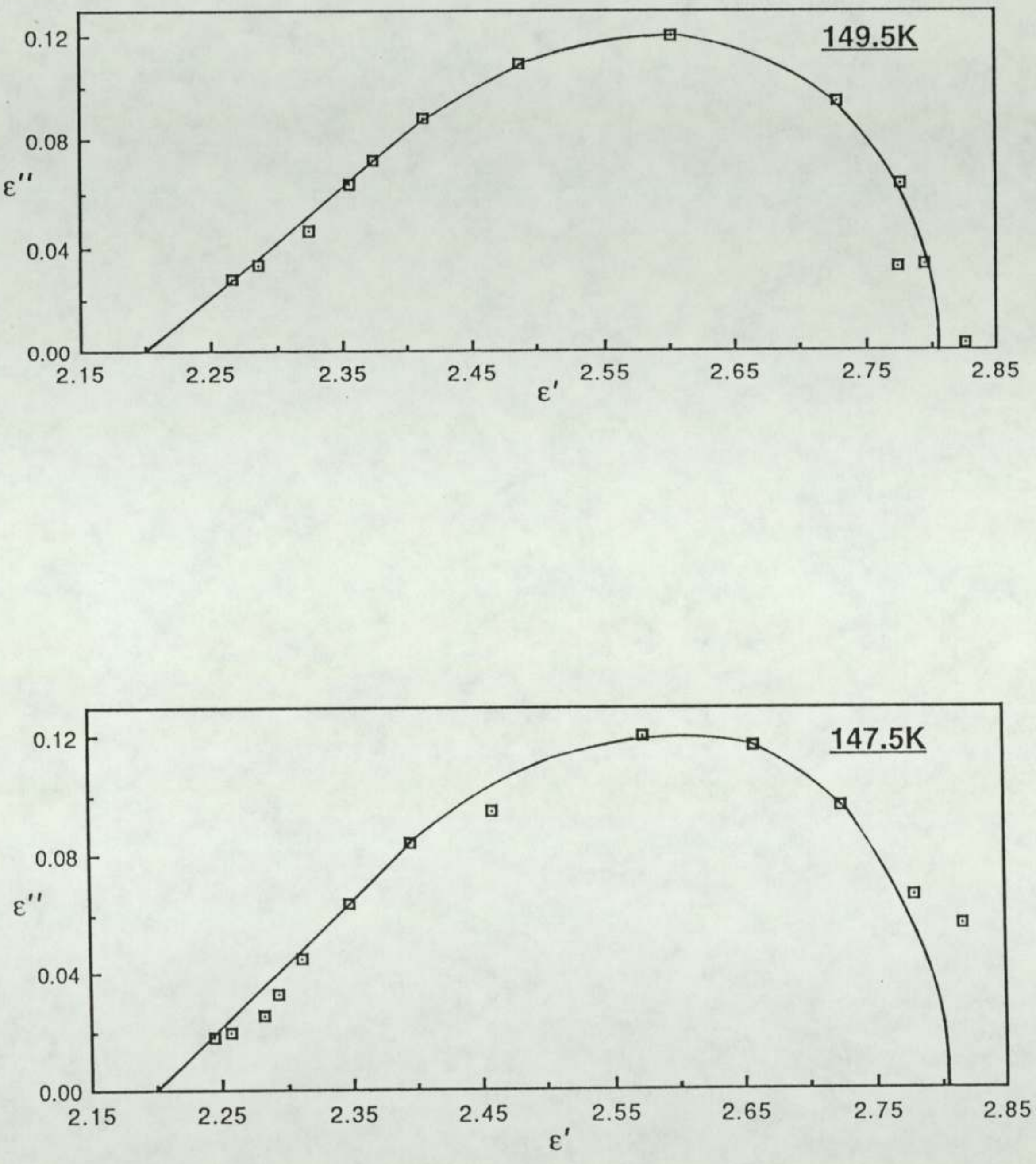

Figure (5-24) Cole-Cole plots for cyclic PDMS with $\bar{n}_n$=35 at various temperatures

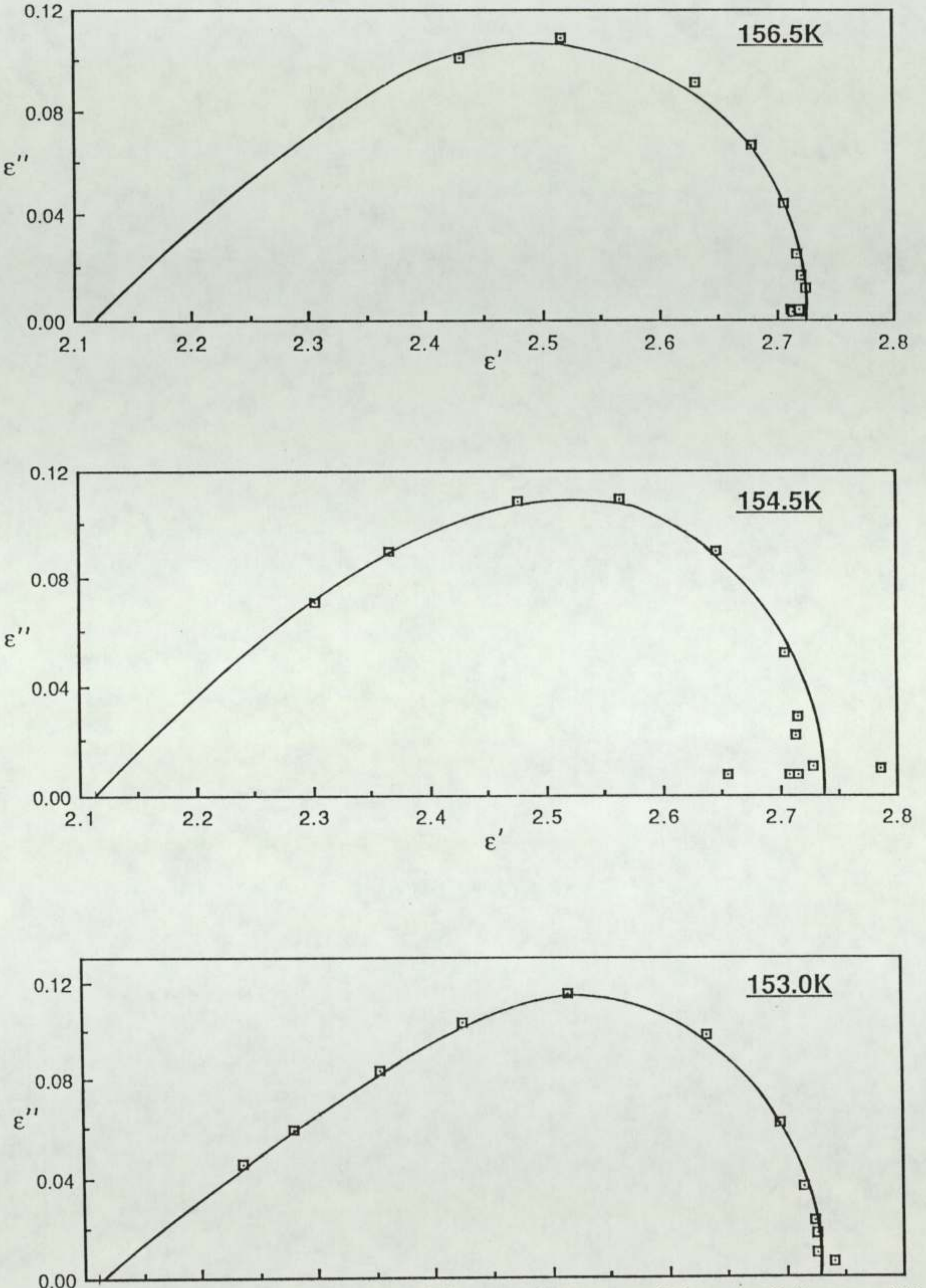

Figure (5-25) Cole-Cole plots for cyclic PDMS with $\bar{n}_n$=50 at various temperatures

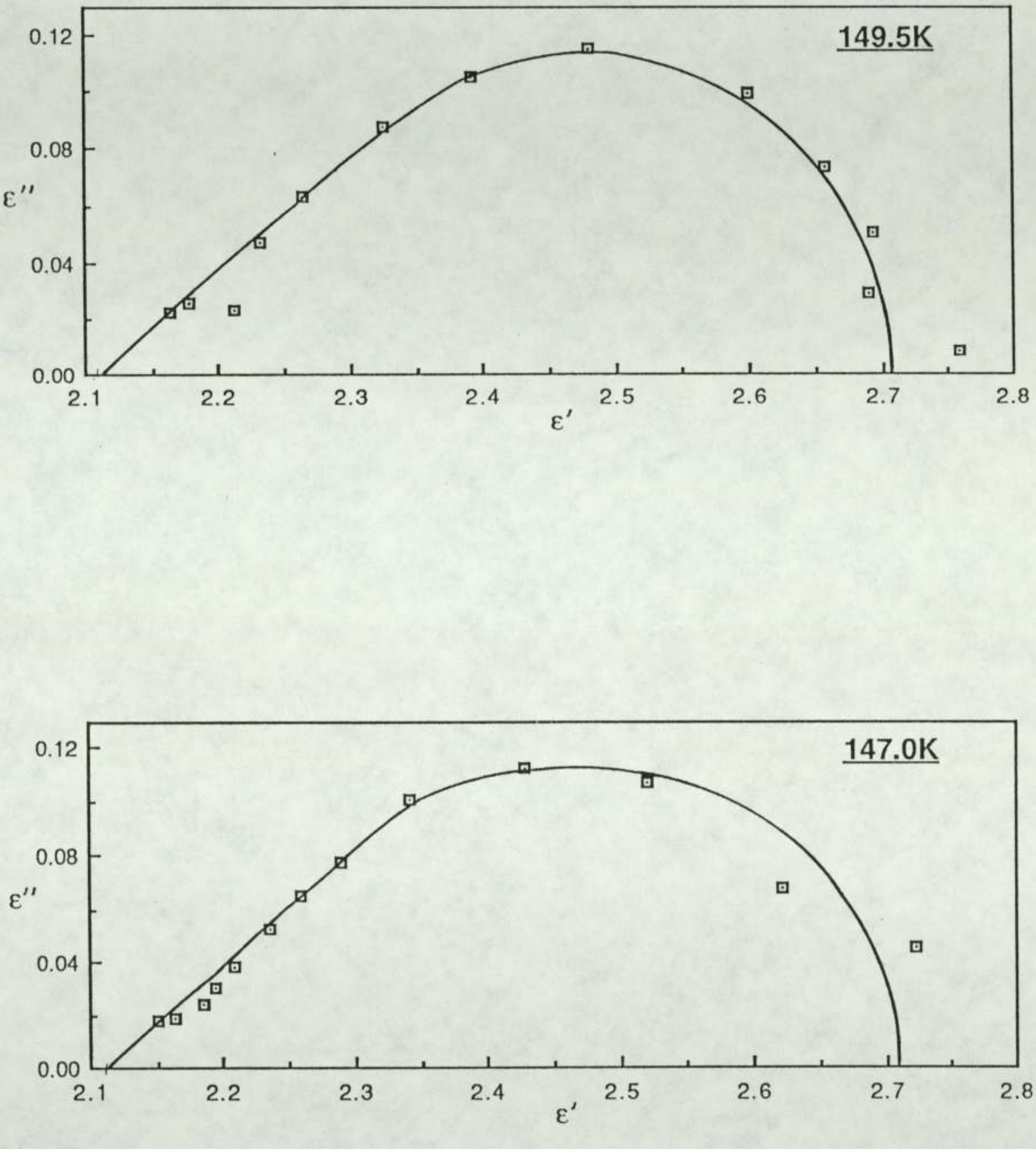

Figure (5-26) Cole-Cole plots for cyclic PDMS with $\bar{n}_n$=50 at various temperatures

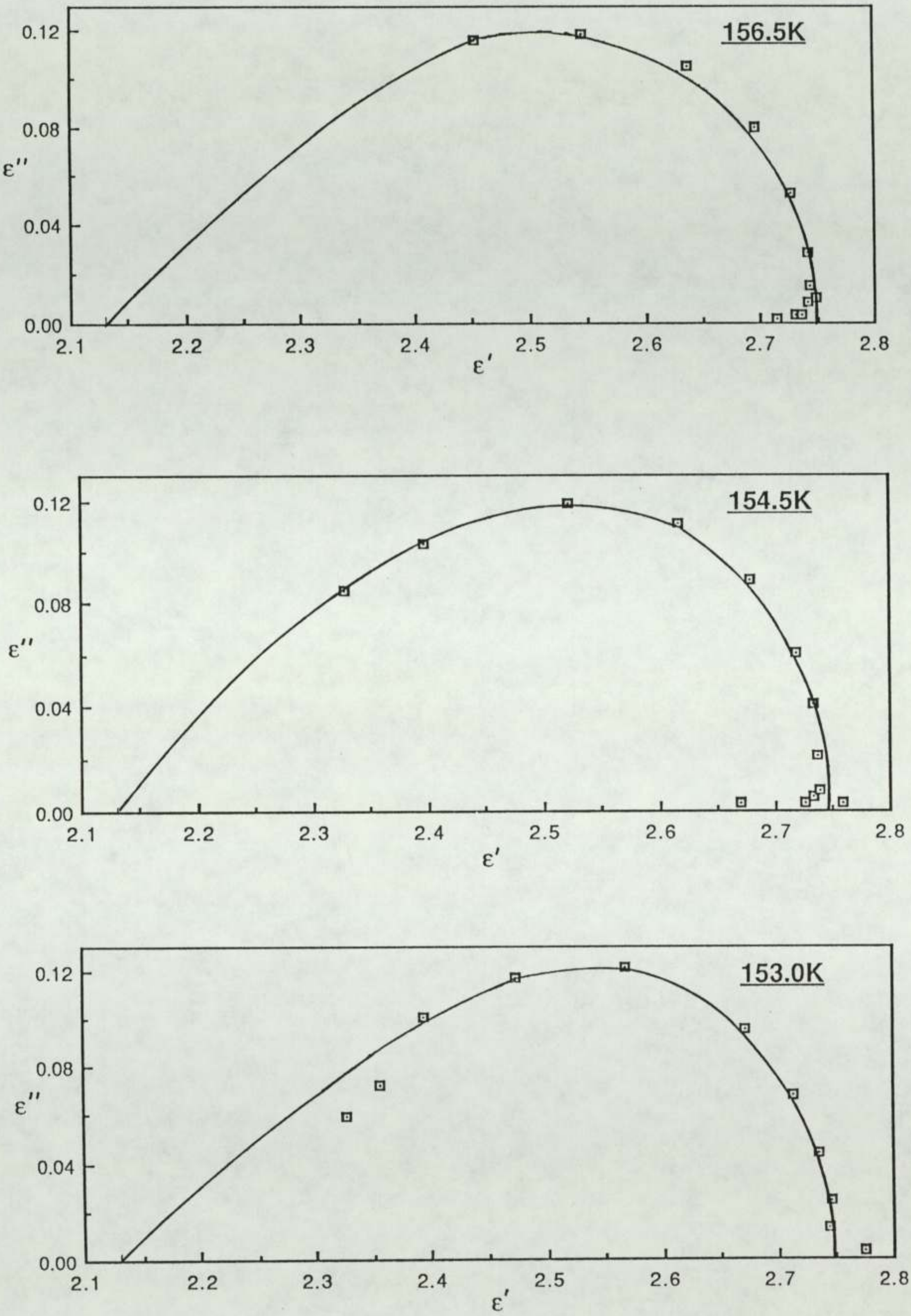

Figure (5-27) Cole-Cole plots for cyclic PDMS with $\bar{n}_n$=66 at various temperatures

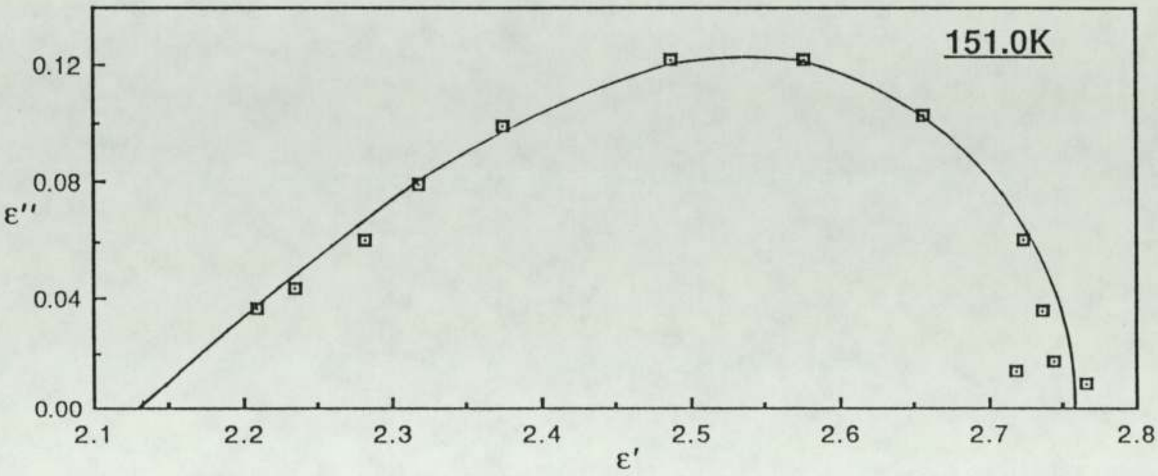

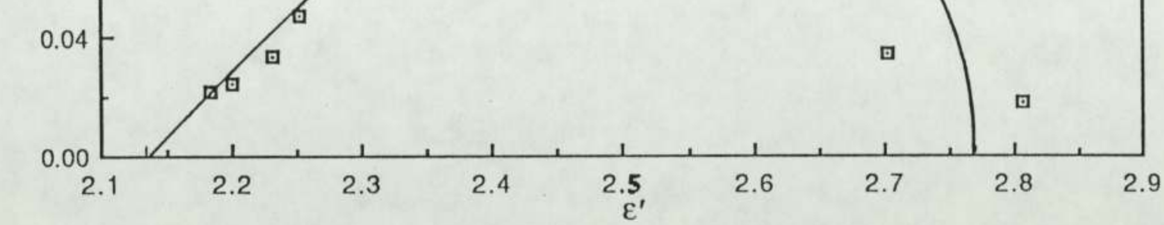

Figure (5-28) Cole-Cole plots for cyclic PDMS with $\bar{n}_n$=66 at various temperatures

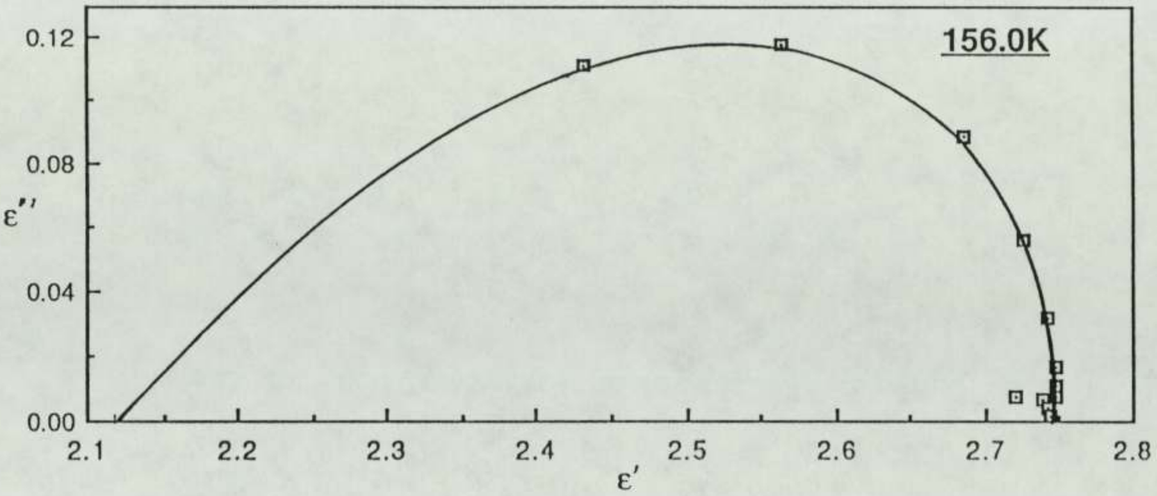

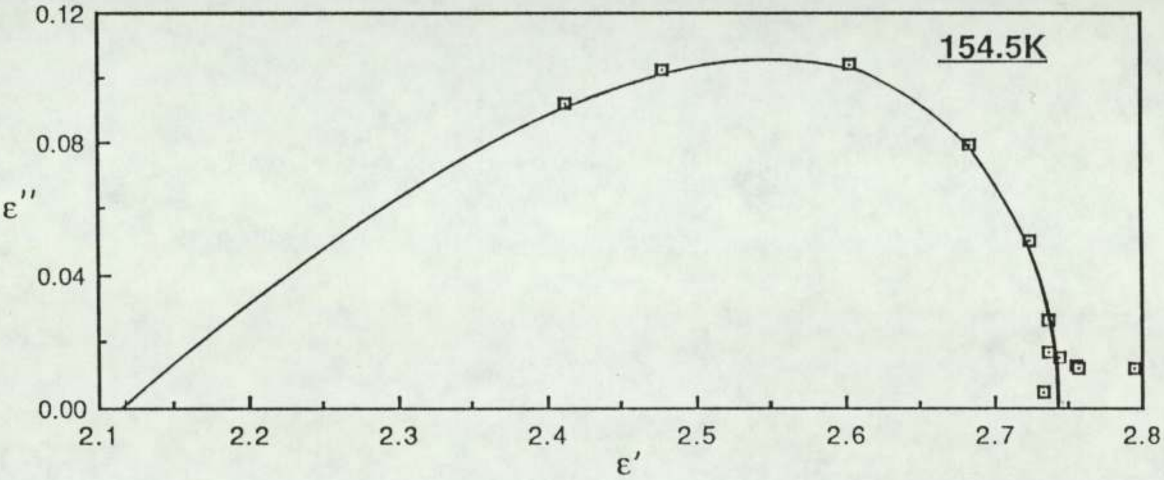

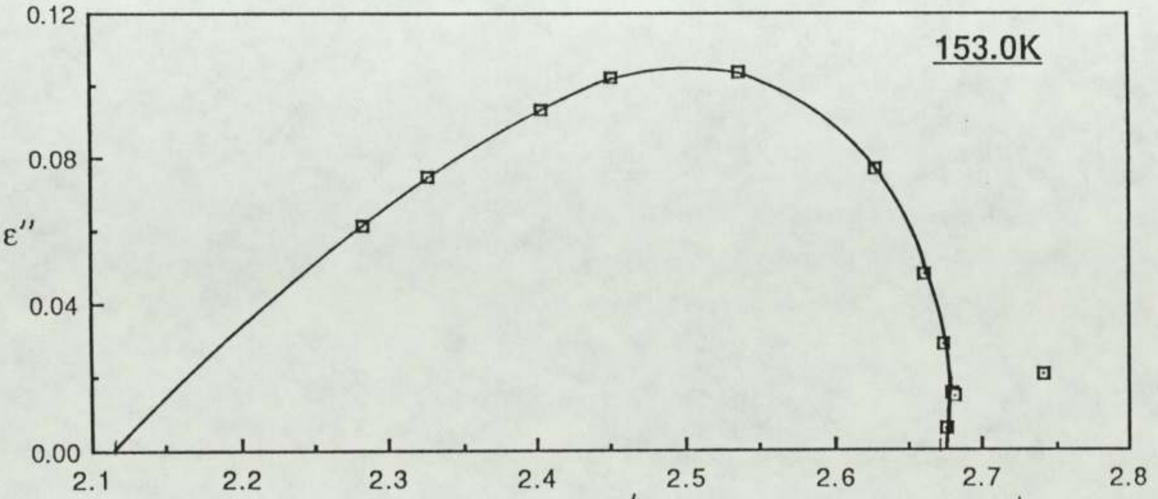

Figure (5-29) Cole-Cole plots for cyclic PDMS with $\bar{n}_n$=99 at various temperatures

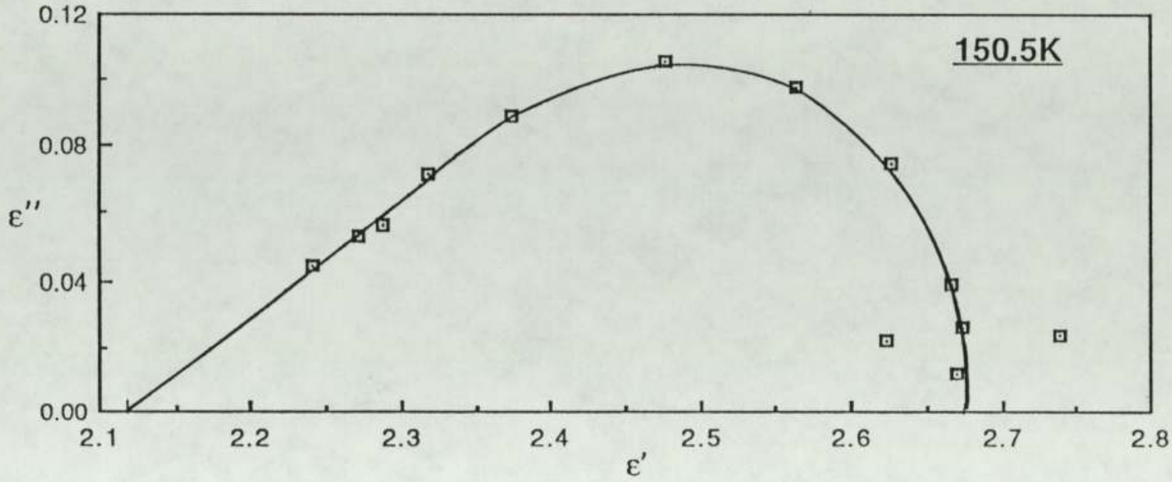

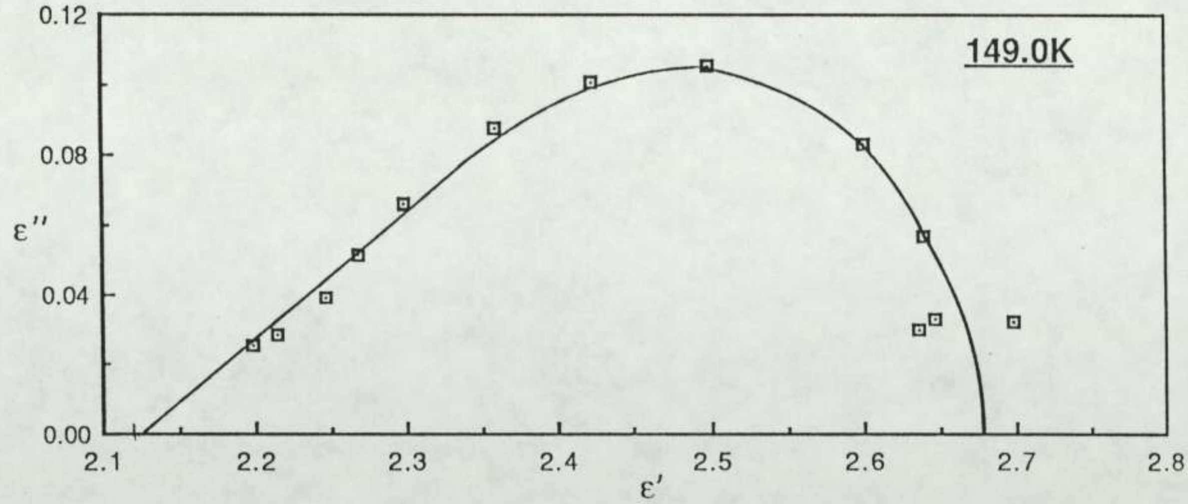

Figure (5-30) Cole-Cole plots for cyclic PDMS with $\bar{n}_n$=99 at various temperatures

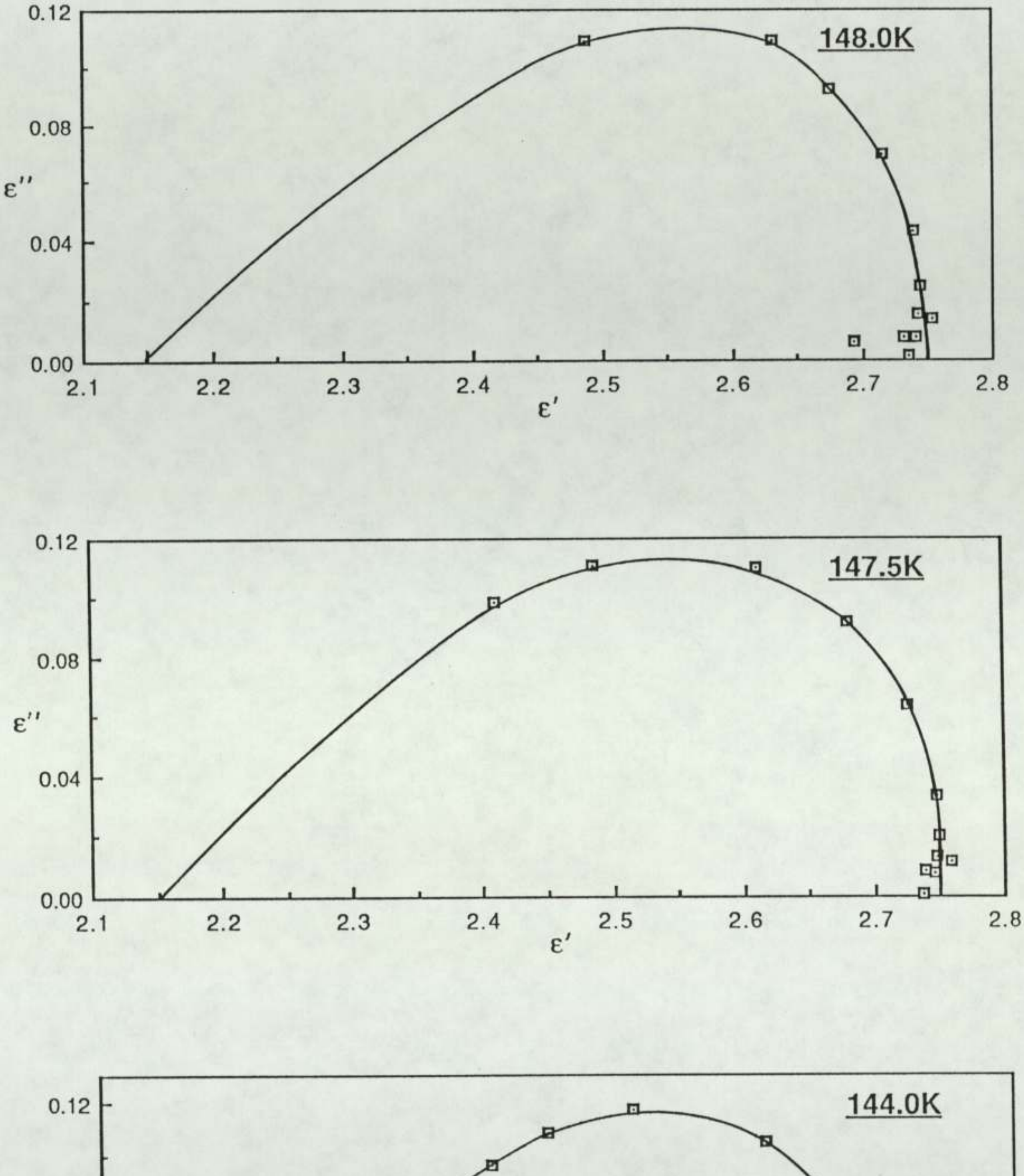

Figure (5-31) Cole-Cole plots for linear PDMS with $\bar{n}_n$=28 at various temperatures

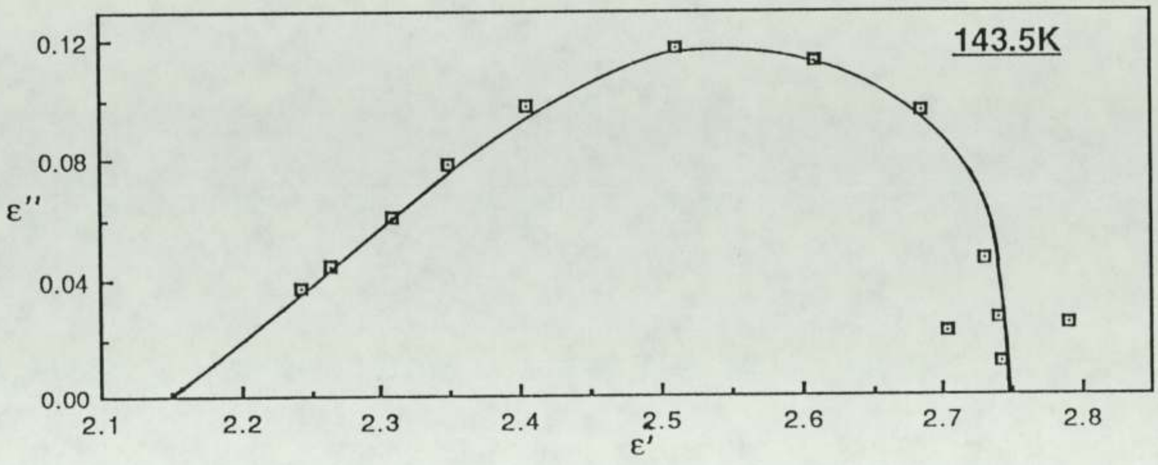

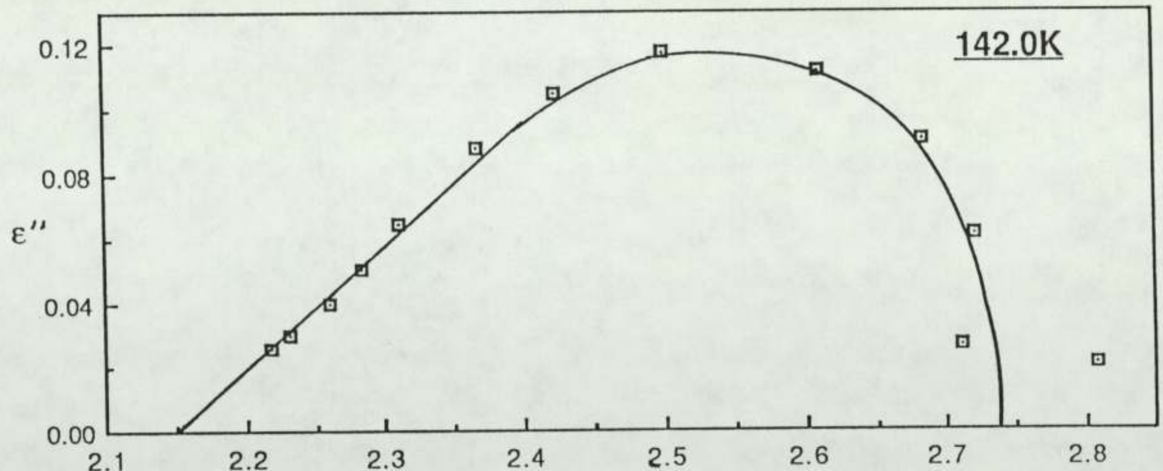

Figure (5-32) Cole-Cole plots for linear PDMS with $\bar{n}_n$=28 at various temperatures

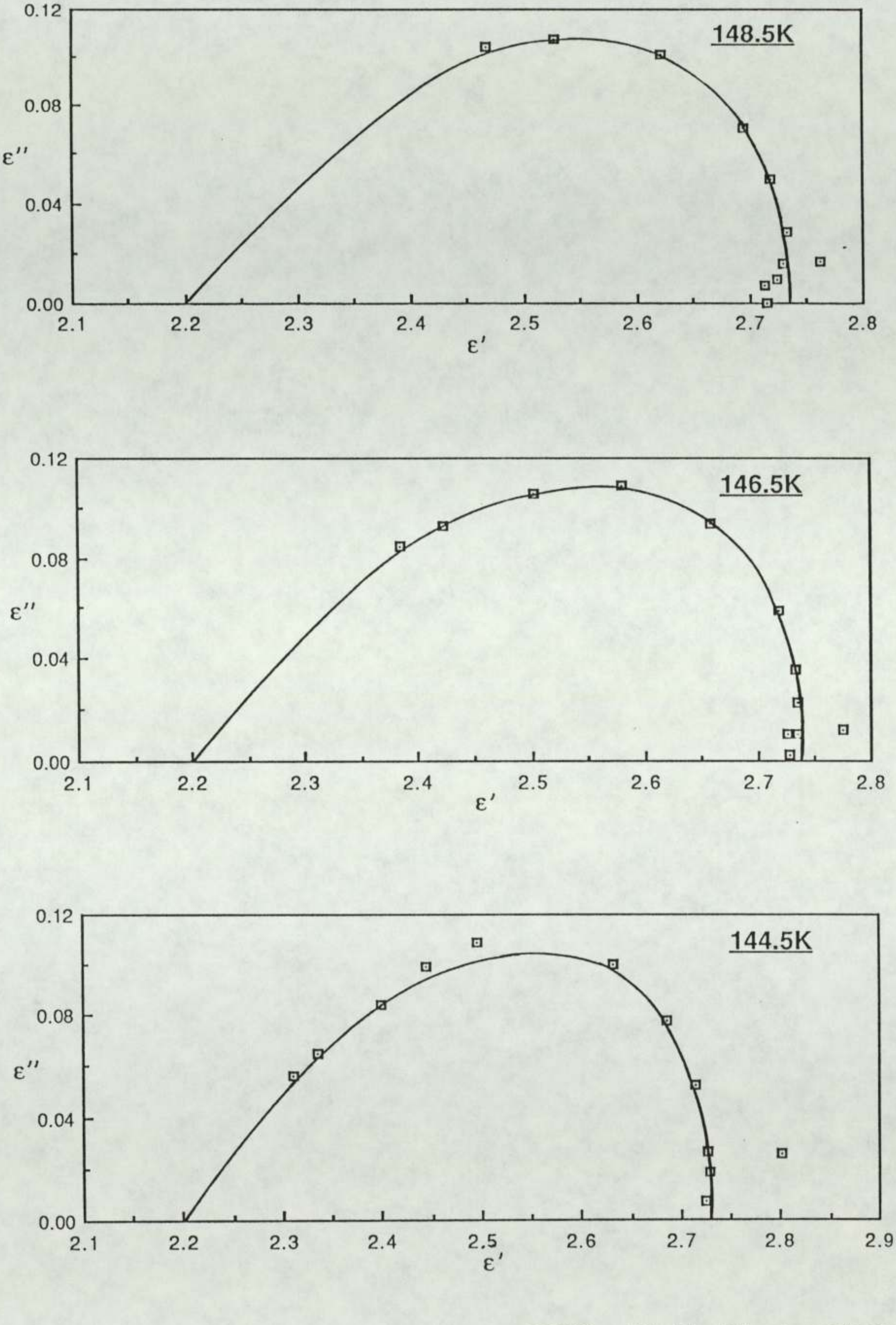

Figure (5-33) Cole-Cole plots for linear PDMS with $\bar{n}_n$=34 at various temperatures

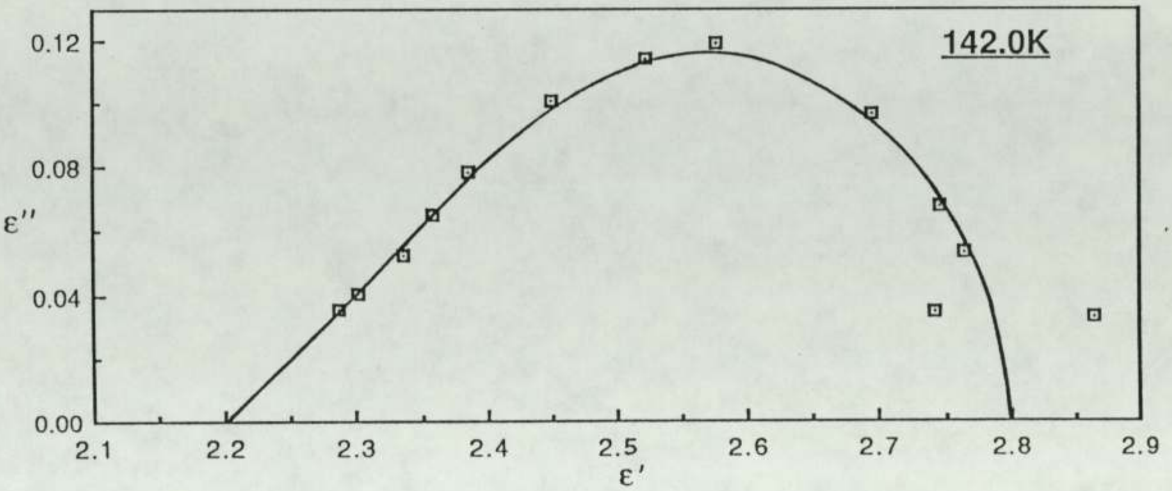

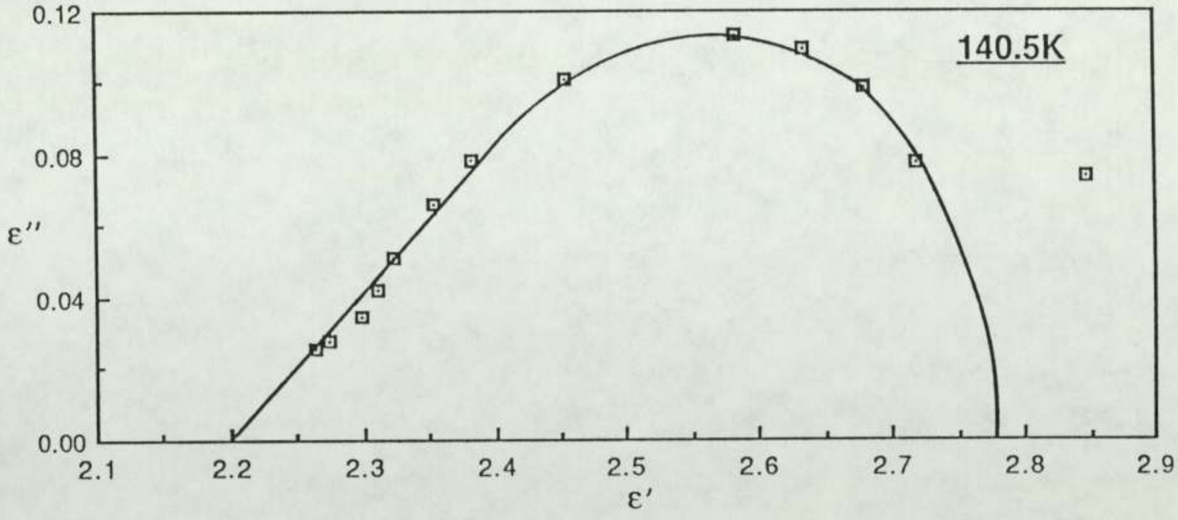

Figure (5-34) Cole-Cole plots for linear PDMS with $\bar{n}_n$=34 at various temperatures

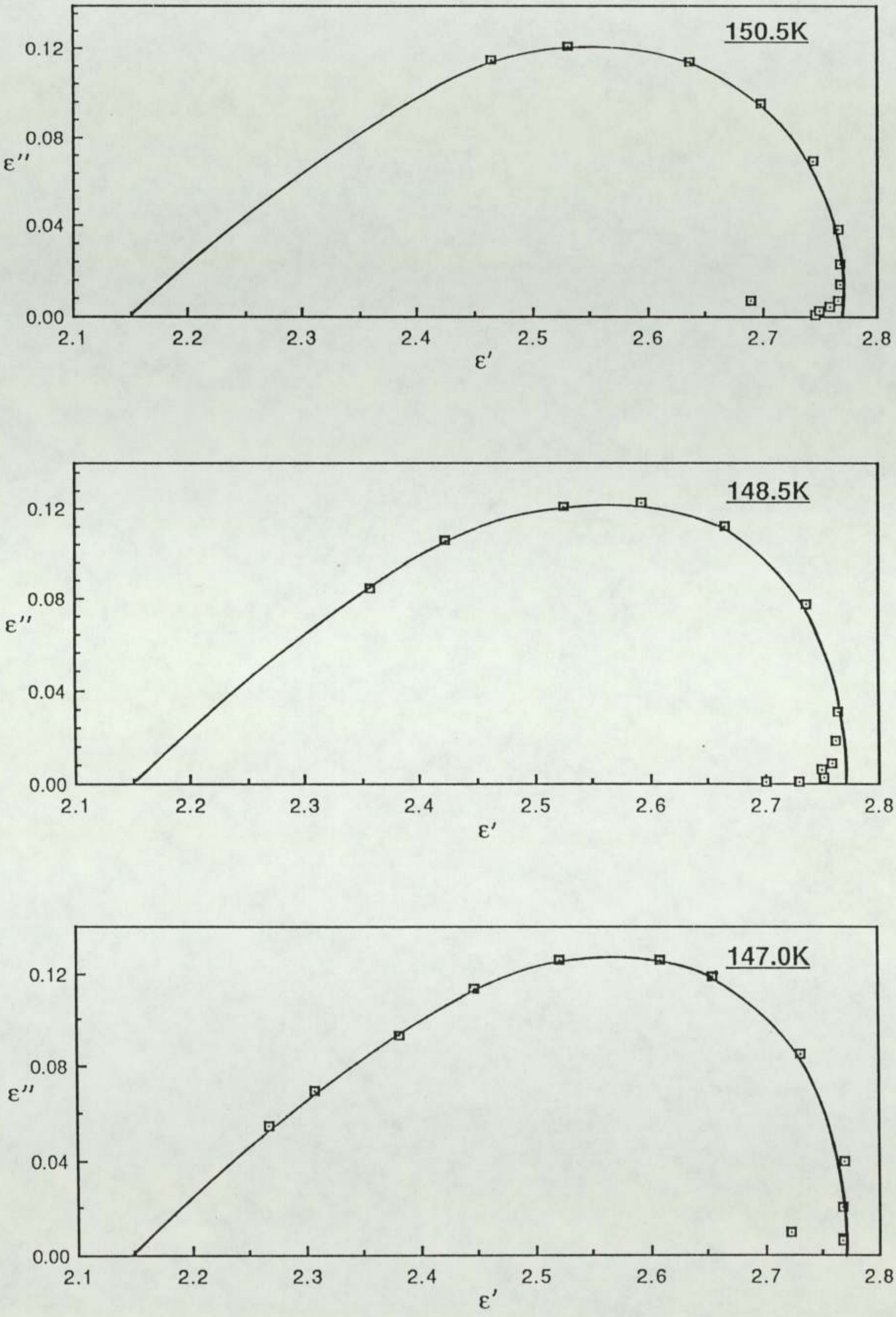

Figure (5-35) Cole-Cole plots for linear PDMS with $\bar{n}_n$=57 at various temperatures

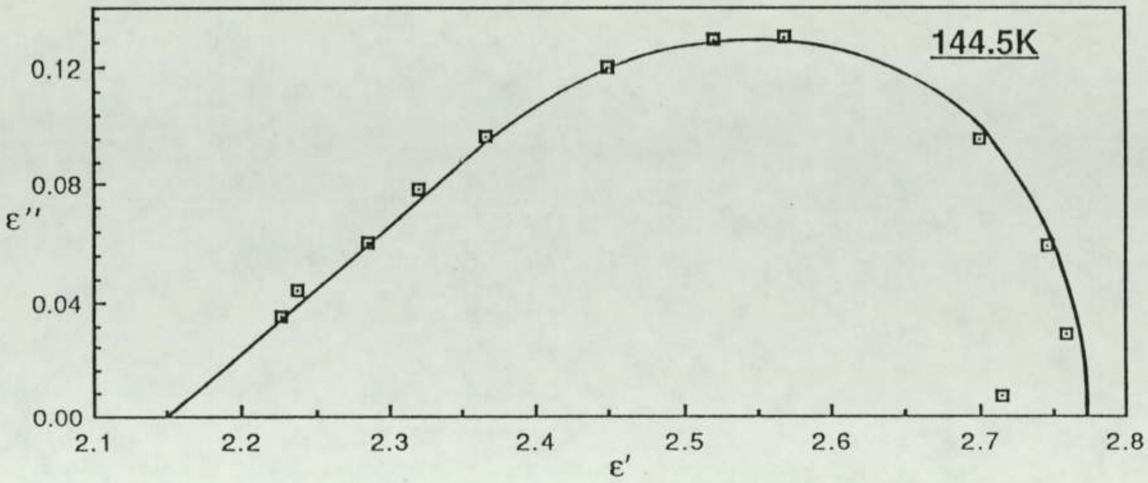

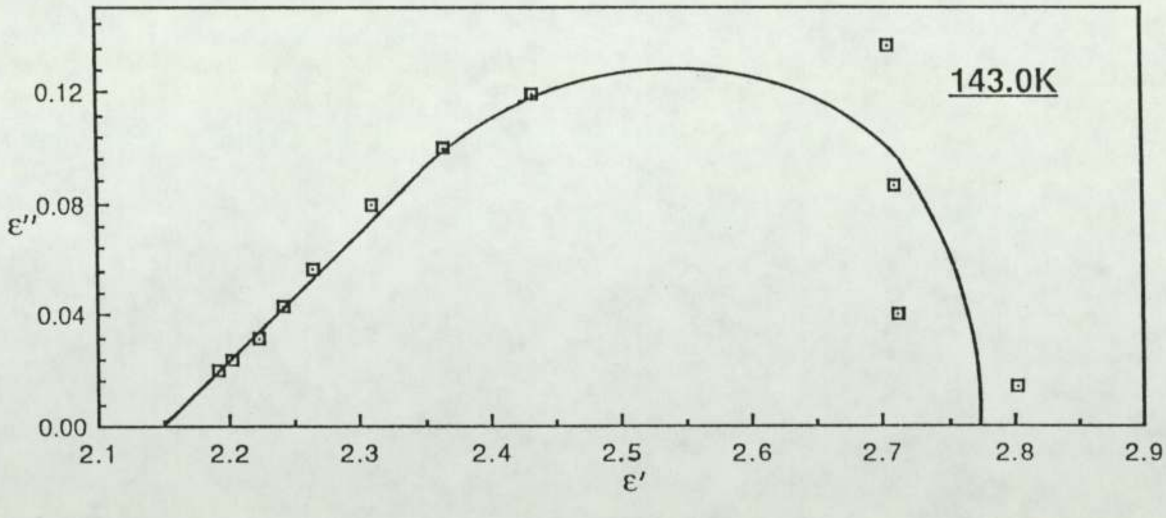

Figure (5-36) Cole-Cole plots for linear PDMS with $\bar{n}_n$=57 at various temperatures

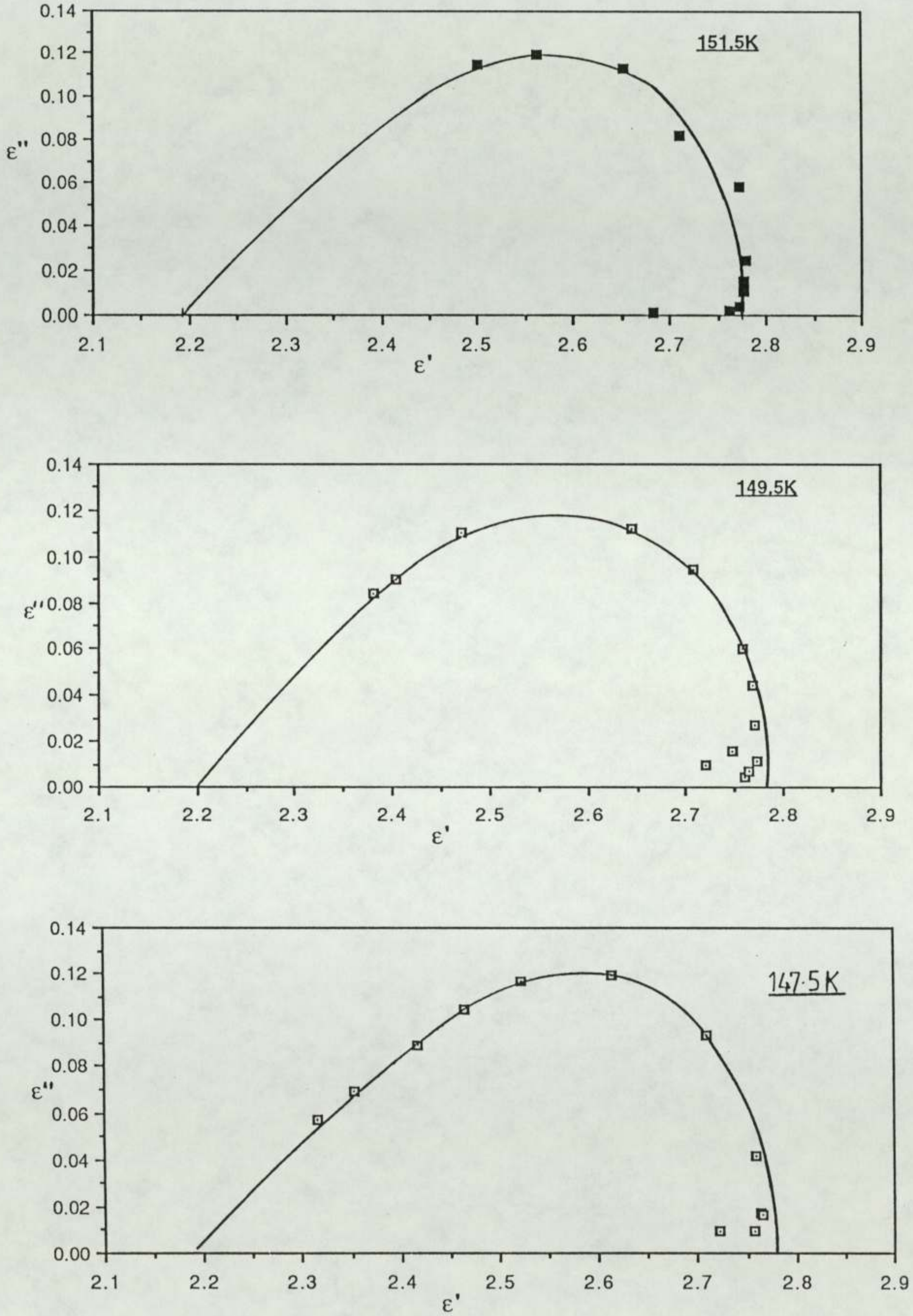

Figure (5-37) Cole-Cole plots for linear PDMS with $\bar{n}_n$=72 at various temperatures

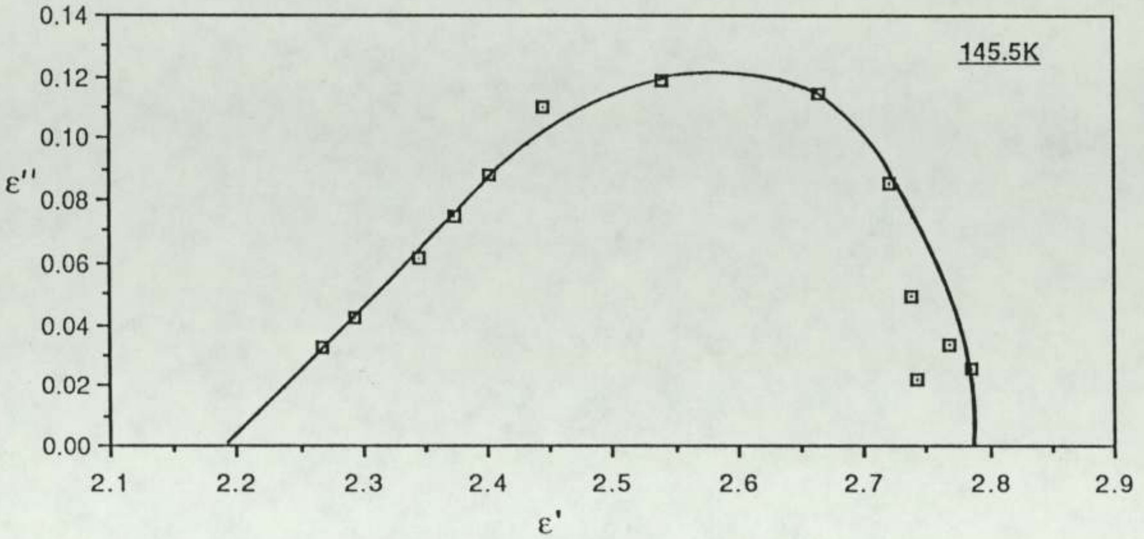

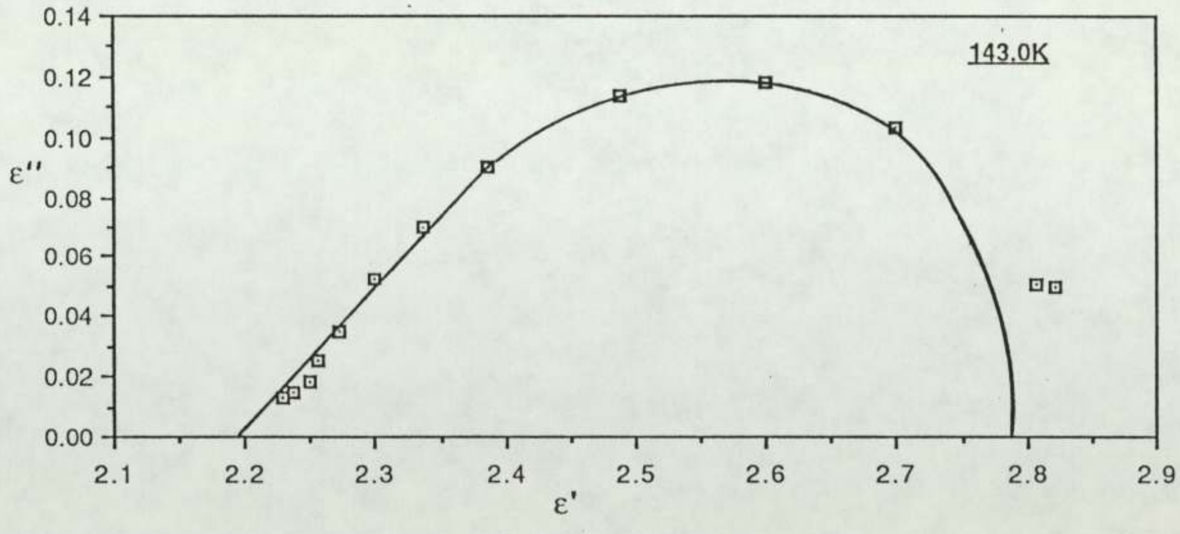

Figure (5-38) Cole-Cole plots for linear PDMS with $\bar{n}_n$=72 at various temperatures

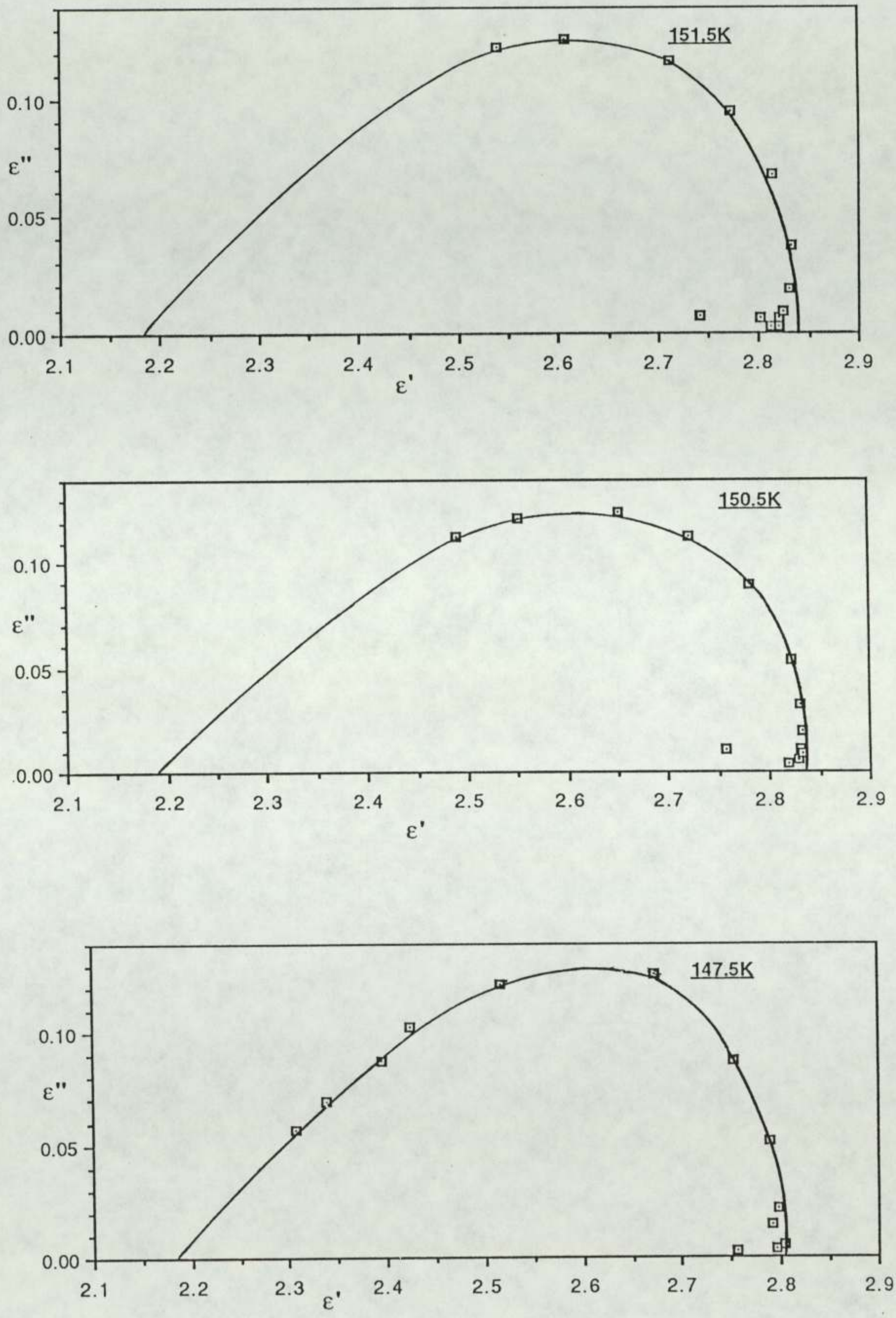

Figure (5-39) Cole-Cole plots for linear PDMS with $\bar{n}_n$=86 at various temperatures

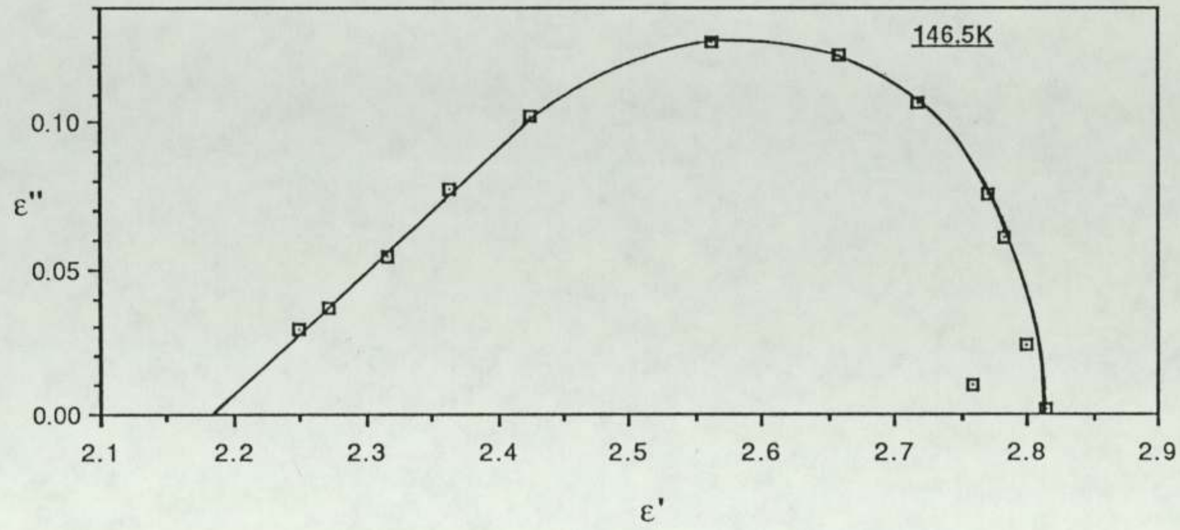

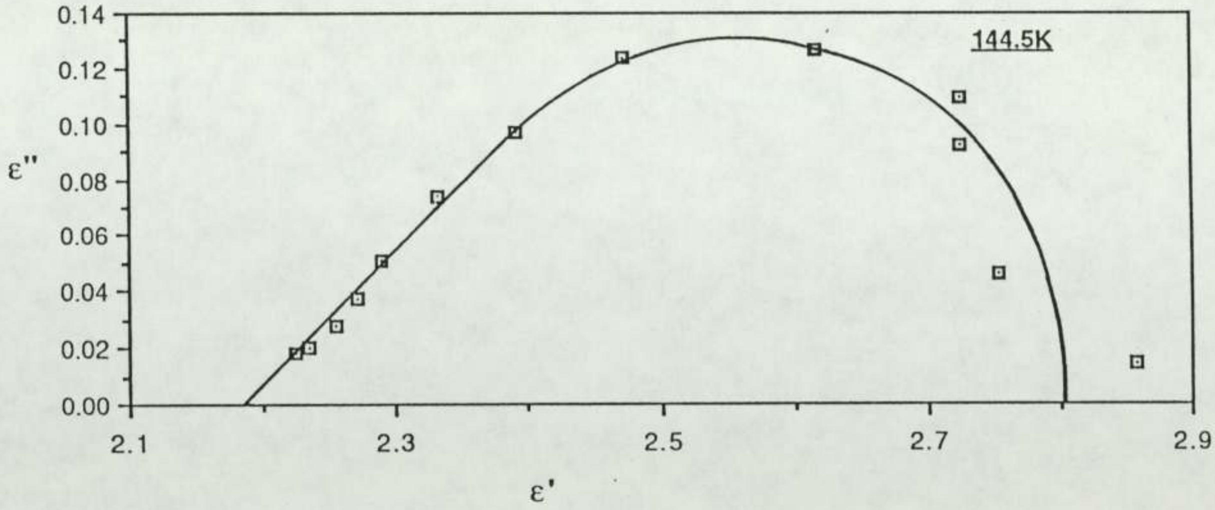

Figure (5-40) Cole-Cole plots for linear PDMS with $\bar{n}_n$ =86 at various temperatures

Davidson-Cole distribution factor, β.

A comparison of the values of permittivity obtained for cyclic and linear fractions of PDMS reveals a range of values for both ε_0 and ε_∞. For cyclic fractions of PDMS ε_0 varies between 2.67±0.02 and 2.83±0.02, while ε_∞ varies between 2.12±0.02 and 2.22±0.02. For linear fractions of PDMS the ε_0 range is 2.73±0.02 to 2.82±0.02 and the ε_∞ range is 2.15±0.02 to 2.20±0.02. The range of ε_0 and ε_∞ values found in this study may, in part, be attributed to experimental error. Additionally, ε_0 and ε_∞ do not appear to exhibit dependence on molecular weight in the range $\bar{n}_n$=28-**99** for cyclics, and in the range $\bar{n}_n$=28-86 for linears.

The magnitude of the dielectric dispersion, $\Delta\varepsilon = (\varepsilon_0 - \varepsilon_\infty)$, lies between 0.58 and 0.63 for cyclic fractions of PDMS and between 0.55 and 0.64 for linear fractions of PDMS. These values differ significantly from a $\Delta\varepsilon$ value of 0.82 measured by Adachi and co-workers[38], with T = 152.5K-155.2K, for an amorphous sample of linear PDMS, possessing an approximate molecular weight of 8.3×10^5. For a partially crystalline sample of linear PDMS, with T=155K-169K, Baird and co-workers[36] reported a $\Delta\varepsilon$ value in the range 0.30-0.45. This lower range of $\Delta\varepsilon$ values, compared to the present study, is probably due to the crystallinity of the sample. For a series of linear dimethyl siloxane oligomers, with n varying between 4 and 12, in the fluid state at 298K, Dasgupta and co-workers[31] reported a maximum $\Delta\varepsilon$ value of 0.29. The difference in the value of $\Delta\varepsilon$ reported by Dasgupta and the higher value of $\Delta\varepsilon$ measured in the present study may be due to the effect of the higher temperature employed in the study carried out by Dasgupta and co-workers.

An examination of the values of the maximum dielectric loss obtained in the present study suggests that differences in values of ε''_{max} for cyclic fractions of PDMS and linear fractions of PDMS are due to experimental errors and that a molecular weight dependence is not detectable. The values of ε''_{max} lie in the approximate range 0.11 to 0.13. For the respective materials mentioned above, Adachi and co-workers reported a value of $\varepsilon''_{max} > 0.2$, Baird and co-workers reported a value of ε''_{max} in the range 0.045-0.049 and Dasgupta and co-workers reported a value of ε''_{max}, equal to 0.11, for a linear oligomer with n =12.

5.05: Dielectric Properties of Oligomers of Methyl Phenyl Siloxane and Poly(methyl phenyl siloxane).

The dielectric relaxation behaviour of a series of undiluted, linear methyl phenyl siloxanes, a series of poly(methyl phenyl siloxanes) and one cyclic oligomer, has been studied as a function of temperature (155.5K-264.0K) and frequency (12Hz-10^5), using the dielectric apparatus described in Chapter 3.

5.06: The Dielectric Loss Results.

Normalised values of the product of the parallel capacitance, C_p, and the dissipation factor, $\tan\delta$, of a series of undiluted, linear methyl phenyl siloxanes, a series of poly(methyl phenyl siloxanes) and one cyclic oligomer, are plotted as a function of the logarithm of the frequency, in Hz, of the applied field in Figures (5-41) to (5-51). The presence of a broad α-type relaxation is readily discernible. There is a steady shift of the frequency corresponding to maximum dielectric loss, $f_{(max)}$, within the frequency range 12-10^5Hz, towards higher temperatures for the oligomers of phenyl methyl siloxane and a greater shift towards even higher temperatures for fractions of PMPS and the cyclic oligomer of methyl phenyl siloxane, as the sample viscosities increase with molecular weight. The width of the loss curves at half height is approximately two decades of frequency, which is comparable to the width at half height measured by Baird and co-workers[37] for an oligomer of methyl phenyl siloxane with a most probable value of n equal to 12.

5.07: Dielectric Relaxation Activation Energy.

Arrhenius plots of the logarithm of the frequency corresponding to maximum dielectric loss plotted against the reciprocal of the absolute temperature, are shown in Figures (5-52) to (5-59), for a series of oligomers of methyl phenyl siloxane, fractions of PDMS and a cyclic methyl phenyl siloxane. All the plots are linear, within experimental error, with a slope proportional to the activation energy for the α-relaxation process.

5.08: Cole-Cole Plots.

Figures (5-60) to (5-81) are Cole-Cole plots of ε" against ε' for oligomers of methyl phenyl siloxane, fractions of PMPS and a cyclic oligomer of methyl phenyl siloxane at various temperatures. The values of ε" and ε' are corrected to allow for the contraction in the volume of the polymer

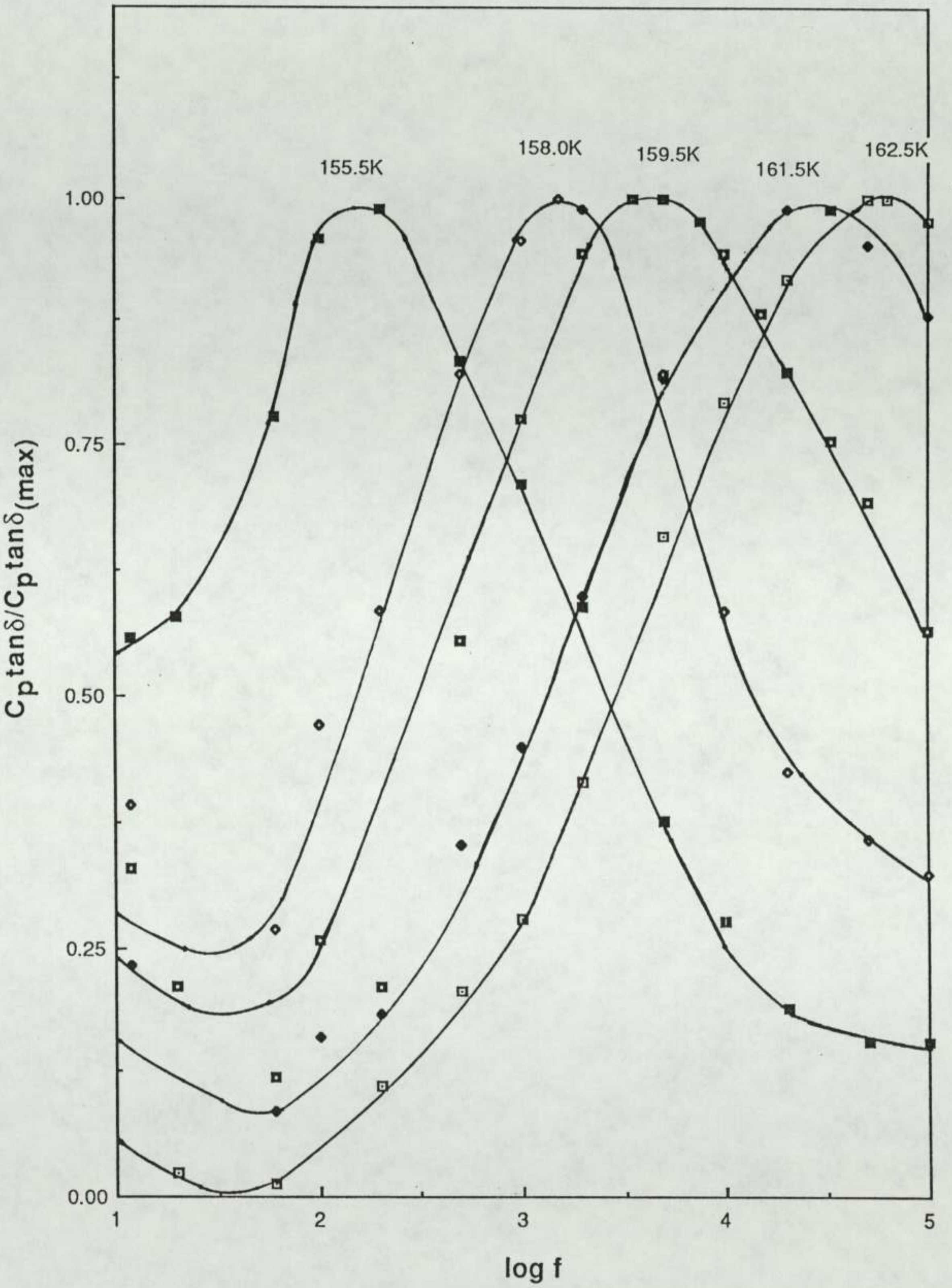

Figure (5-41). Frequency dependence of $C_p\tan\delta/C_p\tan\delta_{(max)}$ for linear MPS with n=4 at various temperatures.

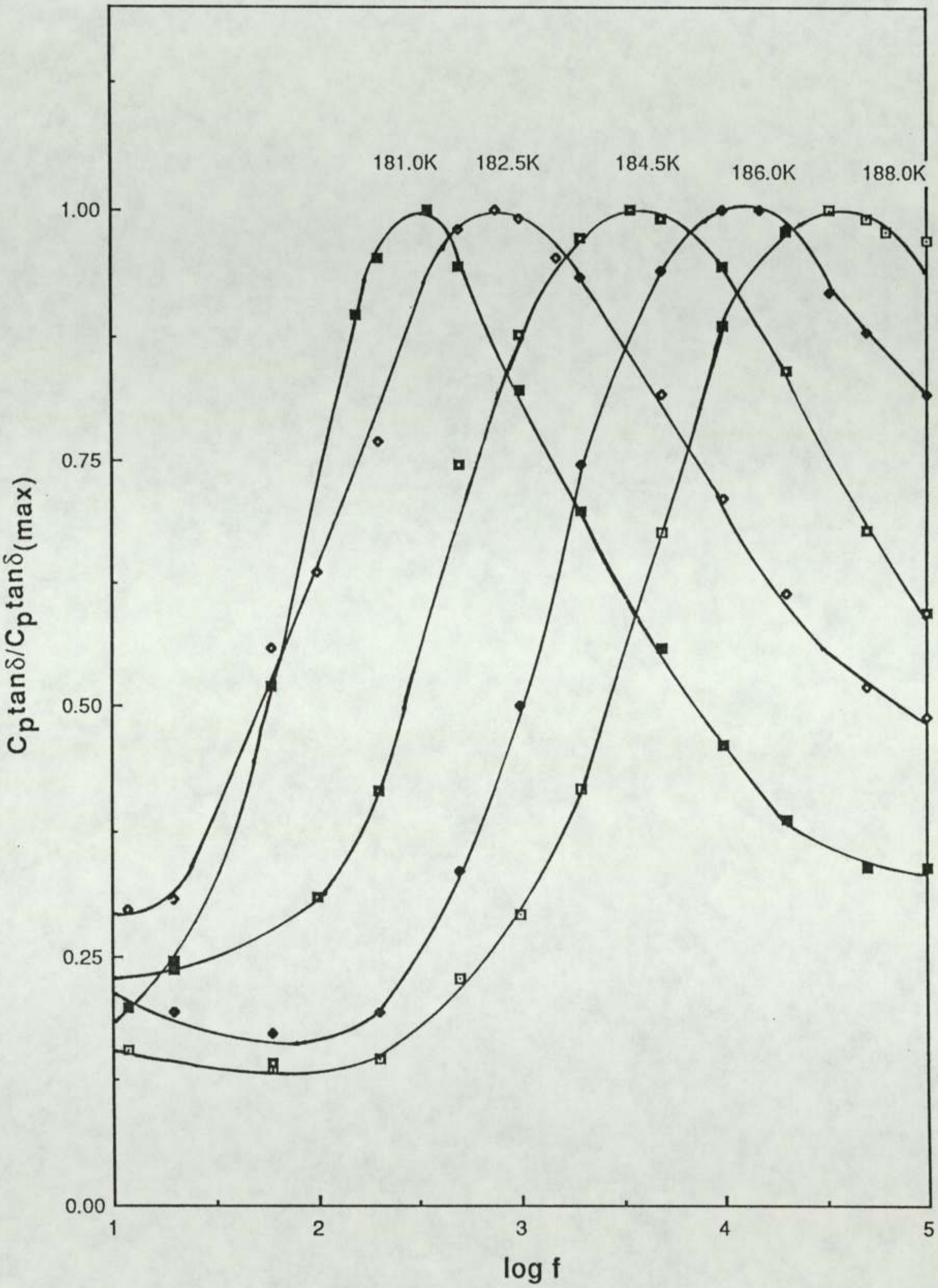

<u>Figure (5-42).</u> **Frequency dependence of $C_p\tan\delta/C_p\tan\delta_{(max)}$ for linear MPS with n=6 at various temperatures.**

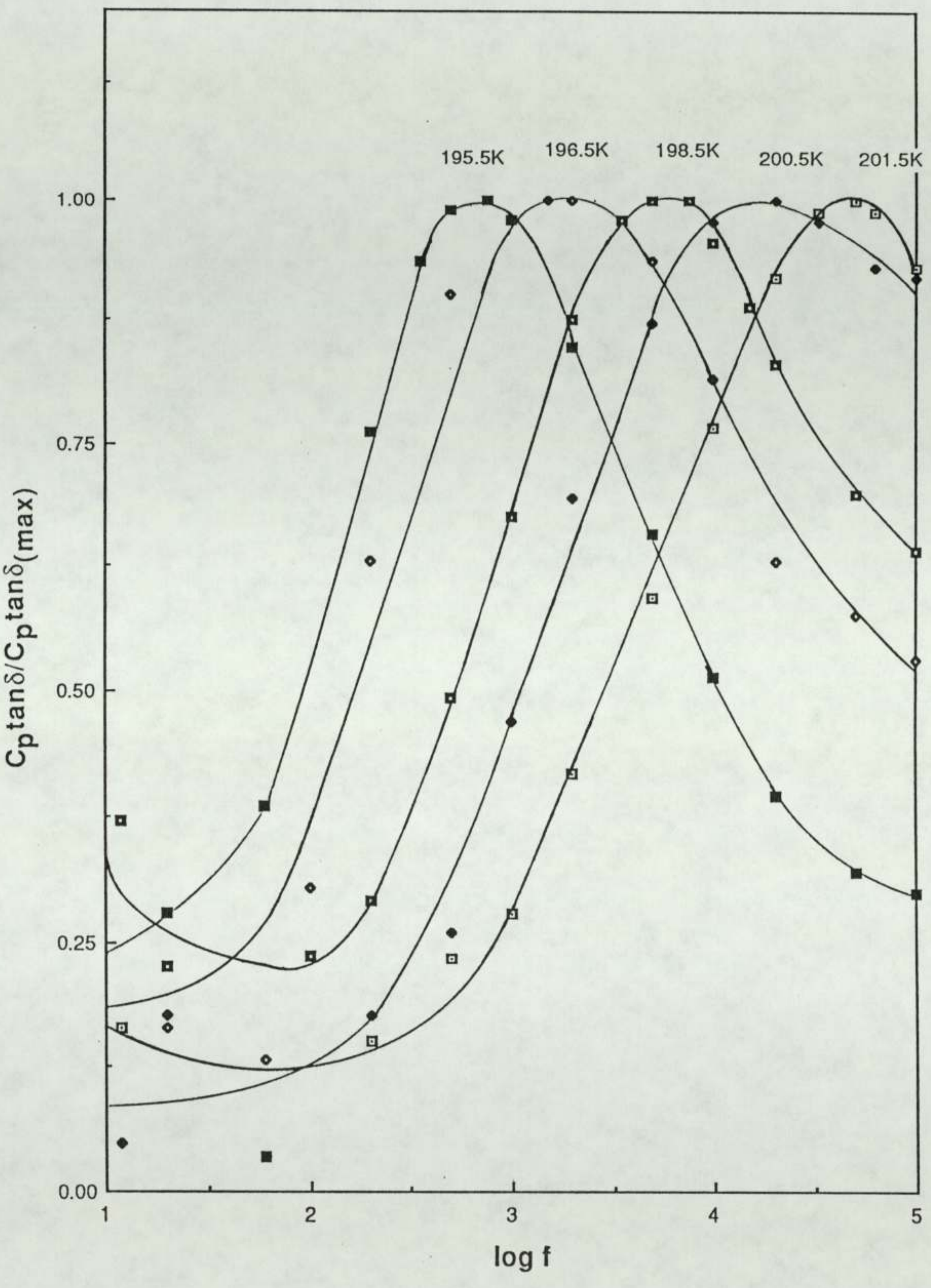

Figure (5-43). Frequency dependence of $C_p\tan\delta/C_p\tan\delta_{(max)}$ for linear MPS with n=8 at various temperatures.

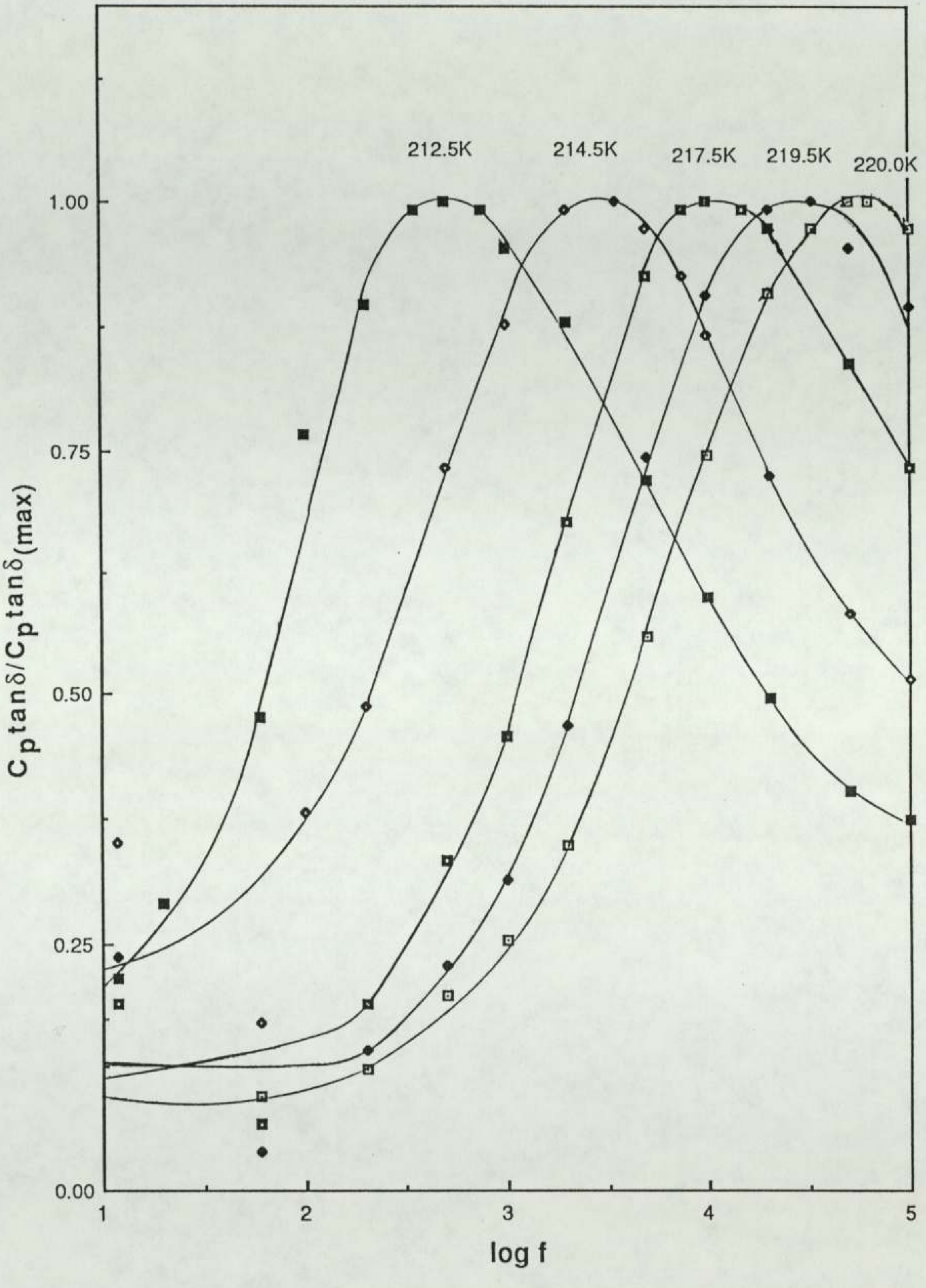

Figure (5-44). Frequency dependence of $C_p\tan\delta/C_p\tan\delta_{(max)}$ for linear MPS with n=10 at various temperatures.

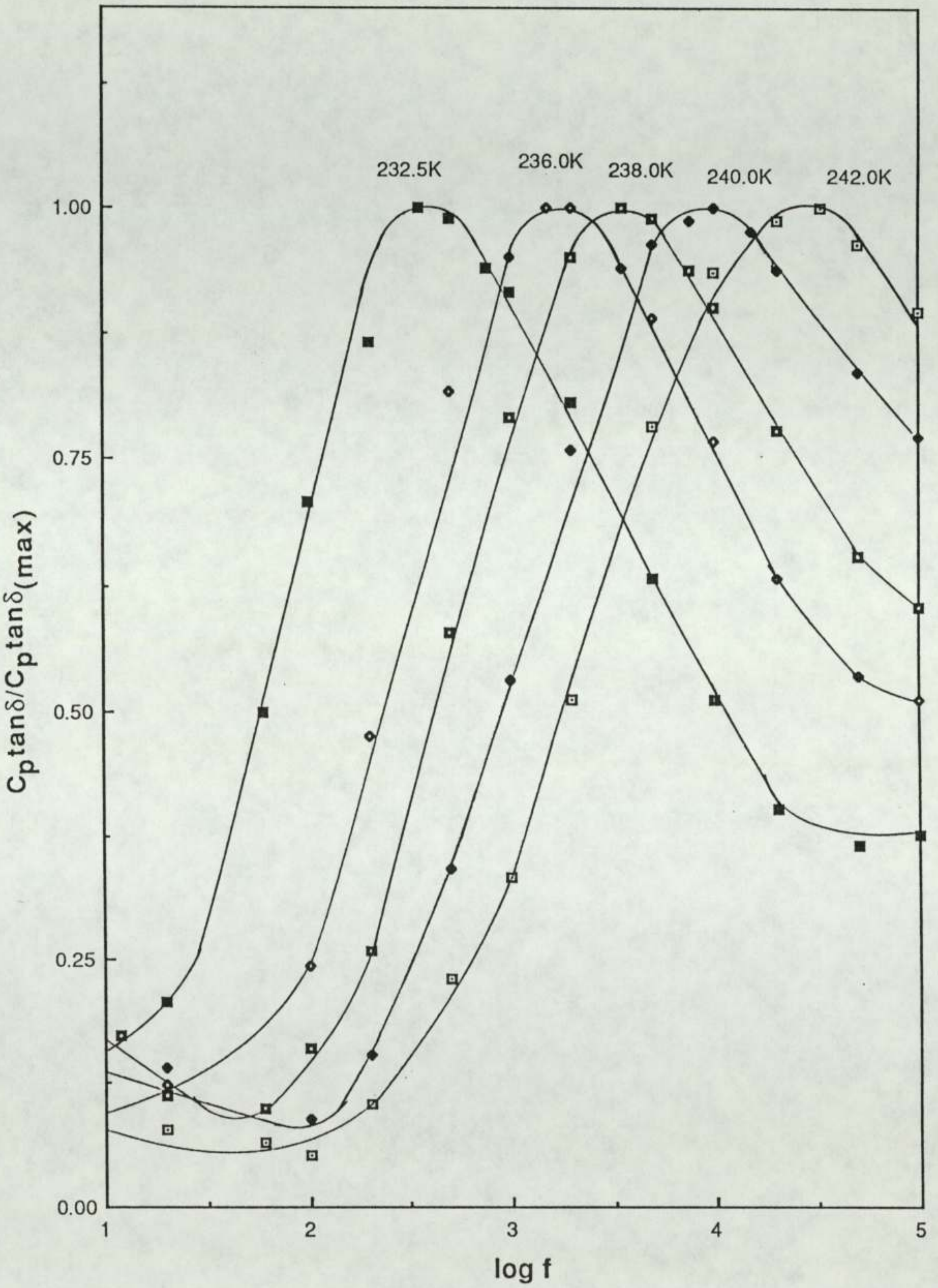

Figure (5-45). Frequency dependence of $C_p\tan\delta/C_p\tan\delta_{(max)}$ for linear PMPS with $\bar{n}_n$=31 at various temperatures.

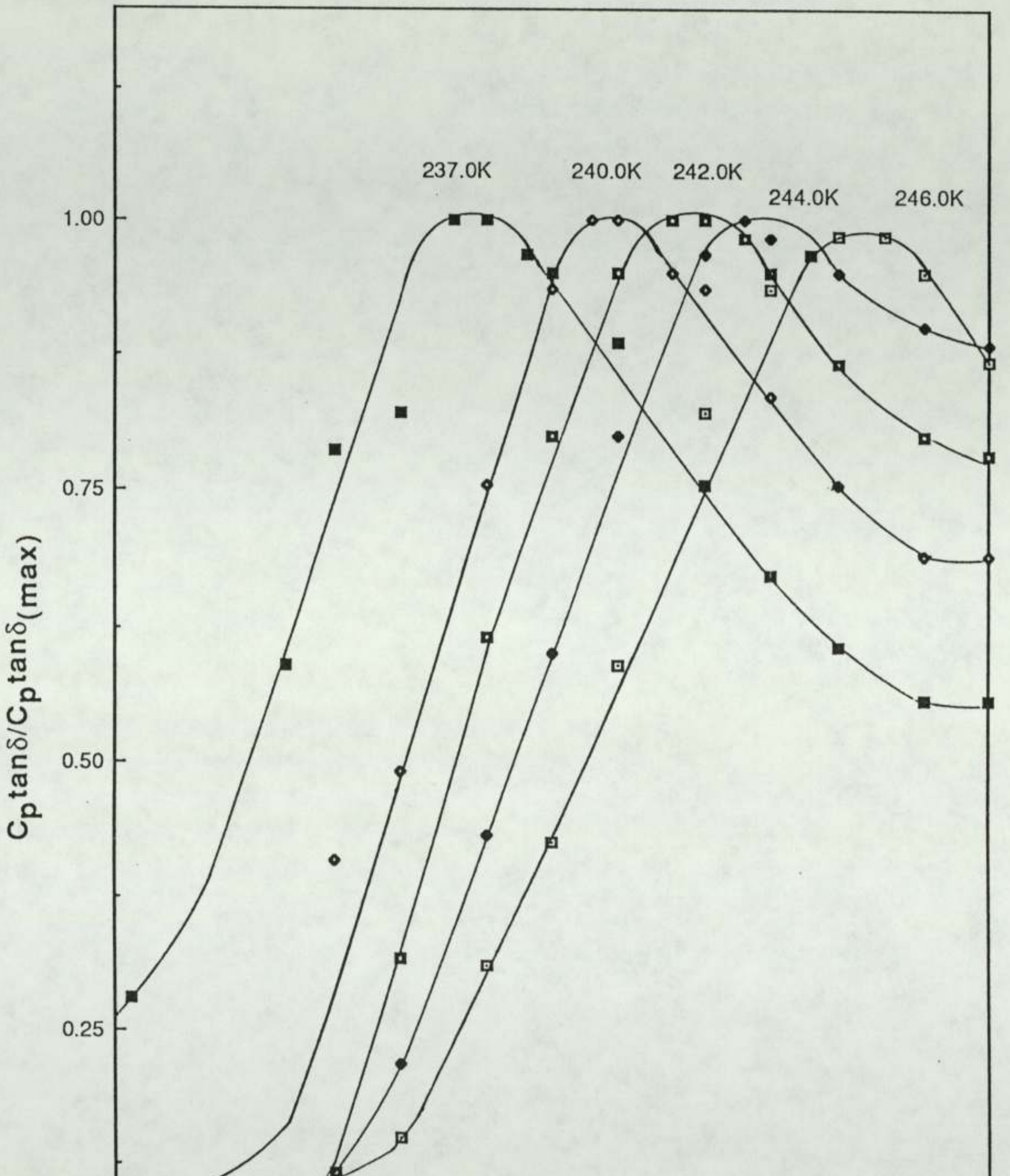

Figure (5-46). Frequency dependence of $C_p \tan\delta / C_p \tan\delta_{(max)}$ for linear PMPS with $\bar{n}_n$=50.5 at various temperatures.

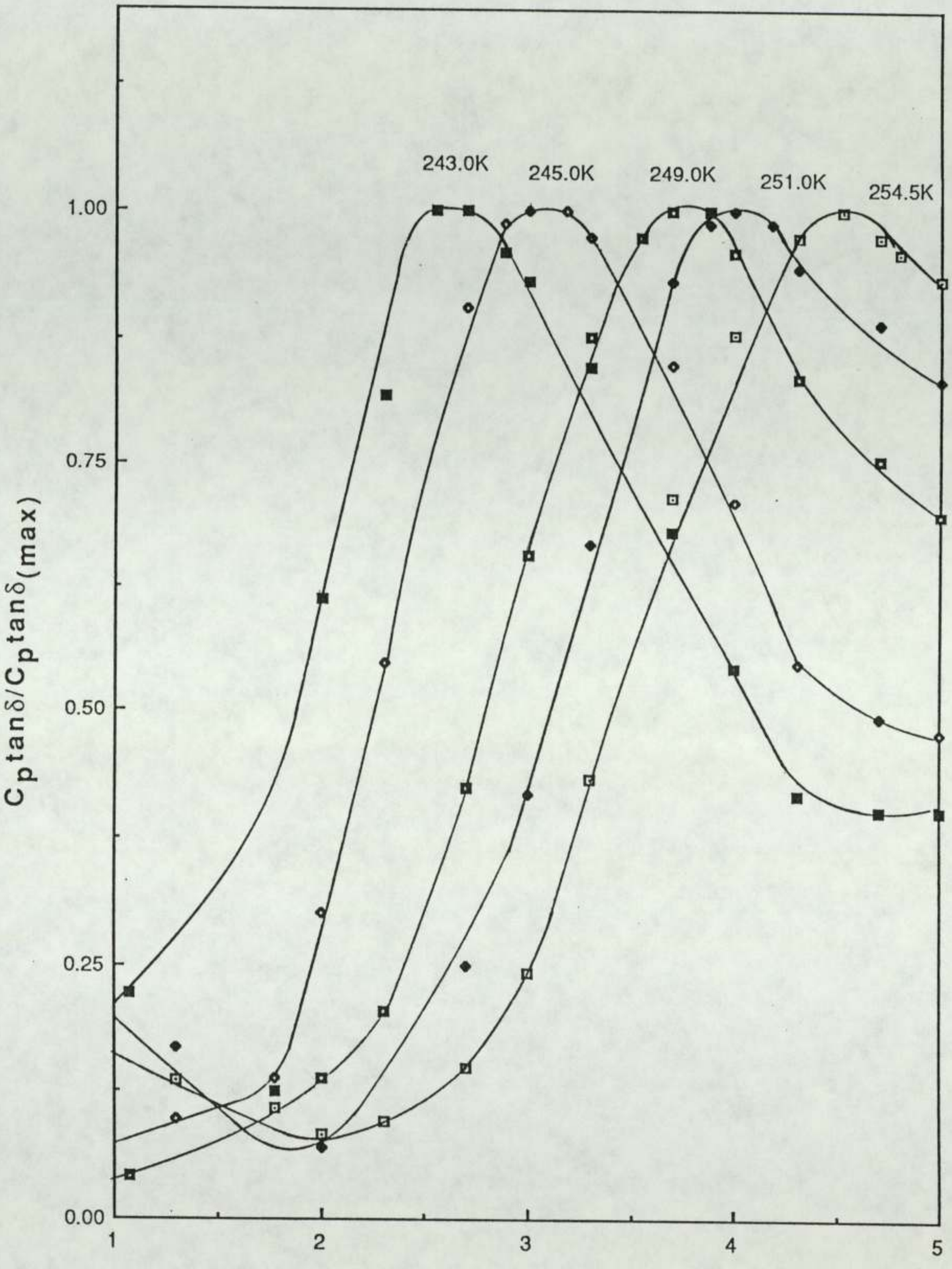

Figure (5-47). Frequency dependence of $C_p\tan\delta/C_p\tan\delta_{(max)}$ for linear PMPS with $\bar{n}_n$=82 at various temperatures.

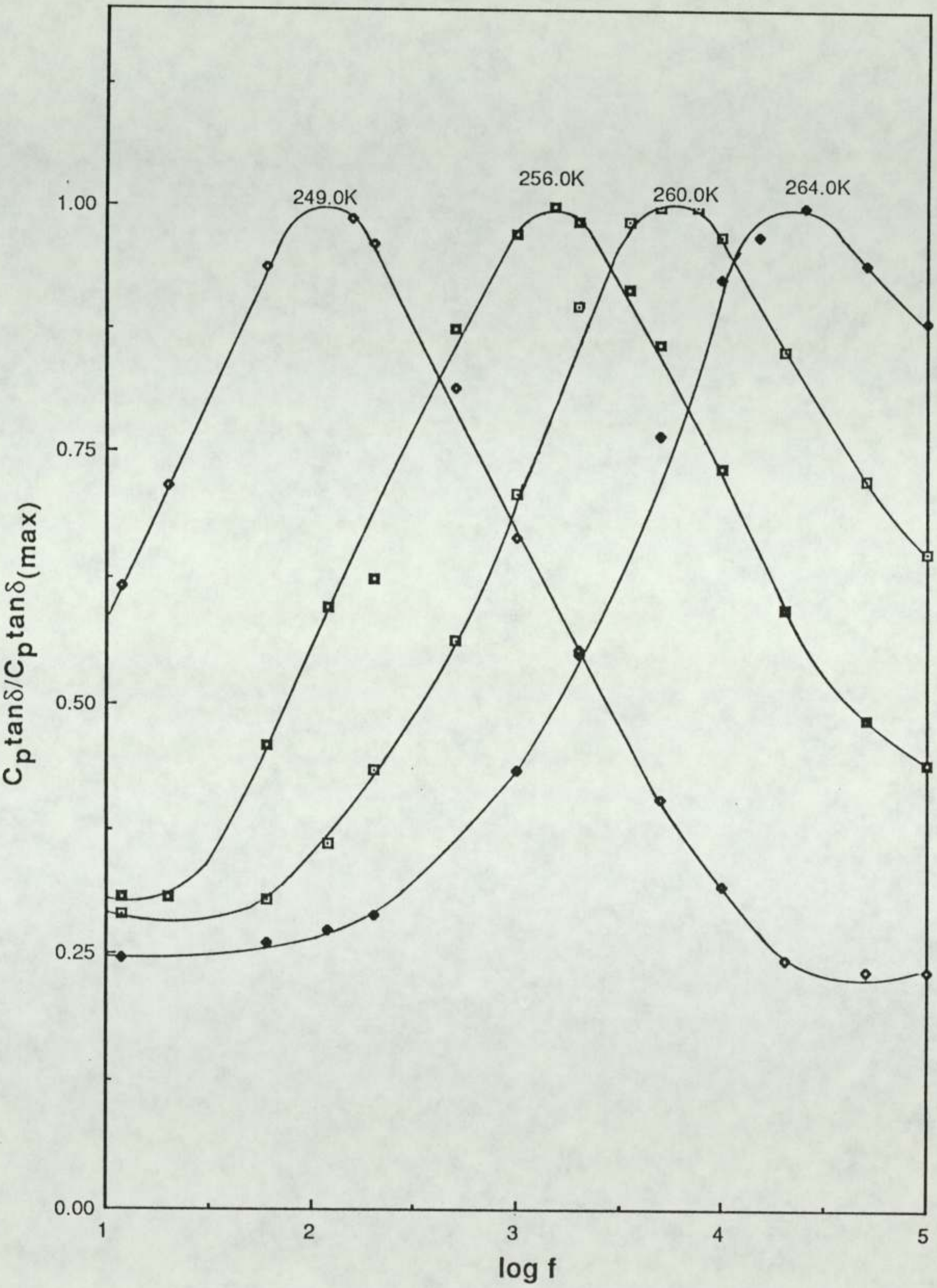

Figure (5-48). Frequency dependence of $C_p\tan\delta/C_p\tan\delta_{(max)}$ for linear PMPS with $\bar{n}_n$=153 at various temperatures.

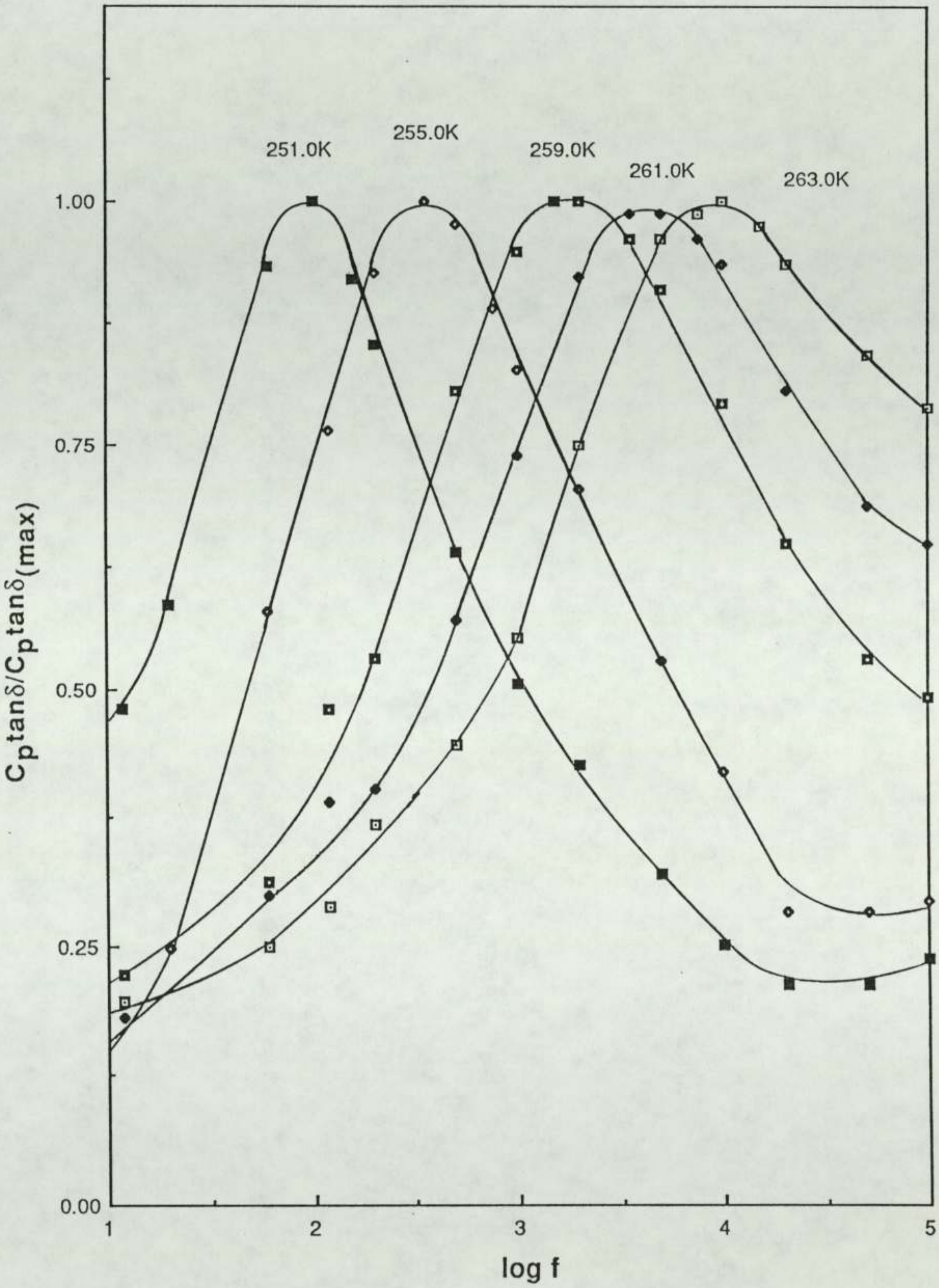

Figure (5-49). Frequency dependence of $C_p\tan\delta/C_p\tan\delta_{(max)}$ for linear PMPS with $\bar{n}_n$=284 at various temperatures.

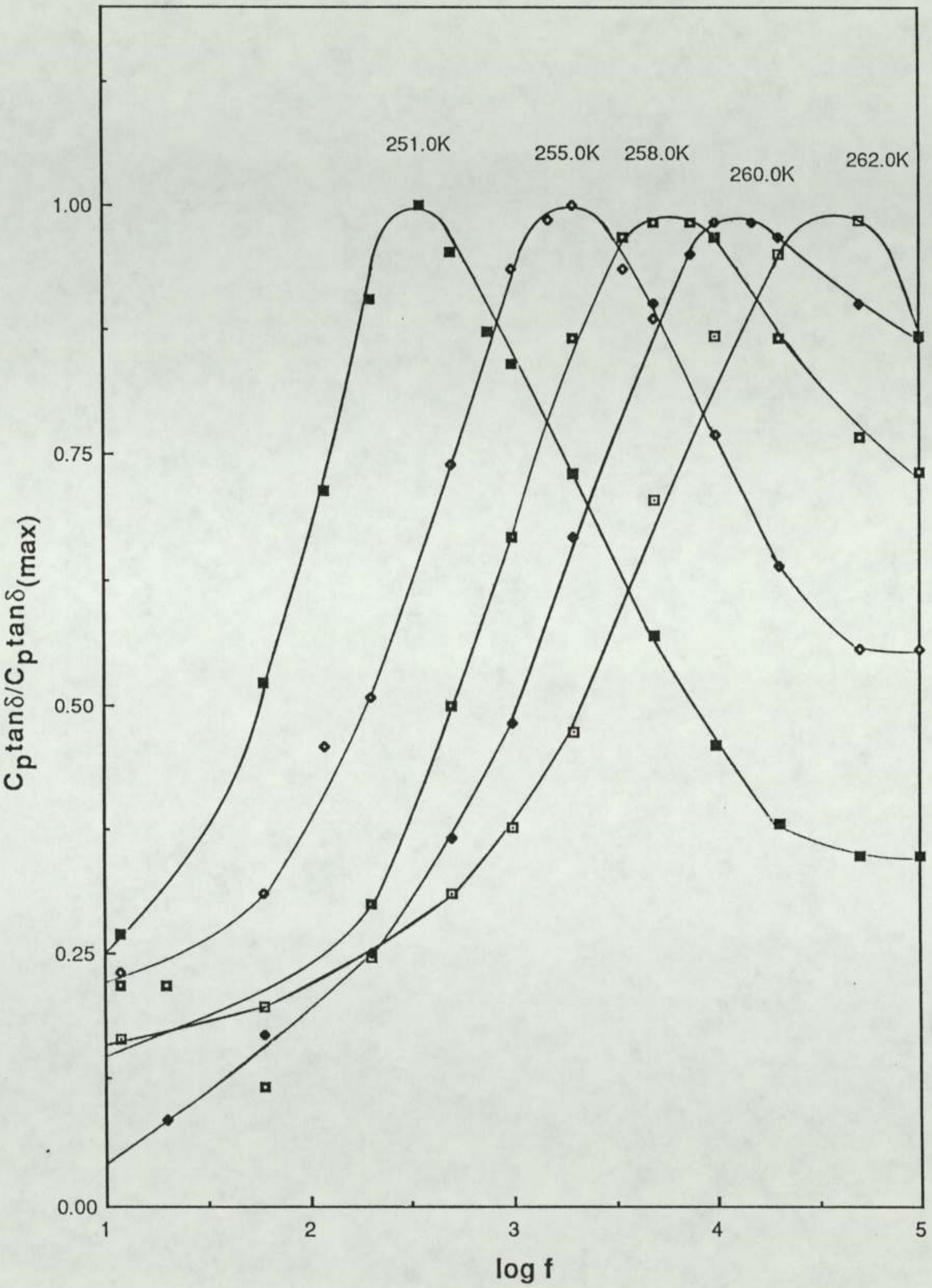

<u>Figure (5-50).</u> Frequency dependence of $C_p\tan\delta/C_p\tan\delta_{(max)}$ for linear PMPS with $\bar{n}_n \sim 1370$ at various temperatures.

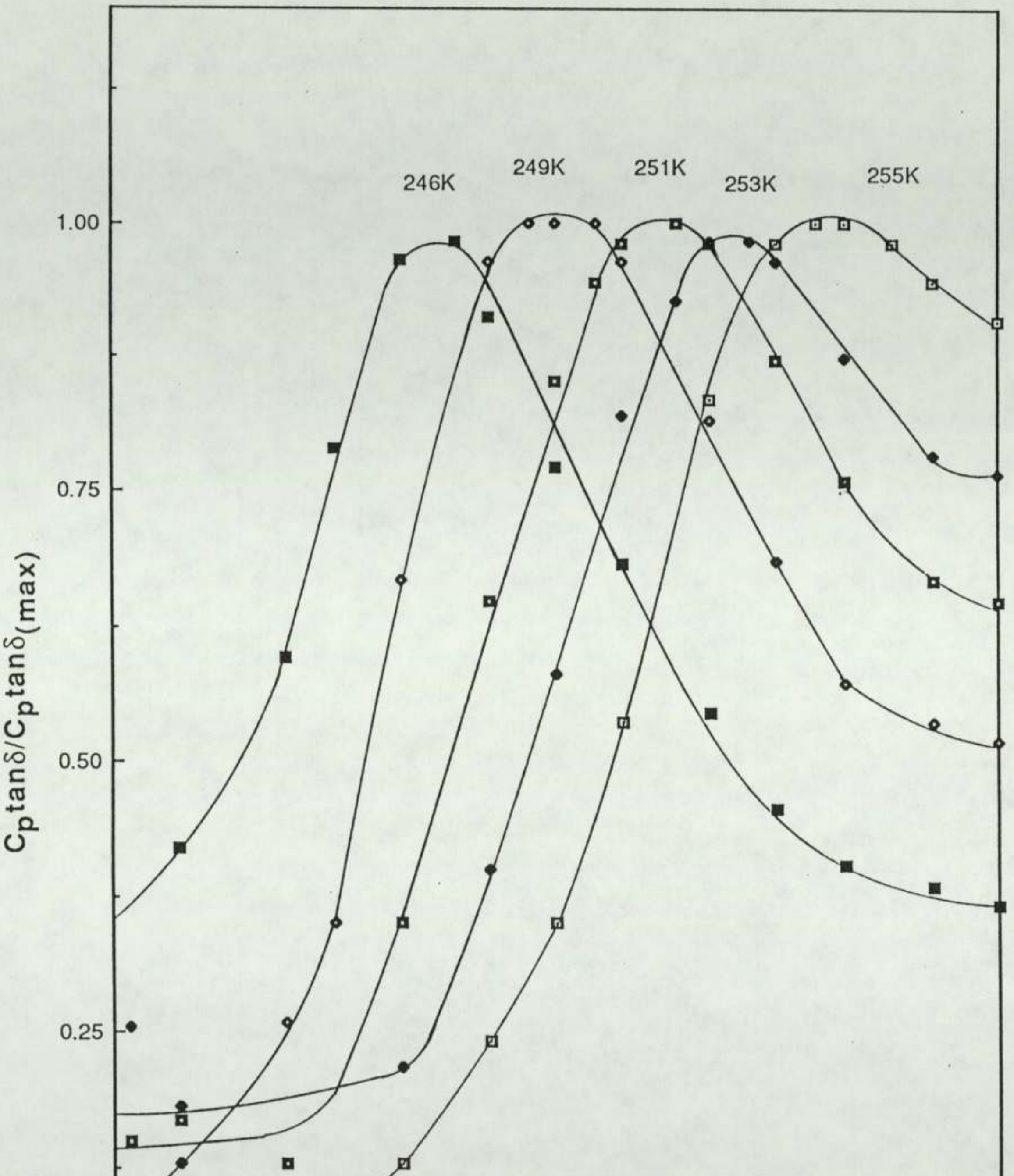

<u>Figure (5-51).</u> Frequency dependence of $C_p\tan\delta/C_p\tan\delta_{(max)}$ for cyclic MPS with n=10 at various temperatures.

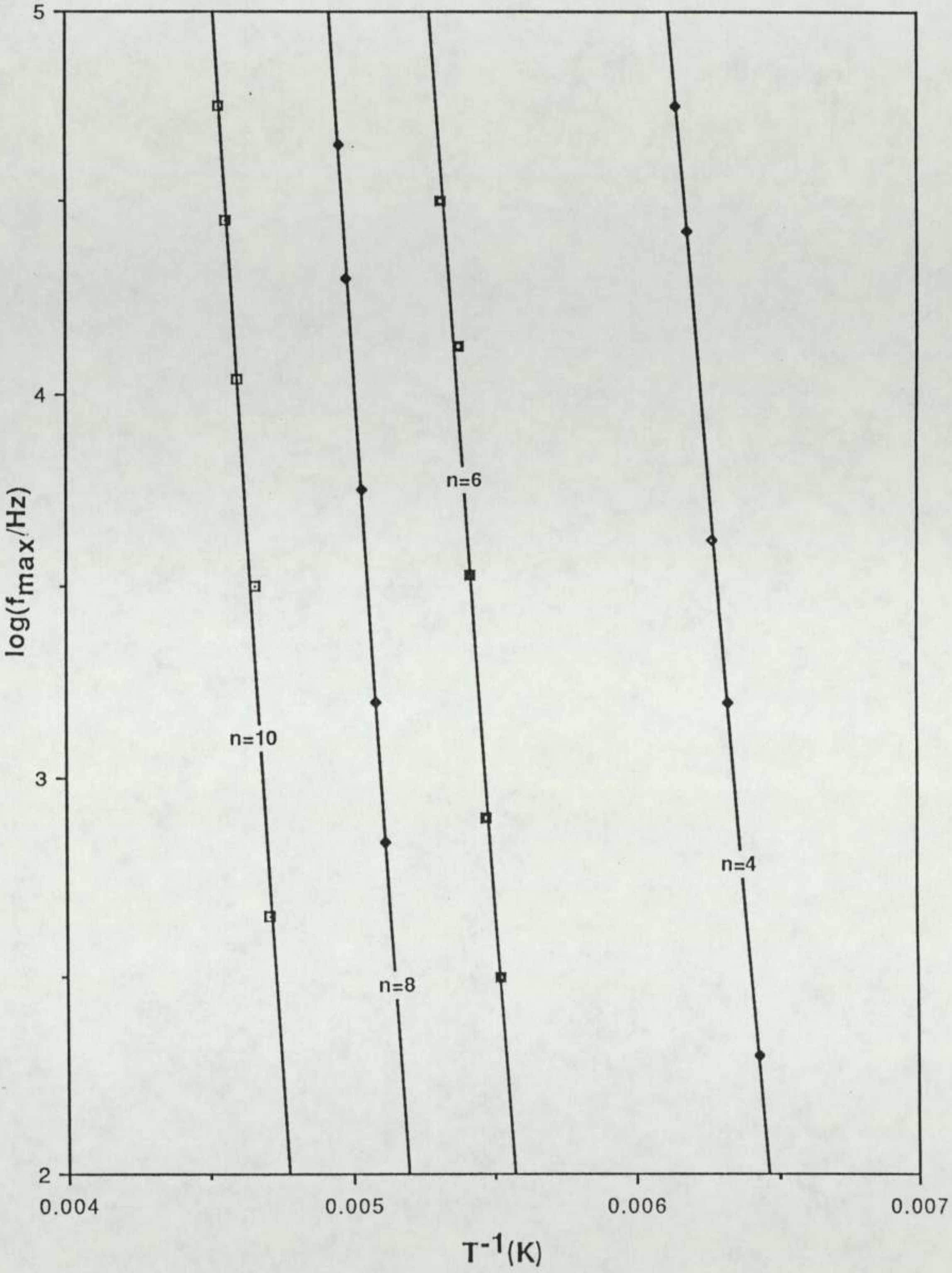

Figure(5-52) Log (f_{max}/Hz) against T^{-1}(K) for linear oligomers of methylphenyl siloxane

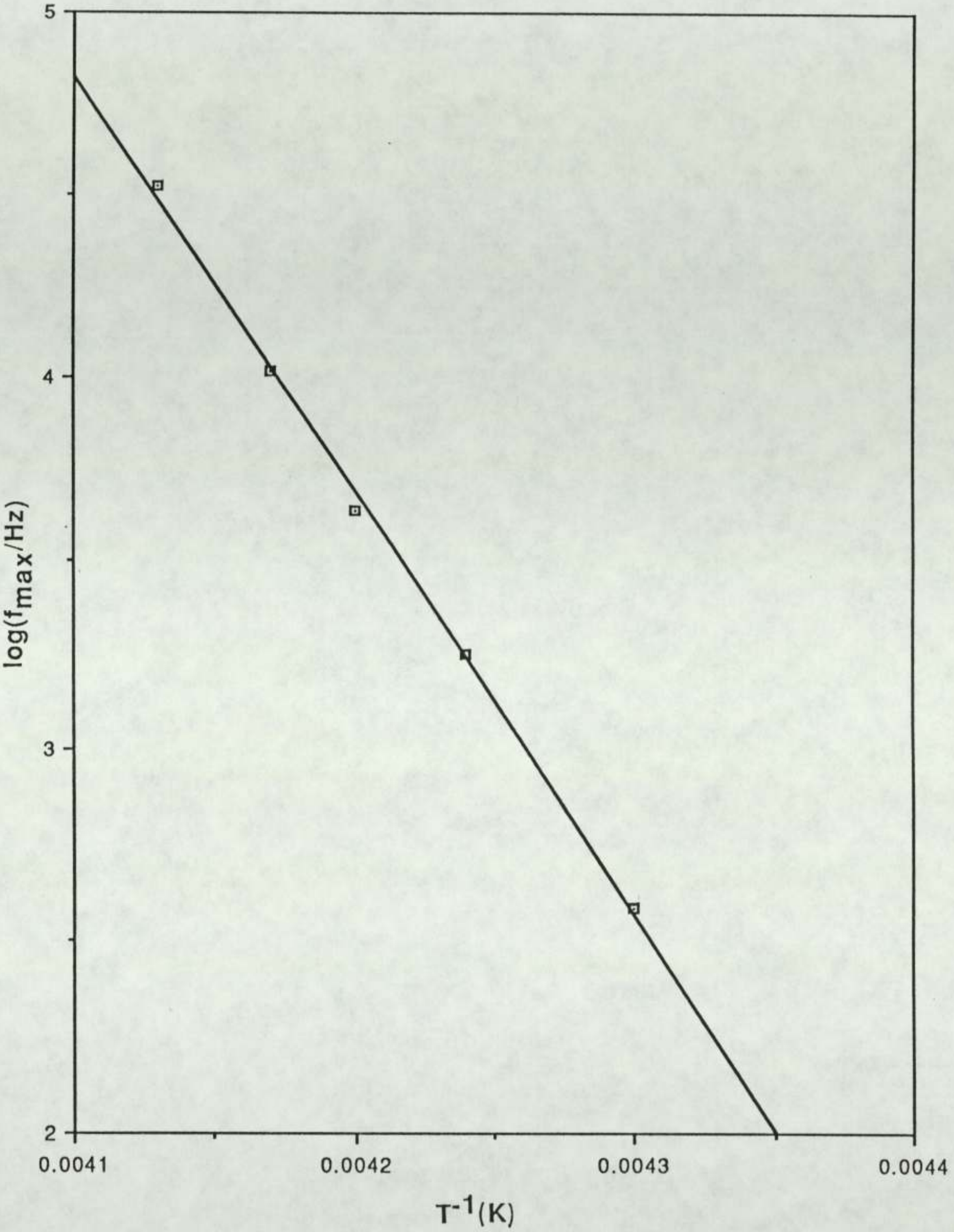

Figure (5-53) Log(f_{max}/Hz) against T^{-1}(K) for linear PMPS with $\bar{n}_n$=31

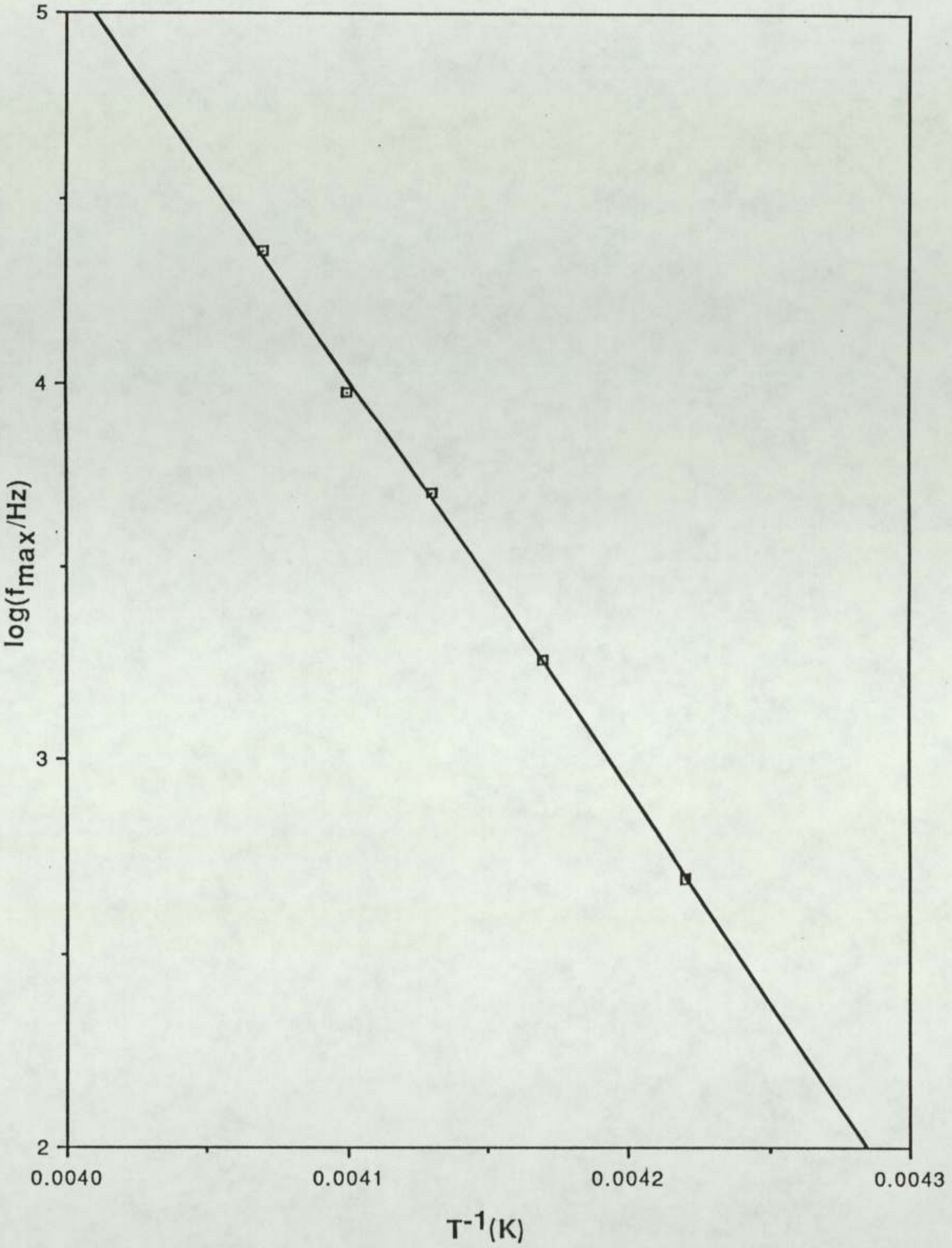

Figure (5-54) Log(f_{max}/Hz) against T^{-1} K for linear PMPS with $\bar{n}_n$=50.5

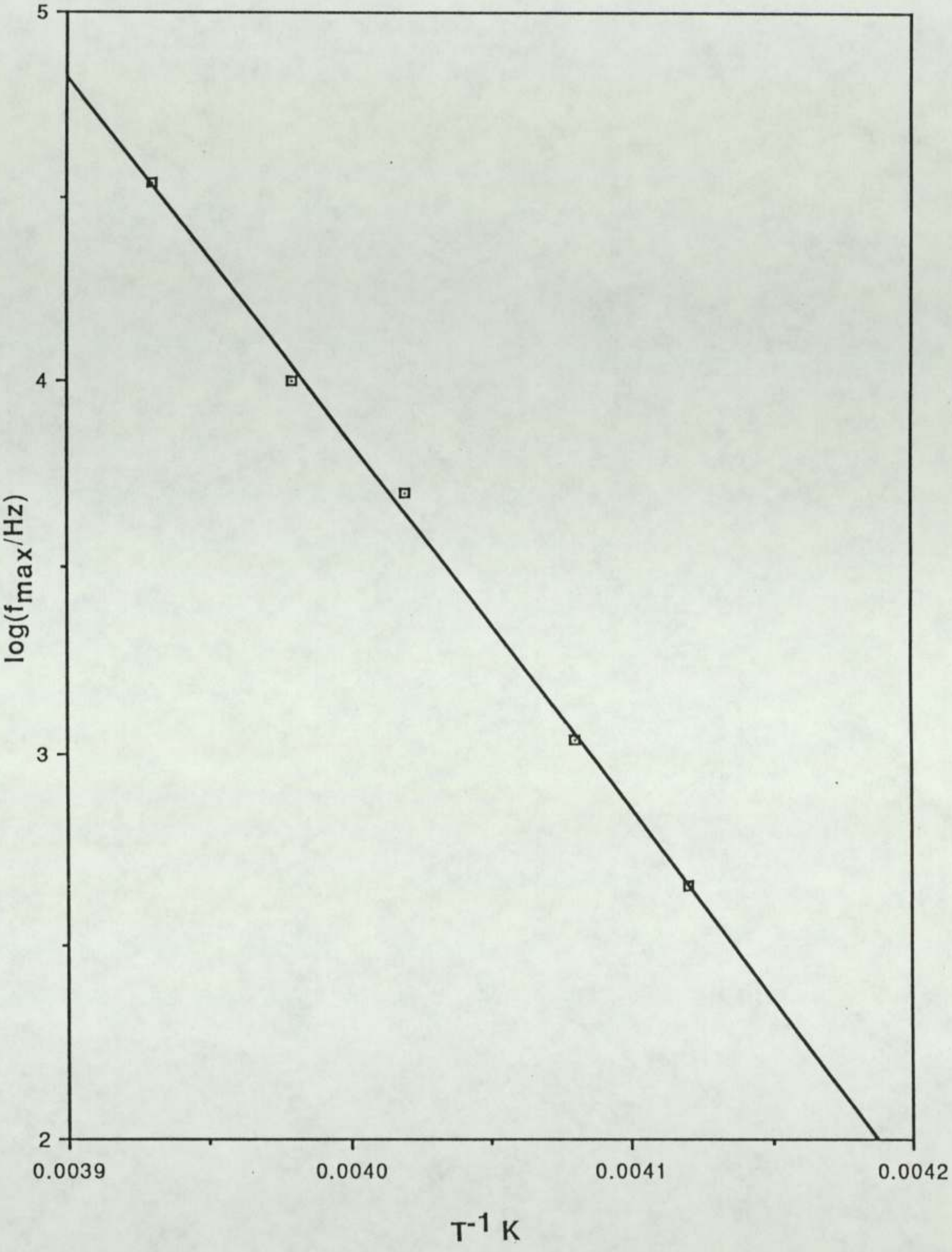

Figure (5-55) Log(f_{max}/Hz) against T^{-1} K for linear PMPS with $\bar{n}_n$=82

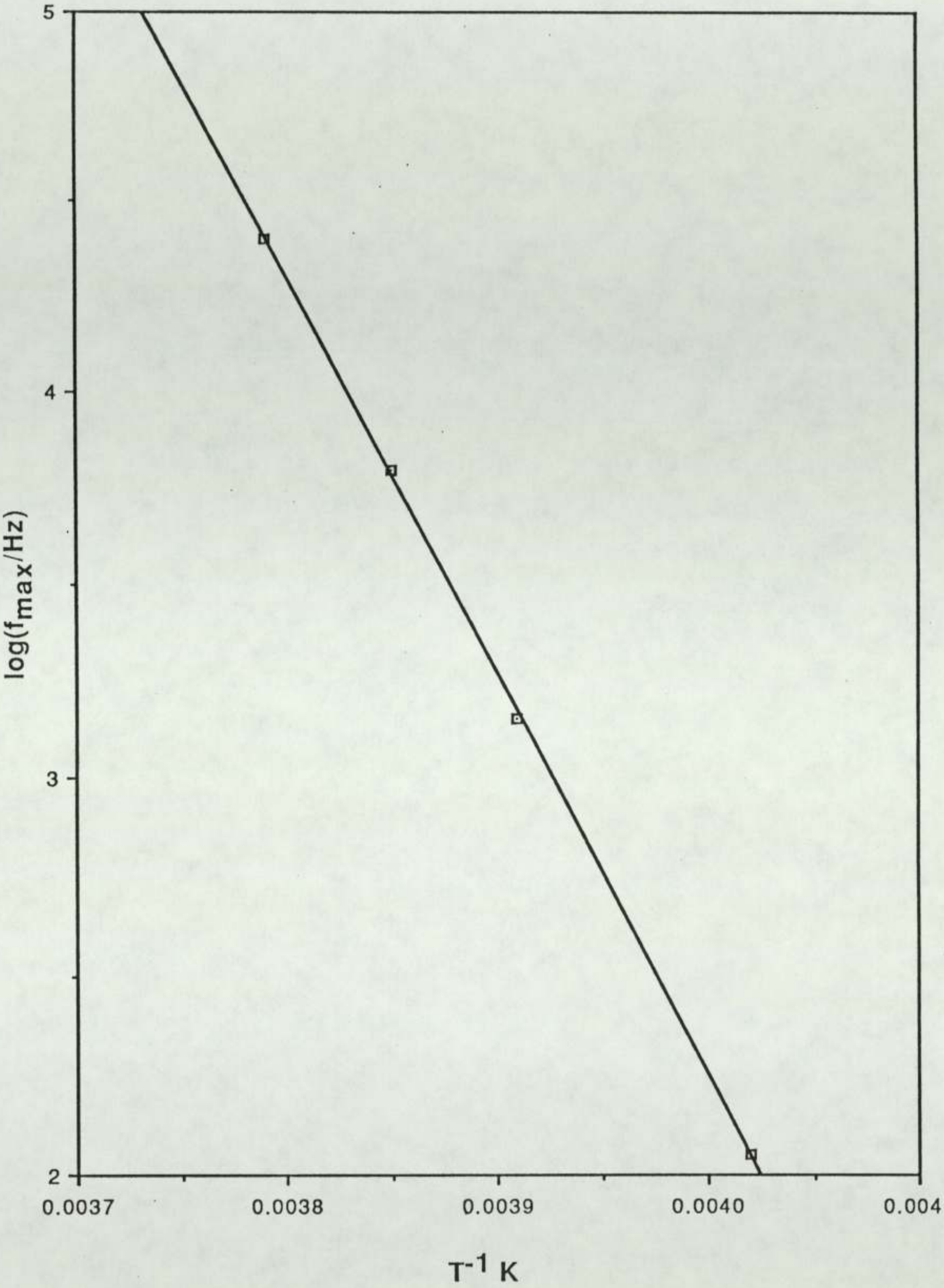

Figure (5-56) Log(f_{max}/Hz) against T^{-1} K for linear PMPS with $\bar{n}_n$=153

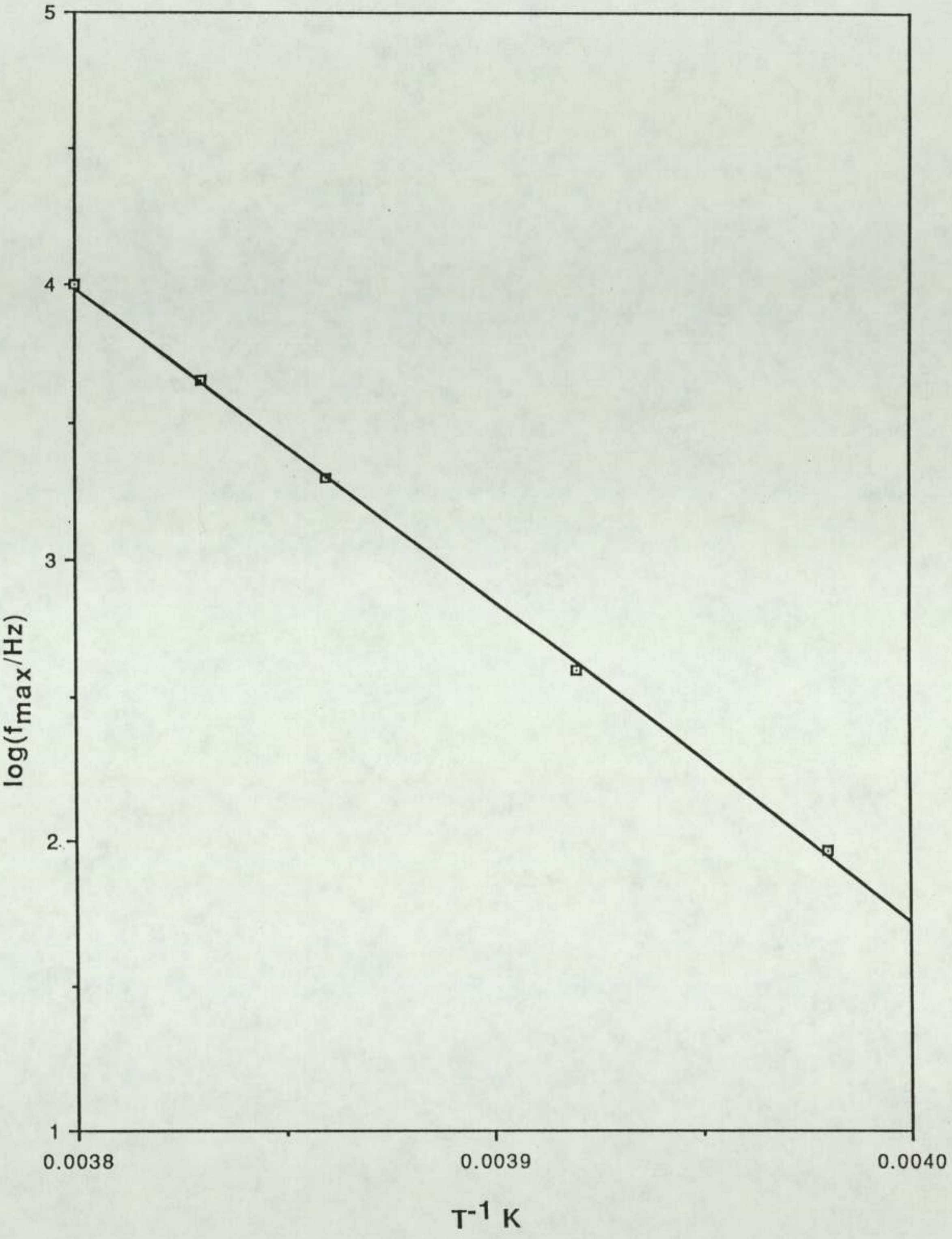

Figure (5-57) Log(f_{max}/Hz) against T^{-1} K for linear PMPS with $\bar{n}_n$=284

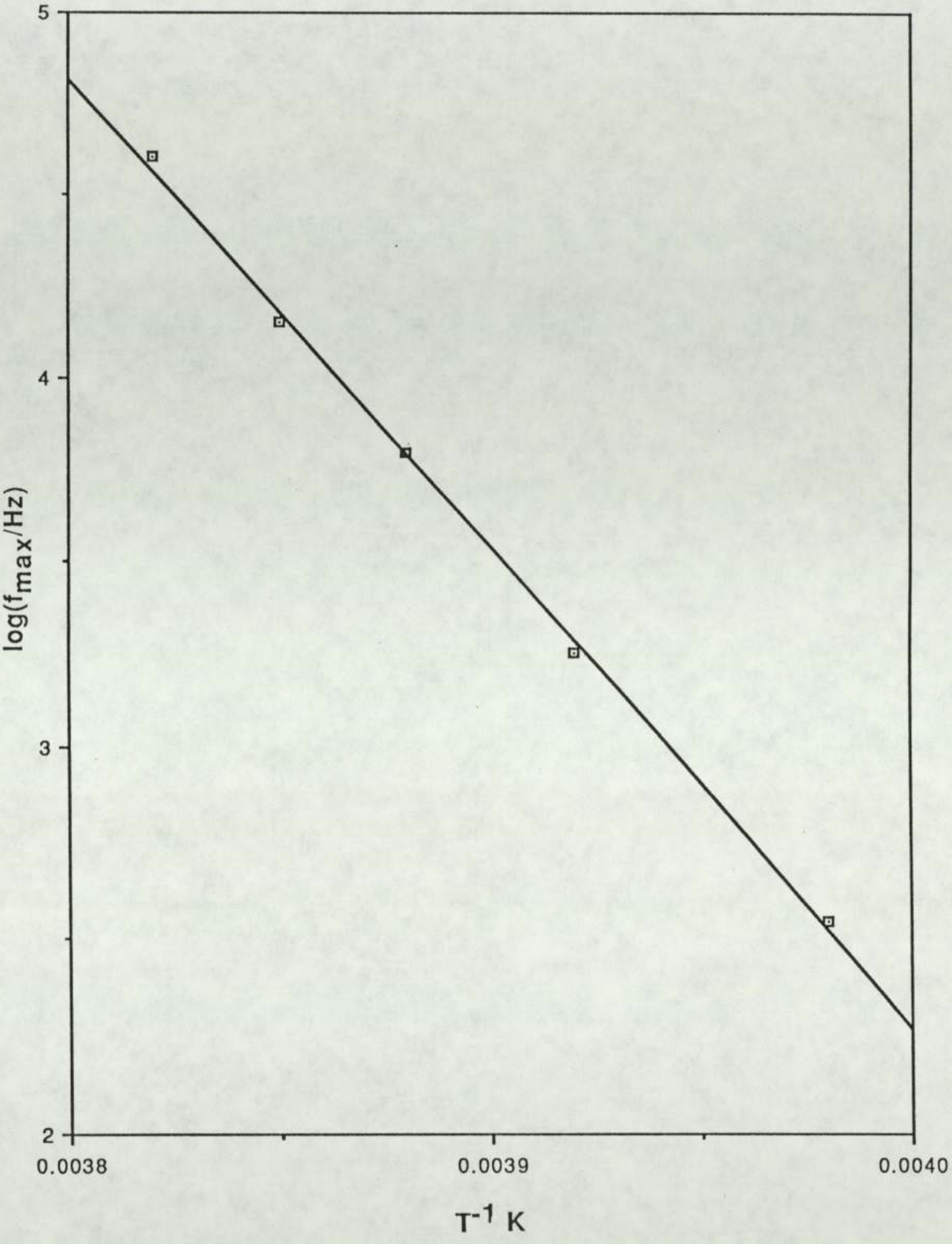

<u>Figure (5-58)</u> Log(f_{max}/Hz) against T^{-1} K for linear PMPS with $\bar{n}_n$~1370

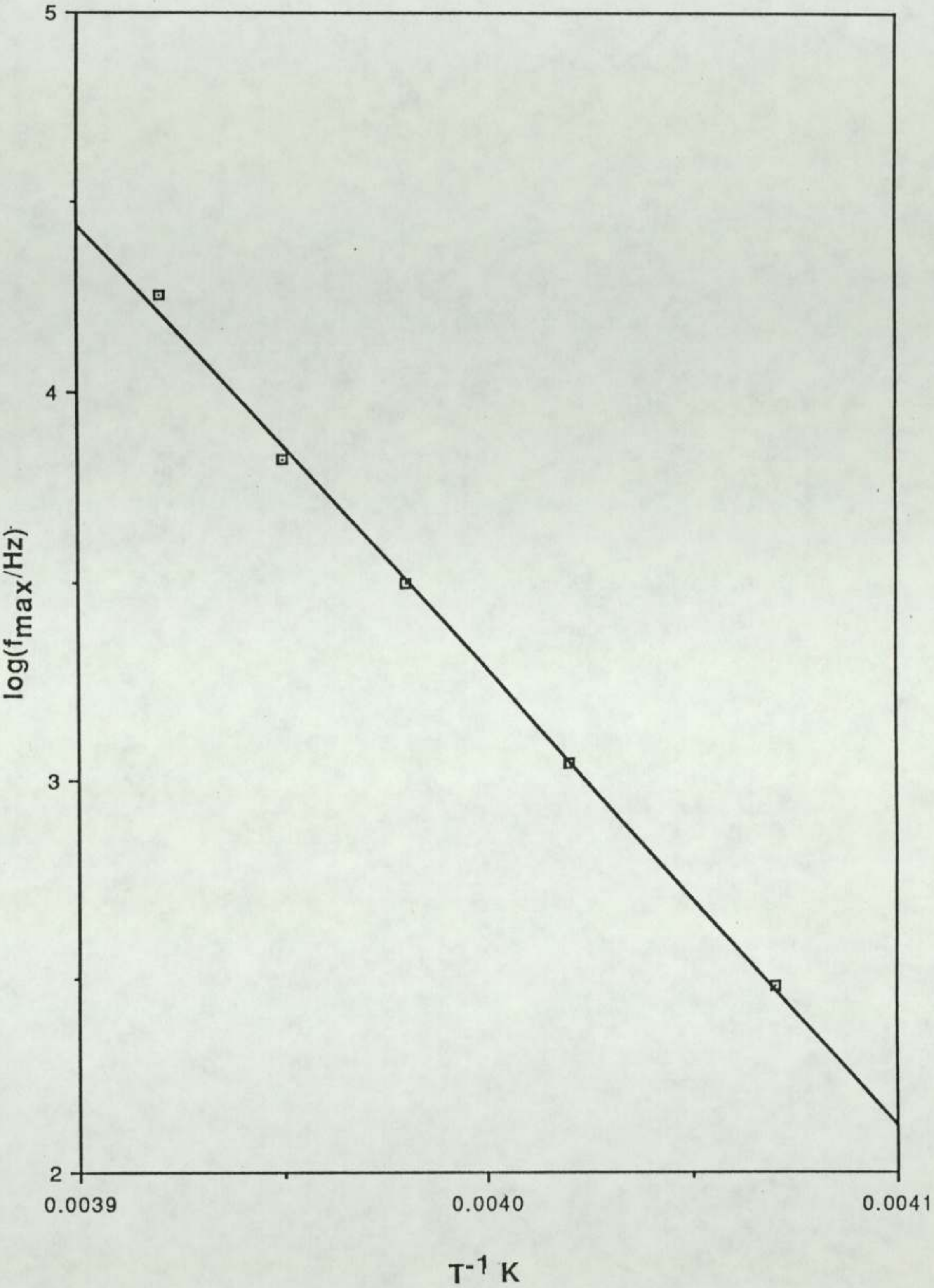

Figure (5-59) Log (f_{max}/Hz) against T^{-1} K for a cyclic oligomer of methylphenyl siloxane with n=10

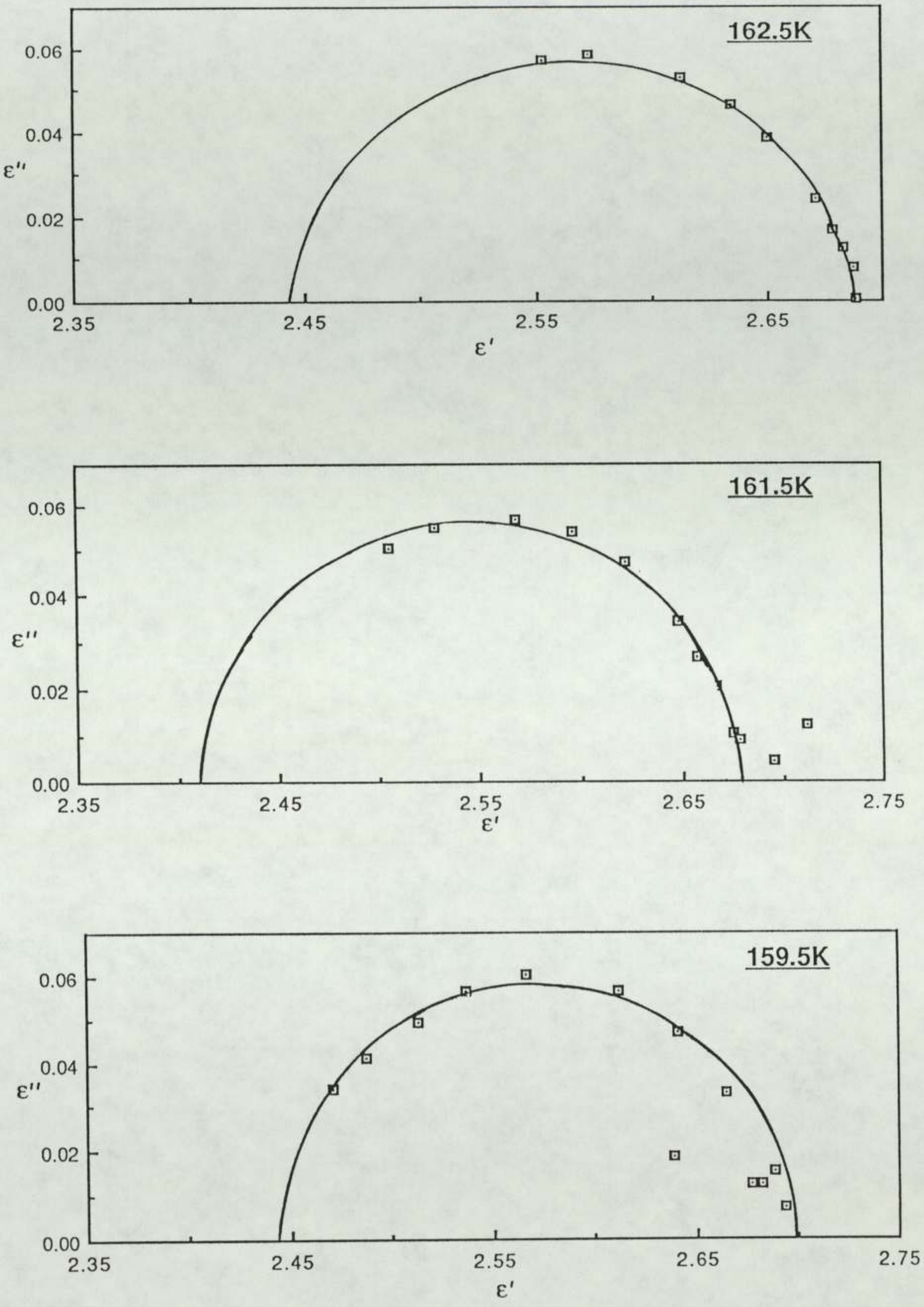

Figure (5-60) Cole-Cole plots for a linear oligomer of methylphenyl siloxane with n=4 at various temperatures

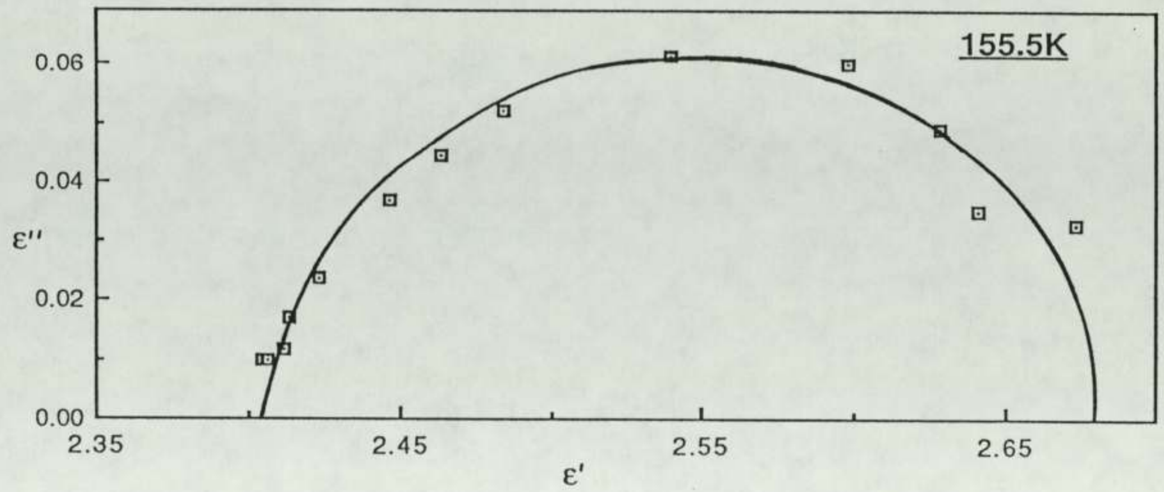

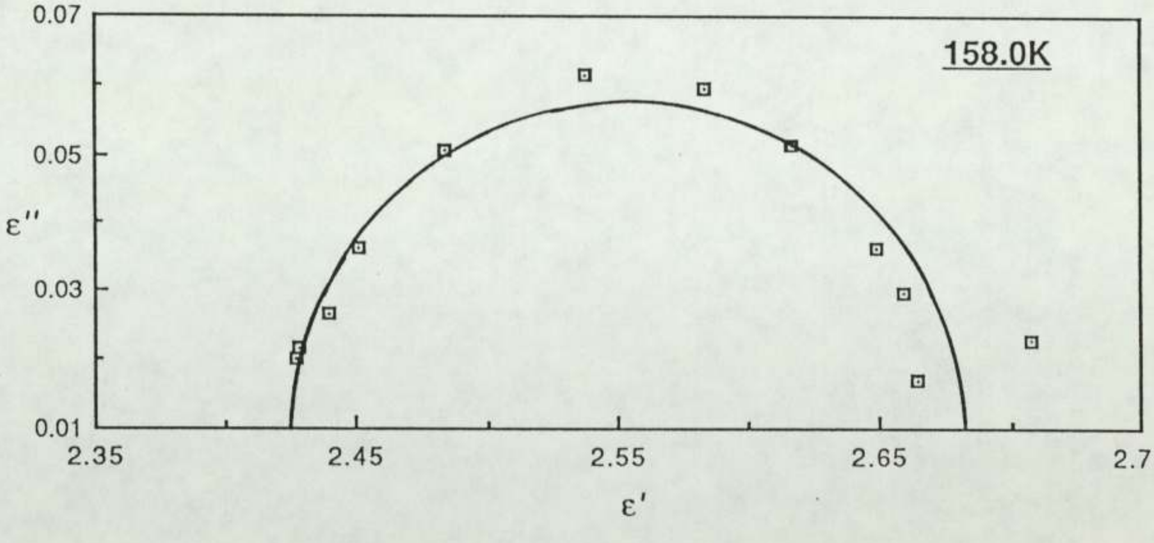

Figure (5-61) Cole-Cole plots for a linear oligomer of methylphenyl siloxane with n=4 at various temperatures

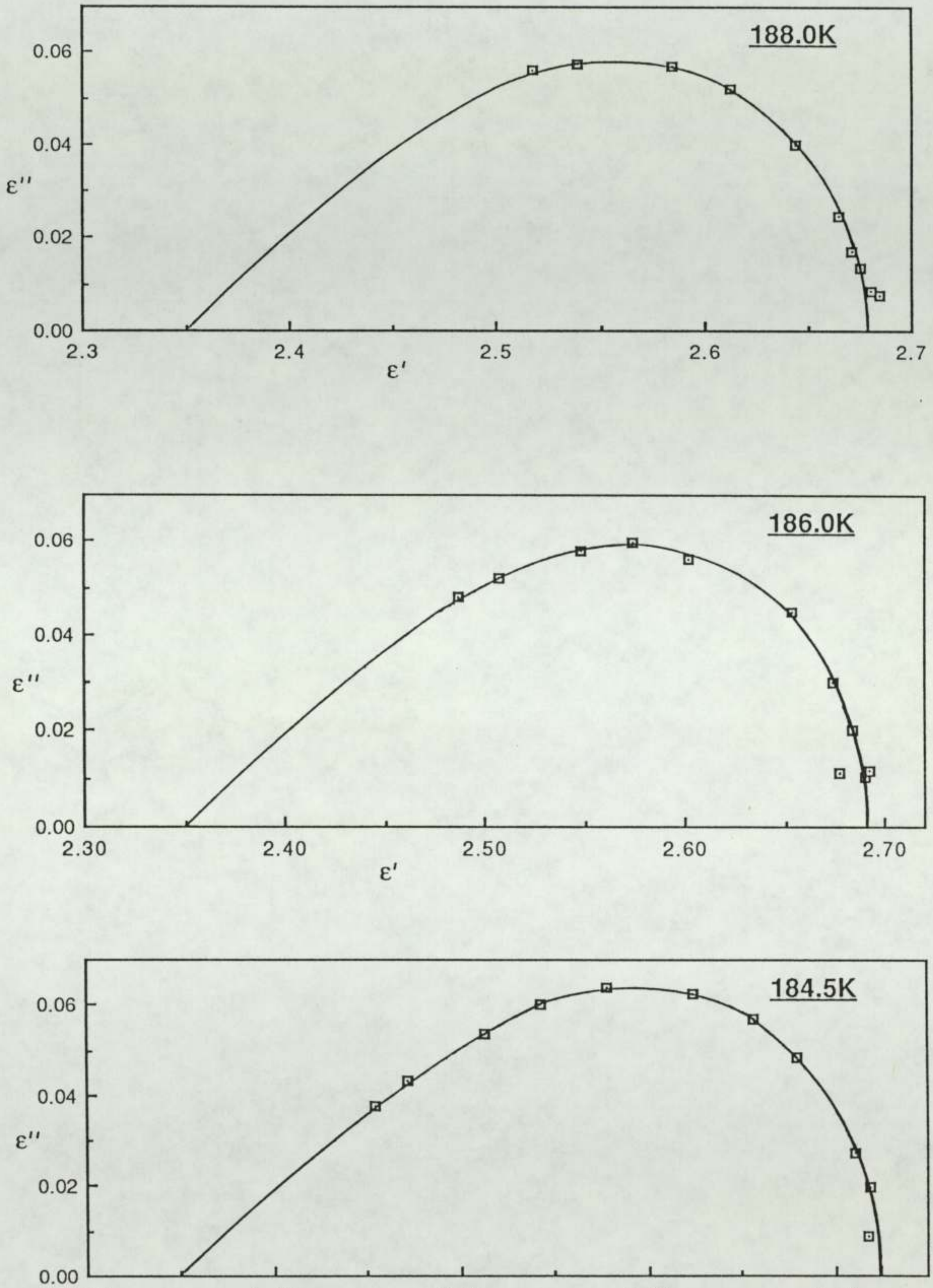

Figure (5-62) Cole-Cole plots for a linear oligomer of methylphenyl siloxane with n=6 at various temperatures

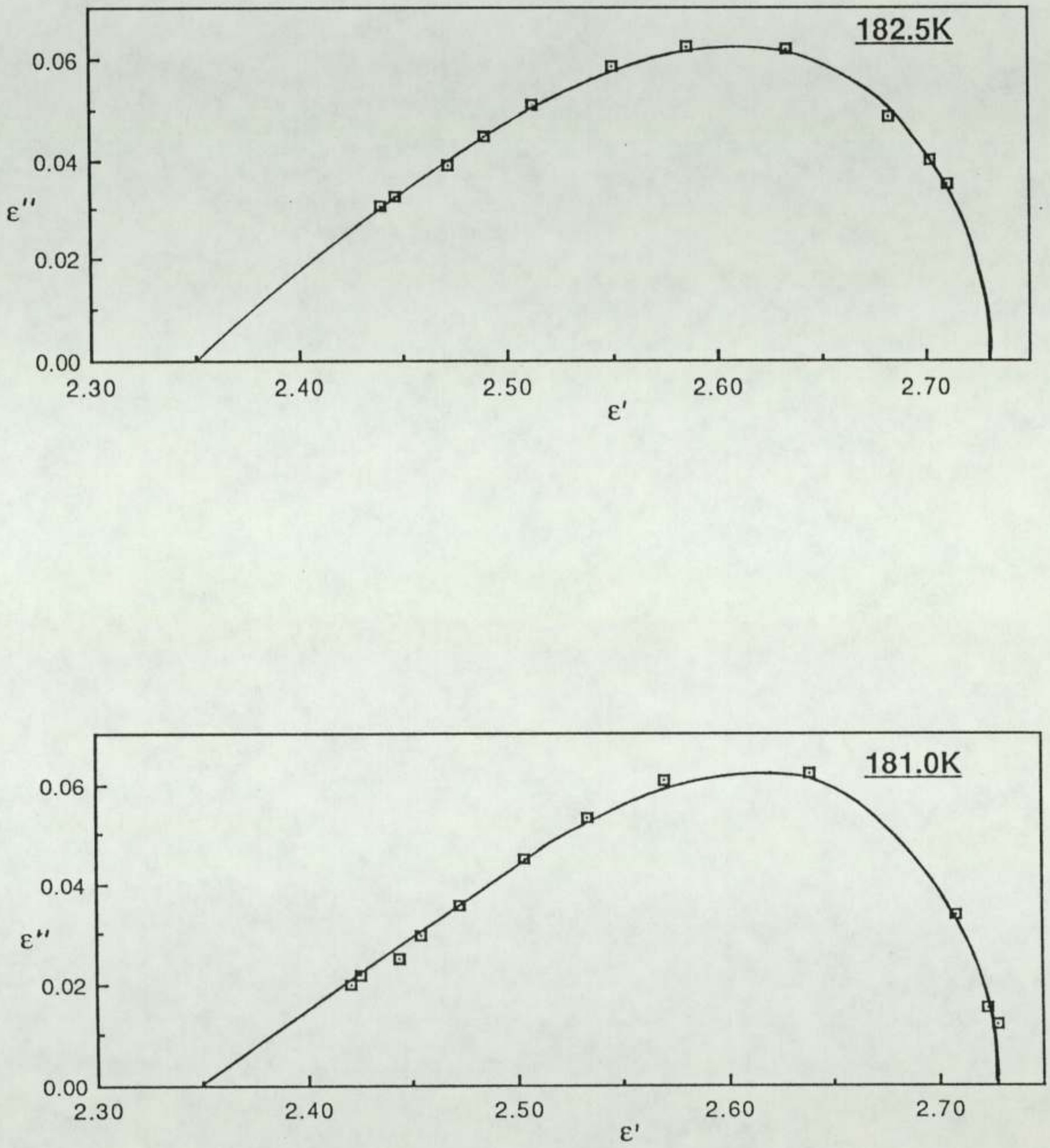

Figure (5-63) Cole-Cole plots for a linear oligomer of methylphenyl siloxane with n=6 at various temperatures

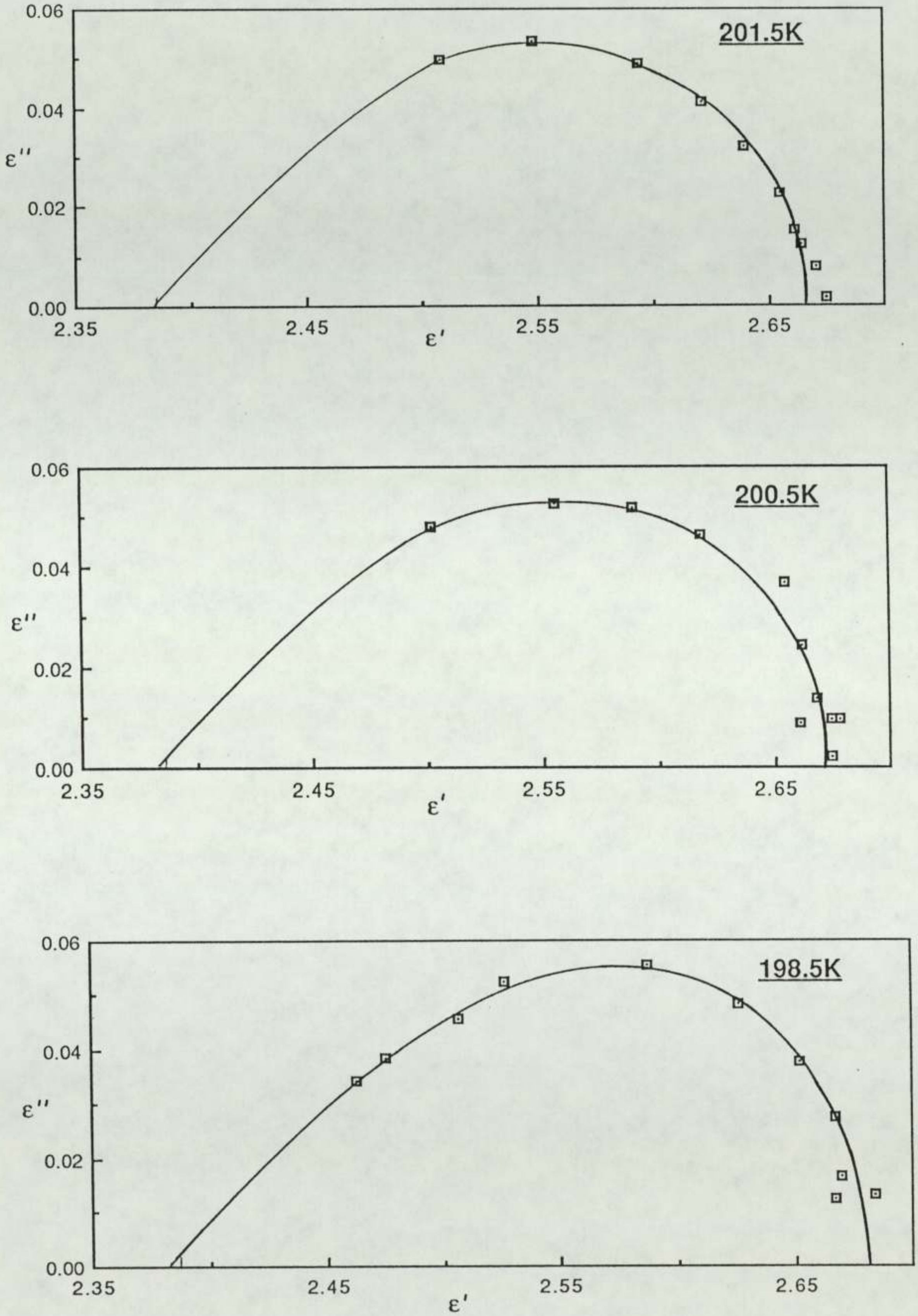

Figure (5-64) Cole-Cole plots for a linear oligomer of methylphenyl siloxane with n=8 at various temperatures

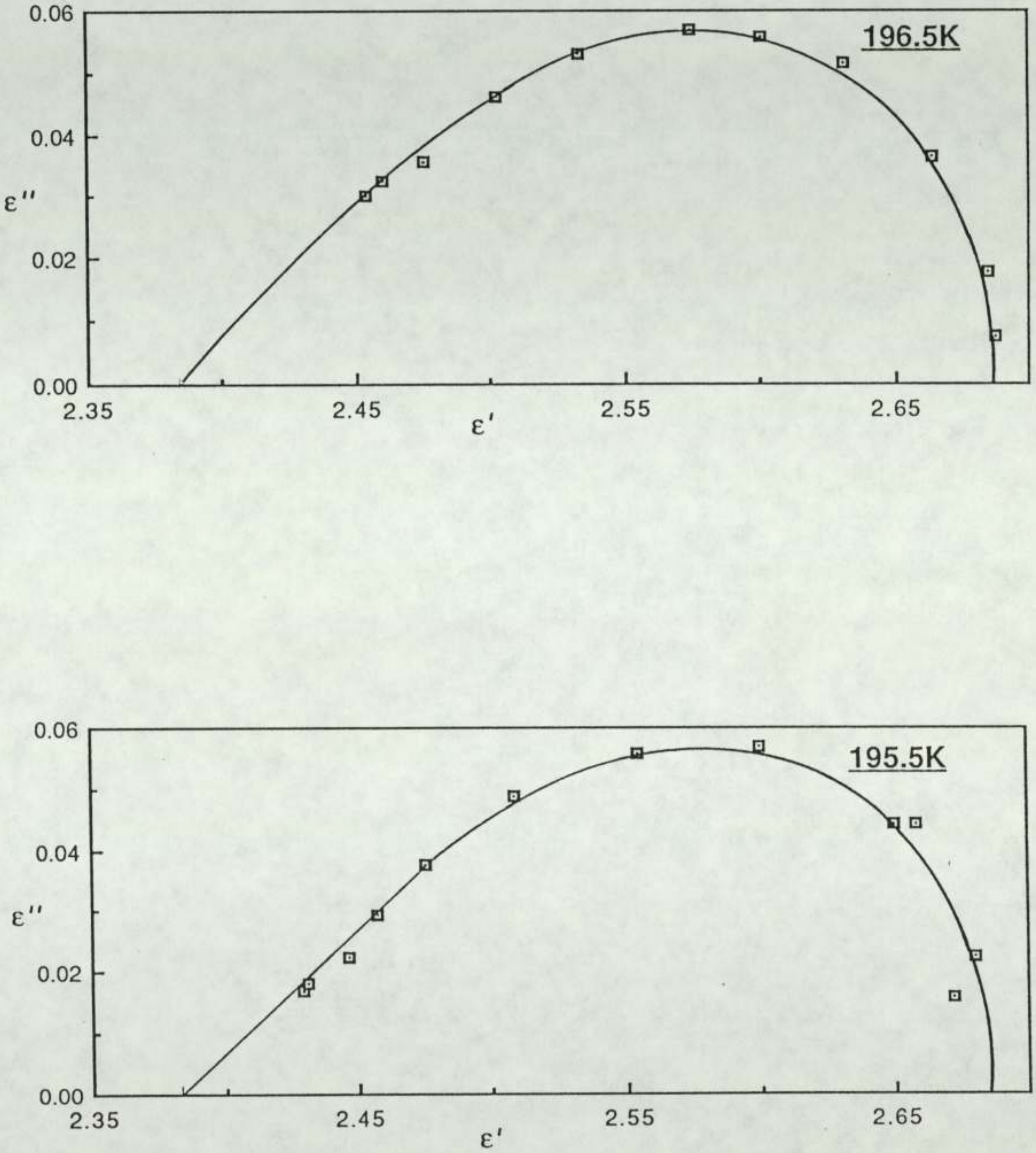

Figure (5-65) Cole-Cole plots for a linear oligomer of methylphenyl siloxane with n=8 at various temperatures

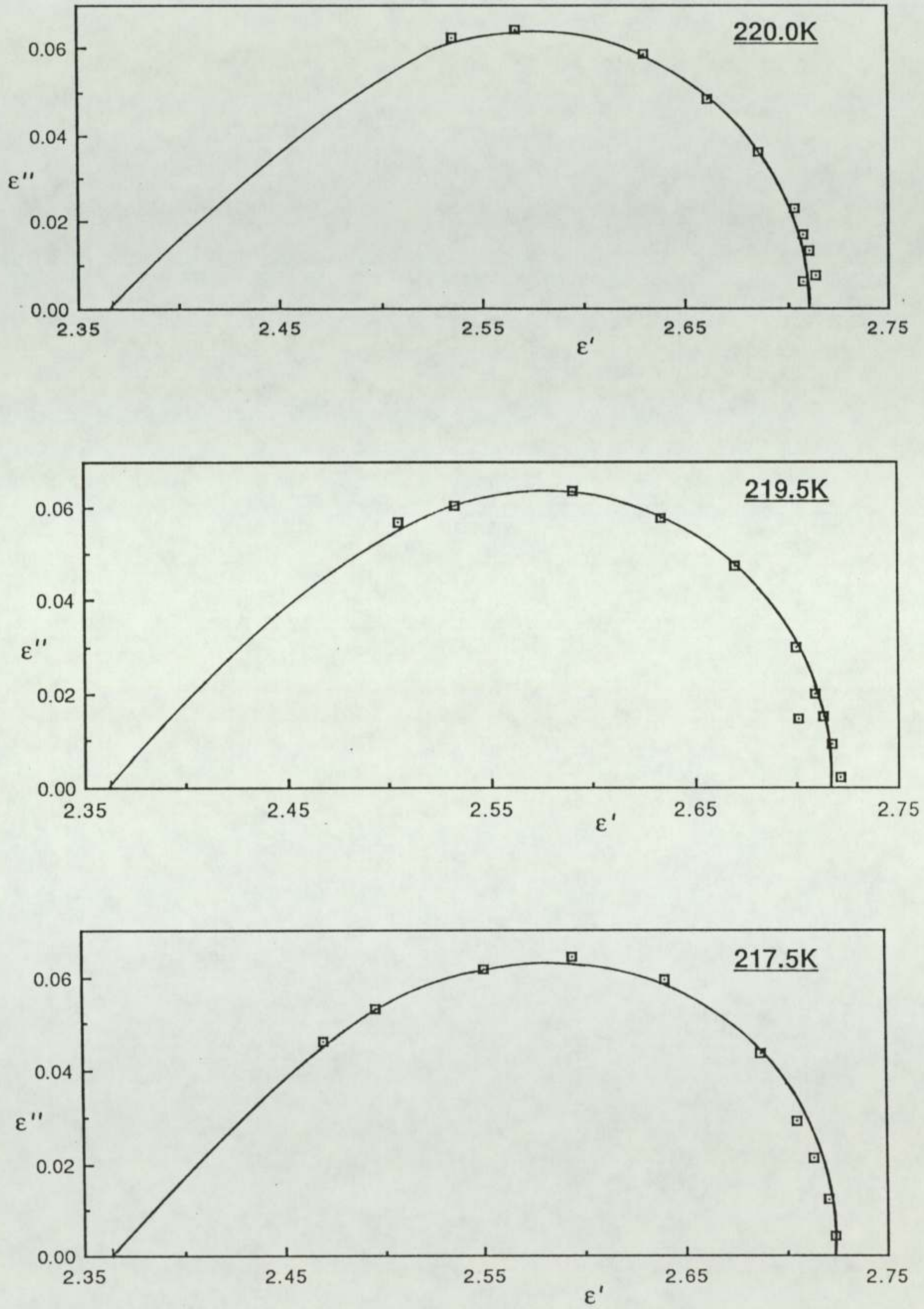

Figure (5-66) Cole-Cole plots for a linear oligomer of methylphenyl siloxane with n=10 at various temperatures

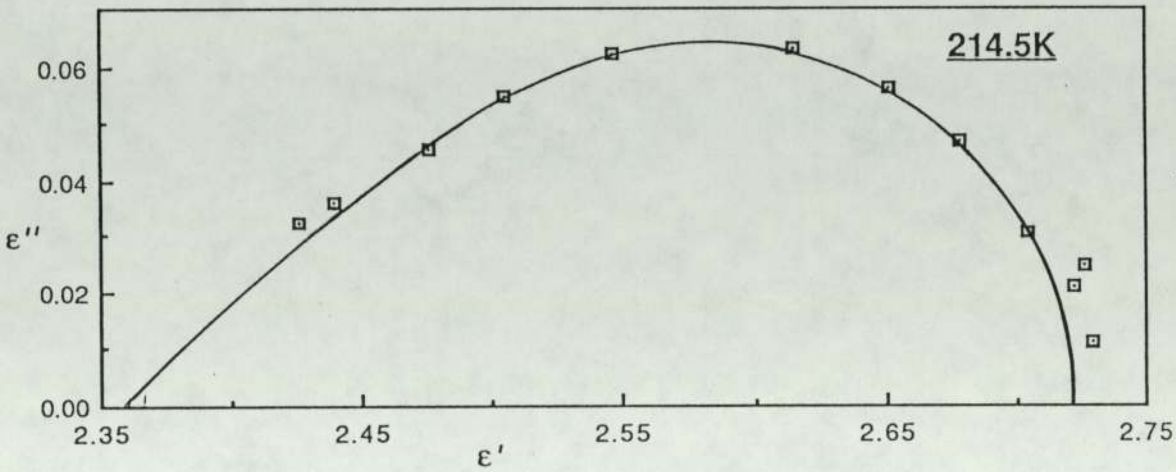

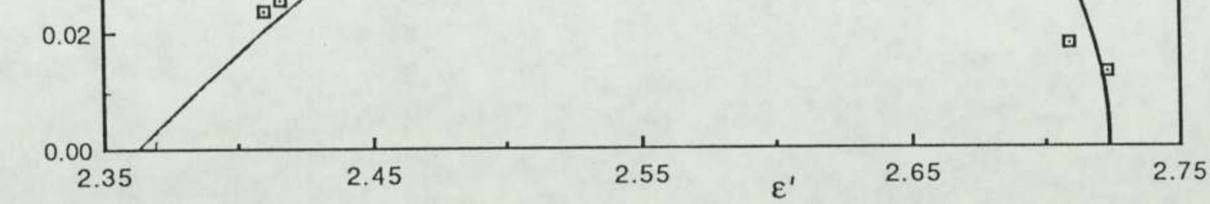

Figure (5-67) Cole-Cole plots for a linear oligomer of methylphenyl siloxane with n=10 at various temperatures

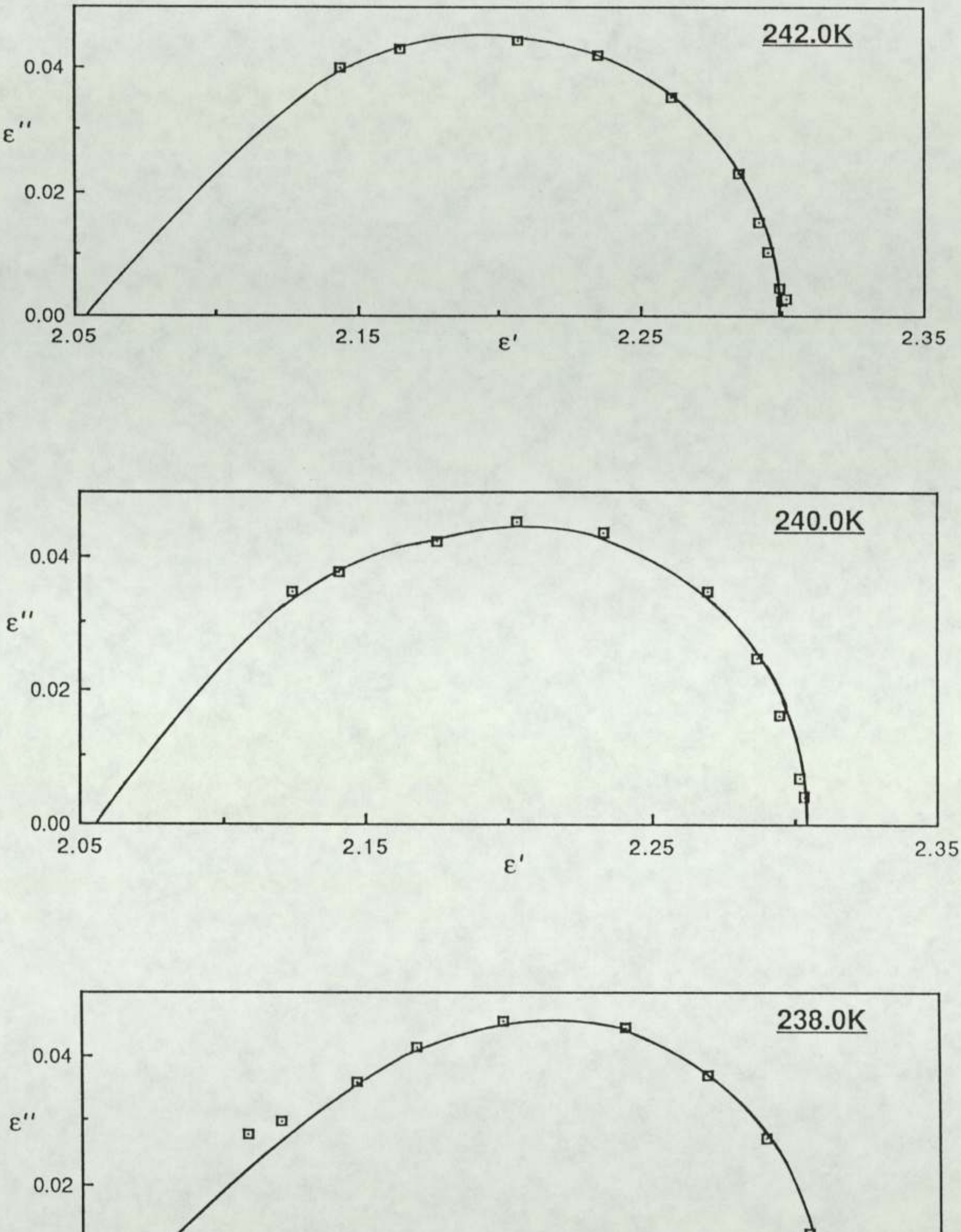

Figure (5-68) Cole-Cole plots for linear PMPS with $\bar{n}_n$=31 at various temperatures

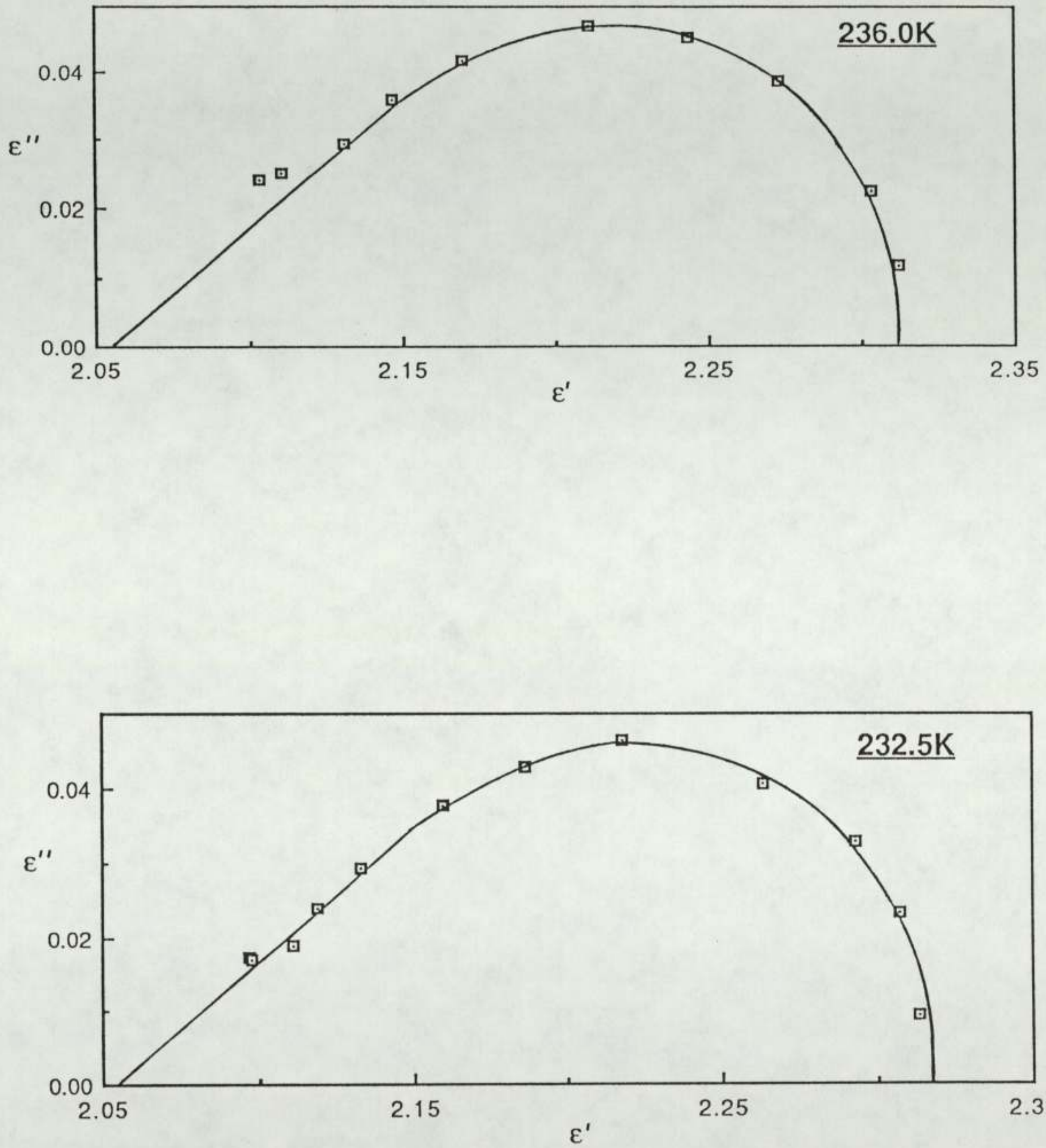

<u>Figure (5-69)</u> Cole-Cole plots for linear PMPS with $\bar{n}_n$=31 at various temperatures

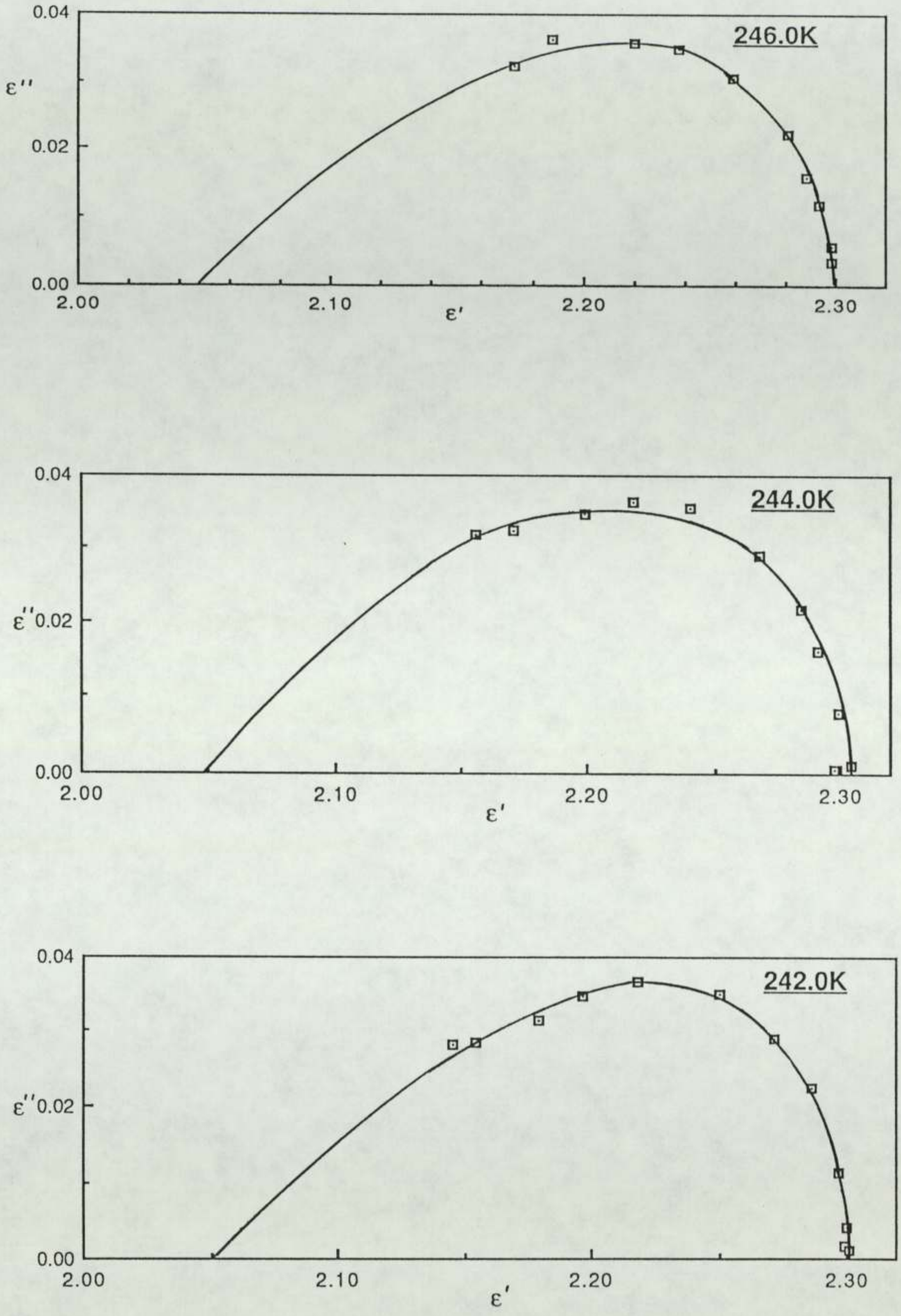

<u>Figure (5-70)</u> Cole-Cole plots for linear PMPS with $\bar{n}_n=50.5$ at various temperatures

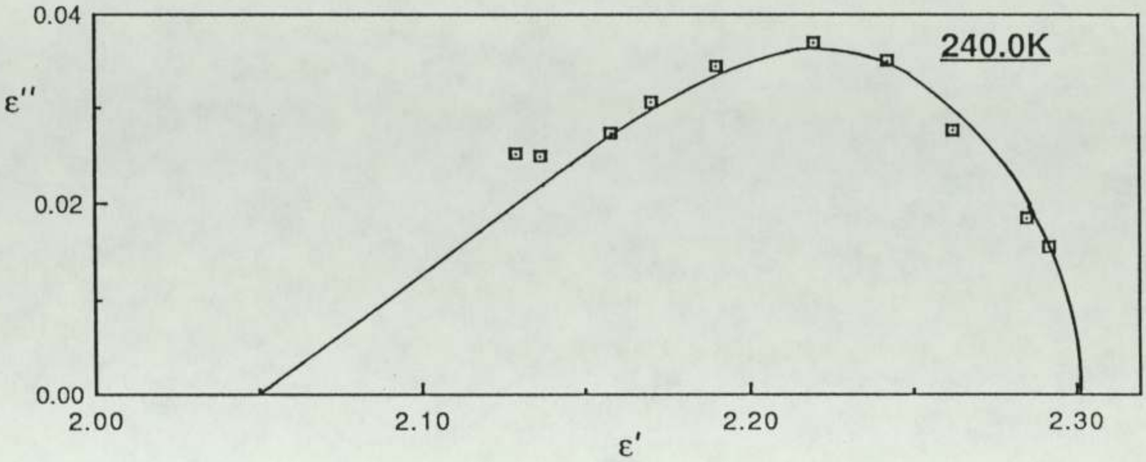

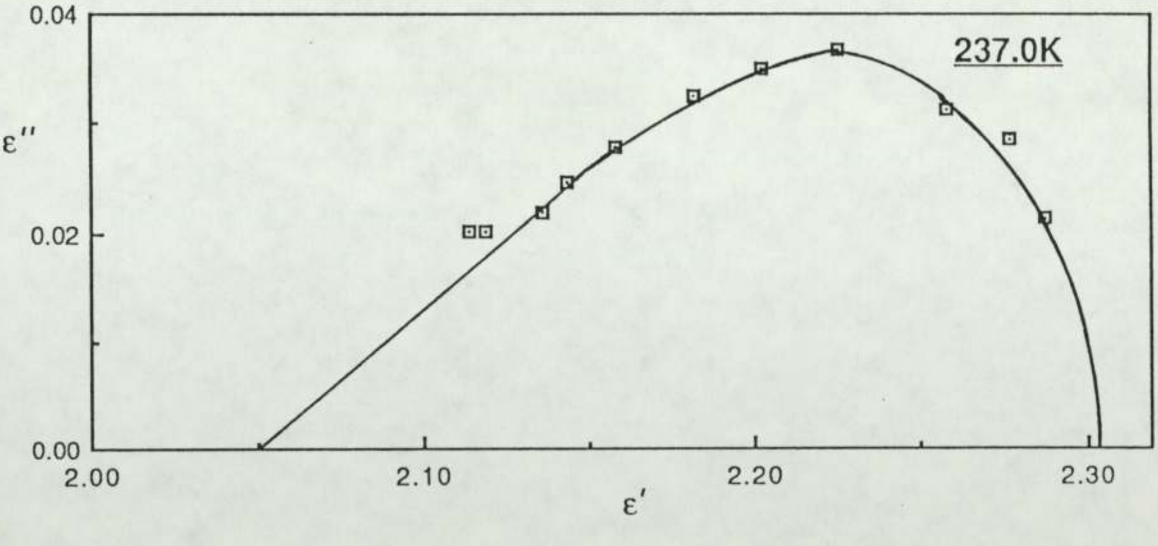

Figure (5-71) Cole-Cole plots for linear PMPS with $\bar{n}_n=50.5$ at various temperatures

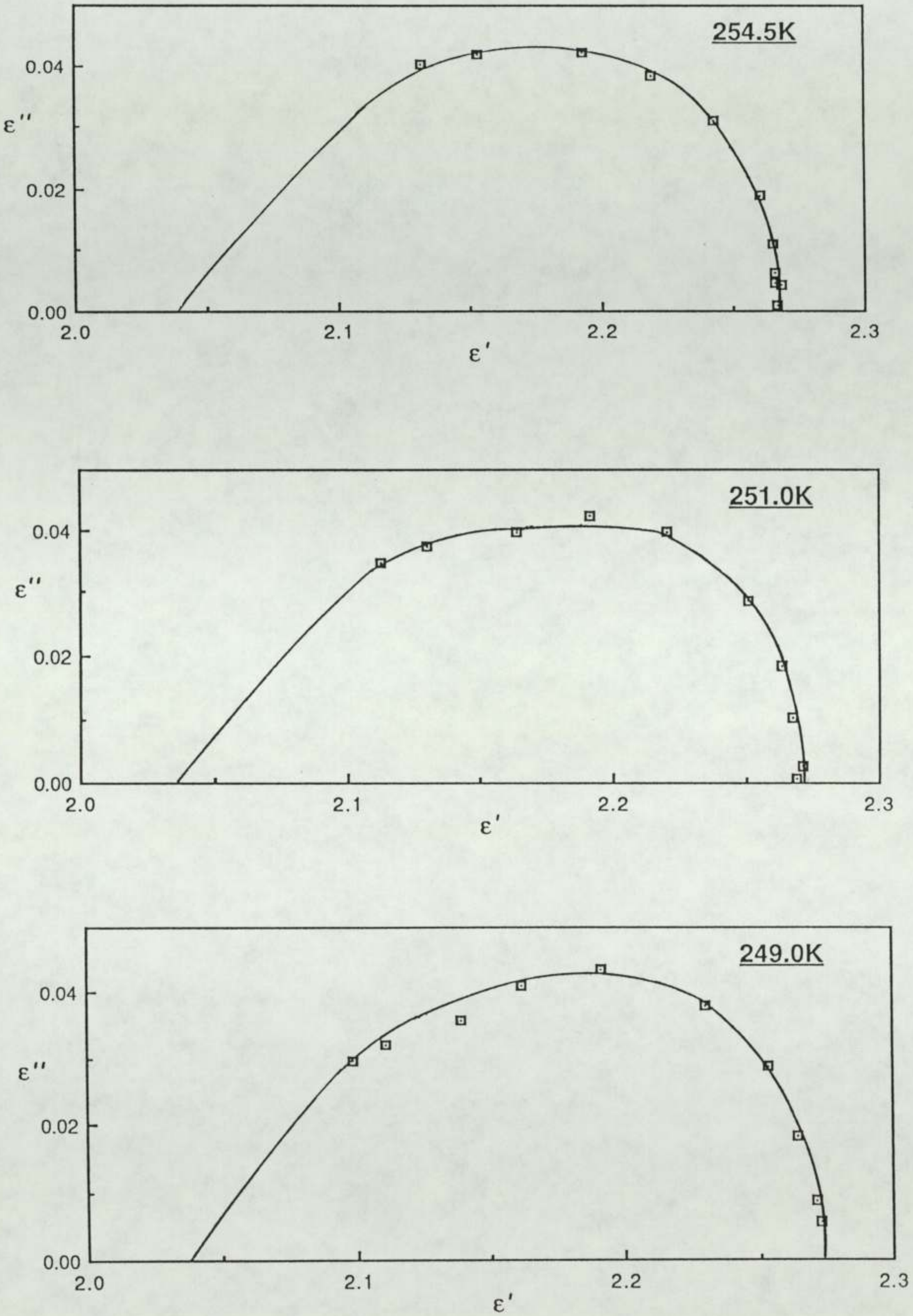

Figure (5-72) Cole-Cole plots for linear PMPS with $\bar{n}_n$=82 at various temperatures

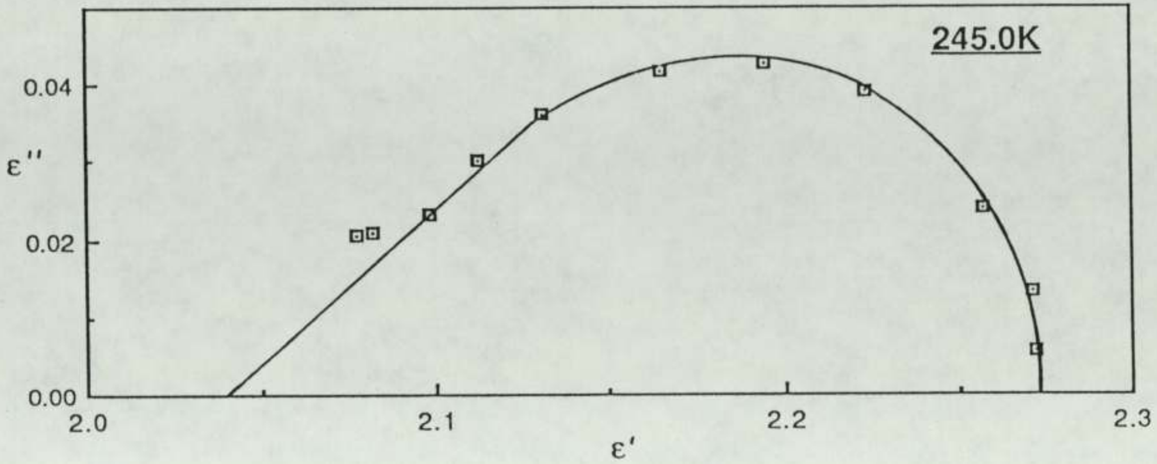

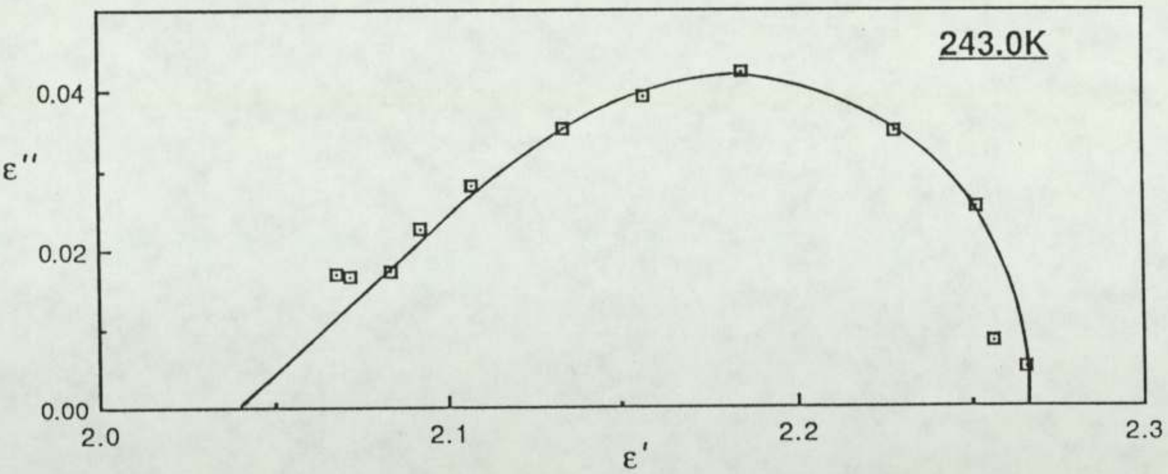

Figure (5-73) Cole-Cole plots for linear PMPS with $\bar{n}_n$=82 at various temperatures

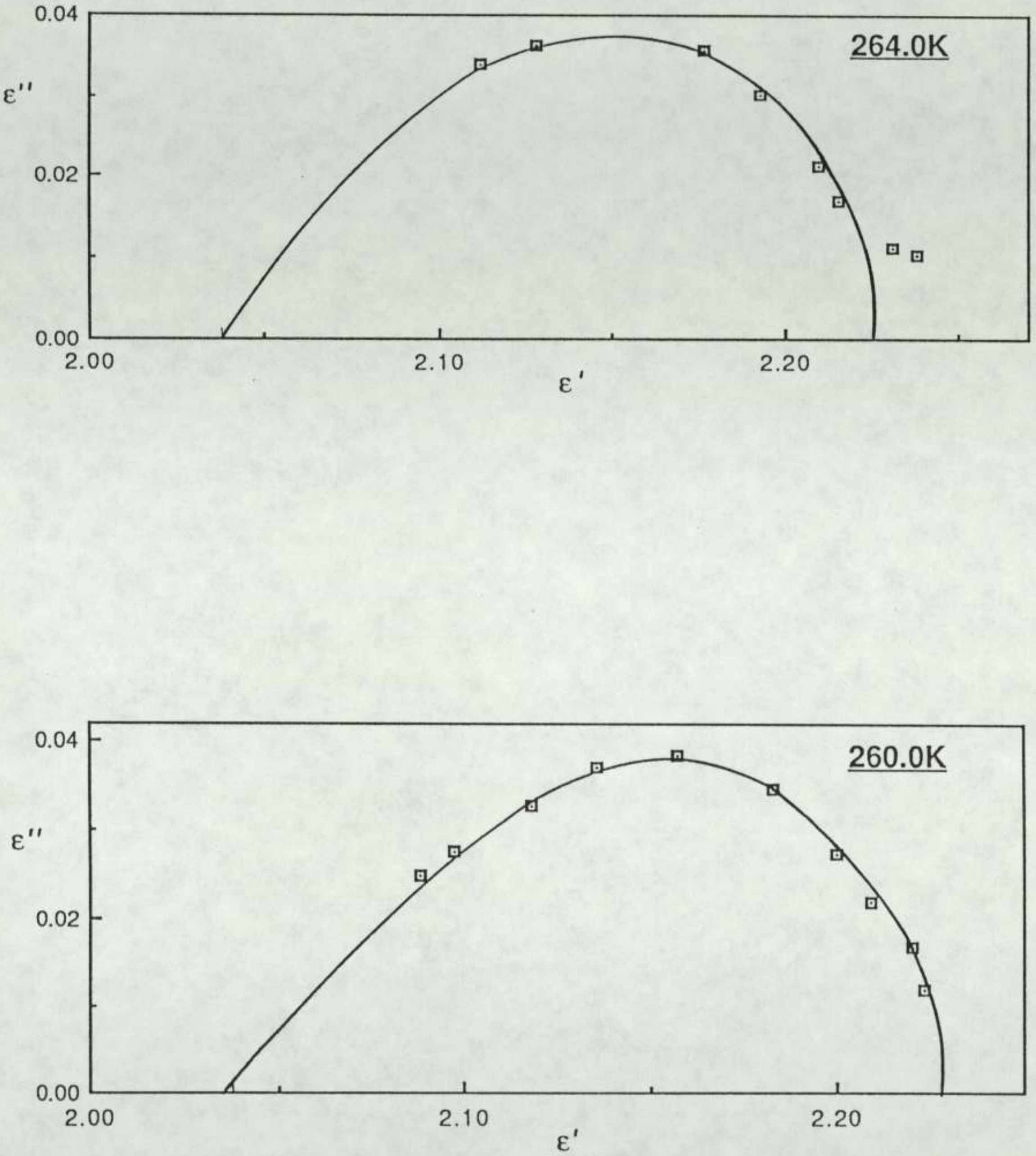

Figure (5-74) Cole-Cole plots for linear PMPS with $\bar{n}_n$=153 at various temperatures

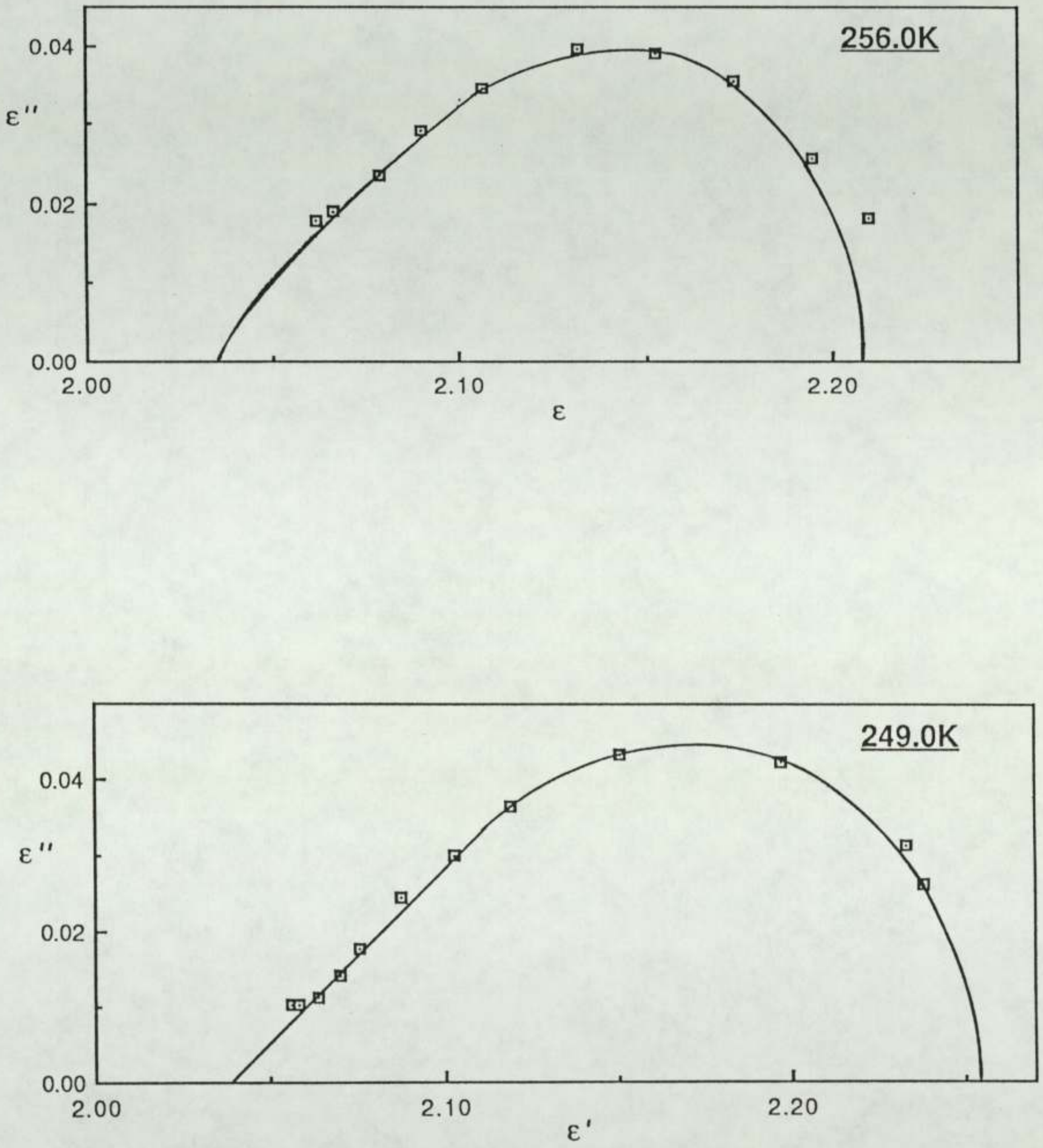

Figure (5-75) Cole-Cole plots for linear PMPS with $\bar{n}_n$=153 at various temperatures

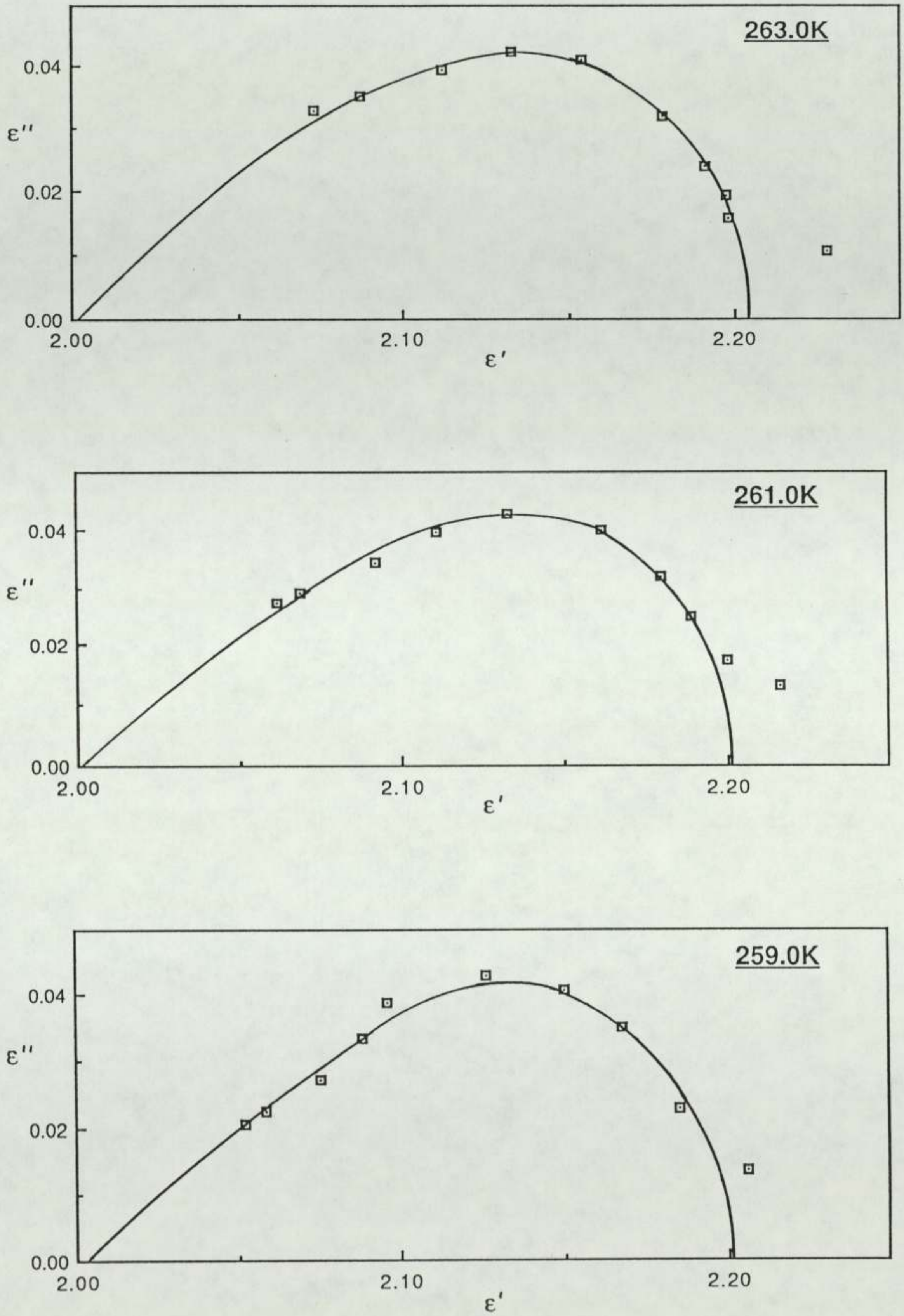

Figure (5-76) Cole-Cole plots for linear PMPS with $\bar{n}_n=284$ at various temperatures

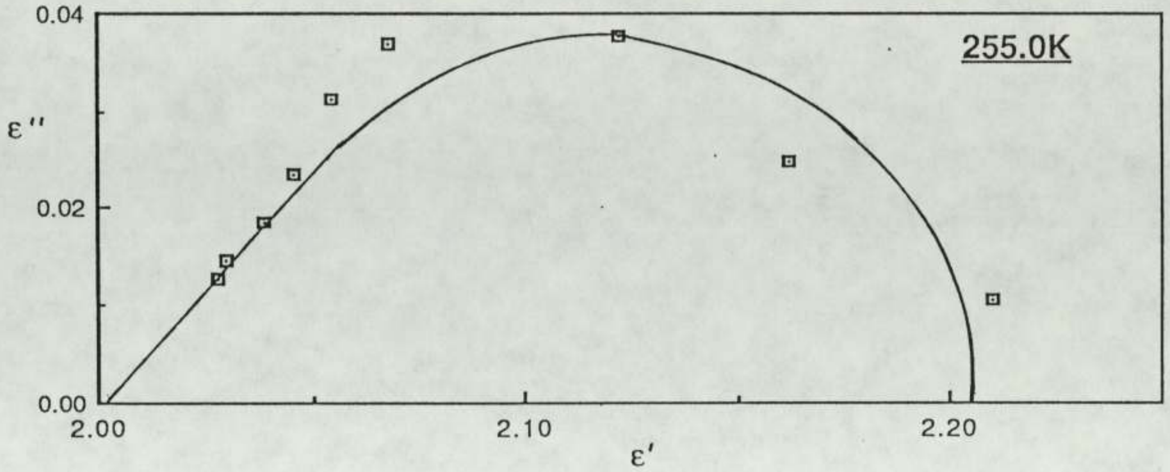

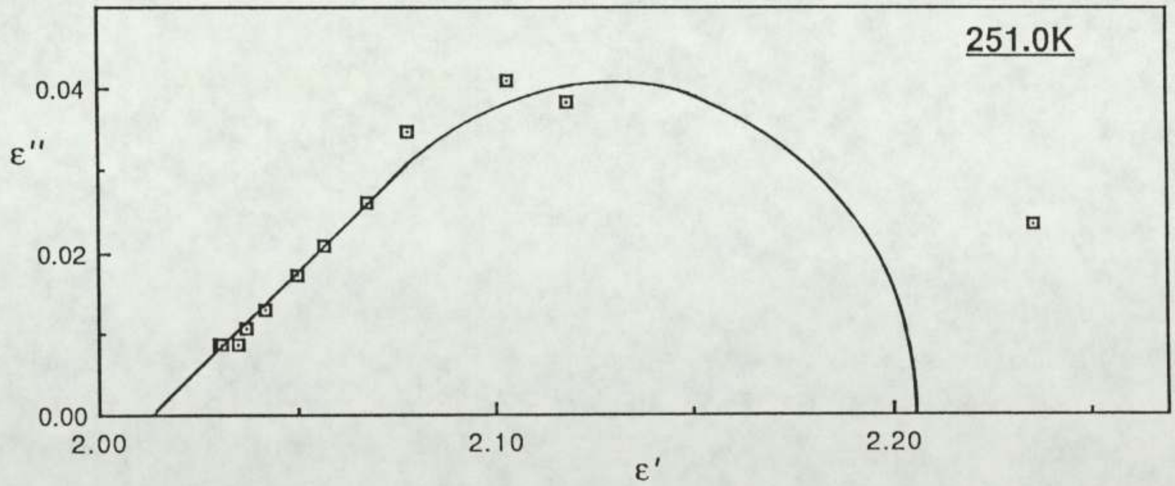

Figure (5-77) Cole-Cole plots for linear PMPS with $\bar{n}_n=284$ at various temperatures

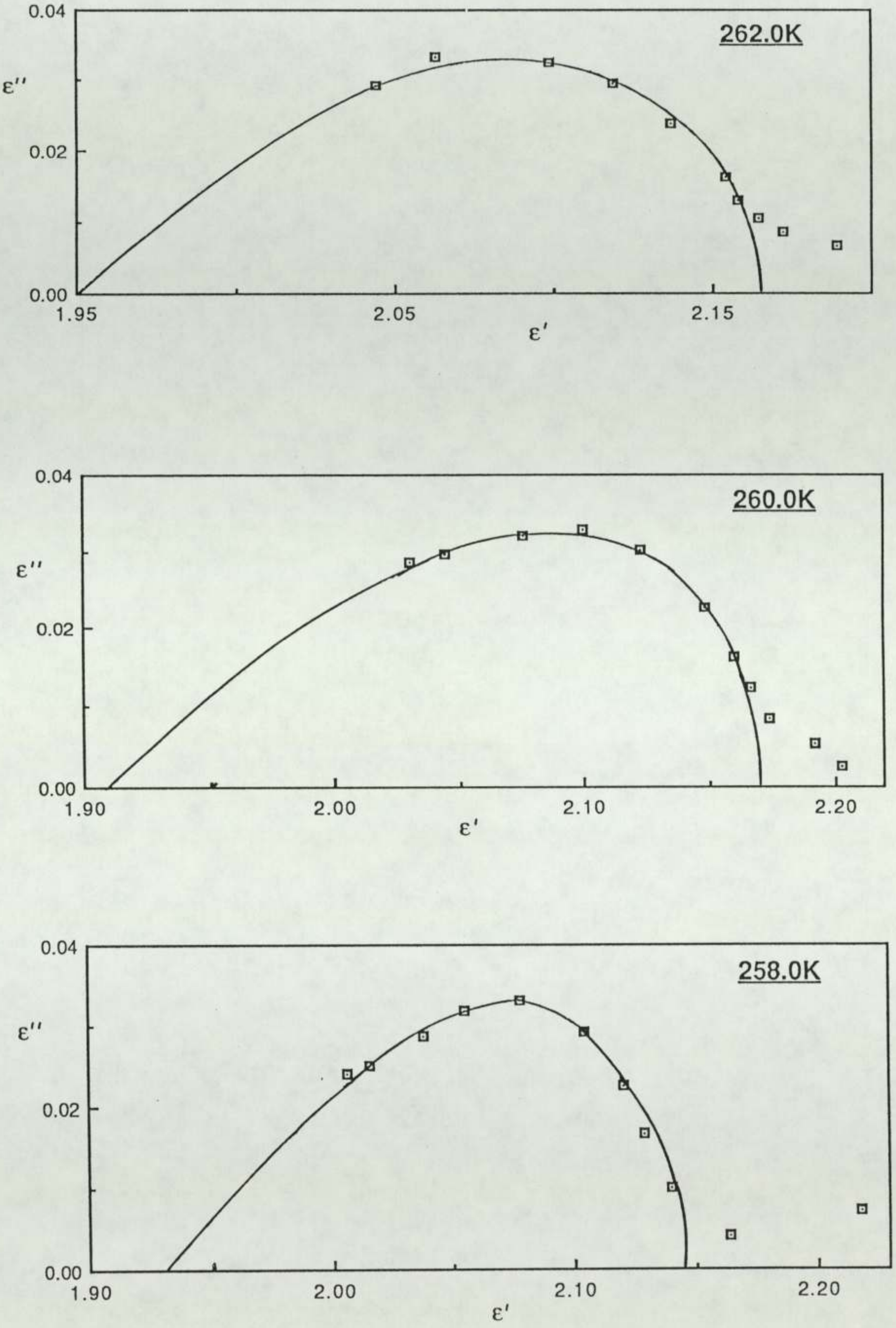

Figure (5-78) Cole-Cole plots for linear PMPS with $\bar{n}_n \sim 1370$ at various temperatures

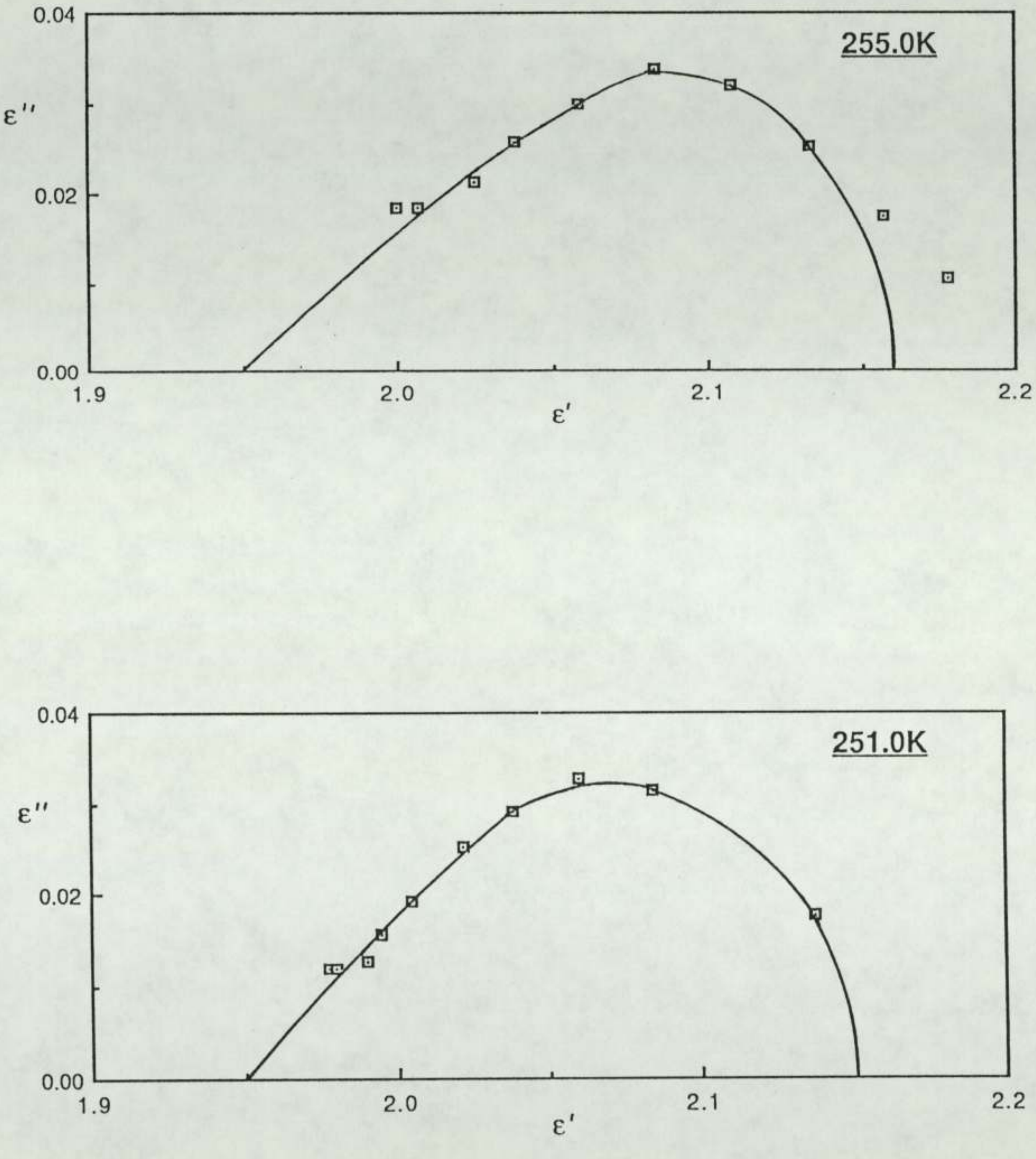

Figure (5-79) Cole-Cole plots for linear PMPS with $\bar{n}_n \sim 1370$ at various temperatures

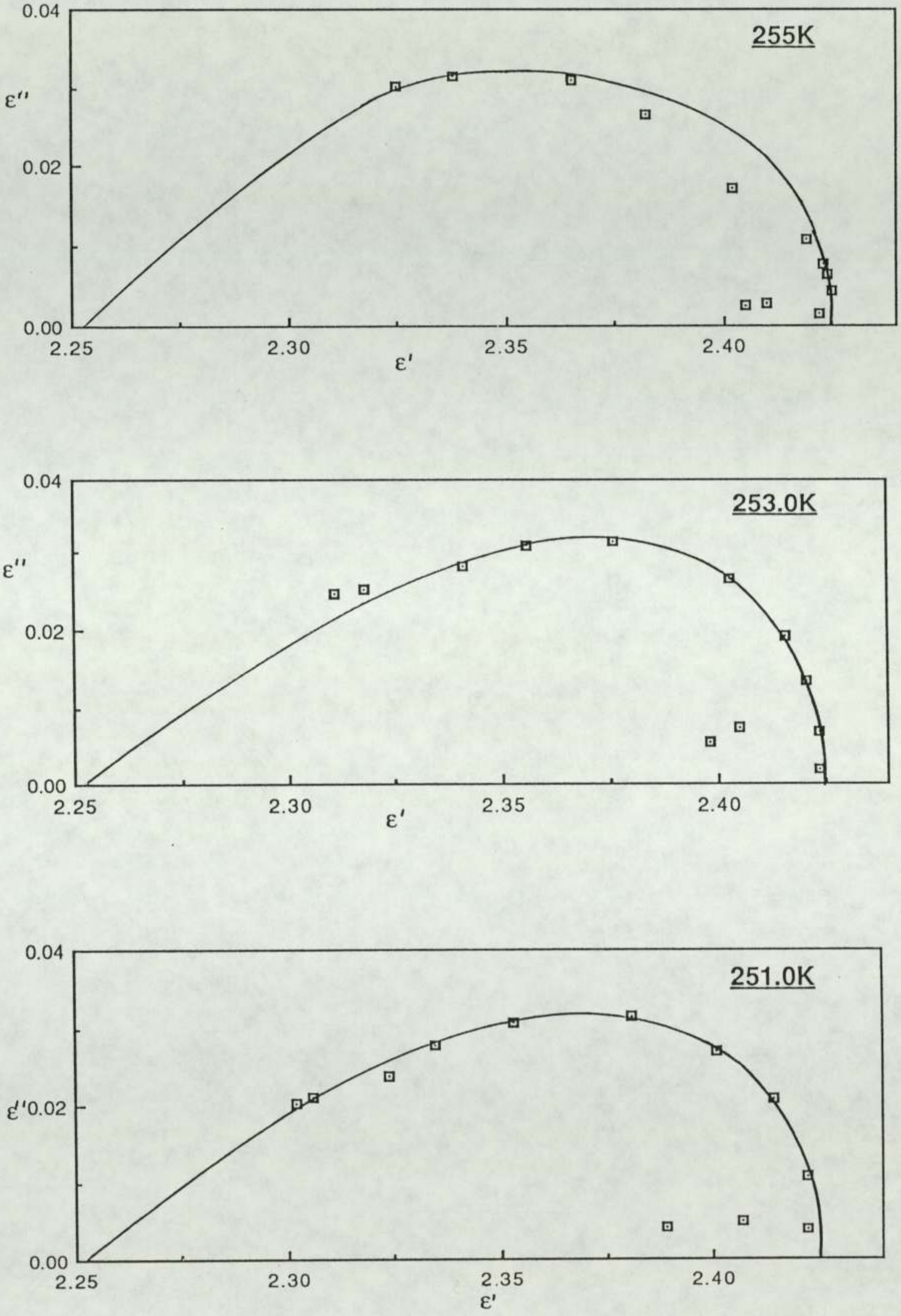

Figure (5-80) Cole-Cole plots for a cyclic oligomer of MPS with n=10 at various temperatures

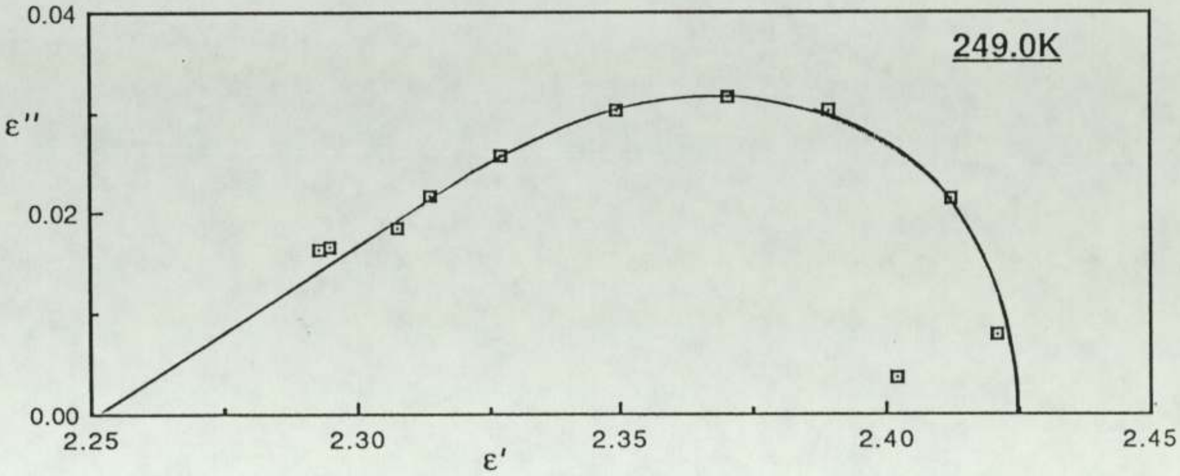

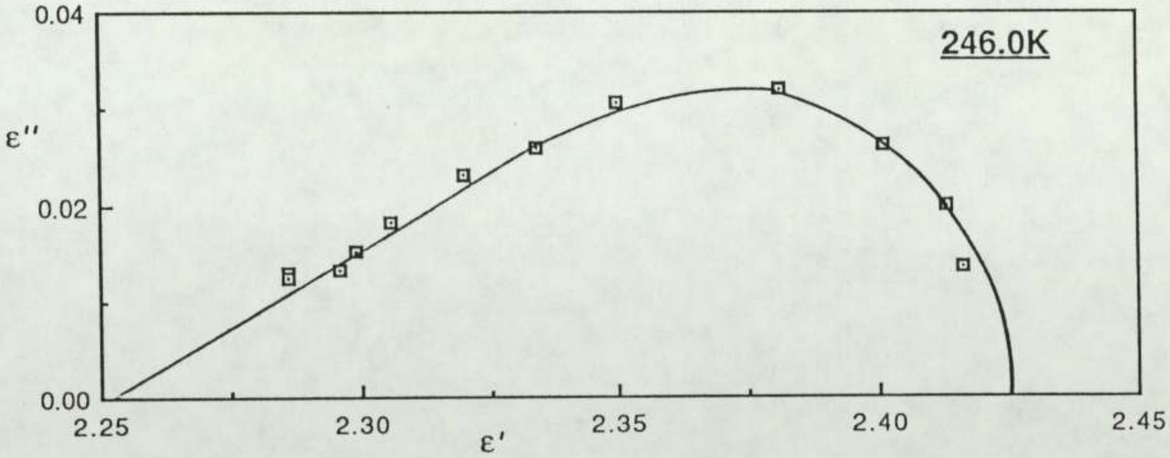

Figure (5-81) Cole-Cole plots for a cyclic oligomer of MPS with n=10 at various temperatures fractions produced by cooling the samples to low temperatures. With the exception of the plot for the linear oligomer of methyl phenyl siloxane with n=4, which is semi-circular, the plots are skewed arcs, and are consistent with the Davidson-Cole analysis. The procedure employed for the estimation of the limiting permittivities from the Cole-Cole arcs is identical to the procedure described for cyclic and linear fractions of PDMS.

The permittivities ε_0 and ε_∞, obtained from the Cole-Cole arcs exhibit a marked dependence on molecular weight. The Cole-Cole plot for the oligomer of methyl phenyl siloxane with n=4, which is semi-circular, gave the highest observed value of ε_∞ equal to 2.43. Thereafter, values of ε_∞ decrease with increasing molecular weight to a value of 1.95 obtained for a fraction of PMPS with $\bar{n}_n$~1370. Values of ε_0 also show a corresponding decrease as molecular weight increases, from 2.73 for an oligomer of methylphenyl siloxane with n=6 to 2.15 for a fraction of PMPS with $\bar{n}_n$~1370. The maximum value of the dielectric increment, $\Delta\varepsilon = (\varepsilon_0 - \varepsilon_\infty)$, is 0.38 for an oligomer of methyl phenyl siloxane with n=6. (In an earlier study, Baird and co-workers^{37} reported a maximum dielectric increment of 0.40. for an oligomer of methyl phenyl siloxane, at 240K, with a most probable value of n equal to 12). In general, values of the dielectric increment are larger for oligomers of methyl phenyl siloxane, varying between 0.31 and 0.38, than for fractions of PMPS, where $\Delta\varepsilon$ varies between 0.19 and 0.26.

For a cyclic oligomer with n=10; ε_∞=2.26, ε_0=2.42-2.45 and $\Delta\varepsilon$= 0.16-0.19.

The maximum values of the dielectric loss for oligomers of methyl phenyl siloxane and fractions of PMPS also decrease with increasing molecular weight. Thus, for the oligomers of methyl phenyl siloxane the maximum dielectric losses lie in the range 5.3×10^{-2} to 6.4×10^{-2}, while for the fractions of PMPS the maximum dielectric losses lie in the range 3.2×10^{-2} to 4.4×10^{-2}.

5.09: Dielectric Properties of Poly(methyl hydrogen siloxane)[PMHS], poly(n-hexyl methyl siloxane) and a Polysiloxane Liquid Crystal.

The dielectric relaxation behaviour for a series of compounds based on a PMHS backbone has been measured, as a function of temperature and frequency, using the apparatus and methods described in Chapter 3.

5.10: The Dielectric Loss Results.

Normalised plots of $C_p\tan\delta$ against log (f/Hz) are shown in Figures (5-82) to (5-85) for PMHS, poly(n-hexyl methyl siloxane) and a polysiloxane liquid crystal.

For PMHS and poly(n-hexyl methyl siloxane) the presence of a broad α-type relaxation process is readily apparent. However, the attachment of n-hexyl to the PMHS backbone has caused the loss curves to broaden considerably(from approximately 2 decades of frequency for PMHS to almost 3 decades of frequency for poly(n-hexyl methyl siloxane)). The frequency corresponding to maximum dielectric loss, within the range $12\text{-}10^5$Hz, is shifted approximately 40K towards higher temperatures for poly(n-hexyl methyl siloxane), with respect to PMHS. This is due to the attached pendant group slowing the rotational motion of the Si-O dipoles.

The loss curves for the polymer liquid crystal measured in the liquid

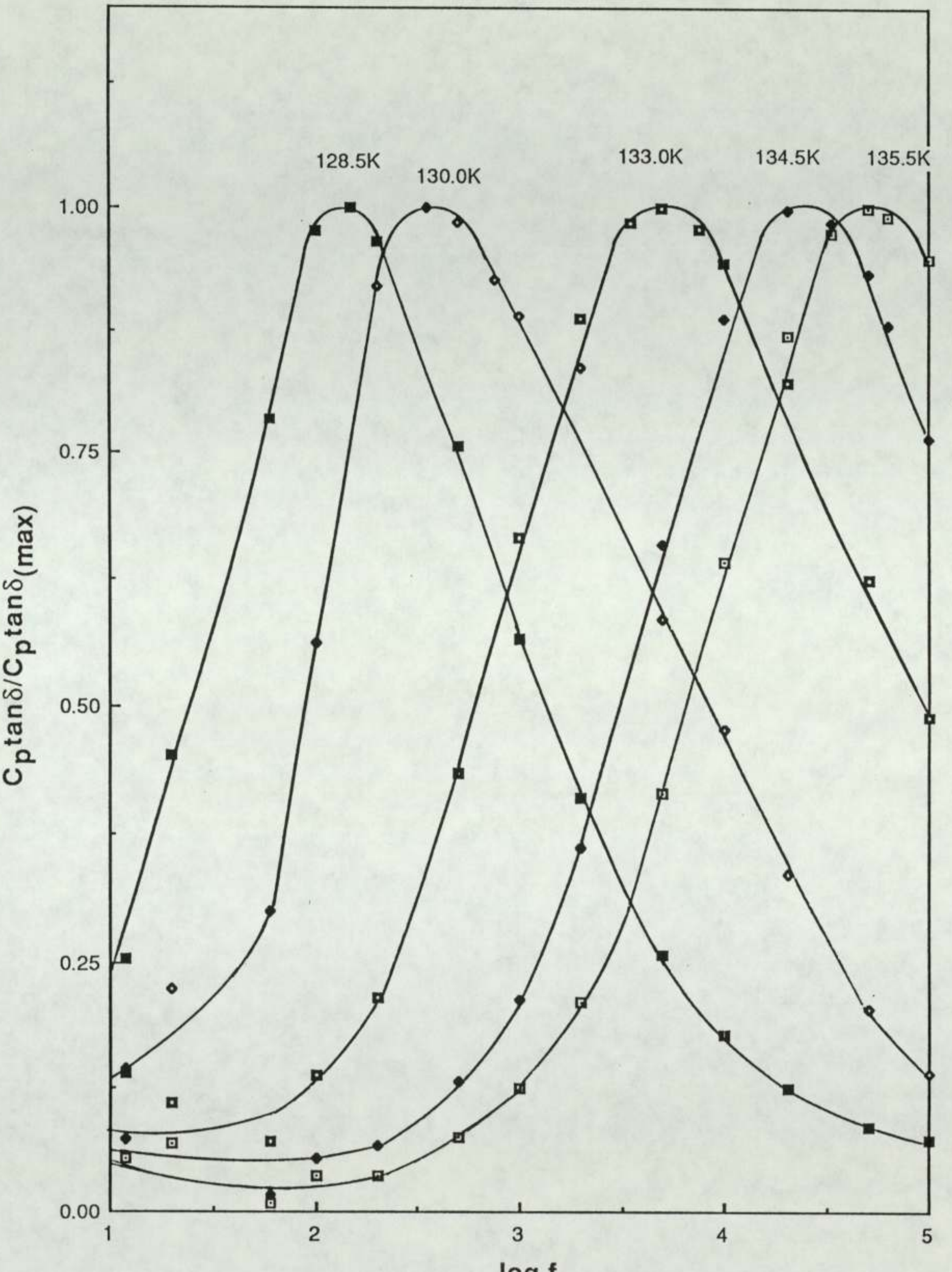

<u>Figure (5-82)</u> Frequency dependence of $C_p\tan\delta/C_p\tan\delta_{(max)}$ for linear PMHS at various temperatures.

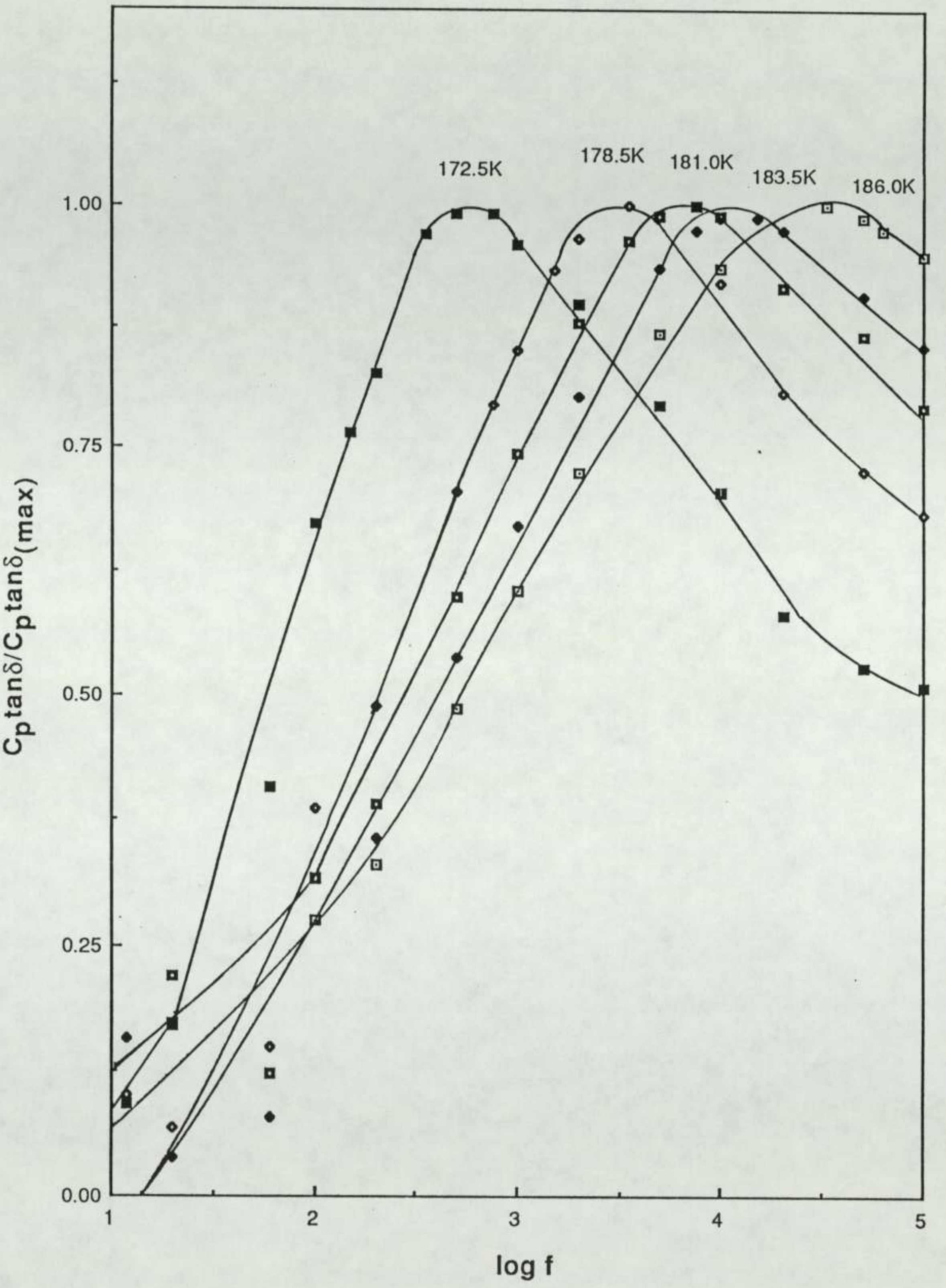

Figure (5-83) Frequency dependence of $C_p\tan\delta/C_p\tan\delta_{(max)}$ for linear poly(n-hexyl methyl siloxane) at various temperatures.

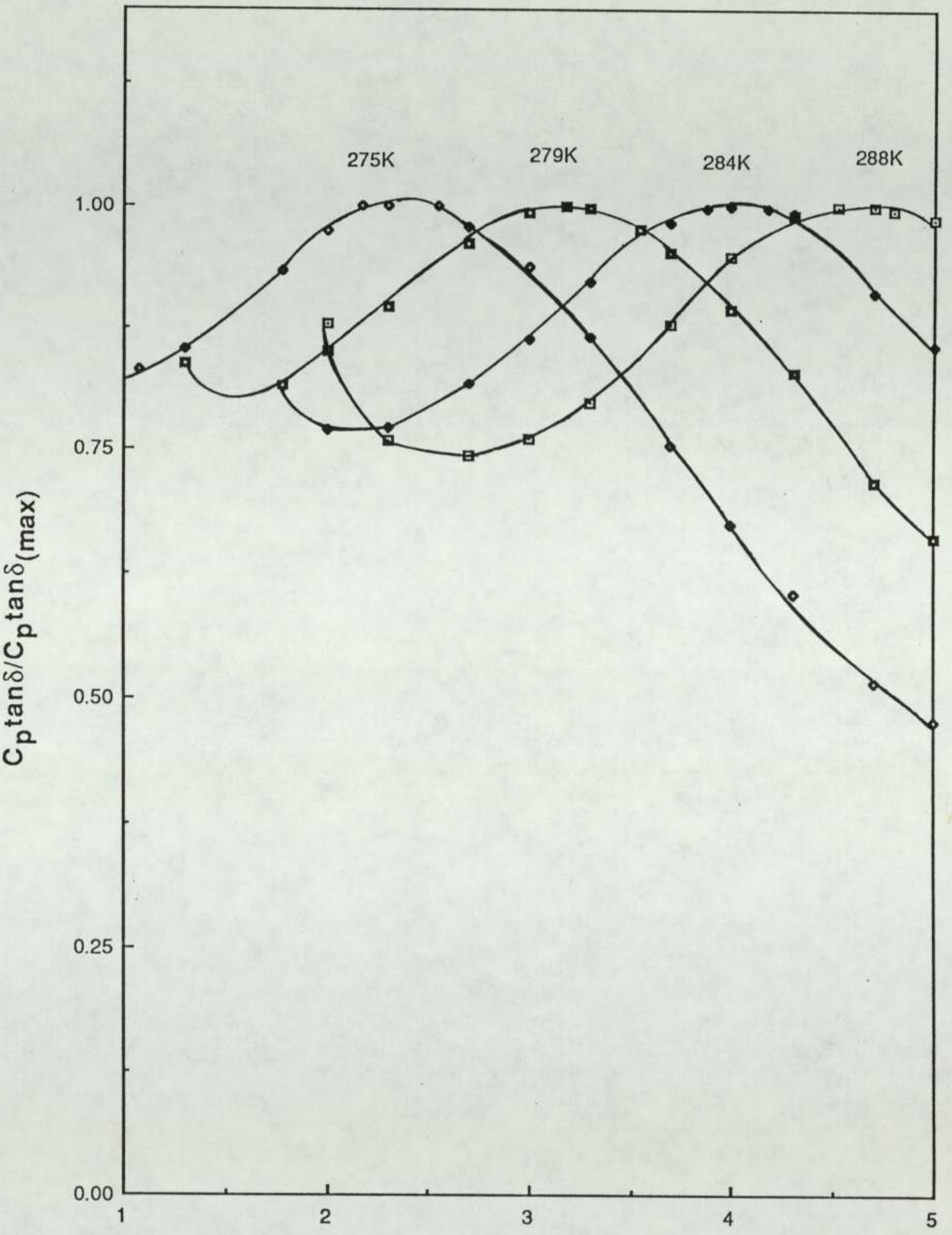

Figure (5-84). Frequency dependence of $C_p\tan\delta/C_p\tan\delta_{(max)}$ for a side chain polymer liquid crystal in the liquid crystalline phase at various temperatures.

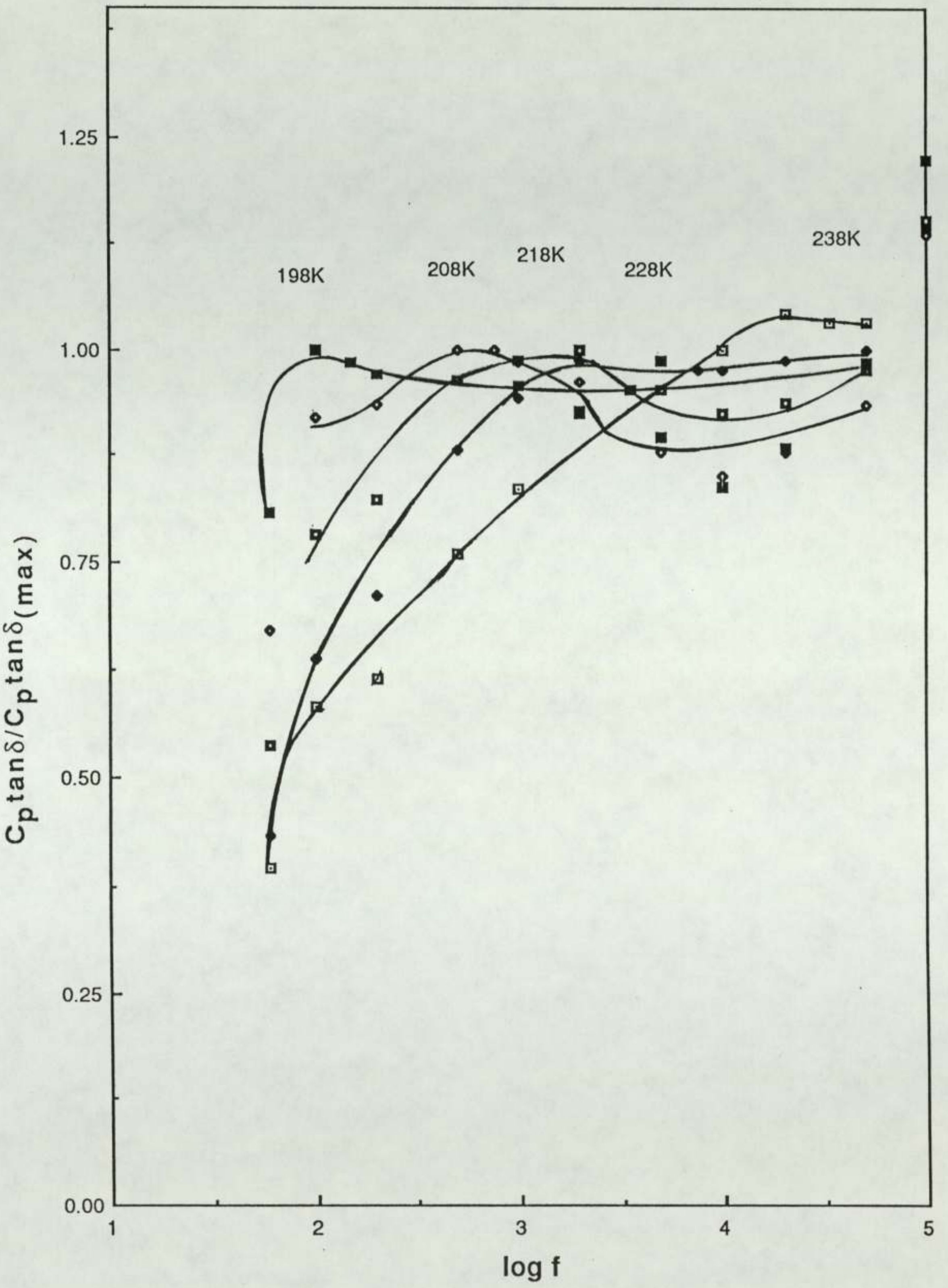

Figure (5-85). Frequency dependence of $C_p\tan\delta/C_p\tan\delta_{(max)}$ for a side chain polymer liquid crystal below T_g at various temperatures.

crystalline phase above T_g are extremely broad, as found in earlier studies by other workers. The high frequency α-process, observed by Williams and co-workers[56], is not apparent. The broadness of each loss curve made the width at half height difficult to estimate. The presence of ionic impurities in the sample resulted in conductive losses as well as dielectric losses, as shown by the low frequency upturn in the curves. At higher temperatures the dielectric losses were completely obscured by the conductive losses, thus no dielectric loss measurements were possible in the isotropic phase of the sample.

In the glassy state of the sample, below T_g, the frequency corresponding to maximum dielectric loss was barely apparent, due to the unusual shape of each loss curve.

5.11:Dielectric Relaxation Activation Energy.

Figures (5-86) and (5-87) show Arrhenius plots of the logarithm of the frequency corresponding to maximum dielectric loss against the reciprocal of the absolute temperature for the samples based on PMHS. All the plots are linear, within experimental error, and have a slope proportional to the activation energy for the relaxation process.

5.12: Cole-Cole Plots.

Figures (5-88) to (5-91) are Cole-Cole plots of ε'' against ε' for PMHS and poly(n-hexyl methyl siloxane) at various temperatures. The PMHS and poly(n-hexyl methyl siloxane) plots are skewed arcs. The limiting values of permittivity, ε_0 and ε_∞, are estimated from the plots using extrapolation procedures previously described..

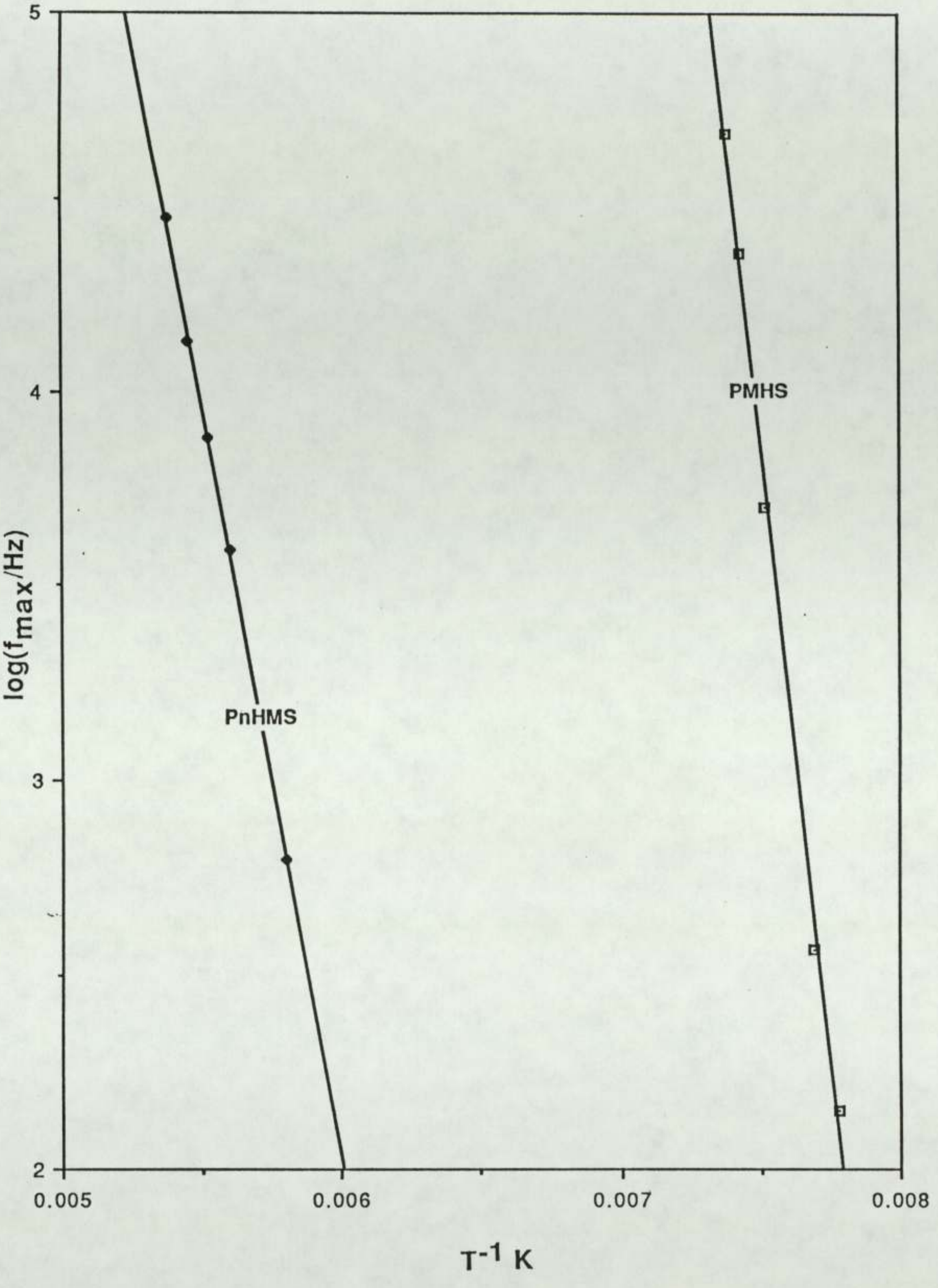

Figure (5-86) Log(f_{max}/Hz) against T^{-1} K for poly(methylhydrogen siloxane) and poly(n-hexyl methyl siloxane)

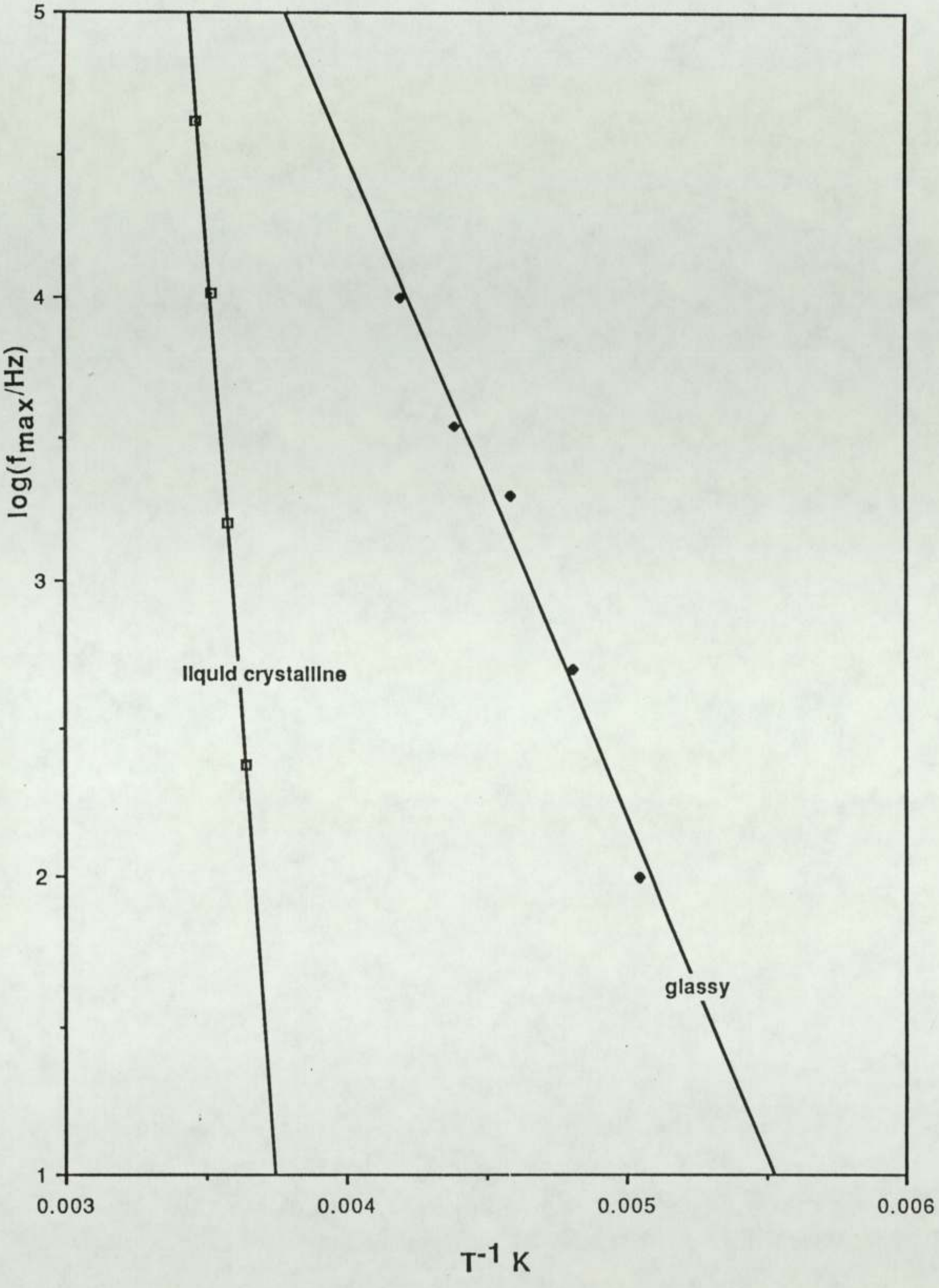

Figure (5-87) Log(f_{max}/Hz) against T^{-1} K for a polysiloxane liquid crystal in the liquid crystalline phase and below T_g

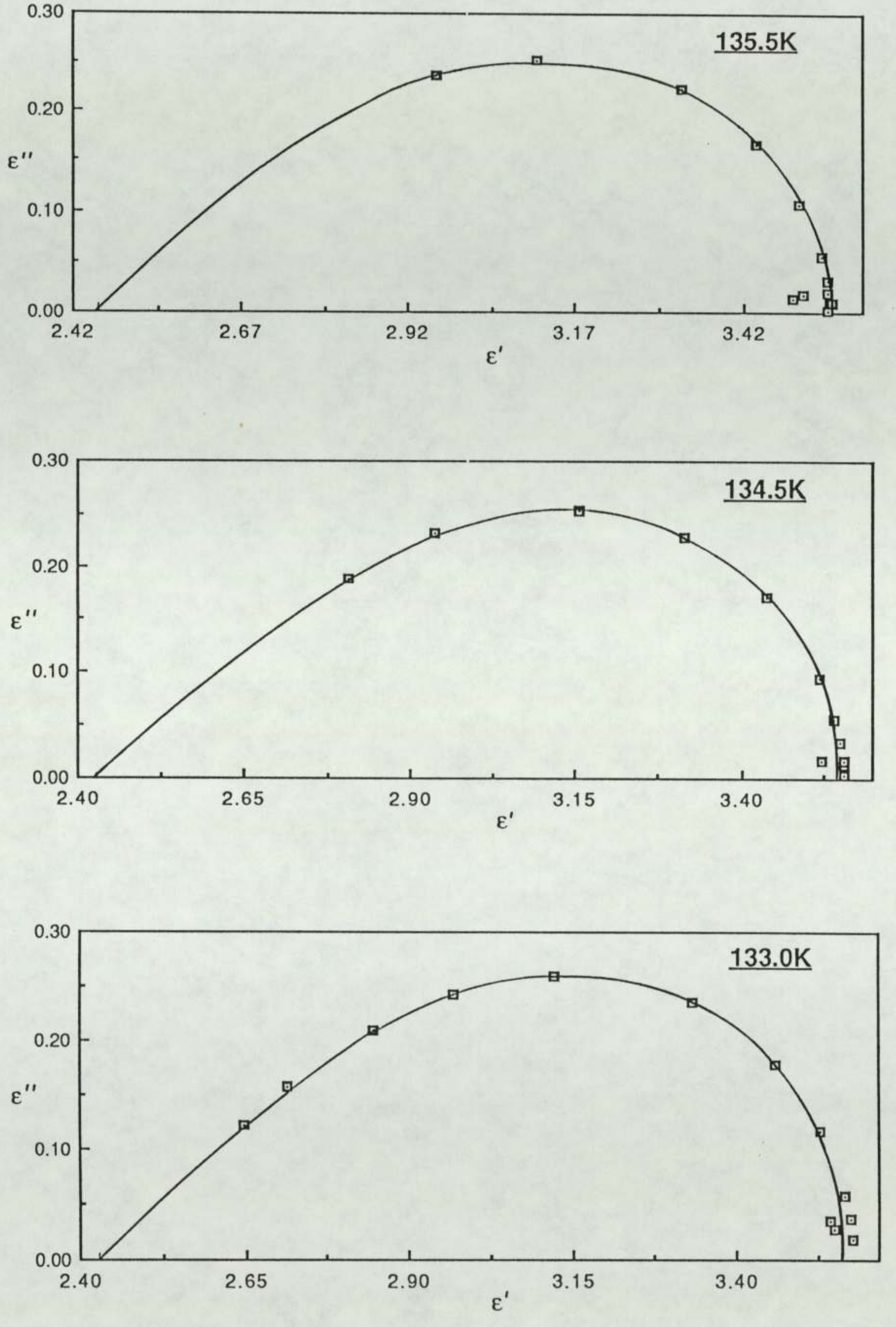

Figure (5-88) Cole-Cole plots for linear poly(methylhydrogen siloxane) at various temperatures

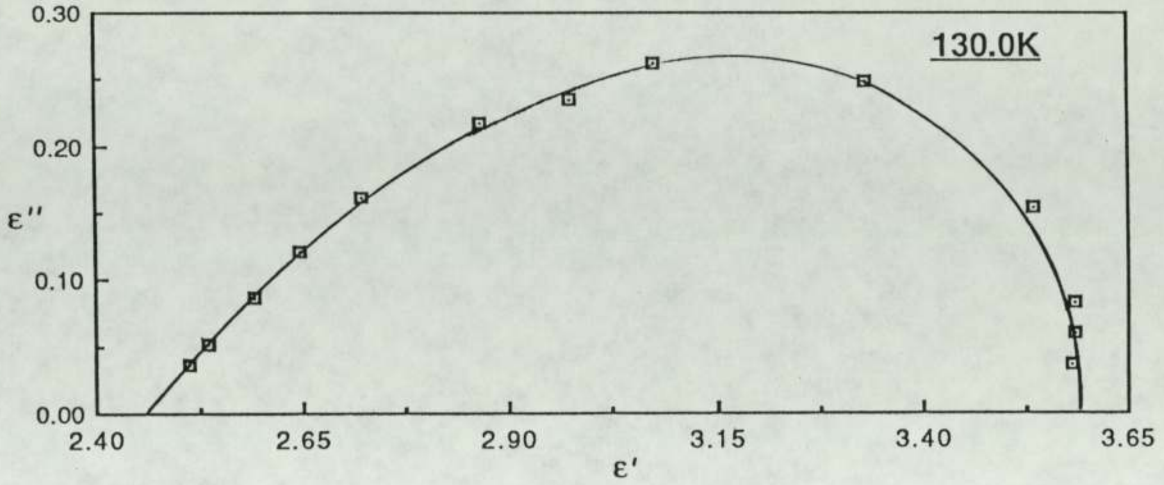

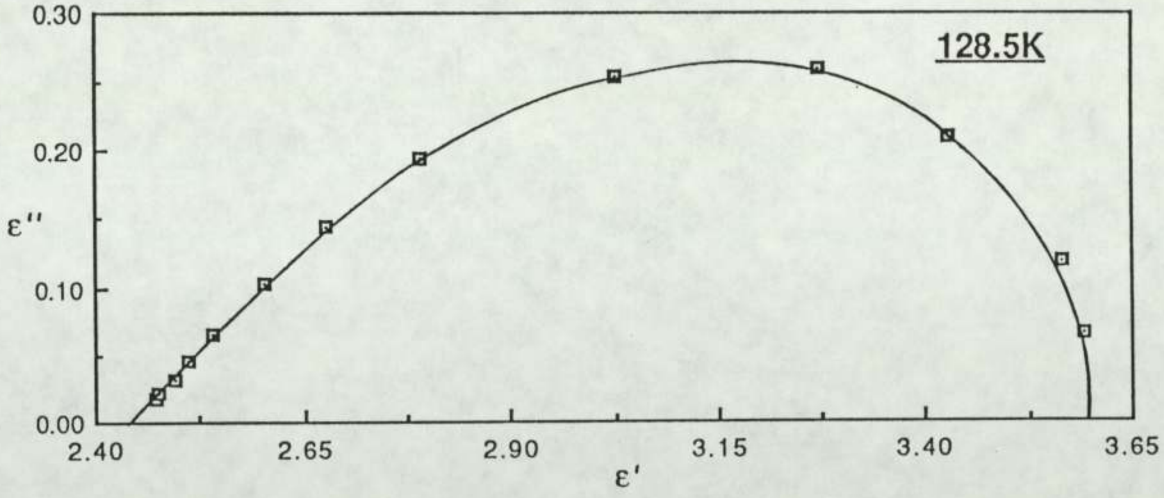

Figure (5-89) Cole-Cole plots for linear poly(methylhydrogen siloxane) at various temperatures

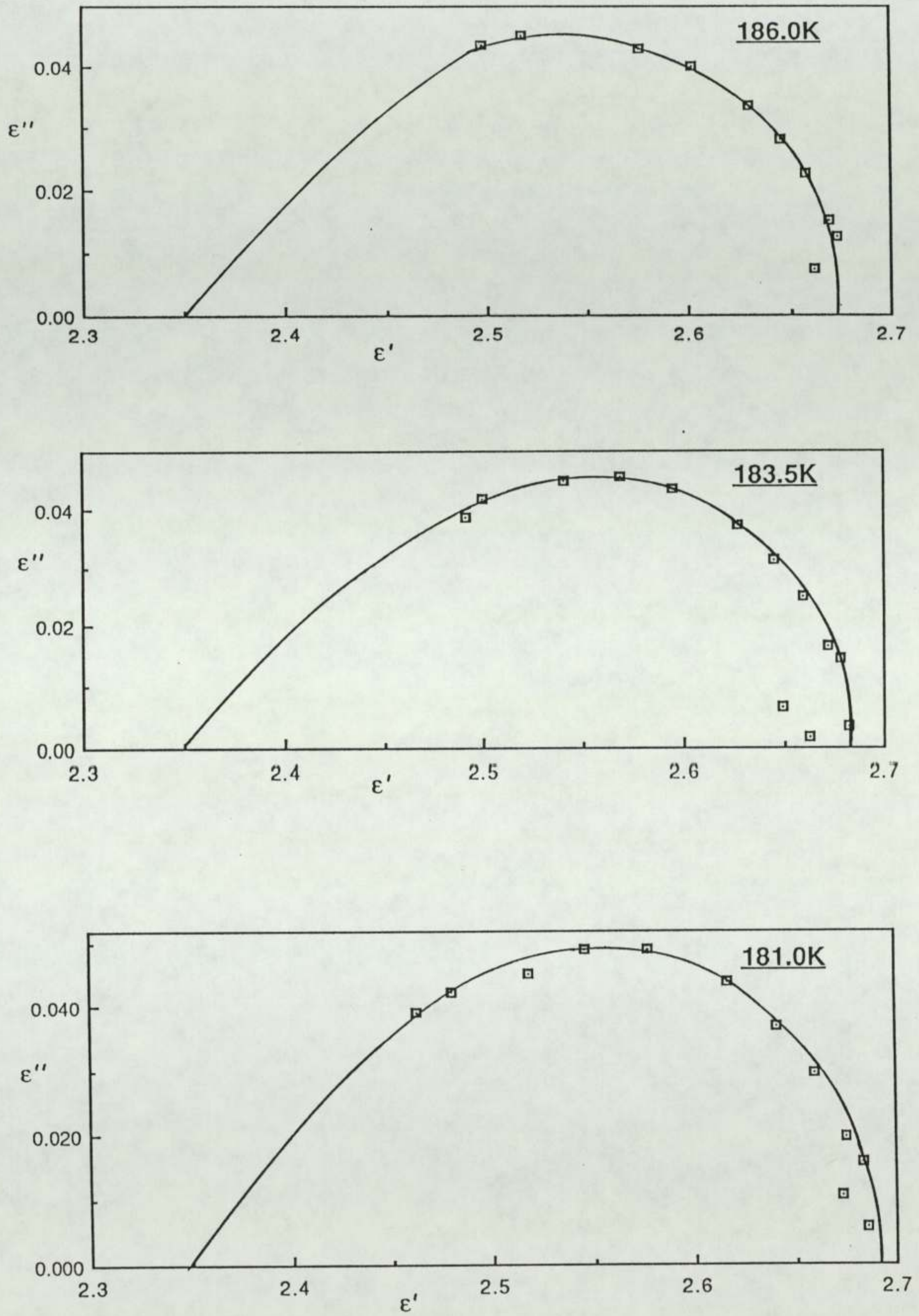

<u>Figure (5-90)</u> **Cole-Cole plots for linear poly(n-hexyl methyl siloxane) at various temperatures**

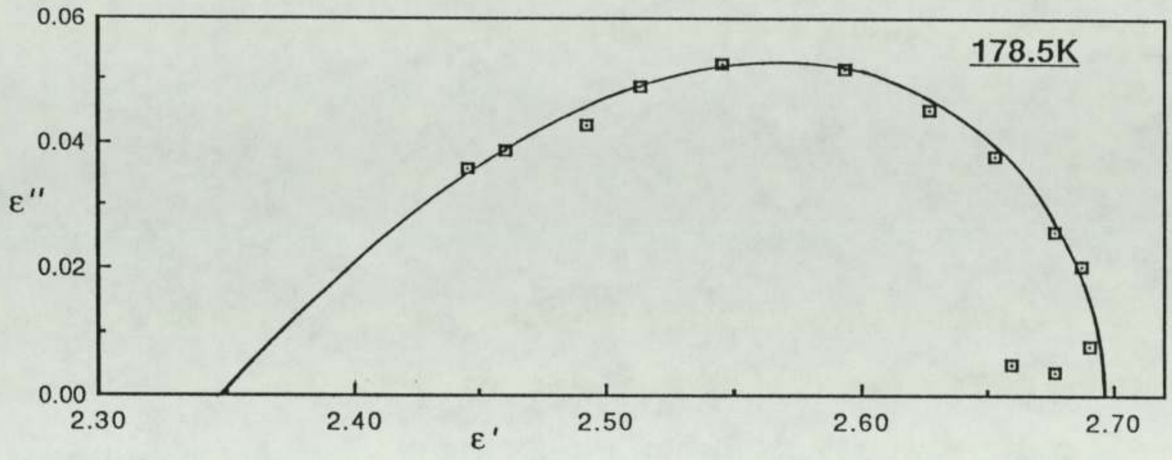

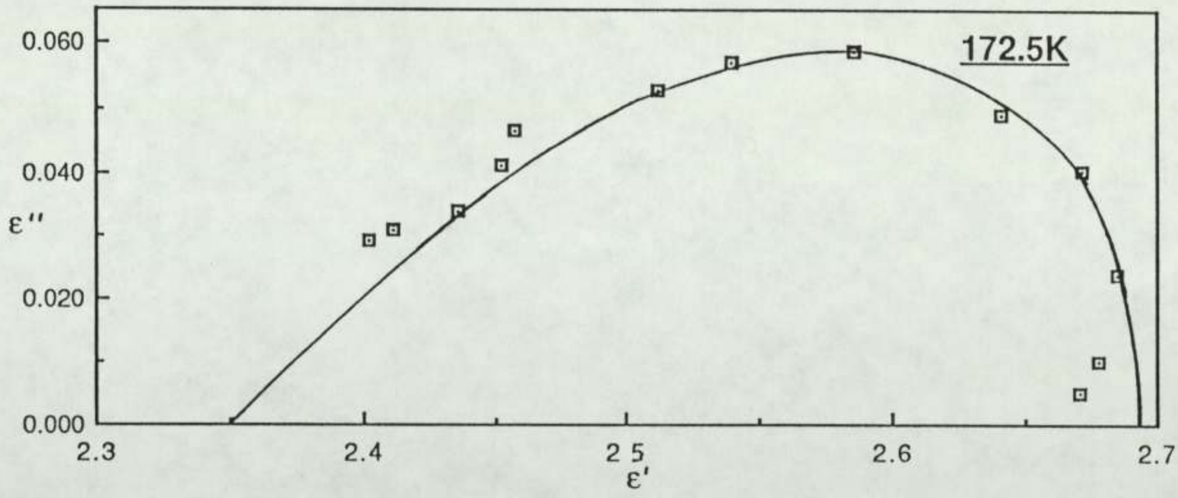

<u>Figure (5-91)</u> **Cole-Cole plots for linear poly(n-hexyl methyl siloxane) at various temperatures**

For PMHS ε_∞ was found to be 2.44 while for poly(n-hexyl methyl siloxane) ε_∞ was estimated to be 2.35. The values of ε_0 for PMHS reach a maximum value of 3.62, compared with a maximum value of ε_0 equal to 2.70 for poly(n-hexyl methyl siloxane).

The values of maximum dielectric loss are also greater for PMHS, being approximately equal to 0.26, while for poly(n-hexyl methyl siloxane) the maximum values of dielectric loss are approximately equal to 0.06. This behaviour may be due to two factors. Firstly, there are fewer dipoles per unit volume in a given amount of poly(n-hexyl methyl siloxane) than there are in the same amount of PMHS, because of the increased volume occupied by the n-hexyl chain compared to the volume occupied by the replaced hydrogen atom. Secondly, the broadness of the loss curve is important, since total dielectric loss is proportional to the area under the loss curve. A dielectric relaxation process characterised by a broad distribution of relaxation times, will have the total dielectric loss spread over a wide frequency range. A similar process, involving the same total dielectric loss, but with a narrower distribution of relaxation times, will have the total dielectric loss spread over a smaller frequency range. Hence, the loss maxima for the latter process will be larger than the loss maxima for the former process.

The gum-like nature of the polymer liquid crystal sample, even at elevated temperatures, led to difficulties in filling the dielectric cell with a known volume of specified geometry, hence it was not possible to calculate absolute values of ε'' and ε'. Instead, Cole-Cole plots for the polymer liquid crystal were drawn as $C_p\tan\delta$ against C_p. These are presented in Figures (5-92) to (5-95).

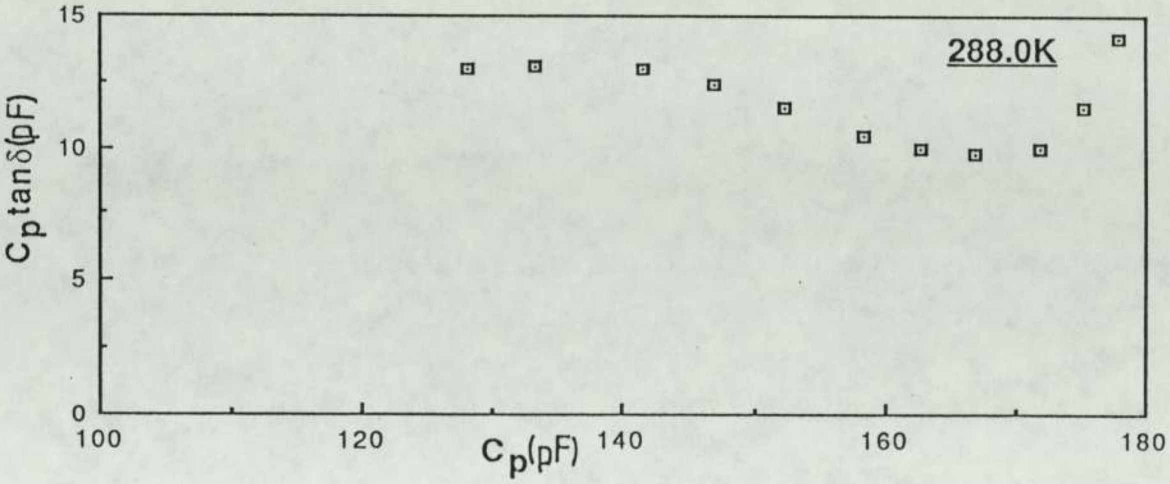

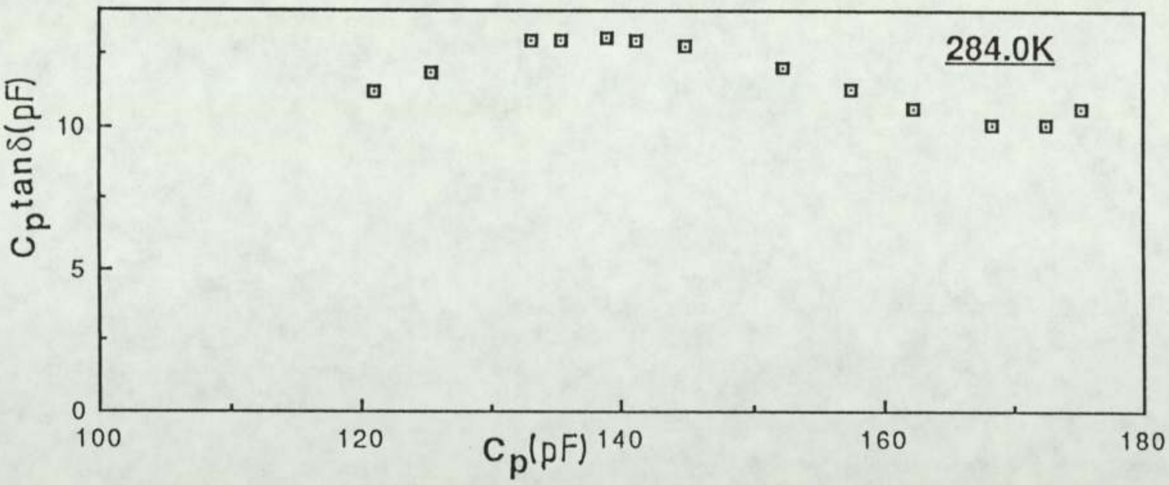

<u>Figure (5-92)</u> **Cole-Cole plots for a polysiloxane liquid crystal in the liquid crystalline phase at various temperatures**

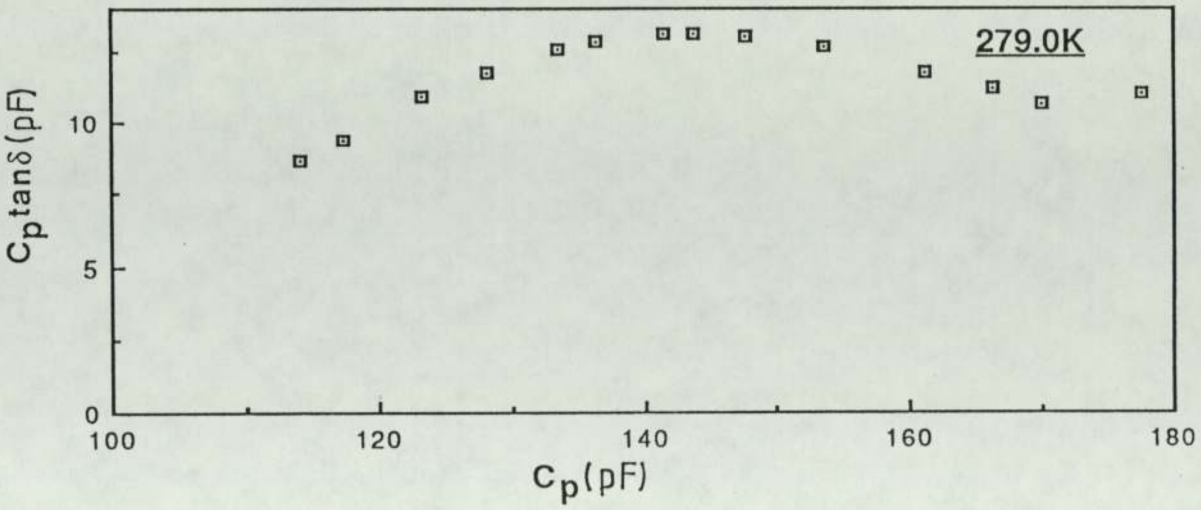

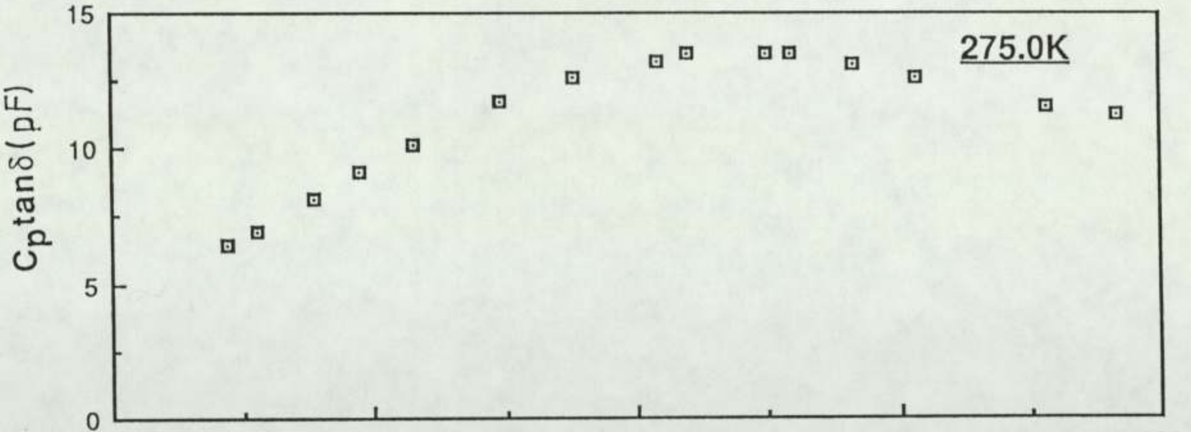

Figure (5-93) Cole-Cole plots for a polysiloxane liquid crystal in the liquid crystalline phase at various temperatures

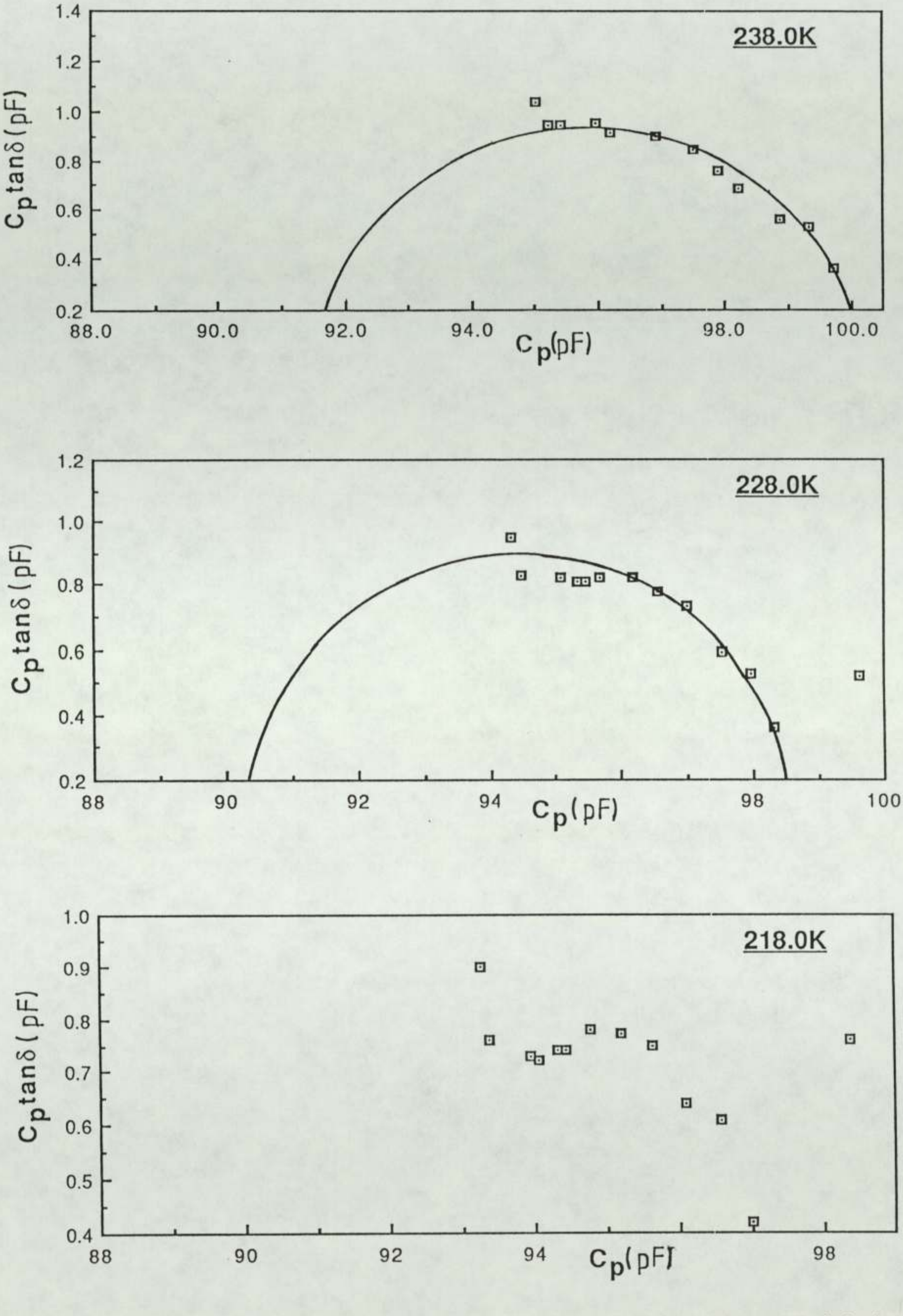

Figure (5-94) Cole-Cole plots for a polysiloxane liquid crystal below T_g at various temperatures

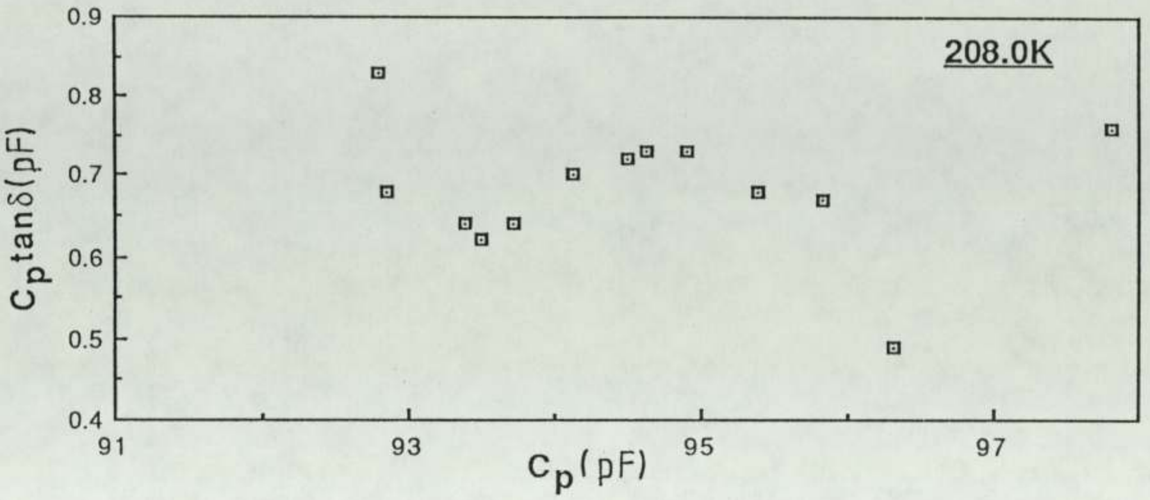

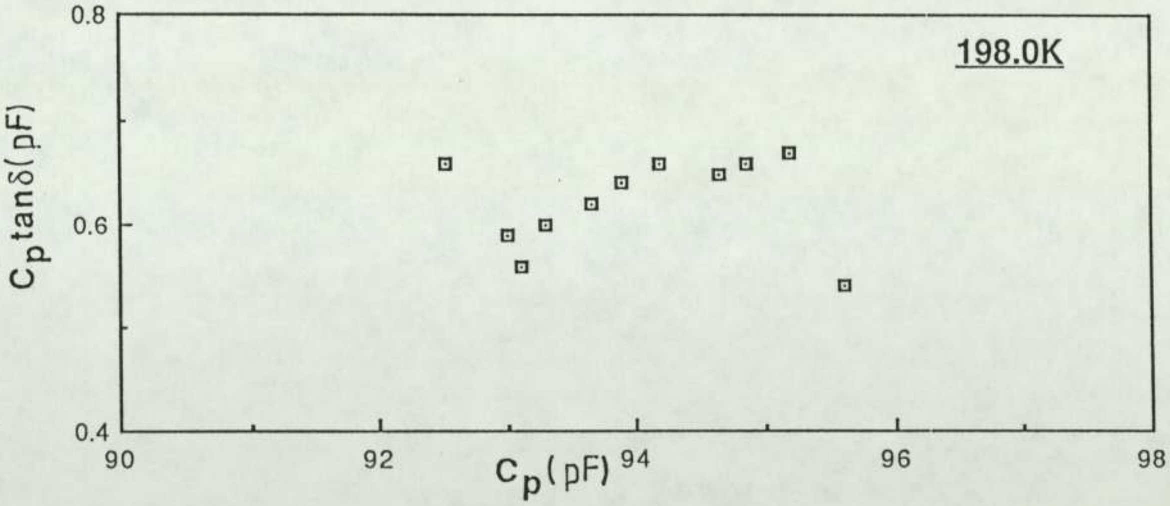

Figure (5-95) Cole-Cole plots for a polysiloxane liquid crystal below T_g at various temperatures

CHAPTER 6

DISCUSSION OF DIELECTRIC RESULTS

6.01: Introduction.

In this chapter the dielectric relaxation activation energies measured from the Arrhenius plots, the Davidson-Cole distribution parameter, β, the Cole-Cole distribution parameter, α, and the mean-square dipole moment $<\mu^2>$, calculated using the Onsager equation, are used as a basis for comparing the dielectric relaxation behaviour of the siloxane based materials discussed in Chapter 5.

6.02: Dielectric Relaxation Activation Energies of Cyclic and Linear Poly(dimethyl siloxanes).

Figure (6-1) shows the variation with molecular weight of the average activation energy for the α-relaxation process of cyclic and linear fractions of PDMS. The plot also includes the standard error associated with each data point. The general non-overlap of the data indicates that cyclic and linear fractions of PDMS, over the range of molecular weights studied, experience different barriers opposing dipolar rotation. For cyclic and linear fractions of PDMS(with the exception of the linear fraction with $\bar{n}_n$=28), the average activation energy increases markedly with increasing molecular weight over the range of molecular weights studied. This behaviour may be interpreted in terms of an increase in the extent of co-operation between neighbouring dipoles that is required for dipolar rotation as molecular weight increases. For a given molecular weight the larger

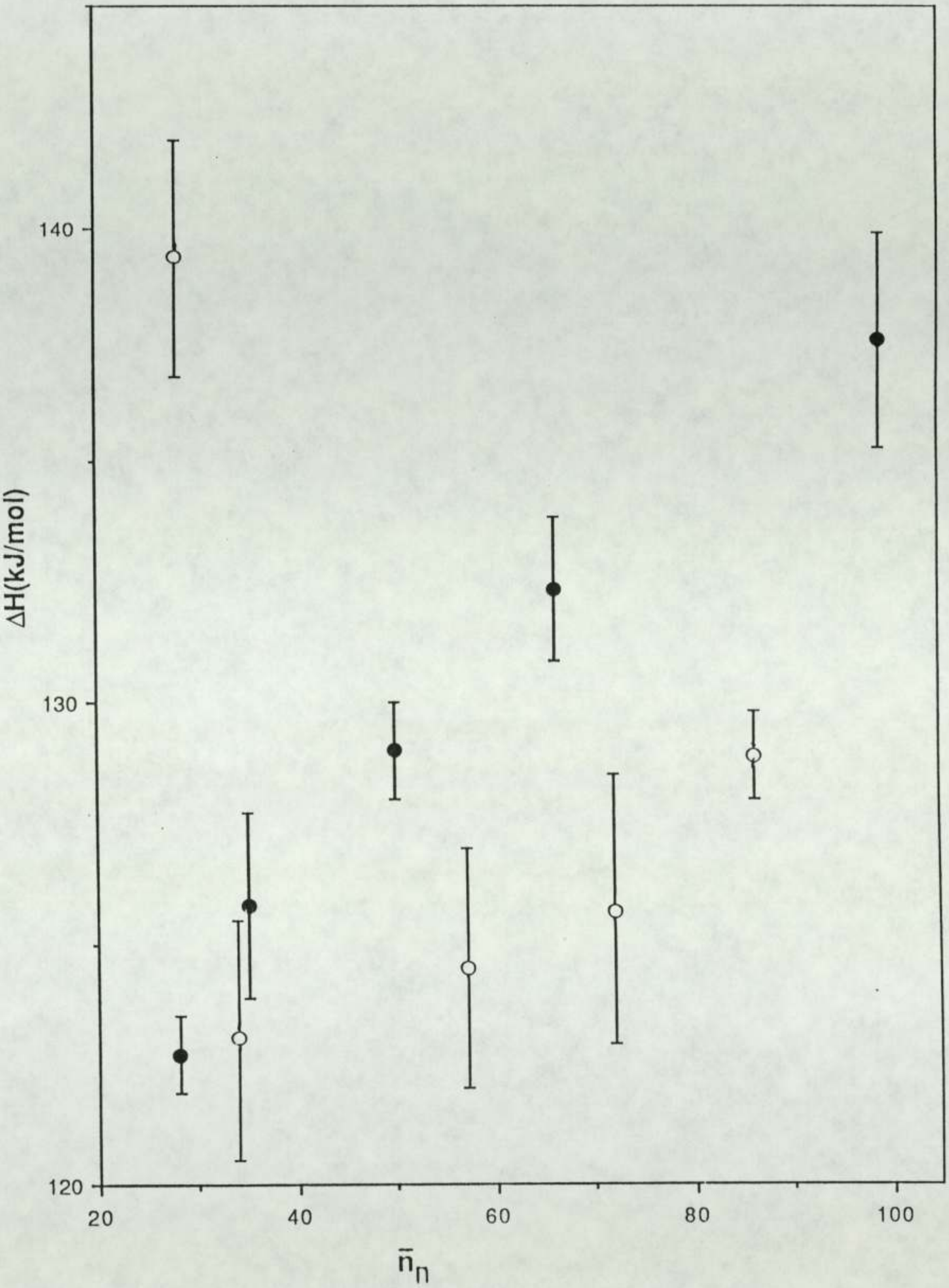

Figure (6-1) Average dielectric relaxation activation energies for cyclic (●) and linear (○) poly(dimethyl siloxanes) value of ΔH_{act} for the cyclic fractions suggests that dipolar rotation is more restricted in the cyclic structure. Because of the absence of any rapid changes in the molecular weight dependence of ΔH_{act} for the fractions studied, it is not possible, using this data alone, to identify a 'critical 'molecular weight region for PDMS. In such a region the onset of long range inter-molecular chain entanglements would be expected to produce a pronounced change in ΔH_{act} for the relaxation process. The critical molecular weight of linear PDMS, estimated from bulk viscosity measurements[111], is 24 500.

A study of the activation energies for molecular weights beyond the current range might be expected to reveal a convergence of ΔH_{act} values for cyclic and linear PDMS as the Si-O dipoles in both structures begin to encounter approximately equal barriers to rotation in sufficiently large molecules.

A direct comparison between the dielectric relaxation activation energies measured in this study and those measured by previous workers is difficult because of the scarcity of published work concerning the dielectric behaviour of amorphous PDMS. A number of different studies[38] of amorphous and partially crystalline samples of linear PDMS have reported ΔH_{act} values in the range ~46 kJ mol^{-1} to ~155 kJ mol^{-1}. For an amorphous sample of linear poly(methyltrifluoropropyl siloxane) Baird and co-workers[112] reported an average activation energy for the α- relaxation process of 112 kJ mol^{-1}.

As far as the author is aware no studies concerning ΔH_{act} for cyclic PDMS have been published to date.

6.03: Davidson-Cole Analysis of Dielectric Data Obtained for Cyclic and Linear Poly(dimethyl siloxanes).

Values of the Davidson-Cole empirical distribution parameter, β, for cyclic and linear fractions of PDMS, are presented in Table (6-1). The values shown are average values of β measured over a small temperature range. With the exception of the linear fraction with $\bar{n}_n$=86 there is an increase in the value of β (i.e. the distribution of relaxation times narrows) as the temperature increases for both cyclic and linear fractions of PDMS. This behaviour is typical of many materials. There is no indication that β depends on molecular weight for cyclic and linear fractions over the range of molecular weights studied.

In general, there appears to be no observable difference in the distribution of relaxation times, within experimental error, between cyclic and linear fractions of PDMS over the range of molecular weights studied (this is an interesting observation, considering that there is a measurable difference in activation energies between cyclic and linear PDMS). Evidently, the effect of the terminal $(CH_3)Si-O$ groups possessed by the linear fractions are unimportant over this molecular weight range. At shorter chain lengths terminal groups would be expected to contribute to the number of different environments experienced by the dipolar segments, and thus lead to an increase in the number of different relaxation times required for dipolar rotation. No such effects are apparent with cyclic polymers since they do not possess terminal groups.

From the Cole-Cole plot presented by Adachi and co-workers[38] the

CYCLICS			LINEARS		
$\bar{n}_n$	T/K	β	$\bar{n}_n$	T/K	β
28	148.0-153.5	0.39	28	142.0-145.0	0.38
28	153.5-157.5	0.43	28	145.0-148.0	0.41
35	147.5-152.0	0.39	34	140.5-144.5	0.39
35	152.0-155.5	0.44	34	144.5-148.5	0.48
50	147.5-153.0	0.42	57	143.0-147.0	0.39
50	153.0-156.5	0.43	57	147.0-150.5	0.40
66	147.0-153.0	0.41	72	143.0-148.0	0.37
66	153.0-156.5	0.42	72	148.0-151.5	0.39
99	149.0-153.0	0.36	86	144.5-147.5	0.44
99	153.0-156.0	0.41	86	147.5-151.5	0.40

Table (6-1) Davidson-Cole distribution parameter, β, for cyclic and linear poly(dimethyl siloxanes). [error in values of β is ±0.02] author has estimated β to be 0.39 for a linear PDMS possessing an approximate molecular weight of 8.3×10^5.

6.04: Mean-Square Dipole Moments of Cyclic and Linear Poly(dimethyl siloxanes).

The magnitude of the dielectric dispersion, $(\varepsilon_0 - \varepsilon_\infty)$, may be used to derive a mean-square dipole moment, $\langle\mu^2\rangle$, for the total number N, of dipolar units present in unit volume of the dielectric.

Experimental values of $\langle\mu^2\rangle$ were calculated for cyclic and linear fractions of PDMS using the Onsager equation discussed in Chapter 2. The limiting values of permittivity, ε_0 and ε_∞, were measured from the Cole-Cole plots, Figures (5-21) to (5-40). The densities of the cyclic and linear fractions of PDMS, reported by previous workers[34], were corrected to allow for an increase in density that occurs as the temperature is lowered.

The experimental mean-square dipole moments per repeat unit, at 148K, are shown in Table (6-2). The values of $\langle\mu^2\rangle$ per repeat unit for cyclic and linear fractions of PDMS, in the molecular weight range studied, are identical, within experimental error.

Figures (6-2) and (6-3) show the variation with $\bar{n}_n$ of $\langle\mu^2\rangle$, for cyclic and linear fractions of PDMS at 148K. Also included are the corresponding values of $\langle\mu^2\rangle$ measured by previous workers at 298K. The values of $\langle\mu^2\rangle$ measured for cyclic and linear fractions of PDMS at 148K show a slight decrease when compared with the values measured at 298K. Because of the uncertainty of the errors associated with the dipole moments measured at 148K it is only possible

CYCLICS		LINEARS	
$\bar{n}_n$	$<\mu^2>$/Debyes	$\bar{n}_n$	$<\mu^2>$/Debyes
28	0.17	28	0.17
35	0.17	34	0.15
50	0.17	57	0.18
66	0.18	72	0.17
99	0.16	86	0.18

Table (6-2) Experimental mean-square dipole moments per repeat unit for cyclic and linear poly(dimethyl siloxanes). [error in $<\mu^2>$ is ± 0.02]

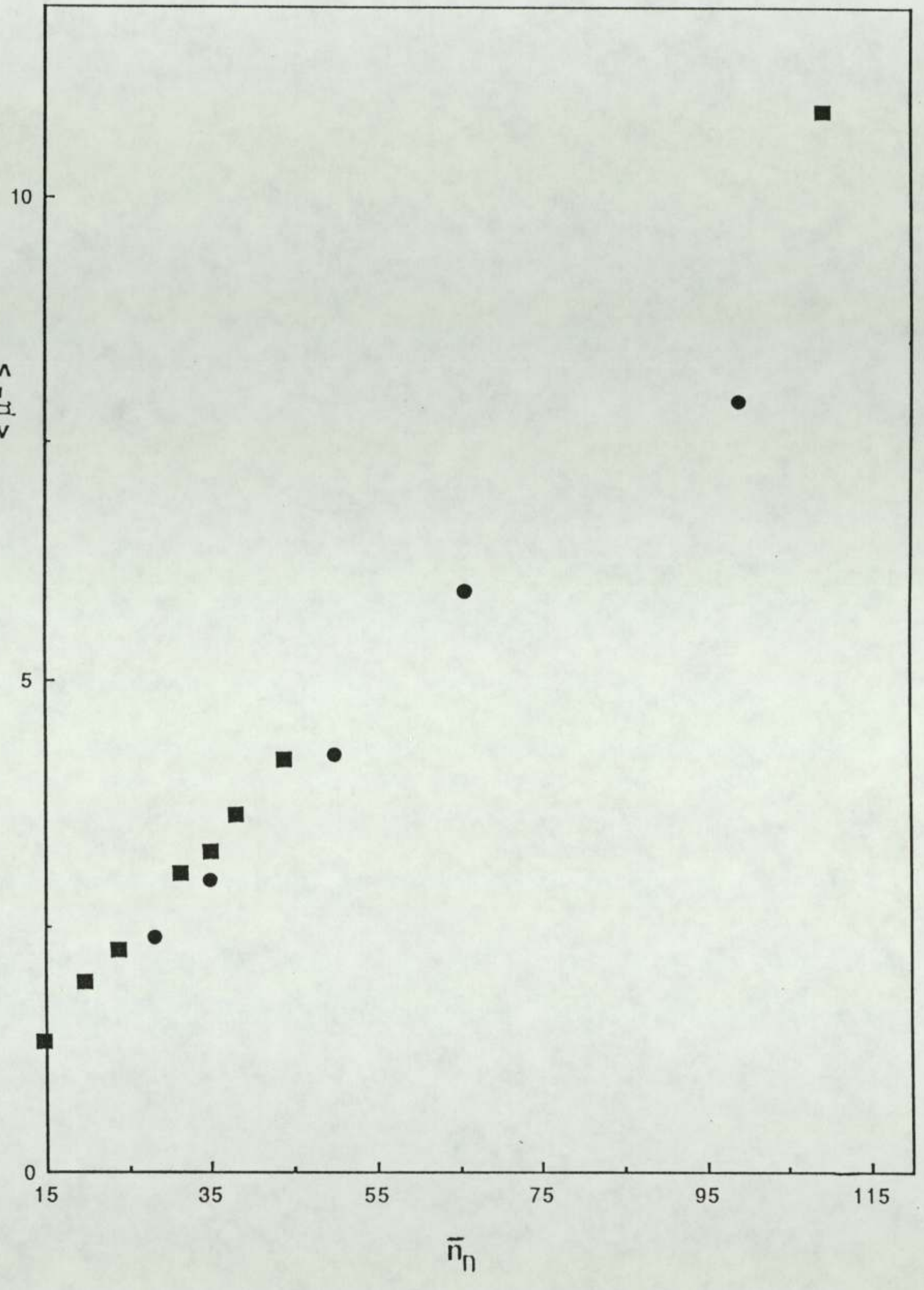

Figure (6-2) Experimental mean-square dipole moments $<\mu^2>$ (Debyes) for cyclic poly(dimethyl siloxanes)

[● present study at 148K; ■ Beevers and Mumby at 298K^{34}]

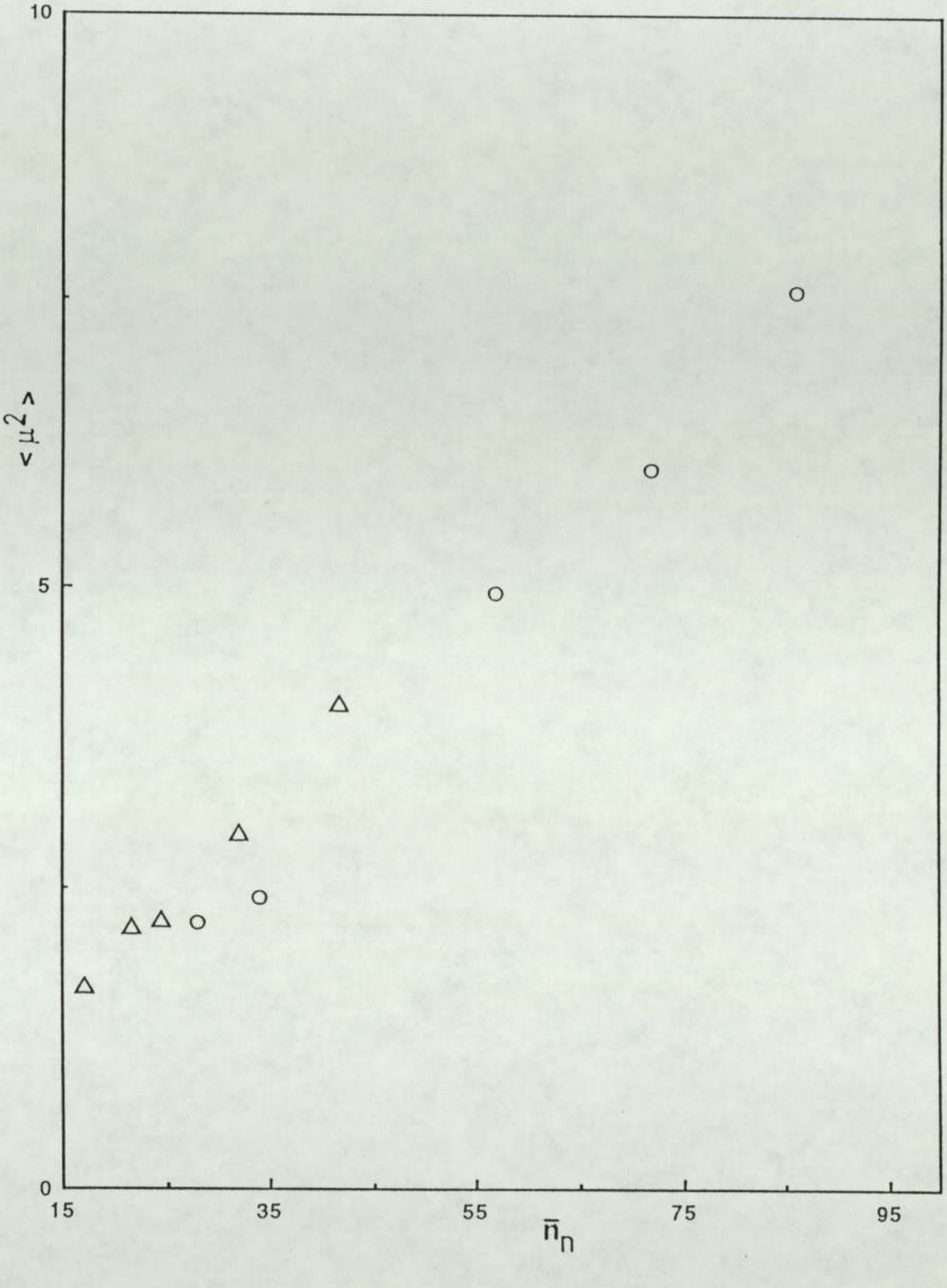

Figure (6-3) Experimental mean-square dipole moments $<\mu^2>$ (Debyes) for linear poly(dimethyl siloxanes)

[○ present study at 148K; △ Beevers and Mumby at 298K[34]] to state that the quantity $\Delta \ln<\mu^2>/\Delta T$, estimated in the present study, is of the same order of magnitude as the related quantity $d\ln<\mu^2>/dT$ measured by Mark for dimethyl siloxane chains over a wide range of molecular weight. According to Mark's calculations the sign of $d\ln<\mu^2>/dT$ changes from negative to positive between $n_n=22$ and $n_n=42$. For a linear fraction of PDMS with $n_n= 66$, Mark calculated $d\ln <\mu^2>/dT$ to be equal to 0.32×10^{-3}.

A quantity which is very sensitive to the conformational properties of flexible polymer molecules is the dipole moment ratio $<\mu^2>/nm^2$, where m is the link dipole moment. The product nm^2, where n is the number of skeletal bonds in the chain, represents an idealised view of a polymer chain in which the dipoles are freely jointed and can rotate independently of each other. The dipole moment ratio represents the factor by which the experimental mean-square dipole moment, $<\mu^2>$, of the actual chain departs from this idealised view. Experimental values of the dipole moment ratio are plotted in Figure (6-4), with m=0.60D. The dipole moment ratios measured by previous workers are also plotted. Differences in the values of the dipole moment ratio measured by previous workers are due to the different methods employed in deriving the atomic polarisations of the materials.

According to the non-statistical vectorial calculations carried out by Mark[32] for linear oligomers of dimethyl siloxane the dipole moment ratio should reach a maximum at n=8. Mark's calculations suggested that, for the hypothetical, planar, all-trans conformation of dimethyl siloxanes, increasing the number of dipoles beyond n=8 would diminish the dipole moment ratio until the dimethyl siloxane chain becomes completely closed, because of unequal bond angles, at

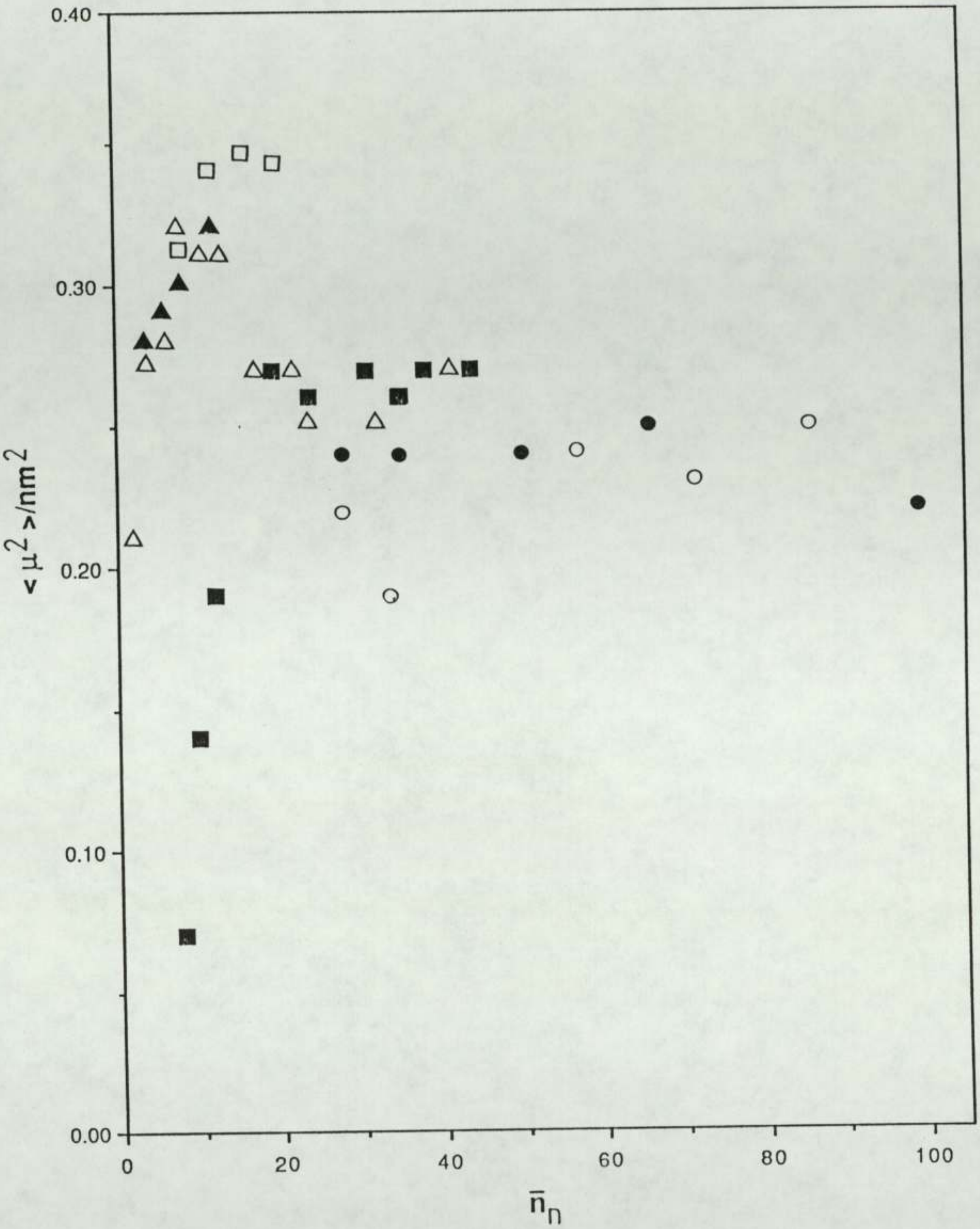

Figure (6-4) Dipole moment ratio $<\mu^2>/nm^2$ for cyclic poly(dimethyl siloxanes) [● present study; ■ Beevers and Mumby[34] ;] and for linear poly(dimethyl siloxanes) [○ present study; △ Beevers and Mumby[34] ; ▲ DasGupta and Smyth[31] ; □ Sutton and Mark[33] ;]

n_n=24. However, the range of molecular weights of cyclic and linear fractions of PDMS which this study is concerned with lies above the molecular weight region discussed by Mark.

6.05: Dielectric Relaxation Activation Energies of Linear Oligomers of Methyl Phenyl Siloxane, Linear Fractions of Poly(methyl phenyl siloxane) and a Cyclic Oligomer of Methyl Phenyl Siloxane.

Figure (6-5) shows the dependence on the molecular weight of the average activation energy for the α- relaxation process of linear oligomers of methyl phenyl siloxane, linear fractions of poly(methyl phenyl siloxane) and a cyclic oligomer of methyl phenyl siloxane. The standard error associated with each data point is also included in the plot. The experimental average activation energies lie in the approximate range 170 kJ mol^{-1} to 240 kJ mol^{-1}. This range of values is significantly lower than the value of 320 kJ mol^{-1} measured by Baird and co-workers[37] for a linear oligomer of methyl phenyl siloxane. However, this oligomer was terminated by bulky phenyl groups which could explain the higher activation energy.

Figure (6-5) may be divided into three regions (indicated on figure). The first region, starting from the linear oligomer of methylphenyl siloxane with n = 4 and finishing at the oligomer with n = 10, shows a sharp increase in ΔH_{act} with increasing molecular size. Taking into account the very short chain lengths of these molecules and the effect of the phenyl groups in reducing chain flexibility, the observed increase in ΔH_{act} in this region is consistent with the idea that, for

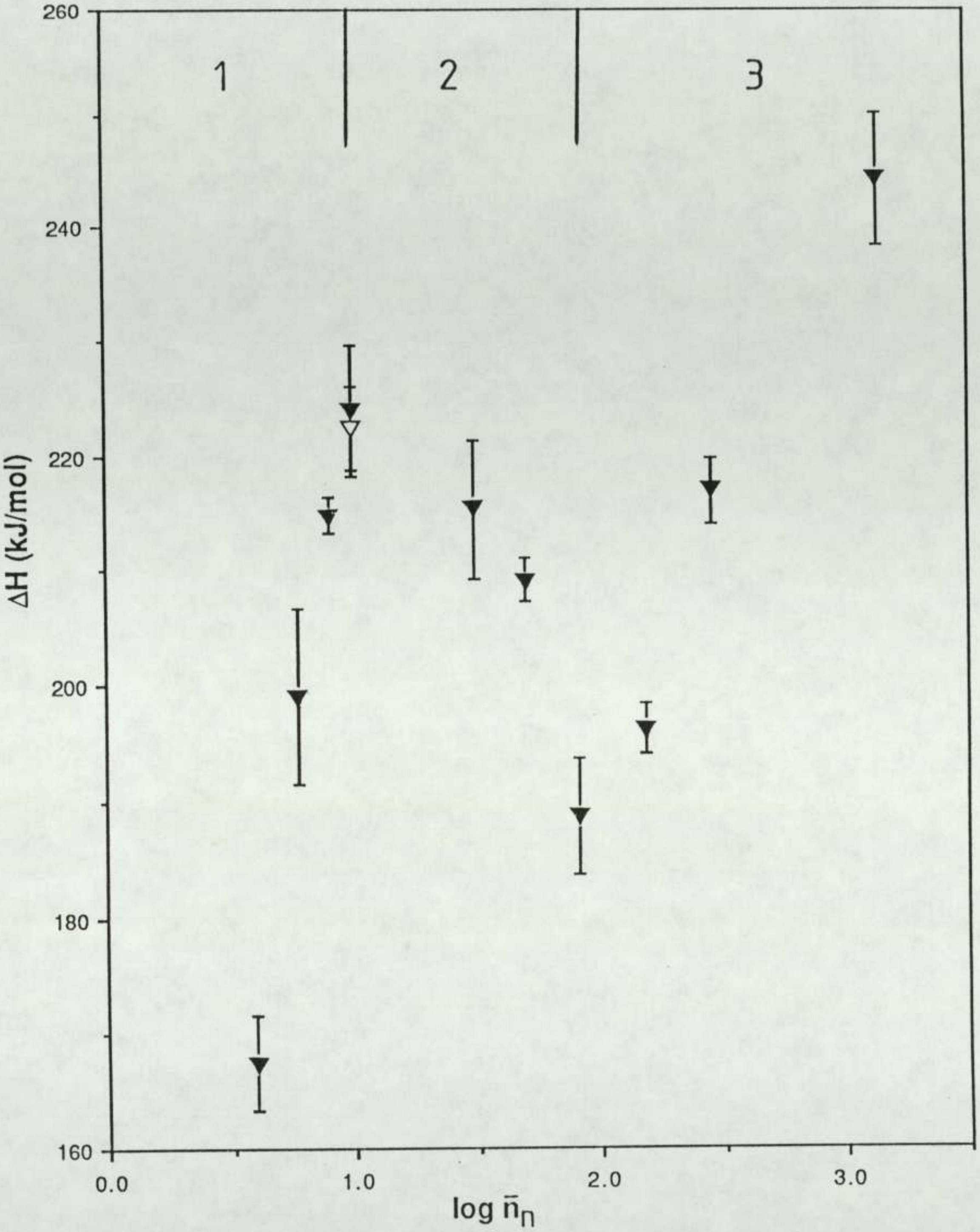

Figure (6-5) Average dielectric relaxation activation energies for linear methyl phenyl siloxanes (▼) and for a cyclic methyl phenyl siloxane (▽)

oligomers of methyl phenyl siloxane, the dominant part of the dielectric relaxation process is rotation of the molecule as a whole. The values of ΔH_{act} for the linear oligomer with n=10 and the cyclic oligomer with n=10 are identical, within experimental error. A comparison with the findings of Dasgupta and co-workers[31] is useful at this point. They measured the dielectric relaxation times and the dielectric relaxation activation energies for a series of linear oligomers of dimethyl siloxane with n=4-12. They concluded that the dominant part of the dielectric relaxation process for linear oligomers of dimethyl siloxane is segmental dipole relaxation. Also, for the small contribution to the relaxation process, due to rotation of the whole molecule, they found that the activation energy increased with increasing molecular size. Hence, it appears that linear oligomers of dimethyl siloxane are more flexible than the corresponding linear oligomers of methyl phenyl siloxane.

The second region of the curve, from n_n=31 to n_n=82, shows a sharp decrease in ΔH_{act} with increasing chain length. In this region the tendency for the average activation energy to increase due to the increase in co-operation required for dipolar relaxation, as the chain length increases, may be more than offset by an opposing tendency for the average activation energy to decrease as the flexibility of the chain increases and as segmental dipolar relaxation takes over from whole molecule rotation as the dominant part of the relaxation process.

The increase in ΔH_{act} in the third and final region of the curve, beginning at n_n=82, can be accounted for by inter-chain interactions, possibly the onset of long range chain entanglements, which would be expected to restrict dipolar rotation and increase ΔH_{act}.

6.06: Davidson-Cole Analysis of Linear Oligomers of Methyl Phenyl Siloxane, Linear Fractions of Poly(methyl phenyl siloxane) and a Cyclic Oligomer of Methyl Phenyl Siloxane.

Empirical distribution parameters, derived from an analysis of the broadness of dielectric loss curves, obtained for the methyl phenyl siloxane system, are presented in Table (6-3). These are the Cole-Cole parameter, α, for the linear oligomer of methyl phenyl siloxane with $n = 4$, and the Davidson-Cole parameter, β, derived for linear oligomers of methyl phenyl siloxane with $n > 4$, a cyclic oligomer of methyl phenyl siloxane and linear fractions of PMPS, measured at various temperatures.

The dielectric relaxation behaviour of the linear oligomer of methyl phenyl siloxane with $n= 4$ was found to be adequately described using a Cole-Cole analysis involving the empirical distribution parameter α. The small value of α, < 0.1, obtained for this sample, suggests that a single relaxation time is sufficient to describe the relaxation process. For such small molecules it is likely that the principal relaxation process corresponds to the rotation of the whole molecule.

For linear oligomers of methyl phenyl siloxane with $n >4$ there are significant increases in the value of β with increasing molecular size, ie; the distribution of relaxation times narrows with increase in molecular weight. This observation is difficult to explain in view of the fact that the segmental contribution to the dielectric relaxation would be expected to become more co-operative as the chain length increases. However, this behaviour may be due to a lessening

	LINEARS	
n	T/K	α
4	155.5-162.5	<0.10
n	T/K	β
6	181.0-184.5	0.32
6	184.5-188.0	0.37
8	195.5-198.5	0.38
8	198.5-201.5	0.45
10	212.5-217.5	0.41
10	217.5-220.5	0.49
31	232.5	0.38
50.5	237.0	0.33
82	243.0	0.36
153	249.0	0.37
284	255.0	0.41
~1370	251.0	0.36
	CYCLIC	
n	T/K	β
10	246.0	0.39

Table(6-3). Cole-Cole and Davidson-Cole analysis of oligomers of methyl phenyl siloxane and fractions of poly(methyl phenyl siloxane). [error in values of β is ± 0.02]

influence of the bulky terminal groups on dipolar rotation as the chain length increases.

For linear fractions of PMPS with $n_n>10$ the distribution of relaxation times broadens to a constant value, within experimental error, characterised by an average value of β equal to 0.37. This reflects the co-operative nature of molecular motion in polymers that results in a spread of relaxation processes associated with different relaxation times.

6.07: Experimental Mean-Square Dipole Moments of Linear Oligomers of Methyl Phenyl Siloxane, Linear Fractions of Poly(methyl phenyl siloxane) and a Cyclic Oligomer of Methyl Phenyl Siloxane.

Experimental values of the mean-square dipole moment per repeat unit were calculated for oligomers of methyl phenyl siloxane and fractions of PMPS, using the Onsager equation. The results are shown in Table (6-4). The permittivities required for the calculations were obtained from the respective Cole-Cole plots. The densities reported by previous workers[113] were corrected to allow for an increase in density caused by cooling the samples to low temperatures.

The smallest value of the experimental mean-square dipole moment per repeat unit for oligomers of methyl phenyl siloxane was found to be 0.15±0.02 Debyes. This value was exhibited by the linear oligomer of methyl phenyl siloxane with $n = 4$ and by the cyclic oligomer of methyl phenyl siloxane with $n = 10$. This behaviour is not unexpected for a small cyclic structure in which the ends are 'tied' together, allowing effective vectorial cancellation of dipole vectors to take place.

The dipole moment ratio, $<\mu^2>/nm^2$, was calculated for the oligomers of

	LINEARS	
n	T/K	$<\mu^2>$/Debyes
4	159.5-162.5	0.15
6	184.5-188.0	0.22
8	198.5-201.5	0.20
10	217.5-220.5	0.24
31	232.5	0.21
50.5	237.0	0.21
82	243.0	0.19
153	249.0	0.19
284	255.0	0.18
~1370	251.0	0.19
	CYCLIC	
n	T/K	$<\mu^2>$/Debyes
10	246.0	0.15

Table (6-4) **Experimental mean-square dipole moments per repeat unit for oligomers of methyl phenyl siloxane and fractions of poly(methyl phenyl siloxane) [error in values is ±0.02]**

methyl phenyl siloxane and fractions of PMPS using a value of m equal to 0.60 Debyes. The results are plotted in Figure (6-6) along with the dipole moment ratio calculated for linear fractions of PDMS by earlier workers (see Figure (6-4)).

The magnitude of the dipole moment ratio for the linear methyl phenyl siloxane chains is lower than the one for the dimethyl siloxane chains, at short chain lengths. For the linear oligomer of methyl phenyl siloxane with $n = 10$ the dipole moment ratio is 0.26; for the corresponding oligomer of PDMS the ratio is 0.31. This may be due to the presence of a cumulative Ph-Si dipole moment and to isomer effects in short chains of methyl phenyl siloxane, features which are absent in short chains of dimethyl siloxane. In addition, the maximum value of the dipole moment ratio is attained at longer chain lengths for PMPS than it is for PDMS. This is an indication of the reduced flexibility of the PMPS chain, when compared to a corresponding PDMS chain, due to the presence of bulky phenyl groups. The reduced flexibility of the PMPS chain prevents the formation of 'closed polygons', a feature of the more flexible short PDMS chains which leads to cancellation of dipole vectors. Thus, the cancellation of dipole moment vectors for short PMPS chains is less effective. At much longer chain lengths, when the polymer chains obey Gaussian statistics, the dipole moment ratio for linear fractions of PMPS and PDMS asymptote to an approximately equal value of 0.26.

Note that the characteristic ratio, $<r^2>/nl^2$, where r is the end-to-end distance of a polymer chain and l is the bond length, does not asymptote to an approximately equal value for high molecular weight linear PMPS and PDMS. The characteristic ratio for PMPS, at 303K, is 8.8[114] while for PDMS, at 383K, the ratio is 6.8[114].

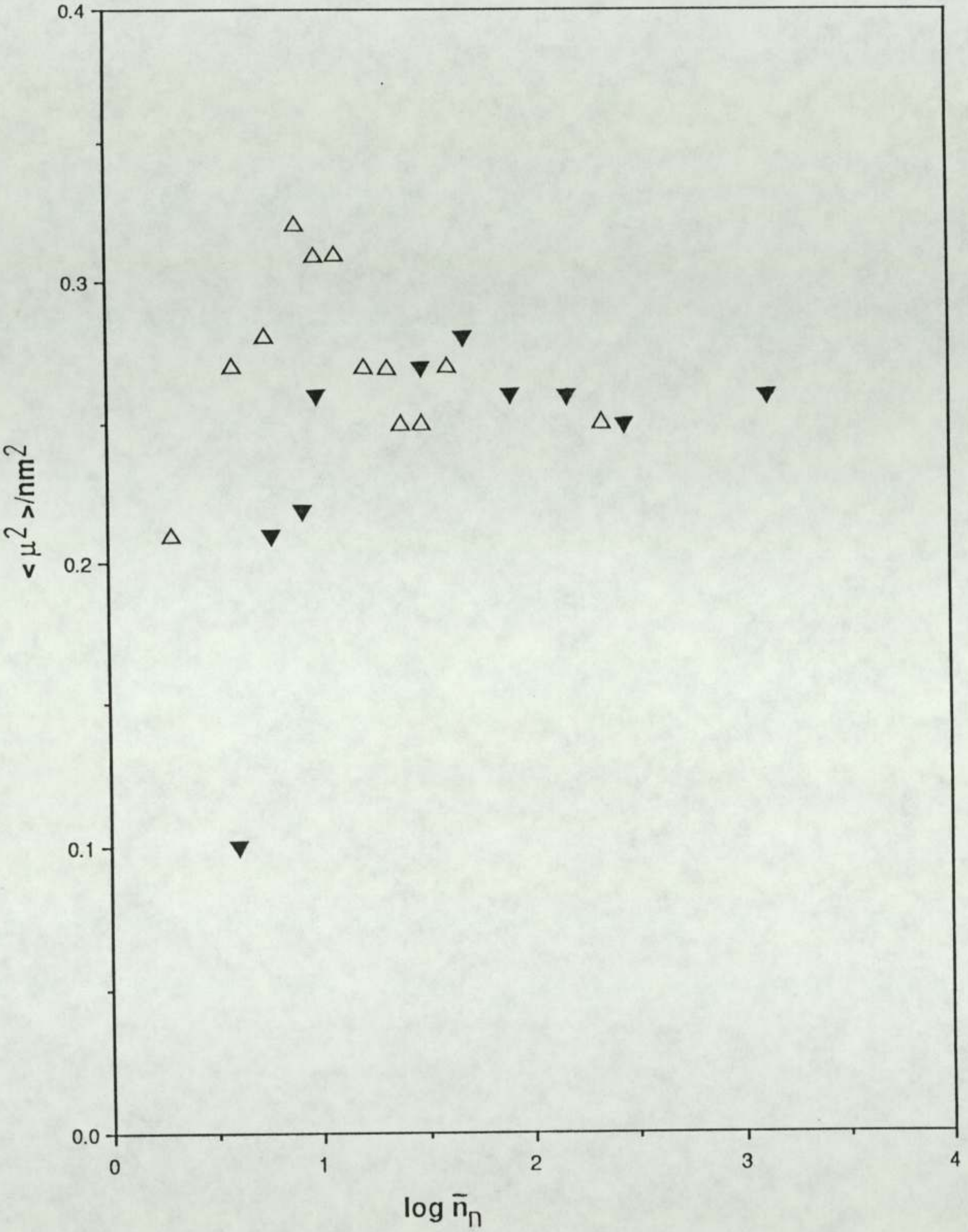

<u>Figure (6-6)</u> Dipole moment ratio, $<\mu^2>/nm^2$, for linear methyl phenyl siloxanes [▼ present study] and for linear dimethyl siloxanes [△ Beevers and Mumby34]

It is generally found, for chain molecules, that the value of the characteristic ratio is typically an order of magnitude higher than the value of the dipole moment ratio. This difference is a characteristic of chemical bonding. It is more likely for bond dipole vectors that are normal to the skeletal backbone to be in relative orientations which lead to effective cancellation, than it is for skeletal bond vectors that add sequentially along the polymer chain. The relatively small values of the dipole moment ratio are a reflection of such cancellation.

The value of m used in the dipole moment ratio calculations for PMPS, namely 0.60 Debyes, may be incorrect since it has been derived from measurements carried out on a dimethyl siloxane structure[30].

6.08: Dielectric Relaxation Activation Energies of Poly(methyl hydrogen siloxane, poly(n-hexyl methyl siloxane) and a Polymer Liquid Crystal.

The dielectric relaxation activation energy for the α-process of poly(methyl hydrogen siloxane) was found to be 123.6kJ mol^{-1}. This value compares well with ΔH_{act} values measured in this study for linear fractions of PDMS. With n-hexyl attached as a pendant group the average activation energy is reduced to 74.3kJ mol^{-1}. This typical 'plasticising' effect has been interpretated by earlier workers in terms of the plasticising group increasing the free volume between the chain segments, thereby reducing inter-molecular forces and lowering the energy barriers opposing dipolar rotation. However, the increased free volume effect would be expected to reduce the degree of co-operation required for dipolar rotation and so cause the loss curves to narrow. For plasticisers added, but not chemically bound, to undiluted poly(dimethyl siloxanes) the observed broadening of the loss curves has been explained by assuming that the plasticiser molecules are concentrated locally, causing relaxation to occur in a variety of environments.

The average activation energy measured for the polymer liquid crystal in the liquid crystalline phase was found to be 253.2±4.4 kJ mol^{-1}. Values of ΔH_{act}, measured in the liquid crystalline phase, of 183 kJ mol^{-1}, 190 kJ mol^{-1} and 220 k mol^{-1} have previously been reported for a nematic polysiloxane[56], a smectic polymethacrylate[48] and a nematic polyacrylate[47], respectively. The high value of ΔH_{act} (compared to PMHS) suggests that the dielectric relaxation process for this material in the mesophase involves motion of the mesogenic group.

The average activation energy measured in the glassy state of the polymer liquid crystal was 44.0±2.2 kJ mol^{-1}. This value is close to the values measured by Haase and co-workers[52] (48kJ mol^{-1}) and by Zentel and co-workers[50] (50±7kJ mol^{-1}) for a polymer liquid crystal, containing an ester group in the side chain, when observed in the glassy state. The relaxation processes in the glassy state involve localised motions of polar groups in the side chain.

6.09: Cole-Cole Plots.

The Davidson-Cole distribution parameter β, measured for PMHS at 135.5K, was found to equal 0.50±0.02. For poly(n-hexyl methyl siloxane), β was found to equal 0.35±0.02, reflecting the plasticising effect of n-hexyl in increasing the extent of co-operation required for dipolar rotation This result, taken with the values of the distribution parameters obtained for dimethyl siloxane and phenyl methyl siloxane structures, suggests that the molecular size of the groups attached to the siloxane backbone is an important factor in determining the breadth of relaxation times. Since β(PMHS) > β(PDMS)> β(PMPS), ie; PMHS has the narrowest distribution of relaxation times, it would appear that the smaller the size of the group(s) attached to the siloxane backbone the lower is the degree of co-operation required for dipolar rotation.

The shape of the Cole-Cole plots for the polymer liquid crystal in the liquid crystalline phase, Figures (5-92) and (5-93), suggests the presence of at least two discrete relaxation processes. Taking into account the high activation energy measured for this sample and the dielectric results published by previous workers it is likely that these processes involve motions of the longitudinal and tranverse components of the resultant dipole moment present in the mesogenic side groups.

The shape of the Cole-Cole plots for the polymer liquid crystal in the glassy state, Figures (5-94) and (5-95), prevents a quantitative interpretation. However, it is possible to describe the relaxation data by constructing a semicircular arc possessing a centre situated below the real axis. This is consistent with the findings of previous workers[53,54] and also with the idea that localised, co-operative motions of the dipolar groups in the side chains may occur, in the glassy state.

6-10: Experimental Mean-Square Dipole Moments for Poly(methyl hydrogen siloxane) and poly(n-hexyl methyl siloxane).

Experimental mean-square dipole moments per repeat unit were calculated for poly(methyl hydrogen siloxane) and poly(n-hexyl methyl siloxane) using the Onsager equation. The limiting permittivities were taken from the respective Cole-Cole plots. The density of poly(methyl hydrogen siloxane) has been reported by earlier workers[115]. The density of poly(n-hexyl methyl siloxane) was estimated by weighing a known volume of the polymer.

The mean-square dipole moment per repeat unit of poly(methyl hydrogen siloxane), in the temperature range 128.5K-135.5K, is 0.20±0.01 Debyes. The corresponding value for poly(n-hexyl methyl siloxane), in the temperature range 172.5K-186.0K, at 0.18±0.02, is identical, within experimental error.

CHAPTER 7

KERR EFFECT THEORY AND RESULTS

Introduction.

In this section a brief history of the development of the electro-optic Kerr effect will be presented as well as a theoretical basis for the interpretation of the Kerr effect data acquired for p-tolaldehyde and the oligomers of p-phenylene vinylene F1 and F2.

7.01: Historical Development of the Kerr Effect.

The announcement of the discovery of electric double refraction was made by John Kerr in the Philosophical Magazine in 1875[116,117]. Kerr reported that when a block of glass was placed between crossed nicols, and the leads from the secondary of a Rumkorff machine attached to it in such a way that the applied electric field was perpendicular to the beam of plane-polarised light passing through the glass, light was found to emerge through the analysing nicol.

The theory of the Kerr effect now usually accepted was developed from 1910 onwards. Langevin[118,119], in that year, assumed that the molecules of a substance may be both electrostatically and optically anisotropic and, as a result of the orientating action of an electric field upon the dipole induced in each of the molecules, the material as a whole became doubly refractive. Born[120] extended this idea in 1918 to include the orientating effect of an electric field on any permanent dipole moments the molecules may possess.

The recognition of a relationship between the Kerr constant and the optical anisotropy of a molecule was first seen by Gans[121] in 1921. Theoretical relationships between molecular optical properties and light scattering were further developed by Debye[122] (1925) and by Debye and Sack[123] (1934). The developments in the theory of the Kerr effect in this period were reviewed by Stuart in 1939[124].

An extensive study of the electro-optical properties of macromolecules was started at Berkeley in 1948 by Zimm and O'Konski. The Kerr effect of flexible polymers has been extensively studied by Le Fevre and co-workers[125-132].

7.02: Theoretical Interpretation.

A molecule can be regarded as having an ellipsoid of polarisability defined by the semi-axes b_1, b_2, and b_3 in the directions of the principal molecular axes 1, 2 and 3. Thus, b_1 is the moment induced by an electric field of unit intensity acting along the 1 axis. Similarly, b_2 and b_3 are moments induced by a unit electric field acting along axes 2 and 3, respectively. The principal axes are such that one of them corresponds to the direction of maximum polarisability of the molecule, another to the direction of minimum polarisability, and the three axes are mutually orthogonal (Figure 7-1). The locations of the principal axes can sometimes be deduced from symmetry considerations. The polarisabilities are relevant to the mathematical treatments given by Langevin, Born and Gans.

The molecular Kerr constant of a molecule is normally regarded as the sum of two contributions; a term θ_1 associated with induced electric dipole moments and a second term, θ_2, associated with permanent electric dipole moments.

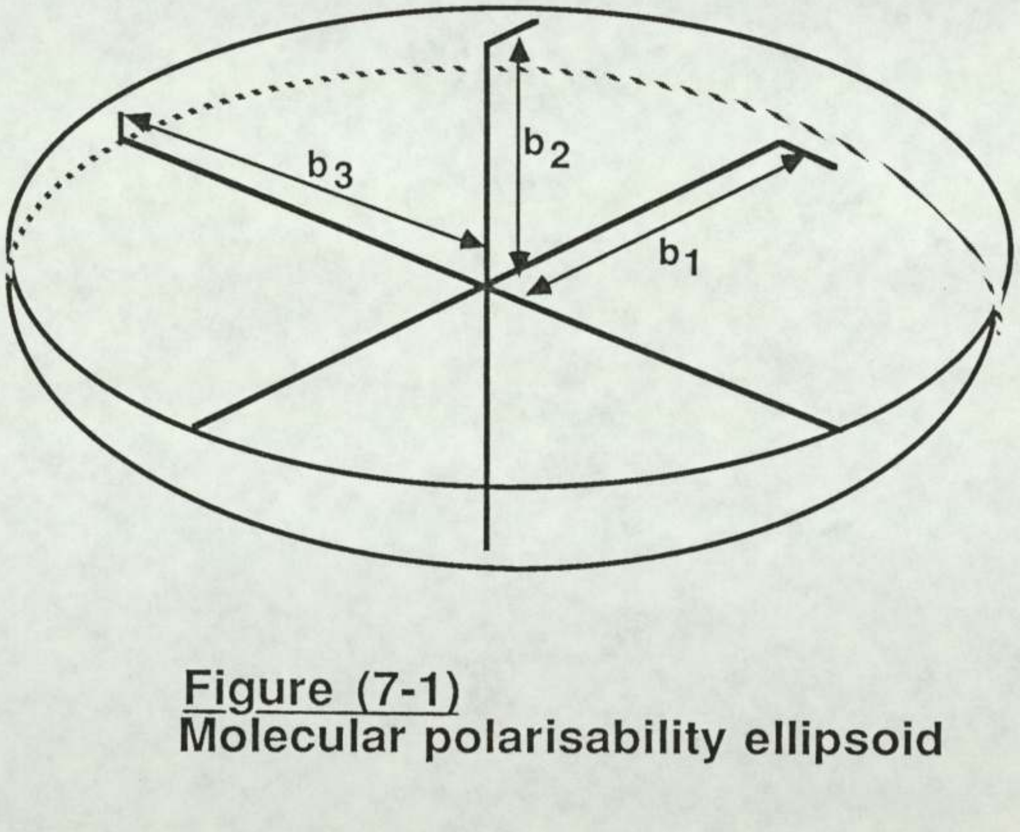

Figure (7-1)
Molecular polarisability ellipsoid

The first term, θ_1, is referred to as the induced anisotropy term and its magnitude, which is always positive, is a measure of the anisotropy of optical and electrical polarisability.

The form of θ_1 is;

$$\theta_1 = \frac{1}{45kT} \frac{(\varepsilon-1)}{(n^2-1)} [(b_1 - b_2)^2 + (b_2 - b_3)^2 + (b_3 - b_1)^2] \qquad (7\text{-}01)$$

In this expression b_1, b_2 and b_3 are the principal electrostatic polarisabilities of the molecule, ε is the dielectric constant, n is the refractive index, k is the Boltzmann constant and T is the absolute temperature.

The second term, θ_2, referred to as the orientation term, is given by equation (7-02);

$$\theta_2 = \frac{1}{45k^2T^2} [(\mu_1^2 - \mu_2^2)(b_1 - b_2) + (\mu_2^2 - \mu_3^2)(b_2 - b_3) + (\mu_3^2 - \mu_1^2)(b_3 - b_1)$$

where μ_1, μ_2 and μ_3 are the components of the permanent dipole moment vector along the directions parallel to b_1, b_2 and b_3, respectively.

From the Langevin-Born-Gans theory, the Kerr constant of the medium is given by;

$$B = \frac{\pi N(n^2 + 2)^2(\varepsilon + 2)^2(\theta_1 + \theta_2)}{27n\lambda} \qquad (7\text{-}03)$$

where N is the number of molecules per unit volume and λ is the wavelength of the light used to make the measurements.

Rearranging equation (7-03) gives;

$$(\theta_1 + \theta_2) = \frac{27n\lambda B}{\pi N(n^2 + 2)^2(\varepsilon + 2)^2} \qquad (7\text{-}04)$$

This may be substituted into;

$$_mK = \frac{2\pi N_A}{9} (\theta_1 + \theta_2) \qquad (7\text{-}05)$$

where $_mK$ is the molecular Kerr constant and N_A is Avogadro's number, to give;

$$_mK = \frac{6nB\lambda}{(n^2 + 2)^2(\varepsilon + 2)^2} \frac{N_A}{N} \qquad (7\text{-}06)$$

N_A/N may be replaced by M/d, where M and d are the molecular weight and density, respectively, to give;

$$_mK = \frac{6nB\lambda M}{(n^2 + 2)^2(\varepsilon + 2)^2 \; d} \qquad (7\text{-}07)$$

7.03: Solution Molar Kerr Constants.

In what follows, the subscripts 1, 2 and 12 refer to solvent, solute and solution, respectively. The equations given above, as written, are strictly applicable only to gaseous dielectrics.

For the purposes of comparing dissolved and gaseous materials equation

(7-07) may be used to calculate a solution molar Kerr constant, ${}_{m}K_{12}$;

$$ {}_{m}K_{12} = \frac{6\underline{n}_{12}\,\underline{B}_{12}\,\underline{\lambda M}_{12}}{(n_{12}^{2}+2)^{2}(\varepsilon_{12}+2)^{2}\ d_{12}} \qquad (7\text{-}08) $$

Using a conventional alligation formula, we have;

$$ {}_{m}K_{12} = f_1\,{}_{m}K_1 + f_2\,{}_{m}K_2 \qquad (7\text{-}09) $$

where ${}_{m}K_1$ and ${}_{m}K_2$ are the molar Kerr constants of the solvent and solute, respectively, and f_1 and f_2 are the corresponding mole fractions. For a dilute solution of a polar solvent the following approximations are acceptable;

$$ n_1 \sim n_{12} \qquad d_1 \sim d_{12} \qquad M_1 \sim M_{12} $$

where n_1, d_1, and M_1 are the refractive index, density and molecular weight of the solvent, respectively. Equation (7-08) then becomes;

$$ {}_{m}K_{12} = 6\lambda n_1 B_{12} M_1/(n_1^{2}+2)^{2}(\varepsilon_{12}+2)^{2} d_1 \qquad (7\text{-}10) $$

Rearranging equation (5-09) gives;

$$ {}_{m}K_2 = ({}_{m}K_{12} - f_1\,{}_{m}K_1)/f_2 \qquad (7\text{-}11) $$

7.04: Solution Molar Kerr Constants at Infinite Dilution.

The procedure for the estimation of molar Kerr constants at infinite dilution involves the extrapolation of measurements of four experimental parameters to infinite dilution before calculating the Kerr constant of a solute.

Rewritng equation (7-09) using specific Kerr constants and weight fractions gives;

$$ {}_{s}K_{12} = {}_{s}K_{1}\omega_{1} + {}_{s}K_{2}\omega_{2} \qquad (7\text{-}12) $$

where ω_1 and ω_2 are the weight fractions of the solvent and solute, respectively, and the specific Kerr constant of a material is defined by;

$$ {}_{s}K = \frac{6nB\lambda}{(n^2+2)^2(\varepsilon+2)^2\ d} \qquad (7\text{-}13) $$

The calculation of the Kerr constant is facilitated by the following relationships which are assumed to apply at high dilution;

$$ \varepsilon_{12} = \varepsilon_1(1+\alpha\omega_2) \qquad (7\text{-}14) $$

$$ d_{12} = d_1(1+\beta\omega_2) \qquad (7\text{-}15) $$

$$ n_{12} = n_1(1+\gamma\omega_2) \qquad (7\text{-}16) $$

$$ B_{12} = B_1(1+\delta\omega_2) \qquad (7\text{-}17) $$

Thus, by making measurements for a series of solutions with different weight fractions, ω_2, of solute, the values of α, β, γ, and δ may be evaluated.

From equation (7-12) we have;

$$ {}_{\infty}({}_{s}K_{2}) = {}_{s}K_{1} + [d_{s}K_{12}/d\omega_{2}]_{\omega_{2}=0} \qquad (7\text{-}18) $$

where ${}_{\infty}({}_{s}K_{2})$ is the specific Kerr constant of the solute at infinite dilution.

By substituting equations (7-14) to (7-17) into equation (7-13) and differentiating with respect to ω_2, equation (7-18) can be rewritten as;

$$_{\infty}({}_{s}K_2) = [1 - \beta + \gamma + \delta + H\gamma - J\alpha\varepsilon_1]_{s}K_1 \qquad (7\text{-}19)$$

where;

$$H = 4n_1^2(n_1^2 + 2) \qquad (7\text{-}21)$$

$$\text{and } J = 2/(\varepsilon_1 + 2) \qquad (7\text{-}22)$$

and ${}_{s}K_1$ is the specific Kerr constant of the solvent. In practice, for polar solutes, β and γ are usually very small relative to α and δ. Thus, a simplified version of equation (7-19) may be used, namely;

$${}_{s}K_2 = (1 + \delta - J\alpha\varepsilon_1)_{s}K_1 \qquad (7\text{-}22)$$

7-05: Calculation of Theoretical Molecular Kerr Constants using Bond Polarisabilities and Dipole Moments.

The following data are required to calculate the theoretical molecular Kerr constant of a specific geometrical form of a molecule: (i) the anisotropic polarisabilities of all bonds or groups; (ii) the permanent electric moments of all dipolar bonds or groups.

Le Fevre and co-workers have demonstrated that the electrical and optical molecular polarisabilities, for a large variety of organic molecules, may be represented by appropriate tensor sums of the constituent bond polarisabilities. The molecular polarisability tensor T_m is given by the tensor sum of the bond polarisability tensors T_i. The latter possess the general form;

$$T_i = \begin{bmatrix} b_L & 0 & 0 \\ 0 & b_T & 0 \\ 0 & 0 & b_V \end{bmatrix} \quad (7\text{-}23)$$

The diagonal components, b_L, b_T and b_V, of the tensor of the i^{th} bond T_i, correspond to the the principal axes of the electro-optical polarisability ellipsoid of the i^{th} bond in the molecule. The electro-optic polarisability tensor of a molecule may be written in the following form;

$$T_m = \sum_{i=1}^{N} S_i \, T_i \, S_i^{-1} \quad (7\text{-}24)$$

where N is the number of bonds in the molecule and S_i is a transformation matrix for representing the bond polarisability in an arbitarily chosen reference co-ordinate system. The matrix S_i^{-1} is the inverse of S_i, and, for transformations in cartesian co-ordinate systems, S_i^{-1} is simply the transpose of S_i. The transformation matrix S_i depends upon the relative orientation of the i^{th} bond and the bond chosen as a reference co-ordinate system.

The general form of the bond transformation matrix applicable to this study, is given by;

$$S_i = \begin{bmatrix} \cos\theta_i & \sin\theta_i & 0 \\ \sin\theta_i & -\cos\theta_i & 0 \\ 0 & 0 & 1 \end{bmatrix} \quad (7\text{-}25)$$

where the elements of the transformation matrix are functions of the bond rotation angle θ_i. If the components of the permanent dipole vector, expressed in the reference co-ordinate system, are μ_x, μ_y and μ_z, then a molecular Kerr constant may be calculated using equations (7-01), (7-02) and

(7-05). (in some cases these equations need to be modified to allow for terms involving off- diagonal elements of T_m).

7.06: Molecular Kerr Constants of p-Tolaldehyde.

Kerr effect measurements and static dielectric permittivity measurements were carried out on dilute solutions of p-tolaldehyde in the solvents 1,4-dioxan or poly(propylene glycol) 2025 (PPG 2025), at 298K, using the Kerr effect apparatus described in Chapter 3. The solution concentrations varied between 1%(v/v) and 5%(v/v).

Experimental solution Kerr constants, B_{12}, and solution permittivity values, ε_{12}, were calculated using the methods discussed in Chapter 3.

Literature values of B_1 and ε_1 for 1,4-dioxan at 298K were found to be 0.075×10^{-14} mV^{-2} and 2.209, respectively[88]. A value of ε_1 for PPG 2025 at 293K, was estimated from the Cole-Cole plots published by Yano and co-workers[133], and found to be 5.5. The experimental Kerr constant, B_1, for PPG 2025 at 298K, calculated using equation (3-10) and the published Kerr constant of cyclohexane, was found to be -0.134×10^{-14} mV^{-2}. Negative values of the experimental Kerr constant for PPG with molecular weights $> 10^3$ have previously been reported[134,135].

Graphs of B_{12} plotted against ω_2 and ε_{12} plotted against ω_2 for solutions of p-tolaldehyde in 1,4-dioxan and PPG 2025 are shown in Figures (7-2) and (7-3). Specific Kerr constants, ${}_sK_1$, have been calculated for 1,4-dioxan and PPG

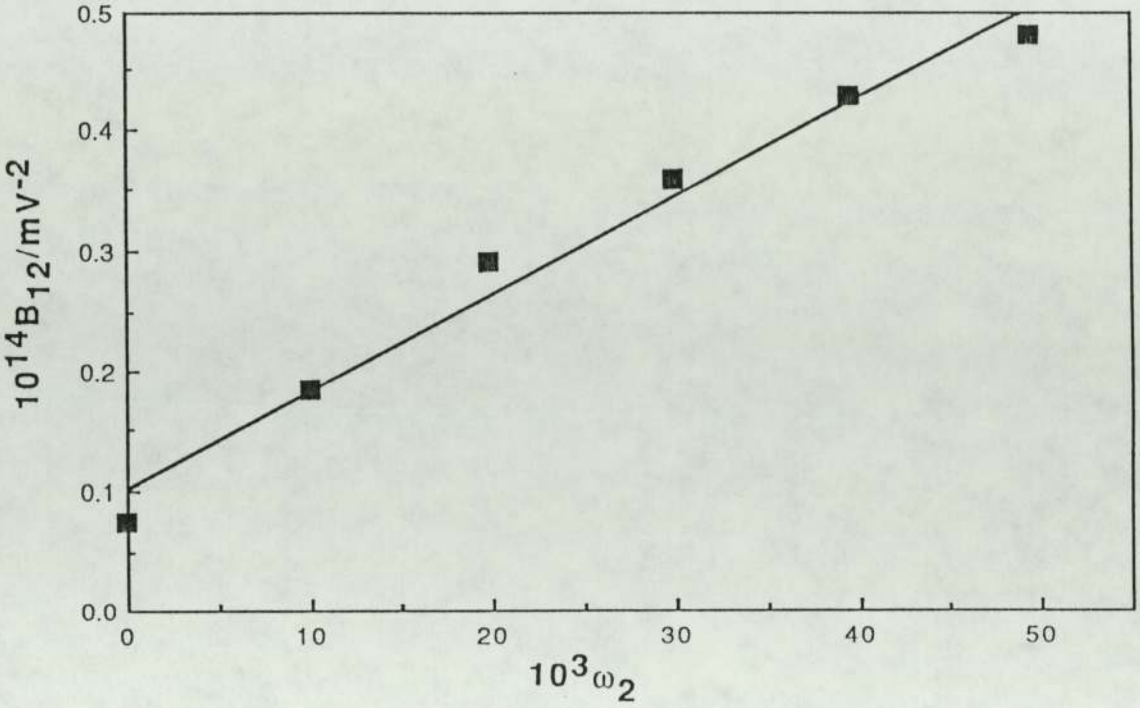

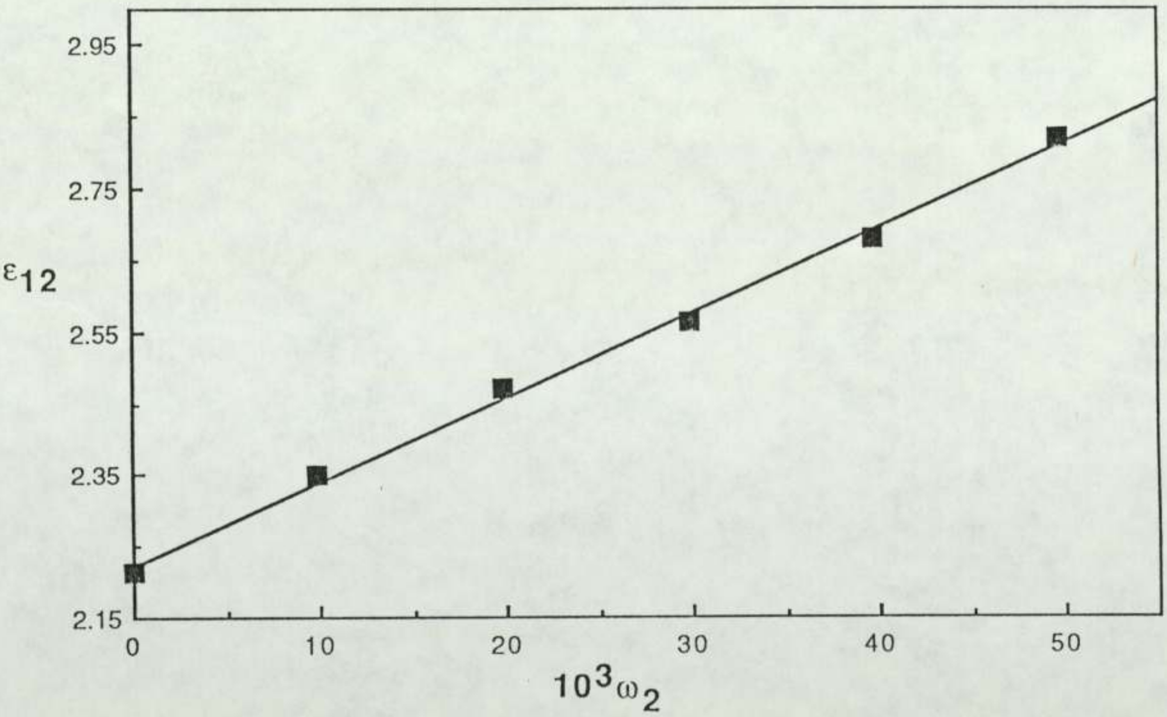

Figure (7-2) B_{12} against ω_2 and ε_{12} against ω_2 for solutions of p-tolaldehyde in 1,4-dioxan at 298K

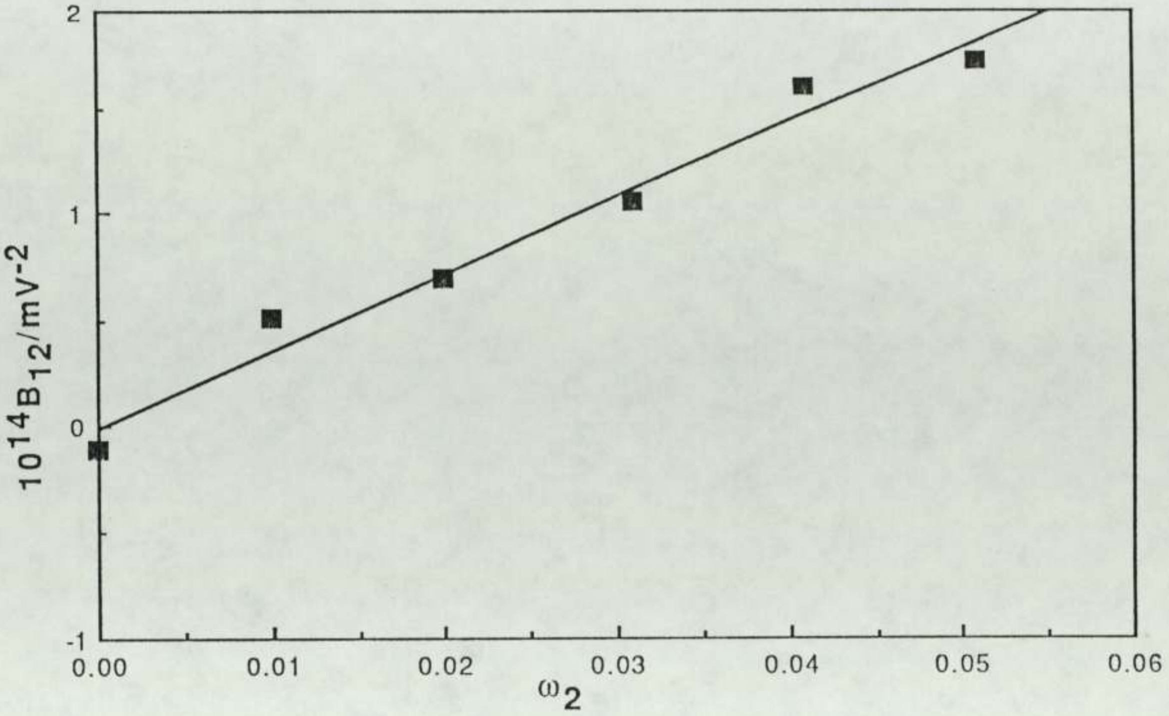

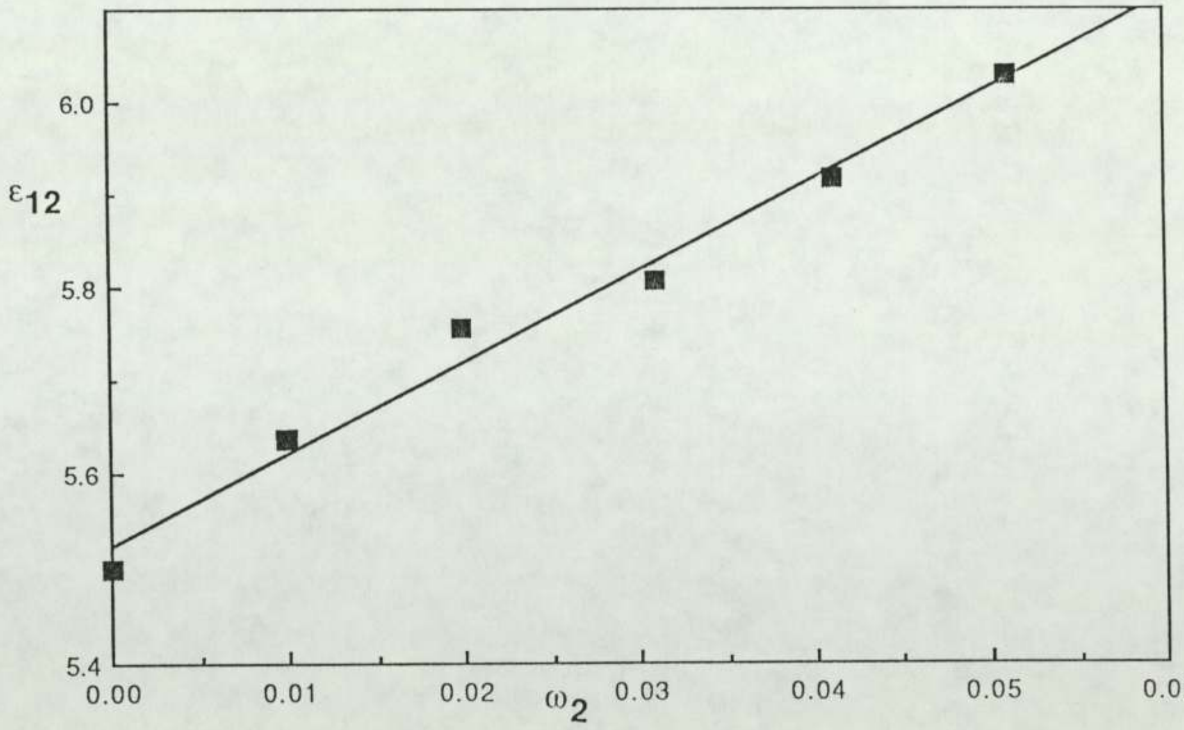

Figure (7-3) B_{12} against ω_2 and ε_{12} against ω_2 for solutions of p-tolaldehyde in PPG 2025 at 298K

2025 at 298K, using equation (7-13). The published values of the density and refractive index for 1,4-dioxan, at 298K, are 1.028×10^{3} kgm $^{-3}$ and 1.4204, respectively[88]. The published values of the density[136], at 293K, and refractive index[137] for PPG 2025, at 298K, are 1.001×10^{3} kgm $^{-3}$ and 1.456, respectively.

${}_{s}K_{1}$ values for 1,4-dioxan and PPG 2025, at 298K, are listed in Table (7-1), along with the molecular Kerr constants, ${}_{m}K_{2}$, calculated for p-tolaldehyde using the infinite dilution method discussed earlier. The values of α and δ were calculated from the slopes of the graphs of ε_{12} plotted against ω_2 and B_{12} plotted against ω_2, respectively.

7.07: Dipole Moment of p-Tolaldehyde.

The dipole moment of p-tolaldehyde, at 298K, was calculated using the Guggenheim-Debye[138] equation, which is given by;

$$\mu_2^2 = \frac{27\varepsilon kT}{N_A(\varepsilon_1 + 2)(n^2 + 2)}(\Delta/c)_{c\to 0} \qquad (7\text{-}26)$$

where μ_2 is the mean-square dipole moment of the solute, ε is the permittivity of free space(8.854×10^{-12} Fm $^{-1}$), k is the Boltzmann constant(1.381×10^{-23} JK $^{-1}$), T is the absolute temperature, N_A is Avogadro's number(6.022×10^{23} mol $^{-1}$), ε_1 is the relative permittivity of the solvent, n_1 is the refractive index of the solvent, $\Delta = (\varepsilon_{12} - n_{12}) - (\varepsilon_1 - n_1)$ [~ $(\varepsilon_{12} - \varepsilon_1)$ for dilute solutions], and c is the concentration of the solute expressed in units of mol/cm^3.

solvent	$10^{26}\ {}_sK_1/m^5V^{-2}kg^{-1}$	$10^{26}\ {}_mK_2/m^5V^{-2}mol^{-1}$
1,4-dioxan	1.28	26.94
PPG 2025	-0.72	23.74

Table (7-1) **Specific Kerr constants for 1,4-dioxan and PPG 2025 and molecular Kerr constants for p-tolaldehyde, at 298K.**

Also;

$$(\Delta/c)_{c\to 0} = (d\varepsilon_{12}/d\omega_2)_{\omega_2\to 0}(M_2/d_1) \qquad (7\text{-}27)$$

where ε_{12} is the relative permittivity of the solution, ω_2 is the weight fraction of the solute, M_2 is the molecular weight of the solute(kg) and d_1 is the density of the solvent(kgm $^{-3}$). Equation (7-26) may be re-expressed as;

$$\mu_2^2 = \frac{27\varepsilon kT\,M_2}{N_A(\varepsilon_1+2)(n^2+2)d_1}(d\varepsilon_{12}/d\omega_2)_{\omega_2\to 0} \qquad (7\text{-}28)$$

Equation (7-28) was used to calculate the dipole moment of p-tolaldehyde, using the slope of the plot of ε_{12} against ω_2 in place of $(d\varepsilon_{12}/d\omega_2)_{\omega_2\to 0}$. The root mean-square dipole moment of tolaldehyde, μ_2, was found to be 3.36 Debyes in 1,4-dioxan and 2.37 Debyes in PPG 2025.

7-08: Molecular Kerr constants of F1 and F2.

Figure (7-4) shows plots of B_{12} against ω_2, for dilute solutions of F1 and F2 in PPG 2025, at 333K, which have been calculated from Kerr effect measurements carried out using the Kerr effect apparatus described in Chapter 3.

The experimental Kerr constant, B_1, of PPG 2025 at 333K, calculated using equation (3-10) and the published Kerr constant of cyclohexane[88], was found to be -0.078x10 $^{-14}$ mV $^{-2}$. The specific Kerr constant of PPG 2025, $_sK_1$, at 333K, calculated using equation (7-13) and a value of ε_1 at 334K, equal to 4.8[133], was found to be -0.511x10 $^{-26}$ m^{5}V $^{-2}$kg $^{-1}$. Solution specific Kerr

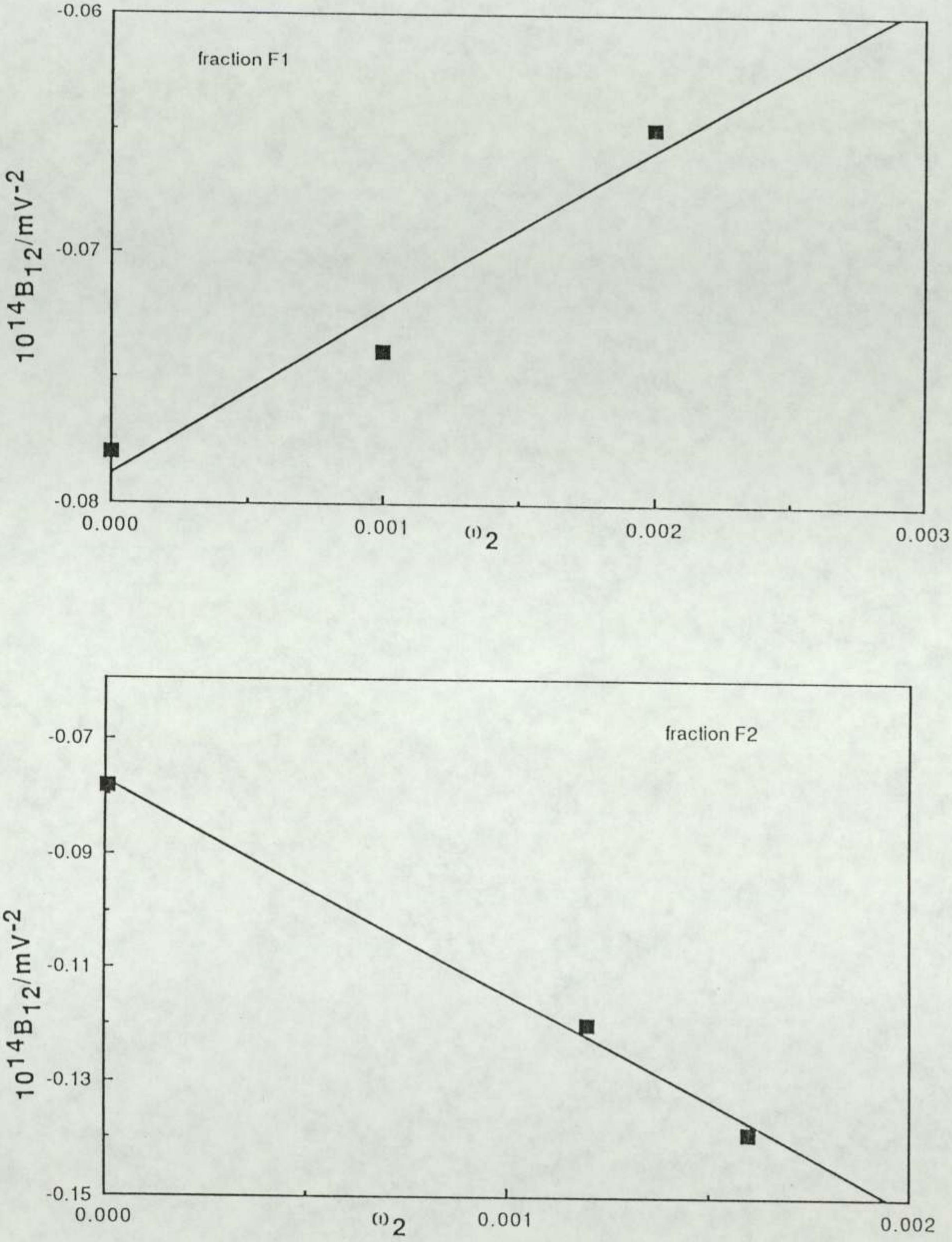

Figure (7-4) B_{12} against ω_2 for solutions of F1 and F2 in PPG 2025 at 333K constants, ${}_{s}K_{12}$, were calculated for solutions of F1 and F2 in PPG 2025 at 333K using equation (7-13). Because of the low solution concentrations, < 0.2%w/v, the following assumptions were made

$$\varepsilon_{12} \sim \varepsilon_1 \qquad n_{12} \sim n_1 \qquad d_{12} \sim d_1$$

Table (7-2) lists specific Kerr constants, ${}_{s}K_2$, for F1 and F2, calculated using the values of ${}_{s}K_{12}$ and equation (7-12), and molecular Kerr constants, ${}_{m}K_2$, for F1 and F2 in PPG 2025 at 333K.

7.09 Theoretical Molecular Kerr Constants of p-Tolaldehyde, F1 and F2.

Theoeretical Kerr constants were calculated for rigid and planar molecular models of p-tolaldehyde, F1 and F2, using the methods described in (7-05).

Individual calculations were carried out for all possible cis and trans configurations of F1 and F2. Two types of transformation matrix were required for bond and group transformations onto a master co-ordinate system. The matrices incorporated θ values of 60° or 120°, depending upon the relative orientation of the bonds/groups and the master co-ordinate system.

The calculations were performed by a computer program which required the molecular polarisabilty tensors and permanent dipole vectors as inputs. Table (7-3) lists the required principal bond and group polarisabilities (in cm^3) and the required permanent dipole vectors (in Debyes). The theoretical results are listed in Table (7-4). Also included, for comparison, are the experimental molecular Kerr constants. The calculations revealed the values of the theoretical molecular Kerr constant, calculated for all possible configurations of F1 and F2, to be almost

fraction	$10^{26}\,{}_{s}K_{2}/m^{5}V^{-2}kg^{-1}$	$10^{26}\,{}_{m}K_{2}/m^{5}V^{-2}mol^{-1}$
F1(x=1)	29.7±5.94	6.59±1.32
F2(x=2)	-242.0±48.4	-78.4±15.68

__Table (7-2)__ **Specific Kerr constants and molecular Kerr constants for oligomers of p-phenylene vinylene F1 and F2, at 333K**

bond/group	$10^{24}b_L$	$10^{24}b_T$	$10^{24}b_V$	μ
C-C	0.99	0.27	0.27	0
C=C	2.80	0.73	0.77	0
C_6H_6	11.1	11.1	0.73	0
C_6H_5CHO	13.36	15.25	8.09	[1.46,2.53,0]
$C_6H_5CH_3$	13.68	12.50	9.04	[0.34, 0, 0]
$CH_3C_6H_4CHO$	14.35	15.52	8.36	[1.8, 2.53, 0]

Table (7-3) Bond and group polarisabilities and dipole vectors used in theoretical calculations[139].

molecule	$10^{26}\,{}_{m}K/m^{5}V^{-2}mol^{-1}$	
	theory	experiment
p-tolaldehyde	44.8	25.3
F1(trans)	76.9	F1; 6.59±1.32
F1(cis)	79.3	"
F2(trans,trans)	167.0	F2; -78.4±15.68
F2(cis,cis)	163.3	"
F2(trans,cis)	165.7	"

<u>Table (7-4)</u> Theoretical and experimental molecular Kerr constants for p-tolaldehyde, at 298K, and oligomers of p-phenylene vinylene, F1 and F2, at 333K; solvent is PPG 2025.

identical.

The discrepancies in the values of the theoretical and experimental Kerr constants and dipole moments may be accounted for in a number of ways.

For p-tolaldehyde the theoretical value of the resultant dipole moment was calculated to be 3.1 Debyes. This compares well with the experimental value of 3.36 Debyes for p-tolaldehyde in 1,4-dioxan. The lower value of $<\mu>$, 2.37 Debyes, measured for p-tolaldehyde in PPG 2025, may be due to complex formation between the carbonyl oxygen of p-tolaldehyde and the OH groups of PPG leading to a reduction in the dipole moment of p-tolaldehyde.

With regard to the Kerr constant results, the assumption that oligomers of p-phenylene vinylene are planar may be incorrect. Since permanent moments are approximately 10^5 times greater than induced moments, the orientative action of an electric field on a polar molecule is overwhelmingly controlled by the disposition of the permanent moment within the molecular framework. Thus, there may be a degree of out-of-plane 'twisting' of the phenyl rings around the C-C bonds which shifts the direction of the dipole moment vector such that it acts at an angle greater than 54.7° to the axis of maximum polarisability. 54.7° is the angle at which, theoretically, the Kerr constant is equal to zero since, in this situation, the parallel and perpendicular components of the light vector will be subject to equal retardation. This may explain the negative value of the experimental Kerr constant observed for F2. In addition, strong solute-solvent interactions may be responsible for the differences in theoretical and experimental behaviour, or, it could be that the assumptions inherent in the addition of polarisability tensors and bond dipole vectors may be invalid for conjugated systems.

There is no indication of an 'exaltation of polarisabilty' effect in these molecules. The nature of such an indication would be a value of the experimental Kerr constant that exceeded the value expected from component group summation, as observed by Le Fevre and co-workers[140] for a series of oligomers of diphenyl-polyene. In addition, they reported that exaltions for benzene derivatives are small and that the exaltation effect reflects increased electron mobilities in conjugated systems.

7.10: Electrical Conductivity Results.

The room temperature electrical conductivities of undoped and doped samples of F1, F2 and P1 have been measured using the apparatus described in Chapter 3.

Doping of the samples was facilitated by enclosing the samples in a sealed dessicator containing solid I_2 for several weeks. The electrical conductivities, σ, of the undoped and doped samples are listed in Table (7-5).

The room temperature electrical conductivity of an undoped P1 disc is $4.44 \pm 0.44 \times 10^{-9}$ $(\Omega cm)^{-1}$. This value is higher than the values reported by Wnek and co-workers[141] [$\sim 10^{-10}$ $(\Omega cm)^{-1}$] and Manecke and co-workers[142] [$\sim 10^{-14}$ $(\Omega cm)^{-1}$] for PPV samples, at 298K, that had been treated, prior to measurement, to give all-trans vinylene units.

The room temperature electrical conductivities of undoped discs F1 and F2 were found to be identical, within experimental error. A study of the electrical conductivities of undoped oligomers of of p-phenylene vinylene, at 298K, has been undertaken by Koßmehl[143]. His findings revealed a molecular weight dependence of conductivity. For an oligomer with x=1, $\sigma < 10^{-20}$

sample	$10^9\sigma/(\Omega cm)^{-1}$	
	undoped	doped
F1	1.96±0.20	1100±110
F2	1.89±0.19	6380±640
P1	4.44±0.44	38900±3900

Table (7-5) **Undoped and I_2 doped electrical conductivities of oligomers of p-phenylene vinylene and poly(p-phenylene vinylene)**

$(\Omega cm)^{-1}$; for x=2, $\sigma = 3x10^{-19} (\Omega cm)^{-1}$; and for x=3, $\sigma = 1x10^{-18} (\Omega cm)^{-1}$.

The differences in the values of conductivity for the polymer and oligomers measured in this study and those measured by other workers are probably due to differences in sample preparation and different experimental techniques employed. Wnek and co-workers[141] measured the conductivity of thin wafers using a four probe d.c. technique. The wafers were formed by pressing PPV powder between Teflon film at a pressure of $2.07x10^6$ Nm^{-2}. Koßmehl[143] and Manecke[142] measured the conductivity with a pressure of $1.47x10^8$ Nm^{-2} maintained on the PPV pellets. (in this study conductivity measurements were carried out at a pressure of $5.88x10^7$ Nm^{-2})

Doping the F1, F2, and P1 powders with I_2 (conductivity of $10^{-7} (\Omega cm)^{-1}$) increases the electrical conductivity by approximately three orders of magnitude for F1 and F2, and by approximately four orders of magnitude for P1. However, the increase in conductivity is not sufficiently large enough to produce a material whose properties could be described as metallic. Iodine is considered not to be sufficiently oxidising enough in the case of PPV (and poly(phenylene).

The electrical conductivities of the doped samples in this study are seen to increase with increasing chain length. This finding is contrary to the findings of Wnek and co-workers[144], who reported that the limiting conductivity of AsF_5 doped PPV ($x \geq 1$) did not appear to depend on the length of the conjugated system present in PPV prior to doping. Their interpretation of this effect, and related effects, is similar to the later interpretation published by Gourley and co-workers, the details of which have already been discussed in Chapter 1.

CHAPTER 8

CONCLUSIONS AND FUTURE WORK

The major part of this study has been concerned with the dielectric relaxation behaviour of cyclic and linear polysiloxanes and the observation of the α-relaxation process.

The measurement of the frequency dependence of the dielectric loss at various temperatures has permitted the calculation of dielectric relaxation activation energies, mean-square dipole moments and relaxation time empirical distribution factors.

The results revealed some differences in the conformational behaviour of dimethyl siloxanes and methyl phenyl siloxanes.

Marked differences in values of ΔH_{act} for cyclic and linear poly(dimethyl siloxanes) suggest that dipolar rotation in cyclic structures is more restricted, compared with chains possessing the same number of skeletal bonds.

Dielectric relaxation activation energies measured for methyl phenyl siloxanes revealed some interesting features. Values of ΔH_{act} were found to increase with increasing molecular size for the linear oligomers. This behaviour was interpretated in terms of the rotation of the whole molecule being mainly responsible for the relaxation process in short chains of methyl phenyl siloxane. This finding, compared with the findings of Dasgupta and co-workers for linear oligomers of dimethyl siloxane, suggests that dimethyl siloxane oligomers are more flexible than the corresponding methyl phenyl siloxane oligomers. For the methyl phenyl siloxane oligomers with chain lengths > n_n=31 ΔH_{act} at first decreases with increasing chain length, as chain flexibility increases, and then increases with increasing molecular size, as inter-chain interactions begin to have an effect on dipolar rotation. The range of values of ΔH_{act} for methyl phenyl siloxanes was found to be higher than the ΔH_{act} range for the corresponding dimethyl siloxanes.

The mean-square dipole moments of cyclic and linear poly(dimethyl siloxanes) were found to be identical, within experimental error, over the range of molecular weights studied. In addition, the differences between the values of $<\mu^2>$ measured in this study at 148K, and those measured by other workers at 298K, were small.

The mean-square dipole moments measured for poly(methyl phenyl siloxanes) with $n_n \geq 31$ were found to be identical, within experimental error, to each other, and were also found to be identical, within experimental error, to the values of $<\mu^2>$ measured for cyclic and linear poly(dimethyl siloxanes) with similar numbers of skeletal bonds.

At short chain lengths, however, the magnitude of the dipole moment ratio measured for linear methyl phenyl siloxane chains, in this study, was found to be lower than the dipole moment ratio measured for some corresponding dimethyl siloxanes by other workers. This reasons for this are not entirely clear, but it may be due to the presence of cumulative dipole moments and isomer effects in short methyl phenyl siloxane chains. Furthermore, it appears that the maximum value of the dipole moment ratio is attained at longer chain lengths for methyl phenyl siloxanes, compared to dimethyl siloxanes. This is an example of the reduced flexibility of methyl phenyl siloxanes. It was also noted that, at chains lengths > n_n=100, values of the dipole moment ratio for poly(methyl phenyl siloxanes) and poly(dimethyl siloxanes) asymptote to an approximately equal value, unlike the values of the characteristic ratio.

The α-relaxation process was also observed in poly(methyl hydrogen siloxane) and poly(n-hexyl methyl siloxane). The attachment of n-hexyl to the polymer backbone produced a typical plasticising effect. This was reflected in a lowering of ΔH_{act} and a broadening of the distribution of relaxation times, relative to PMHS. Although the presence of n-hexyl would be expected to the alter the conformation of the polymer chain through steric interactions, thereby altering the proportion of bonds occupying trans, g+ and g- states, this is not reflected in the values of $<\mu^2>$ per repeat unit for PMHS and poly(n-hexyl methyl siloxane), which are identical, within experimental error.

Calculation of values of β for PDMS, PMPS and PMHS suggests that the extent of co-operation required for dipolar rotation in polymers is dependent upon the size of the group(s) attached to the polymer backbone.

Because of the difficulties in calibrating the dielectric cell used to observe the dielectric relaxation of a polysiloxane liquid crystal, and the heterogeneity of the sample, the amount of quantitative information that could be extracted from this system was limited. However, it was concluded, from the high activation energy measured for this system and the broadness of the loss curves (reflected in the Cole-Cole plots), that the dielectric relaxation behaviour of a polymer liquid crystal, of this type, in the liquid crystalline phase, cannot be explained by a simple α-process. Instead, this behaviour is likely to be composed of different motions of the dipole moment components contained within the side chains. This is also true of the dielectric relaxation behaviour observed for this sample below T_g.

Future work concerning the dielectric behaviour of the above materials should involve some dilute solution work, in order to reduce inter-chain interactions.

A problem with the synthesis of cyclic and linear polysiloxanes, $(R(Me)SiO)_x$ ($R \neq Me$), is the lack of stereoregularity. As with vinyl polymers the substituents R and Me may be placed along the chain in isotactic, syndiotactic or atactic configurations. The synthesis of stereoregular siloxane polymers, containing isotactic or syndiotactic blocks, would be expected to affect the physical properties of these materials. This may be particularly relevant to the production of liquid crystal polymers for practical applications. To date, this aspect of polysiloxane chemistry has received little attention, with just a few published studies[145,146].

The remainder of this study was concerned with the synthesis, characterisation, electro-optic properties and electrical properties of poly(p-phenylene vinylene) and oligomers of p-phenylene vinylene.

Although the chemical structure of the polymer was established by a variety of techniques, an accurate determination of molecular weight proved impossible, because of the low solubility of the polymer and its oligomers. Thus. certain assumptions regarding the molecular weight of the oligomers were necessary to facilitate the calculation of Kerr constants.

The difference between the values of the experimental and theoretical Kerr constants are not easily explained, although a number of factors may be important. A more complex theoretical model is required to take account of the possible non-planar conformation of oligomers of p-phenylene vinylene.

It is possible that the electrical conductivities measured in this study are dependent on sample preparation. This problem is commonly encountered when attempts are made to measure reproducible electrical conductivities of doped powders. Recently, thin films, foams and fibres of high molecular weight poly(p-phenylene vinylene) have been produced. The synthesis of homogenous substrates, such as thin films, is likely to simplify the electrical and structural investigations into these materials, as well as improving processibility and durability. In addition, the ability of such films to be stretched during formation allows the conductivity to be systematically altered. Thus, future work on the electrical properties of PPV is likely to involve films rather than powders, in conjunction with suitable dopants, such as AsF_5.

APPENDIX 1

COMPUTER PROGRAMS

The computer programs employed in the analysis of experimental and theoretical data are presented in this appendix. Each program is accompanied by an outline of its function together with a list of parameters required as input by the program. All of the programs were written in Basic and were run on an Apple II computer in the department of Applied Chemistry.

Program 1-Davidson-Cole analysis.

This program calculates theoretical values of dielectric permittivity and dielectric loss, at a series of spot frequencies in the range 12-10^5Hz, for particular values of β, ε_o, ε_∞ and the frequency corresponding to maximum loss, f_{max}. The program requires as input the following data:

1. Values of the Davidson-Cole empirical distribution factor,β.(the program can accomodate up to 12 values in a single input)
2. The limiting low frequency permittivity, ε_o.
3. The limiting high frequency permittivity, ε_∞
4. The frequency corresponding to maximum loss, f_{max}.
5. Experimental values of ε' and ε'' measured at various spot frequencies in the range 12-10^5Hz.

Using the first input value of β, the value of f_{max}, and equation (2-32), the program is able to calculate a value of τ_1. This permits the program to calculate a value of ϕ (from $\tan\phi=\omega\tau_1$) at each spot frequency. Equations (2-30) and (2-31) are then used to calculate the values of ε' and ε''.

The final routine of the program calculates the errors between the experimental and theoretical values of ε' and ε''.

The program then repeats the calculation sequence outlined above, each time altering only the value of β, until all the values of β have been used. The theoretical values of permittivity, loss and the calculated errors corresponding to each value of β are stored on file and can be displayed on the screen.

PROGRAM 1

```
5  REM  FIT DIELECTRIC RELAXATION DATA
7  REM  TO DAVIDSON-COLE EQUATION
10  ONERR  GOTO 12000
20  VTAB 5: HTAB 8
30  REM
40  REM  THE NOMENCLATURE:
50  REM  ESP = REAL PERMITTIVITY
60  REM  EDP = REAL PERMITTIVITY
70  REM  EU = HIGH FREQ. PERMITTIVITY
80  REM  ER = LOW FREQ. PERMITTIVITY
90  REM  GAM = DAVIDSON-COLE PARAMETER
100  REM  WM = FREQ.(RAD) CORRESPONDING
110  REM  TO MAXIMUM LOSS
120  REM  TAU1 = RELAXATION TIME/SEC
130  REM  PHI = LOSS ANGLE
140  REM  CP = COSINE(LOSS ANGLE*GAM)
150  REM  SP = SINE(LOSS ANGLE*GAM)
160  REM  TP = TANGENT(LOSS ANGLE)
170  REM  PI = 3.14159265
180  REM  W= FREQ. IN RADIANS
190  REM  F = FREQUENCY IN HZ
200  REM  NA = NORMALISED ABSORPTION
210  REM  ND = NORMALISED DISPERSION
220  REM -----------------------
230  REM
250  DIM ESP(14),EDP(14),PHI(14),CP(14),SP(14),W(14)
,F(14),NA(14),ND(14),EU(5),GA(12),DE(14),AE(14)
260 PI = 3.14159265:RAD = 0.0174533:FG = 0
270  REM  ----------------------
280  REM
300  REM  DO SOME INITIALISING
310 NA$ = "M S BEEVERS"
320 DA$ = "15 OCTOBER 1986"
330 TI$ = "DAVIDSON-COLE ANALYSIS"
340 CO$ = "DIELECTRIC RELAXATION DATA"
350 EU = 2.5:ER = 3.5:GAM = .5:WM = 1000:ER(3) = 999
:ER(6) = 999:MG = .1:E1 = 999:E2 = 999
360 F2 = 0:PF = 0:F1 = 0: REM   SET PRINT FLAGS
370  FOR I = 1 TO 14:DE(I) = 999:AE(I) = 999: NEXT I

380  REM
390  REM   ---------------------
400  REM
500  REM  MAIN MENU SECTION
510  HOME :NM = 0
520  GOSUB 1000: GOSUB 3500: REM  TITLE & FREQ.ALC.
530  HOME : VTAB 6
540  PRINT  SPC( 5)"1 - TITLE SCREEN"
550  PRINT  SPC( 5)"2 - INFORMATION"
560  PRINT  SPC( 5)"3 - INPUT TEXT"
570  IF FG = 0 THEN  PRINT  SPC( 5);: FLASH : PRINT
"4 - GET DATA FROM KEYBOARD": NORMAL
575  IF FG = 1 THEN  PRINT  SPC( 5)"4 - GET DATA FRO
```

```
M KEYBOARD"
580  PRINT  SPC( 5)"5 - CALCULATE"
590  PRINT  SPC( 5)"6 - RESULTS TO SCREEN"
600  PRINT  SPC( 5)"7 - RESULTS TO PRINTER"
610  PRINT  SPC( 5)"8 - GET DATA/RESULTS FROM FILE"
620  PRINT  SPC( 5)"9 - QUIT PROGRAM": PRINT
625  PRINT "(EU,GA, DISP.ERROR = ";ER(1);" ";ER(2);"
 "; INT (1000 * ER(3)) / 1000;: PRINT ")"
627  PRINT "(EU,GA, ABS.ERROR =  ";ER(4);" ";ER(5);"
 "; INT (1000 * ER(6)) / 1000;: PRINT ")": PRINT
630  HTAB 6: PRINT "PRESS A KEY (1-8)..."
640  IF NM > 0 THEN  HTAB 6: PRINT : PRINT "<LAST CH
OICE WAS ";NM;">"
650  VTAB 19: HTAB 28: GET A$
660  IF A$ <  > "" THEN NM =  VAL (A$)
670  IF NM < 1 OR NM > 9 THEN 530
680  ON NM GOSUB 1000,1500,2000,2500,900,6000,4500,9
500,10000
690  GOTO 530
700  REM ----------------------
710  REM
900  REM  RUN CALCULATION SEQUENCE
905  GOSUB 3000: IF F2 = 1 THEN 950
908 ER(3) = 999:ER(6) = 999
910  FOR II = 1 TO NE:EU = EU(II)
915  FOR JJ = 1 TO NG:GAM = GA(JJ)
920  GOSUB 4000: REM  CALC E' & E'' PAIRS AT 'SPOT'
FREQUENCIES
925  GOSUB 8000: REM  CALC ERRORS BETWEEN EXPL AND T
HEORY
930  GOSUB 9000: REM  SEND RESULTS TO FILE ON DISC
935  IF PF = 1 AND F1 = 0 THEN  GOSUB 4500:F1 = 1
940  IF PF = 1 AND F1 = 1 THEN  GOSUB 5080
945  NEXT JJ: NEXT II: RETURN
950  GOSUB 4000
960  RETURN
1000  REM  TITLE SCREEN
1010  HOME
1020  VTAB 5: HTAB 8
1030  PRINT "DAVIDSON-COLE ANALYSIS": PRINT
1040  HTAB 18: PRINT "OF": PRINT
1050  HTAB 6: PRINT "DIELECTRIC RELAXATION DATA"
1060  FOR TD = 1 TO 1000: NEXT TD
1070  RETURN
1200  REM  FILE NOT FOUND ERROR
1210  REM
1500  REM  BRIEF INFORMATION SCREEN
1510  HOME
1520  PRINT "THIS PROGRAM READS IN": PRINT
1530  PRINT "LOW FREQUENCY PERMITTIVITY"
1540  PRINT "HIGH     -          -   "
1550  PRINT "DAVIDSON-COLE PARAMETER"
1560  PRINT "FREQ/HZ OF MAXIMUM LOSS"
1580  PRINT : PRINT "AND CALCULATES THE NORMALISED"
1590  PRINT "DISPERSION AND ABSORPTION DATA FOR "
1600  PRINT "PLOTTING COLE-COLE CURVES"
1610  PRINT : FLASH : PRINT "PRESS A KEY TO CONTINUE
": NORMAL
1620  GET A$
1630  HOME : PRINT "MORE INFORMATION (Y/N) "
```

```
1640  GET A$
1650  IF A$ = "N" THEN  RETURN
1660  IF A$ <  > "Y" THEN 1640
1670  LIST 50 - 100
1680  PRINT : FLASH : PRINT "ANY KEY TO CONTINUE": NORMAL

1690  GET A$
1700  LIST 110 - 160
1710  PRINT : FLASH : PRINT "ANY KEY TO CONTINUE": NORMAL

1720  GET A$
1730  LIST 170 - 210
1740  PRINT : FLASH : PRINT "ANY KEY TO CONTINUE": NORMAL

1750  GET A$
1760  RETURN
1800  REM ---------------------------
1810  REM
2000  REM  INPUT TITLE & COMMENTS
2010  HOME
2020  PRINT "TITLE"
2030  PRINT "<";TI$;">"
2040  INPUT A$
2050  IF A$ <  > "" THEN TI$ = A$
2060  PRINT "COMMENTS"
2070  PRINT "<";CO$;">"
2080  INPUT A$
2090  IF A$ <  > "" THEN CO$ = A$
2100  PRINT "YOUR NAME"
2110  PRINT "<";NA$;">"
2120  INPUT A$
2130  IF A$ <  > "" THEN NA$ = A$
2140  PRINT "THE DATE"
2150  PRINT "<";DA$;">"
2160  INPUT A$
2170  IF A$ <  > "" THEN DA$ = A$
2180  RETURN
2200  REM  ---------------
2210  REM
2500  REM  INPUT DIELECTRIC DATA
2510  HOME : PRINT : PRINT "LOW FREQUENCY PERMITTIVI
TY"
2520  PRINT "<";ER;"> ";
2530  INPUT A$
2540  IF A$ <  > "" THEN ER =  VAL (A$)
2550  PRINT : PRINT "HIGH FREQUENCY PERMITTIVITY"
2560  PRINT "<";EU;"> ";
2570  INPUT A$
2580  IF A$ <  > "" THEN EU =  VAL (A$)
2590  PRINT : PRINT "DAVIDSON-COLE PARAMETER"
2600  PRINT "<";GAM;"> ";
2610  INPUT A$
2620  IF A$ <  > "" THEN GAM =  VAL (A$)
2630  PRINT : PRINT "FREQ/HZ OF MAXIMUM LOSS"
2640  PRINT "<";WM;"> ";
2650  INPUT A$
2660  IF A$ <  > "" THEN WM =  VAL (A$)
2665  PRINT : PRINT "MAXIMUM LOSS <";MG;">";: INPUT
MG$: IF  VAL (MG$) <  > 0 THEN MG =  VAL (MG$)
2670 FG = 1: REM  SET FLAG TO SHOW DATA INPUT
```

```
2680  GOSUB 7000: REM  SET UP EU'S & GAMMAS
2690  RETURN
2700  REM  ----------------------
2710  REM
3000  REM  CALCULATE RELAXATION TIME
3005  REM  CORRESPONDING TO MAX. LOSS
3010  HOME : IF FG = 0 THEN  POP : GOTO 530
3020  VTAB 10: HTAB 14: FLASH : PRINT "CALCULATING":
 NORMAL
3030 ARG = PI / (GAM + GAM + 2): REM  CHECK ANGLE CO
NVERSION HERE
3040 TAU1 =  TAN (ARG) / (WM * 2 * PI)
3050  RETURN
3200  REM ----------------------
3210  REM
3500  REM  CALCULATE SPOT FREQUENCIES
3520 F(1) = 12: REM  IN UNITS OF HZ
3530 F(2) = 20:F(3) = 50:F(4) = 60
3540 F(5) = 100:F(6) = 200:F(7) = 500
3550 F(8) = 1000:F(9) = 2000:F(10) = 5000
3560 F(11) = 10000:F(12) = 20000:F(13) = 50000
3570 F(14) = 100000
3580  FOR I = 1 TO 14
3590 W(I) = F(I) * PI * 2: NEXT I
3600  RETURN
3700  REM  -------------------------
3710  REM
4000  REM  CALCULATE
4010  FOR I = 1 TO 14
4020 PHI(I) =  ATN (W(I) * TAU1)
4030 CP(I) =  COS (PHI(I) * GAM)
4040 SP(I) =  SIN (PHI(I) * GAM): NEXT I
4050  REM  CALC NORMALISED DISPERSION
4060  FOR I = 1 TO 14
4070 ND(I) = ( COS (PHI(I)) ^ GAM) * CP(I): NEXT I
4080  FOR I = 1 TO 14
4090 NA(I) = ( COS (PHI(I)) ^ GAM) * SP(I): NEXT I
4100  REM  CALCULATE EPSILONS E' & E''
4110 MAX = .05: FOR I = 1 TO 14
4120 ESP(I) = ((ND(I) * (ER - EU)) + EU)
4130 EDP(I) = (NA(I) * (ER - EU))
4135  IF EDP(I) > MAX THEN MAX = EDP(I)
4136  NEXT I
4140  FOR I = 1 TO 14
4150 EDP(I) = (EDP(I) / MAX) * MG: NEXT I
4160  RETURN
4170  REM ----------------------
4500  REM  PRINT INITIAL DATA READ IN
4510  HOME
4520  PRINT "IS PRINTER READY ? (Y)"
4530  GET A$: PRINT
4540  IF A$ = "Y" THEN 4560
4550  IF A$ = "N" THEN  PRINT "SETUP PRINTER": GOTO
4520
4555  GOTO 4530
4560  PRINT  CHR$ (4);"PR£ 1": REM  OPEN PRINTER CHA
NNEL
4570  PRINT : PRINT : PRINT : PRINT : PRINT  SPC( 5)
;TI$: PRINT
4580  PRINT  SPC( 5);NA$;"        ";DA$: PRINT
```

```
4590  PRINT  SPC( 5);CO$: PRINT : PRINT
4600  PRINT  SPC( 5);"LOW FREQUENCY PERMITTIVITY:  "
; INT (1000 * ER + .1) / 1000
4610  PRINT  SPC( 5);"HIGH FREQUENCY PERMITTIVITY: "
; INT (1000 * EU + .1) / 1000
4620  PRINT
4630  PRINT  SPC( 5);"DAVIDSON-COLE PARAMETER "; INT
(1000 * GAM + .1) / 1000
4640  PRINT
4650  PRINT  SPC( 5);"FREQUENCY/HZ OF MAXIMUM LOSS:
"; INT (WM)
4655  PRINT : PRINT  SPC( 5)"MAXIMUM LOSS: "; INT (1
000 * MG + .1) / 1000
4660  PRINT
4670  PRINT  CHR$ (4);"PR£ 0": PRINT : PRINT  SPC( 5
);: FLASH : PRINT "ANY KEY TO CONTINUE";: NORMAL
4680  GET K$: PRINT
4690  GOSUB 5000
4700  RETURN
4710  REM ----------------------
4720  REM
5000  REM  SEND RESULTS TO THE PRINTER
5010  PRINT  CHR$ (4);"PR£ 0": PRINT
5020  HOME : IF NM = 6 THEN 5085
5080  IF NM = 7 THEN  PRINT  CHR$ (4);"PR£ 1"
5085  IF NM = 6 THEN  PRINT "F/HZ   W/RAD  E'      E'
'    ABS    DIS": GOTO 5170
5090  PRINT  SPC( 5)"F/HZ         ";
5100  PRINT "W/RAD       ";
5110  PRINT "E'          ";
5120  PRINT "E''         ";
5130  PRINT "NORMALISED";
5140  PRINT " NORMALISED"
5150  PRINT  SPC( 44)"ABSORPTION";
5160  PRINT " DISPERSION"
5170  PRINT
5180  FOR I = 1 TO 14
5240  GOSUB 5500
5242  IF NM = 6 THEN  PRINT OS$
5244  IF NM = 7 THEN  PRINT "      ";OS$
5246  NEXT I
5250  PRINT : HTAB 5
5260  PRINT "DISPERSION (E') ERROR IS  "; INT (1000 *
E1 + 0.1) / 1000
5270  PRINT : HTAB 5
5280  PRINT "ABSORPTION (E'') ERROR IS  "; INT (1000
 * E2 + .1) / 1000
5290  PRINT  CHR$ (4);"PR£0": PRINT : INVERSE : PRINT
"ANY KEY TO CONTINUE";: NORMAL : GET K$: PRINT
5310  RETURN
5320  REM ----------------------
5340  REM
5500  REM  TIDY OUTPUT TO THE PRINTER
5510 BL$ = "            ":OS$ = ""
5520 TS$ =  STR$ ( INT (F(I))): GOSUB 6500
5530 TS$ =  STR$ ( INT (W(I))): GOSUB 6500
5540 TS$ =  STR$ ( INT (1000 * ESP(I) + .1) / 1000):
 GOSUB 6500
5550 TS$ =  STR$ ( INT (1000 * EDP(I) + .1) / 1000):
 GOSUB 6500
```

```
5560 TS$ =  STR$ ( INT (1000 * NA(I) + .1) / 1000): GOSUB
6500
5570 TS$ =  STR$ ( INT (1000 * ND(I) + .1) / 1000):O
S$ = OS$ + TS$
5580  RETURN
5590  REM ---------------------
5600  REM
6000  REM  RESULTS DISPLAYED ON THE SCREEN
6010  HOME
6020  GOSUB 4570
6040  RETURN
6200  REM -----------------------
6210  REM
6500  REM  STRING ROUTINE FOR OUTPUT
6505 CW = 10: IF NM = 6 THEN CW = 7
6510 LN =  LEN (TS$)
6520 OS$ = OS$ + TS$ +  LEFT$ (BL$,CW - LN)
6530  RETURN
6540  REM -------------------------
6550  REM
7000  REM  THIS ROUTINE, IF REQUESTED, CAN RUN THE
7010  REM  PROGRAM WITH A RANGE OF EU'S AND
7020  REM  GAMMAS. IF THIS IS DESIRED THEN
7030  REM  EXPL E' AND E'' MUST BE INPUT
7040  HOME : VTAB 10
7050  PRINT "DO YOU WANT THE PROGRAM TO CALCULATE": PRINT

7060  PRINT "E' AND E'' FOR VARIOUS VALUES OF EU AND
": PRINT
7070  PRINT "GAMMA ? (Y/N)";
7080  GET K$
7090  IF K$ <  > "Y" AND K$ <  > "N" THEN 7080
7100  IF K$ = "N" THEN F2 = 1: RETURN
7105  IF K$ = "Y" THEN F2 = 0
7110  HOME : VTAB 10: HTAB 3
7120  PRINT "HOW MANY VALUES OF EU ARE THERE ";
7130  INPUT K$
7140  IF  VAL (K$) = 0 OR  VAL (K$) > 5 THEN 7110
7150 NE =  VAL (K$)
7160  HOME : VTAB 2: HTAB 5
7170  PRINT "ENTER EACH EU WITH <RETURN>  KEY": PRINT

7180  FOR I = 1 TO NE
7190  VTAB 5: PRINT "EU(";I;") = ";: PRINT "          "
;: HTAB 9: INPUT K$
7200  IF  VAL (K$) = 0 THEN 7190
7210  IF  VAL (K$) < 1.5 OR  VAL (K$) > 3 THEN 7190
7220 EU(I) =  VAL (K$)
7230  NEXT I
7240  HOME : VTAB 10: HTAB 3
7250  PRINT "HOW MANY VALUES OF GAMMA";
7260  INPUT K$
7270  IF  VAL (K$) = 0 OR  VAL (K$) > 12 THEN 7240
7280 NG =  VAL (K$)
7290  HOME : VTAB 2: HTAB 5
7300  PRINT "ENTER EACH GAMMA WITH <RETURN> KEY": PRINT

7310  FOR I = 1 TO NG
7320  VTAB 5: PRINT "GAMMA(";I;") = ";: PRINT "
   ";: HTAB 13: INPUT K$
```

```
7330  IF  VAL (K$) = 0 OR  VAL (K$) < 0.1 OR  VAL (K
$) > 1.0 THEN 7320
7340 GA(I) =  VAL (K$)
7350  NEXT I
7360  HOME : VTAB 2
7370  PRINT "INPUT EXPL. VALUES OF E' AND E'' FOR": PRINT

7380  PRINT "THE FOLLOWING 'SPOT' FREQUENCIES. PRESS
": PRINT
7390  PRINT "<RETURN> TO GET DEFAULT VALUE. VALUES":
 PRINT
7395  PRINT "OF 999 ARE NOT USED IN THE CALCULATION"
: PRINT
7400  PRINT
7410  INVERSE : PRINT "PRESS ANY KEY TO CONTINUE";: NORMAL

7420  GET K$
7430  REM
7440  FOR I = 1 TO 14: HOME : VTAB 8: HTAB 5
7450  PRINT "FREQUENCY = ";F(I);"HZ": PRINT
7460  VTAB 10: HTAB 5
7470  PRINT "E' <";DE(I);"> ";: INPUT K$
7480  IF K$ <  > "" THEN DE(I) =  VAL (K$)
7500  VTAB (12): HTAB 5
7510  PRINT "E'' <";AE(I);"> ";: INPUT K$
7520  IF K$ <  > "" THEN AE(I) =  VAL (K$)
7540  NEXT I
7550  HOME : VTAB 10
7560  PRINT "FILE NAME FOR RESULTS ? (<31 CHAR.)"
7565  PRINT : PRINT "ADVISE THE USE OF QUOTES": PRINT

7570  PRINT : HTAB 5: INPUT K$
7580  IF K$ =  CHR$ (13) OR K$ =  CHR$ (32) THEN 755
0
7590 F$ = K$
7600  HOME : VTAB 10
7610  PRINT "DO YOU WANT TO AUTOMATICALLY SEND THE":
 PRINT
7620  PRINT "DATA/RESULTS TO PRINTER ? (Y/N)";
7630  GET K$
7640  IF K$ <  > "Y" AND K$ <  > "N" THEN 7630
7650  IF K$ = "Y" THEN PF = 1
7660  RETURN
8000  REM  ROUTINE FOR CALCULATING ERRORS BETWEEN EX
PERIMENTAL
8010  REM  AND THEORETICAL VALUES OF E'(AND E'')
8020 N = 14:E1 = 0
8030  FOR I = 1 TO 14
8040  IF DE(I) = 999 THEN N = N - 1: GOTO 8060
8050 E1 =  ABS (ESP(I) - DE(I)) + E1
8060  NEXT I
8070  IF N <  > 0 THEN E1 = E1 / N
8075  IF N = 0 THEN E1 = 999
8080 N = 14:E2 = 0
8090  FOR I = 1 TO 14
8100  IF AE(I) = 999 THEN N = N - 1: GOTO 8120
8110 E2 =  ABS (EDP(I) - AE(I)) + E2
8120  NEXT I
8130  IF N <  > 0 THEN E2 = E2 / N
8135  IF N = 0 THEN E2 = 999
```

```
8140  IF E1 < ER(3) THEN ER(1) = EU:ER(2) = GA:ER(3)
 = E1
8150  IF E2 < ER(6) THEN ER(4) = EU:ER(5) = GA:ER(6)
 = E2
8160  END
9000  REM  RESULTS TO DISC FILE
9010  REM
9020 NF$ = F$ + "EU" +  STR$ (II) + "GA" +  STR$ (JJ
)
9030 D$ =  CHR$ (4): REM  CTRL-D
9040  PRINT D$;"OPEN ";NF$
9050  PRINT D$;"DELETE ";NF$
9060  PRINT D$;"CLOSE ";NF$
9070  PRINT D$;"OPEN ";NF$
9075  PRINT D$;"WRITE ";NF$
9080  PRINT TI$: PRINT CO$
9090  PRINT NA$: PRINT DA$
9100  PRINT ER: PRINT EU: PRINT GAM: PRINT WM: PRINT
MG
9110  FOR I = 1 TO 14
9120  PRINT DE(I): PRINT ESP(I): PRINT AE(I): PRINT
EDP(I): PRINT ND(I): PRINT NA(I)
9130  NEXT I
9140  PRINT E1: PRINT E2: REM  DISPERSION AND ABSORP
TION ERRORS
9150  PRINT D$;"CLOSE ";NF$
9160  RETURN
9500  REM  GET DATA/RESULTS FROM FILE
9510  REM
9520  HOME : VTAB 10: HTAB 5:D$ =  CHR$ (4)
9530  PRINT "CATALOG DISC ? (Y/N) ";
9540  GET K$: PRINT
9550  IF K$ <  > "Y" AND K$ <  > "N" THEN 9540
9560  IF K$ = "Y" THEN  PRINT  CHR$ (4);"CATALOG"
9565  IF K$ = "Y" THEN  PRINT : INVERSE : PRINT "ANY
 KEY TO CONTINUE";: NORMAL : GET K$: PRINT
9570  PRINT : PRINT
9580  PRINT "WHICH FILE DO YOU WANT ": PRINT
9590  HTAB 5: INPUT K$:NF$ = K$
9600  IF K$ =  CHR$ (13) THEN 9570
9610  PRINT D$;"VERIFY ";NF$
9620  HOME : VTAB 10: HTAB 5
9630  PRINT "FOUND FILE <";NF$;">"
9640  PRINT D$;"OPEN ";NF$
9645  PRINT D$;"READ ";NF$
9650  INPUT TI$: INPUT CO$: INPUT NA$
9660  INPUT DA$
9670  INPUT ER: INPUT EU: INPUT GAM: INPUT WM: INPUT
MG
9680  FOR I = 1 TO 14
9690  INPUT DE(I): INPUT ESP(I): INPUT AE(I): INPUT
EDP(I): INPUT ND(I): INPUT NA(I)
9700  NEXT I
9710  INPUT E1: INPUT E2
9720  PRINT D$;"CLOSE ";NF$
9730  RETURN
10000  REM  THE QUIT ROUTINE
10010  HOME : VTAB 10: HTAB 6: PRINT "DO YOU WANT TO
 QUIT ? (Y/N)"
10020  GET A$
```

```
10030  IF A$ = "N" THEN  RETURN
10040  HOME : VTAB 10: HTAB 10: INVERSE : PRINT "
          "
10042  HTAB 10: PRINT " ";: NORMAL : PRINT " END OF
PROGRAM ";: INVERSE : PRINT " "
10044  HTAB 10: PRINT "                     "
10050  FOR TD = 1 TO 1000: NEXT TD
10060  NORMAL : HOME
10070  END
12000  REM  FILE NOT FOUND ERROR ROUTINE
12010  REM
12030  HOME : VTAB 10: HTAB 5
12040  FLASH : PRINT "FILE NOT FOUND": NORMAL
12050  FOR TD = 1 TO 1000: NEXT TD
12055  CALL  - 3288: REM  CLEAR THE STCK
12060  HOME : POP : GOTO 500
12070  END
20000  PR£ 1
20010  PR£ 1
20020  FOR I = 1 TO 14
20030  PRINT DE(I);" ";ESP(I);"  "AE(I);" ";EDP(I)
20040  NEXT I
20050  PRINT
20060  PRINT "E1 ";E1;" ";"E2 ";E2
20070  END
```

Program 2-Calculation of the mean-square dipole moment per repeat unit.

Mean-square dipole moments per repeat unit, $<\mu^2>$, were calculated using the Onsager equation. The computer program requests the following input:

1. Static dielectric permittivity, ε_0.

2. Infinite frequency dielectric permittivity, ε_∞.

   (these values normally being derived from Cole-Cole plots)
3. Absolute temperature, T.
4. Number of dipolar units per unit volume, N.(molecules per cm^3)

The quantity N may be input from the keyboard directly, or calculated by the program. The latter action results in the display of a short menu in which three options are provided for the evaluation of N. These options concern the units which the user of the program wishes to employ for the concentration of components; these being weights, moles or mole fractions. Once a choice has been made, the user is then requested to input the appropriate quantities for the chemical system. The density, in units of g/cm^3, of the medium and the molecular weight of each component are also requested by the program.

The program then prints (to screen) the mean-square dipole moment and the root-mean square dipole moment.

PROGRAM 2

```
10  REM  EVALUATION OF ONSAGER EQUATION
20  REM  TO CALCULATE THE MEAN-SQUARE
30  REM  ELECTRIC DIPOLE MOMENT
40  HOME
50  PRINT  SPC( 5)"EVALUATION OF ONSAGER'S EQUATION"

60  PRINT
70  PRINT "STATIC PERMITTIVITY ";
80  INPUT EO
90  PRINT : PRINT "INF. FREG. ’’ ";
100  INPUT EI
140  PRINT
150  PRINT "ABSOLUTE TEMPERATURE /K ";
160  INPUT T
170  PRINT
180  PRINT : PRINT "   CALCULATE DIPOLES PER CM^3 ?
(Y/N)"
185  GET K$: IF K$ = "" THEN 185
186  IF K$ = "Y" THEN  GOSUB 1000: GOTO 190
187  IF K$ <  > "N" THEN 185
188  GOTO 200
190  HOME : PRINT : PRINT "  DIPOLAR UNITS PER CM^3
(*10^-20)": PRINT
191  PRINT "    TOTAL            = "; INT (NT * 100) /
100
192  PRINT "    COMPONENT 'A'  = "; INT (N1 * 100) /
100
193  PRINT "    COMPONENT 'B'  = "; INT (N2 * 100) /
100
200  PRINT : INPUT "        INPUT VALUE.....";ND
205 NU = (EO - EI) * (2 * EO + EI) * 9 * 1.3805 * T
210 DE = EO * (EI + 2) * (EI + 2) * 4 * 3.14153 * ND

220 MS = NU / DE
230 M =  SQR (MS)
240  PRINT
250  PRINT "MEAN-SQUARE MOMENT PER DIPOLAR UNIT"
260  PRINT "IS (DEBYES)^2.....  "; INT (MS * 100) /
100
270  PRINT
280  PRINT "ROOT-MEAN-SQUARE DIPOLE MOMENT PER"
290  PRINT "DIPOLAR UNIT (DEBYES).....    "; INT (M *
100) / 100
300  PRINT : PRINT : PRINT  SPC( 10)"ANOTHER GO ? (Y
/N) "
310  GET K$: IF K$ = "" THEN 310
320  IF K$ = "Y" THEN 40
330  IF K$ <  > "N" THEN 310
340  HOME
350  END
1000  HOME : PRINT "  CALCULATION OF DIPOLAR UNITS P
ER CM^3"
1010  PRINT
1020  PRINT  SPC( 5)"1. WORK IN WEIGHTS (GRAMS)"
1030  PRINT
1040  PRINT  SPC( 5)"2. WORK IM MOLES"
```

```
1050  PRINT
1060  PRINT  SPC( 5)"3. WORK IN MOLE FRACTIONS"
1070  PRINT
1080  PRINT  SPC( 6)"   CHOOSE NUMBER REQUIRED"
1090  GET K$: IF K$ = "" THEN 1090
1100 K =  VAL (K$): IF K < 1 OR K > 3 THEN 1090
1110  ON K GOTO 1200,1500,1800
1200  HOME : PRINT
1210  INPUT "WEIGHT OF COMPONENT 'A'    ";WA
1220  INPUT "MOLECULAR WEIGHT OF 'A'    ";MA
1230  PRINT
1240  INPUT "WEIGHT OF COMPONENT 'B'    ";WB
1250  INPUT "MOLECULAR WEIGHT OF 'B'    ";MB
1260  PRINT
1270  INPUT "DENSITY OF SOLUTION G/CM^3 ";DS
1280 NT = ((WA / MA) + (WB / MB)) * DS * 6022 / (WA +
WB)
1285 N1 = (WA / MA) * DS * 6022 / (WA + WB)
1287 N2 = (WB / MB) * DS * 6022 / (WA + WB)
1290  GOTO 1910
1500  HOME : INPUT "MOLES OF COMPONENT  'A' ";NA
1510  PRINT
1520  INPUT "MOLECULAR WEIGHT OF 'A' ";MA
1530  PRINT
1540  INPUT "MOLES OF COMPONENT  'B' ";NB
1550  PRINT
1560  INPUT "MOLECULAR WEIGHT OF 'B' ";MB
1570  PRINT
1580  INPUT "DENSITY OF SOLUTION G/CM^3 ";DS
1590 NT = (NA + NB) * DS * 6022 / (NA * MA + NB * MB
)
1595 N1 = NA * DS * 6022 / (NA * MA + NB * MB)
1597 N2 = NB * DS * 6022 / (NA * MA + NB * MB)
1600  GOTO 1910
1800  HOME
1810  INPUT "MOLE FRACTION OF 'A' ";FA
1820  PRINT
1830  INPUT "MOLECULAR WEIGHT OF 'A' ";MA
1840  PRINT
1850  INPUT "MOLE FRACTION OF 'B' ";FB
1860  PRINT
1870  INPUT "MOLECULAR WEIGHHT OF 'B' ";MB
1880  PRINT
1890  INPUT "DENSITY  OF SOLUTION  G/CM^3 ";DS
1900 NT = DS * 6022 / (FA * MA + FB * MB)
1905 N1 = FA * DS * 6022 / (FA * MA + FB * MB)
1907 N2 = FB * DS * 6022 / (FA * MA + FB * MB)
1910  RETURN
```

Program 3-Calculation of molar Kerr constants.

This program calculates the molar Kerr constant using the components of the molecular electro-optical polarisability tensor and the components of the molecular permanent dipole moment vector. It is also possible to calculate molar Kerr constants corresponding to different temperatures. All dipole moments are listed in Debyes and all polarisations in cm^3. A Gans ratio of 1.1 was used throughout.

PROGRAM 3

```
1  REM  PROGRAM MOLARK(BASIC VERSION)
2  REM  CALCULATES MOLECULAR KERR CONSTANT
3  REM  USING COMPONENTS OF THE MOLECULAR
4  REM  OPTICAL TENSOR AND COMPONENTS OF
5  REM  MOLECULAR DIPOLE MOMENT VECTOR
6  REM  ****
7  REM  DISTORTION POLARISATION(DP) AND
8  REM  ELECTRONIC POLARISATION(DE) REQD
20  DIM TE(20),MK(20),T(3,3),V(3)
30 BOLTZ = 1.38054
40 AVOGAD = 6.02252
50 PI = 3.14159265
52  HOME
55  INPUT "SHORT TITLE: ";HEADING$
60  INPUT "GANS RATIO (TYPICALLY 1.1): ";GANS
70  INPUT "NUMBER OF TEMPERATURES: ";NTEMP
80  FOR I = 1 TO NTEMP
90  PRINT "TYPE IN TEMPERATURE: ";I
100  INPUT TE(I): NEXT I
110  FOR I = 1 TO 3
120  PRINT "TYPE IN ROW ";I" OF OPTICAL TENSOR (*10^
40 CM2V-1)"
130  INPUT T(I,1),T(I,2),T(I,3): NEXT I
140  PRINT "DIPOLE MOMENT ? (Y/N):"
150  GET K$: IF K$ = "" THEN 150
160  IF K$ = "N" THEN 210
165  IF K$ <  > "Y" THEN 150
170  PRINT "X,Y,Z COMPONENTS OF DIPOLE MOMENT (*10^3
0 CM)"
180  INPUT "X COMPONENT: ";U(1)
190  INPUT "Y COMPONENT: ";U(2)
200  INPUT "Z COMPONENT: ";U(3)
210  GOSUB 1000
220  IF K$ = "N" THEN 240
230  GOSUB 2000
240 A = A * GANS
250  FOR I = 1 TO NTEMP
260 CA = 1 / (45 * BOLTZ * TE(I))
270 TA = CA * A
280 TB = 0.0
290  IF K$ = "N" THEN 315
300 CB = CA / (BOLTZ * TE(I))
310 TB = CB * B
315 MK(I) = 2 * PI * AVOGAD * (TA * 10 ^ ( - 34) + T
B * 10 ^ ( - 31)) / 9
317 MK(I) = MK(I) / (4 * PI * 8.854 * 10 ^ ( - 12))
320  NEXT I
330  HOME : PRINT HEADING$: PRINT
540  PRINT : PRINT "--------MOLAR KERR CONSTANT-----
-TEMP/K:PRINT
545  PRINT : PRINT "      (SI)      (ESU)": PRINT
550  FOR I = 1 TO NTEMP
560  PRINT MK(I),MK(I) / (1.11265 * 10 ^ ( - 15));"
  ";TE(I);" K": NEXT
570  END
1000  REM ***SUBROUTINE STATIC****
```

```
1010 A = (T(1,1) - T(2,2)) ^ 2 + (T(2,2) - T(3,3)) ^
2
1020 A = A + (T(3,3) - T(1,1)) ^ 2 + 3 * (T(1,2) ^ 2
 + T(2,1) ^ 2)
1030 A = A + 3 * (T(1,3) ^ 2 + T(3,1) ^ 2 + T(2,3) ^
2 + T(3,2) ^ 2)
1040  RETURN
2000  REM  ****SUBROUTINE PERMAN****
2010 B = (T(1,1) - T(2,2)) * (U(1) ^ 2 - U(2) ^ 2) +
(T(2,2) - T(3,3)) * (U(2) ^ 2 - U(3) ^ 2)
2020 B = B + (T(3,3) - T(1,1)) * (U(3) ^ 2 - U(1) ^
2) + 3 * (U(1) * U(2) * T(1,2) + U(2) * U(3) * T(2,3
))
2030 B = B + 3 * (U(1) * U(3) * T(1,3) + U(2) * U(1)
 * T(2,1) + U(3) * U(2) * T(3,2) + U(3) * U(1) * T(3
,1))
2040  RETURN
```

APPENDIX 2

EXPERIMENTAL DATA

To check the reproducibility of the experimental dielectric data, repeated measurements using identical apparatus, separated by a number of days, were carried out on a linear oligomer of methyl phenyl siloxane with n=4 and a cyclic fraction of poly(dimethyl siloxane) with n=50. The measurements were repeated at two temperatures for each sample, and the results are listed in the following tables. The initial measurements are listed under (1) and the repeated measurements are listed under (2).

Sample 1. methyl phenyl siloxane with n=4

	162.5K				155.5K			
	(1)		(2)		(1)		(2)	
f(kHz)	C_p(pF)	tanδ	C_p(pF)	tanδ	C_p(pF)	tanδ	C_p(pF)	tanδ
0.012					47.96	.0120	48.23	.0113
0.02	46.17	.0005	47.02	.0007	45.86	.0129	46.38	.0125
0.06	45.01	.0002	46.24	.0006	44.32	.0181	45.47	.0176
0.1	44.78	.0028	45.21	.0025	43.75	.0226	44.19	.0215
0.2					42.85	.0236	43.32	.0230
0.5	44.37	.0045	44.85	.0051	42.06	.0205	42.75	.0212
1	44.24	.0060	44.56	.0063	41.76	.0176	42.38	.0181
2	44.11	.0088	44.30	.0085	41.51	.0147	42.09	.0151
5	43.82	.0142	44.07	.0147	41.19	.0095	41.87	.0104
10	43.62	.0171	43.75	.0173	41.07	.0068	41.63	.0076
20	43.35	.0198	43.44	.0203	41.03	.0048	41.52	.0055
50	42.78	.0220	42.68	.0223	40.84	.0040	41.35	.0046
100	42.53	.0217	42.41	.0215	40.82	.0040	41.32	.0044

Sample 2. cyclic PDMS with $\bar{n}_n$=50

	156.5K				147.0K			
	(1)		(2)		(1)		(2)	
f(kHz)	C_p(pF)	tanδ	C_p(pF)	tanδ	C_p(pF)	tanδ	C_p(pF)	tanδ
0.012	48.61	.0012	49.23	.0015	48.78	.0162	49.05	.0165
0.02					46.68	.0251	47.13	.0260
0.06	46.00	.0012	47.15	.0017	43.96	.0412	44.77	.0419
0.1	45.79	.0014	46.93	.0018	42.67	.0450	43.59	.0457
0.2	45.61	.0016	46.72	.0022	41.33	.0419	42.22	.0425
0.5	45.48	.0042	46.44	.0039	40.53	.0331	41.29	.0336
1	45.37	.0060	46.19	.0063	40.06	.0279	40.85	.0284
2	45.26	.0090	45.99	.0087	39.68	.0230	40.47	.0232
5	45.03	.0161	45.66	.0155	39.27	.0170	39.95	.0175
10	44.70	.0244	45.32	.0241	39.06	.0135	39.75	.0140
20	44.12	.0338	44.89	.0330	38.93	.0105	39.54	.0110
50	42.78	.0421	43.06	.0415	38.64	.0086	39.37	.0091
100	41.84	.0404	42.17	.0408	38.58	.0082	39.26	.008

LIST OF REFERENCES

1 McCrum N.G., Read B.E., Williams G. 'Anelastic and dielectric effects in polymeric solids' Wiley 1967 London

2 Bur A.J. 'Dielectric properties of polymers at microwave frequencies: a review' Polymer Vol. 26, 963-977 (1985)

3 Heatley F. 'Nuclear magnetic relaxation of synthetic polymers in dilute solution' Prog. NMR Spec. Vol. 13, 47-85 (1979)

4 Cuniberti C. 'Proton magnetic relaxation times and molecular motion in polydimethylsiloxane' J. Polym. Sci. A-2 Vol. 8, 2051-2065 (1970)

5 Matsuo K., et. al. 'Fluorine magnetic relaxation in poly(p-fluorostyrene) and poly(m-fluorostyrene)' J. Polym. Sci. Polym. Phys. Ed. Vol. 15, 1347-1361 (1977)

6 McCall D.W. 'NMR studies of molecular relaxation mechanisms in polymers' Acc. Chem. Res. Vol. 4, 223- (1971)

7 Aroney M.J. 'The electro-optical Kerr effect in conformational analysis' Angew. Chem. Int. Ed. Engl. Vol. 16, 663-734 (1977)

8 Stuart H.A., Peterlin A. 'Optische anisotropie und form von fadenmolekulën II. Kunstliche doppelbrechung' J. Pol. Sci. Vol. 5, 551-563 (1950)

9 Champion J.V., Meeten G.H., Southwell G.W. 'Electro-optic Kerr birefringence of polystyrenes in dilute solution' Polymer Vol. 17, 651-655 (1976)

10 Khanarian G., Tonelli A.E. 'Kerr effect and dielectric study of poly(oxyethylene glycols)' Macromolecules Vol. 15, 145-148 (1982)

11 Khanarian G., Schilling F.C., Rudolf E.C., Tonelli A.E. 'Kerr effect and dielectric study of poly(vinyl chloride) and its oligomers' Macromolecules Vol. 16, 287-291 (1983)

12 Tsvetkov V.N., Rjumtsev E.I., Andreeva L.N., Pogodina N.V., Lavrenko P.N., Kutsenko L.I. 'Electric birefringence in solutions of cellulose carbanilate as a function of molecular weight' Eur. Polym. J. Vol. 10, 563-570 (1974)

13 Jennings B.R., Brown B.L. 'The physical properties of isocyanates in solution' Eur. Polym. J. Vol.7, 805-826 (1971)

14 Tsvetkov V.N., Andreeva L.N. 'Flow and electric birefringence in rigid-chain polymer solutions' Adv. Polym. Sci. Vol 39, 95-207 (1981)

15 Williams G. 'Molecular aspects of multiple dielectric relaxation in solid polymers' Adv. Polym. Sci. Vol 33, 59-92 (1979)

16 Williams G. 'Dielectric relaxation of solid polymers' NATO Adv. Study Inst. Series C, C94, 213-239 (1982)

17 Dodgson K., Semlyen J.A. 'Studies of cyclic and linear poly(dimethyl siloxanes):1. Limiting viscosity number-molecular weight relationships' Polymer Vol 18, 1265-1268 (1977)

18 Bannister D.J., Semelyn J.A. 'Studies of cyclic and linear poly(dimethyl siloxanes):6. Effect of heat' Polymer Vol. 22, 377-381 (1981)

19 Burton D.J., Harris R.K., Dodgson K., Pellow C.J., Semlyen J.A. 'Silicon-29 n.m.r. chemical shifts of cyclic dimethyl siloxane oligomers' Polymer Commun. Vol. 24, 278-281 (1983)

20 Clarson S.J., Dodgson K., Semlyen J.A. 'Studies of cyclic and linear poly(dimethyl siloxanes):19. Glass transition temperatures and crystallisation behaviour' Polymer Vol. 26, 925- (1985)

21 Dodgson K., Higgins J.S., 'Neutron scattering from cyclic polymers' in 'Cyclic Polymers', 167-196, edited by J.A. Semlyen, Elsevier A.S.P. (1986)

22 Edwards C.J.C., Stepto R.F.T., Semlyen J.A. 'Studies of cyclic and linear poly(dimethyl siloxanes):5. Diffusion behaviour in dilute solution' Polymer Vol. 21, 781-786 (1980)

23 Dodgson K., Bannister D.J., Semlyen J.A. 'Studies of cyclic and linear poly(dimethyl siloxanes):4. Bulk viscosities' Polymer Vol. 21, 663-667 (1980)

24 Bass S.L., Kauppi T.A. 'Silicones- a new class of high polymers of interest to the radio industry' Proc. I.R.E. Vol. 33, 441- (1945)

25 Baker E.B., Barry A.J., Hunter M.J. 'Dielectric constants of dimethyl siloxane polymers' Ind. Eng. Chem. Vol. 38, 1117- (1946)

26 Warrick E.L., Hunter M.J., Barry A.J. 'Polymer chemistry of the linear siloxanes' Ind. Eng. Chem. Vol. 44, 2196- (1952)

27 Young O.B., Dickerman C.E. 'Dielectric constants of dimethylsilicones' Ind. Eng. Chem. Vol. 46, 364- (1954)

28 Andrianov K.A., Golubkov G.E. 'The electrical properties and the structure of organo-silicon polymers' Soviet. Phys. Tech. Phys. Vol. 26, 1642-1646 (1956)

29 Golubkov G.E., Talykov V.E. 'Heteroorganic plastics. Electrical properties of polyorganosiloxanes of branched structure with regular alternation of units" Soviet Plastics Vol. 5, 15- (1969)

30 Dasgupta S., Garg S.K., Smyth C.P. 'Microwave absorption and molecular structure in liquids LXIX. Atomic polarisation and relaxation in several siloxanes and hexamethyldisilazine' J. Am. Chem. Soc. Vol. 89, 2243-2246 (1967)

31 Dasgupta S., Smyth C.P. 'Microwave absorption and molecular structure in liquids LXX. Dipole moment, atomic polarisation and dielectric relaxation in poly methylpolysiloxanes' J. Chem Phys. Vol. 47, 2911-2916 (1967)

32 Mark J.E. 'Dipole moments of dimethylsiloxane chains' J. Chem. Phys. Vol. 49, 1398-1402 (1968)

33 Sutton C., Mark J.E. 'Dipole moments of dimethylsiloxane oligomers and poly(dimethylsiloxane)' J. Chem. Phys. Vol. 54, 5011-5014 (1971)

34 Beevers M.S., Mumby S.J., Clarson S.J., Semlyen J.A. 'Studies of cyclic and linear poly(dimethyl siloxanes):13. Static dielectric measurements and dipole moments' Polymer Vol. 24, 1565-1570 (1983)

35 Huggins C.M., St. Pierre L.E., Bueche A.M. 'Nuclear magnetic resonance study of molecular motion in polydimethylsiloxanes' J. Phys. Chem. Vol. 64, 1304-1309 (1960)

36 Baird M.E., Sengupta C.R. 'Dielectric relaxation in poly(dimethyl siloxane)' Polymer Vol. 12, 802-804 (1971)

37 Baird M.E., Sengupta C.R. 'Dielectric relaxation in siloxane polymers' J. Chem. Soc. Faraday Trans. II Vol. 68, 1795-1799 (1972)

38 Adachi H., Adachi K., Ishida Y., Kotaka K. 'Dielectric relaxation of poly(dimethyl siloxane)' J. Polym. Sci. Polm. Phys. Ed. Vol. 17, 851-857 (1979)

39 Sengupta C.R. 'Anomalous dielectric relaxation in poly(dimethyl siloxane)' Polymer Vol. 23, 1394-1395 (1982)

40 Baird M.E., Sengupta C.R. 'Dielectric α relaxation in siloxane oligomer + diluent systems' J. Chem. Soc. Faraday Trans. II Vol. 70, 1741-1747 (1974)

41 Sengupta C.R. 'Dielectric relaxation and effect of plasticisers on siloxane polymers' Eur. Polym. J. Vol. 19, 251-254 (1982)

42 Finkelmann H., Rehage G. 'Liquid crystal side chain polymers' Adv. Polym. Sci. Vol. 60/61, 99-172 (1984)

43 Shibaev V.P., Platè N.A. 'Thermotropic liquid-crystalline polymers with mesogenic side groups' Adv. Polym. Sci. Vol. 60/61, 173-252 (1984)

44 Geib H., Hisgen B., Pschorn U., Ringsdorf., Spiess H.W. 'Deuteron NMR study of molecular order and motion in a liquid crystakkine polymer' J. Am. Chem. Soc. Vol. 104, 917- (1982)

45 Wassmer K.H., Ohmes E., Kothe G., Portugall M., Ringsdorf H., 'Structure and dynamics of a liquid crystalline side chain polymer' Makromol. Chem. Rapid Commun. Vol. 3, 282- (1982)

46 Kresse H. 'Dielectric behaviour of liquid crystals' Adv. Liq. Cryst. Vol. 6, 109-172 (1983)

47 Kresse H., Talrose R.V. 'Dielectric investigations on a comb-like polymer with a liquid crystal phase' Makromol. Chem. Rapid Commun. Vol. 2, 369-374 (1981)

48 Kresse H., Kostromin M.V., Shibaev V.P. 'Thermotropic liquid crystalline polymers, 10. Comparitive dielectric investigations of smectic and nematic polymers' Makromol. Chem. Rapid Commun. Vol. 3, 509-513 (1982)

49 Kresse H., Shibaev V.P. 'Thermotropic liquid crystalline polymers, 15. Dielectric investigations at the glass transition' Makromol. Chem. Rapid Commun. Vol. 5, 63-66 (1984)

50 Zentel R., Strobl G.R., Ringsdorf H., 'Dielectric relaxation of liquid crystalline polyacrylates and polymethacrylates' Macromolecules Vol. 18, 960-965 (1985)

51 Kresse H., Zentel R., Tennstedt E. 'Dielectric investigations on liquid-crystalline side group polymers' Makromol. Chem. Rapid Commun. Vol. 6, 261-265 (1985)

52 Haase W., Pranato H. 'Properties of some liquid crystalline side chain polymers in the electric field' in Polymeric Liquid Crystals, edited by A. Blumstein, Plenum Press (1983)

53 Haase W., Pranato H., Bormuth F.J. 'Dielectric properties of some side chain liquid crystalline polymers' Ber Bunsenges. Phys. Chem. Vol. 89, 1229-1234 (1985)

54 Pranato H., Bormuth F.J., Haase W., Kiechle U., Finkelmann H. 'Dielectric properties of a liquid crystalline siloxane copolymer' Makromol. Chem. Vol. 187, 2453-2460 (1986)

55 Attard G.S., Williams G. 'The effect of a directing electric field on the physical structure of a liquid crystalline side chain polymer. The preparation of aligned thin films and their study using dielectric relaxation spectroscopy' Polym. Commun. Vol. 27, 2-5 (1986)

56 Attard G.S., Williams G., Gray G.W., Lacey D., Gemmel P.A. 'Molecular dynamics of liquid crystalline side chain polymers: The dielectric relaxation behaviour of a siloxan polymer in the nematic and isotropic phases' Polymer Vol. 27, 185-189 (1986)

57 Attard G.S., Williams G. 'The effect on the cooling rate on the alignment of a liquid crystalline polymer as studied by dielectric relaxation spectroscopy' Polym. Commun. Vol. 27, 66-68 (1986)

58 Attard G.S., Williams G. 'Molecular dynamics of a smectic liquid-crystalline side-chain in its unaligned and aligned states as studied by dielectric relaxation spectroscopy' Liquid Crystals Vol. 1, 253-269 (1986)

59 Araki K., Attard G.S. 'Dielectric relaxation in the planarly-aligned nematic phase of a siloxane side-chain polymer' Liquid Crystals Vol. 1, 301-304 (1986)

60 Attard G.S. 'The determination of the orders parameters and director alignment in the nematic phase of a liquid crystalline side-chain polymer by the resolution of dielectric loss spectra' Mol. Phys. Vol. 58, 1087-1100 (1986)

61 Attard G.S., Araki K., Williams G. 'Two-frequency addressing of a siloxane liquid crystalline side-chain polymer for different thermal electrical treatments as studied by dielectric relaxation spectroscopy' J. Molec. Elec. Vol. 2, (1986)

62 Attard G.S., Araki K., Williams G. 'A simple approach to the dielectric relaxation behaviour of a liquid crystalline polymer and its application to the determination of the director order parameter for partially aligned materials' Br. Polym. J. Vol. 19, 119-127 (1987)

63 Simon R., Coles H.J. 'Electrically-induced optical storage effects in smectic polysiloxanes. A variable transmission device' Liq. Cryst. Vol. 1, 281-286 (1986)

64 Coles H.J., Simon R. 'Electro-optic effects in a smectogenic polysiloxane side-chain liquid crystal polymer' in Recent Advances in Liquid Crystalline Polymers, 323-334, edited by L.L. Chapoy, Elsevier ASP (1985)

65 Coles H.J., 'Electro-optic effects in side-chain polymer liquid crystals' Faraday Discuss. Chem. Soc. 79 (1985)

66 Gourley K.D., Lillya C.P., Reynolds J.R., Chien J.C.W. 'Electrically conducting polymers. AsF_5-doped poly(phenylenevinylene) and its analogues' Macromolecules Vol. 17, 1025-1033 (1984)

67 Gagnon D.R., Capistran J.D., Karasz F.E., Lenz R.W. 'Conducting polymers. Conductivity anisotropy in orientated poly(p-phenylene vinylene)' Polym. Bull. Vol. 12, 293-298 (1984)

68 Karasz F.E., Capistran J.D., Gagnon D.R., Lenz R.W. 'High molecular weight polyphenylene vinylene' Mol. Cryst. Liq. Cryst. Vol. 118, 327-332 (1985)

69 Murase I., Ohnishi T., Noguchi T., Hirooka M. 'Highly conducting poly(p-phenylene vinylene) prepared from a sulphonium salt' Polym. Commun. Vol. 25, 327-329 (1984)

70 Murase I., Ohnishi T., Noguchi T., Hirooka M. "Highly conducting poly(p-phenylene vinylene) prepared from a sulfonium salt' Mol. Cryst. Liq. Cryst. Vol. 118, 333-336 (1985)

71 Murase I., Ohnishi T., Noguchi T., Hirooka M. 'Alkoxy-substituent effect of poly(p-phenylene vinylene)' Polym. Commun. Vol. 26, 362-364 (1985)

72 Gagnon D.R., Capistran J.D., Karasz F.E., Lenz R.W., Antoun S., 'Synthesis, doping and electrical conductivity of high molecular weight poly(p-phenylene vinylene)' Polymer Vol. 28, 567-573 (1987)

73 Potember R.S., Hoffman R.C., Hu H.S., Cocchanio J.E., Viands C.A., Murphy R.A., Poehler T.O., 'Conducting organics and polymers for electronic and optical devices' Polymer Vol. 28, 574-580 (1987)

74 Nigrey P.J., MacInnes D., Nairns D.P., MacDiarmid A.G., Heeger A.J., 'Lightweight rechargeable storage batteries using polyacetylene, $(CH)_x$, as the cathode-active material' J. Electrochem. Soc. Vol. 128, 1651-1654 (1981)

75 Yoshino K., Kaneto K., Inuishi Y. 'Proposal of electro-optical switching and memory devices utilizing doping and undoping processes of conducting polymers' Jpn. J. Appl. Phys. Vol. 22, L157-L158 (1983)

76 Kaneto K., Yoshino K., Inuishi Y. 'Characteristics of electro-optic device using conducting polymer, polythiophene and polypyrrole films' Polym. Commun. Vol. 26, 103- (1985)

77 Debye P., Polar Molecules, Chem. Catalog. New York (1929)

78 Onsager L. 'Electric moments of molecules in liquids' J. Am. Chem. Soc. Vol. 58, 1486-1493 (1936)

79 Kirkwood J.G. 'The dielectric polarisation of polar liquids' J. Chem. Phys. Vol. 7, 911-919 (1939)

80 Fröhlich H., Theory of Dielectrics, Oxford University Press (1949)

81 Cole R.H., Cole K.S. 'Dispersion and absorption in dielectrics. Alternating current characteristics' J. Chem. Phys. Vol. 9, 341-351 (1941)

82 Davidson D.W., Cole R.H., 'Dielectric relaxation in glycerine' J. Chem. Phys. Vol. 18, 1417- (1950)

83 Havriliak S., Negami S. 'A complex plane analysis of α- dispersions in some polymer systems' J.Polym. Sci. Vol. 14, 99-117 (1966)

84 Cook M., Watts D.C., Williams G. 'Correlation function approach to the dielectric behaviour of amorphous polymers' Trans. Faraday Soc. Vol. 66, 2503-2511 (1970)

85 Eyring H. 'Viscosity, plasticity and diffusion (a) examples of absolute reaction rates' J. Chem. Phys. Vol. 4, 283-291 (1936)

86 Handbook of Chemistry and Physics, edited by R.C. Weast, 53rd edition, CRC press 1972/3

87 Experimental and Theoretical Investigations of the Dielectric and Electro-Optical Properties of Polycarbazoles and Polysiloxanes, S.J. Mumby, PhD thesis, University of Aston, (1983)

88 Le Fevre C.G., Le Fevre R.J.W. 'The Kerr effect' in Physical Methods of Chemistry, edited by A. Weissberger 399-452, Vol. 1, Pt. IIIC Wiley-Interscience (1972)

89 Finkelmann H., Rehage G. 'Investigations on liquid crystalline polysiloxanes, 1. Synthesis and characterisation of linear polymers' Makromol Chem. Rapid Commun. Vol. 1, 1-4 (1980)

90 Ringsdorf H., Schneller A. 'Liquid crystalline side chain polymers with low glass transition temperatures' Makromol Chem. Rapid Commun. Vol. 3, 557-562 (1982)

91 Apfel M.A., et. al. 'Synthesis and properties of high temperature mesomorphic polysiloxane solvents: Biphenyl and terphenyl-based nematic systems' Anal. Chem. Vol. 57, 651-658 (1985)

92 Jones B.A., Bradshaw J.S., Nishioka M., Lee M.L. 'Synthesis of smectic liquid-crystalline polysiloxanes from biphenylcarboxylate esters and their use as stationary phases for high resolution gas chromatography' J. Org. Chem. Vol. 49, 4947-4951 (1984)

93 Gray G.W., 'The chemistry of liquid crystals' Phil. Trans. R. Soc. Lond. A309 77-92 (1983)

94 Gray G.W. 'Relationship between chemical structure and properties for low molecular weight liquid crystals' in Polymer Liquid Crystals, 1-33, edited by A.Ciferri Academic Press (1982)

95 Gray G.W. 'The Clifford Paterson Lecture, 1985. Liquid crystals: an arena for research and industrial collaboration among chemists, physicists and engineers' Proc. R. Soc. Lond. A402 1-36 (1985)

96 Finkelmann H. 'Liquid crystalline side chain polymers' Phil. Trans. R. Soc. Lond. A309 105-114 (1985)

97 Janini G.M., Laub R.J., Shaw T.J. 'Synthesis and properties of high temperature mesomorphic polysiloxane (MEPSIL) solvents. Amide, ester and Schiff's base linked systems' Makromol Chem. Rapid Commun. Vol. 6, 57-63 (1985)

98 Gemmel P.A., Gray G.W., Lacey D. 'Effects of molecular structure on the properties of teminally cyano-substituted side chain liquid crystalline polysiloxanes' Mol. Cryst. Liq. Cryst. Vol. 122, 205-218 (1985)

99 Gray G.W., Lacey D., Nestor G., White M.S. 'Preparation of liquid crystalline polysiloxanes with terminal cyano groups in the side chain' Vol. 7, 71-76 (1986) **Polymer**

100 McDonald R.N., Campbell T.W. 'The Wittig reaction as a polymerisation method' J. Am. Chem. Soc. Vol. 82 4669-4671 (1960)

101 Hoeg D.F., Lusk D.I., Goldberg E.P. 'Poly-p-xylylidene' J. Pol. Sci. B2 697-701 (1964)

102 Ouchi K. 'An ayyempt to synthesise poly-p-xylylidene and related compounds by a Wurtz-Fittig type reaction' Aust. J. Chem. Vol. 19, 333-335 (1966)

103 Rajarman L., Balasubramanian M., Nanjan M.J., 'Synthesis of poly-p-xylylidene' Curr. Sci. Vol. 49, 101-102 (1980)

104 McMurry J.E., Fleming M.P. 'A new method for the reductive coupling of carbonyls to olefins. Synthesis of β-carotene' J. Am. Chem. Soc. Vol. 96, 4707-4709 (1974)

105 Hörhold H.H., Gottschaldt J., Opfermann J. 'Untersuchungen über poly(ayrlenvinylene) XVII. Poly(1,4-phenylen-1,2-diphenylvinylen' J. Prakt. Chem. Vol. 319, 611-621 (1977)

106 Wessling R.A., Zimmerman R.G. U. S. Patent no. 3 401 152 (1968)

107 Kanbe M. 'Synthesis of poly-p-xylylidene from p-xylenebis(dimethylsulfonium) tetrafluoroborate' J.Polym Sci. A-1 Vol. 6, 1058-1060 (1968)

108 Koßmehl G., Yaridjanian A. 'Über polyarylenalkenylene und polyheteroarylalkenylene, 11. Synthesen von poly(1,4-diphenylvinylen), poly(2,5-thiophendiylvinylen) und poly(2,5-furandiylvinylen) aus methylsubstituierten aldehyden' Makromol Chem. Vol. 182, 3419-3426 (1981)

109 Levy J., et. al., Carbon-13 Nuclear Magnetic Resonance Spectroscopy, Wiley (1980)

110 Ishida Y. 'Dielectric relaxation of high polymers in the solid state' J.Polym Sci. A-2 1835-1861 (1969)

111 Ferry J.D., Viscoelastic Properties of Polymers, Wiley, New York (1980)

112 Baird M.E., Sengupta C.R. 'Dielectric relaxation in polymethyltrifluoropropylsiloxane' Polymer Vol. 15, 608-609 (1974)

113 Noll W., Chemistry and Technology of Silicones, Academic Press, (1968)

114 Wright P.V., Beevers M.S. 'Preparation of cyclic polysiloxanes' in Cyclic Polymers, edited by J.A. Semlyen, Elsevier ASP (1986)

115 Freeman G.G. 'Silicones-an introduction to their chemistry and applications', ILIFFE Books, London (1962)

116 Kerr J. 'A new relation between electricity and light: Dielectrified media birefringent' Phil. Mag. Vol. 50, 337-348 (1875)

117 Kerr J. 'A new relation between electricity and light: Dielectrified media birefringent(second paper)' Phil. Mag. Vol. 50, 446-458 (1875)

118 Langevin P. Radium Vol. 7, 249- (1910)

119 Langevin P. Compt. Rend. Vol. 475, 151- (1910)

120 Born M. 'Elektrononen theorie des naturülichen optischen drehungsvermögens isotroper und anisotroper flüssigkeiten' Ann. Physik. Vol. 55, 177- (1918)

121 Gans R. 'Asymmetrie von gasmolekularen. Ein beittragzur bestimmungdermolekularen form' Ann. Physik. Vol. 65, 97-123 (1921)

122 Debye P., Handbuch Radiol., Vol. 6, (1925)

123 Debye P., Sack H. Ann. Physik. Vol. 69, 179- (1934)

124 Stuart H.A., Hand-und-Jahrbuch der Chemischen Physik., Vol. 10, (1939)

125 Le Fevre R.J.W., et. al. 'Molecular polarisability. The specific Kerr constants and polarisation of various polystyrenes dissolved in carbon tetrachloride' J.Chem. Soc. Pt. 2 1468-1474 (1958)

126 Le Fevre R.J.W., et. al. 'Molecular polarisability. The specific Kerr constants and polarisation of vinyl acetates and various polyvinylacetates dissolved in carbon tetrachloride or benzene' J.Chem. Soc. Pt. 2 1468-1474 (1958)

127 Le Fevre R.J.W., Sundaram K.M.S. 'Molecular polarisabilty. Molar Kerr constants and dipole moments of vinyl chloride and six polyvinylchlorides as solutes in dioxan' J.Chem. Soc. Pt. 1 1494-1502 (1962)

128 Le Fevre R.J.W., Sundaram K.M.S. 'Molecular polarisabilty. Molar Kerr constants and dipole moments of vinyl bromide and six polyvinylbromides as solutes in dioxan' J.Chem. Soc. Pt. 3 4003-4008 (1962)

129 Le Fevre R.J.W., Sundaram K.M.S. 'Molecular polarisabilty. The molar Kerr constants of methyl methacrylate and its polymers' J.Chem. Soc. Pt. 2 1880-1887 (1963)

130 Le Fevre R.J.W., Sundaram K.M.S. 'Molecular polarisability. The molar Kerr constants, apparent dipole moments, etc., of methyl acrylate and five of its polymers' J.Chem. Soc. Pt. 3 3188-3193 (1963)

131 Le Fevre R.J.W., Sundaram K.M.S. 'Molecular polarisability. The molar Kerr constants, dipole moments, etc., of isoprene, polyisoprenes and some related hydrocarbons' J.Chem. Soc. Pt. 3 3547-3554 (1960)

132 Aroney M., et. al. 'The molar Kerr constants and dipole moments of six polyethylene glycols as solutes in benzene' J.Chem. Soc. Pt. 3 2890-2895 (1960)

133 Yano S., Rahalkar R.R., Hunter S.P., Wang C.H., Boyd R.H. 'Studies of molecular relaxation of poly(propylene oxide) solutions by dielectric relaxation and brillouin scattering' J.Polym. Sci. Polym. Phys. Ed. Vol. 14, 1877- (1976)

134 Le Fevre R.J.W., Sundaram K.M.S. 'Molecular polarisability. The apparent dipole moments and molar Kerr constants of six polypropylene glycols as solutes in benzene' J.Chem. Soc. Perkin II 2323-2325 (1972)

135 Beevers M.S., Elliot D.A., Williams G. 'Molecular motion in melt samples of poly(propylene glycol) studied using dielectric and Kerr effect relaxation techniques' Polymer Vol. 21, 13-20 (1980)

136 Interaction of Metal Salts with Polyethers, F. Hakiempoor, PhD thesis, University of Aston (1985)

137 Wetton R.E., Williams G. 'Dielectric relaxation in polytetramethylene oxide' Trans. Faraday. Soc. Vol. 61, 2132-2139 (1965)

138 Guggenheim E.A. 'A proposed simplification in the procedure for computing electric dipole moments' Trans. Faraday. Soc. Vol. 45, 714-720 (1949)

139 Le Fevre C.G., Le Fevre R.J.W., 'The Kerr effect. Its measurement and applications in chemistry' Rev. Pure. Appl. Chem. Vol. 5, 260-318 (1955)

140 Le Fevre R.J.W. 'Applications in chemistry of properties involving molecular polarisability' J. and Proc. R. Soc. N.S.W. Vol. 95, 1-11 (1961)

141 Wnek G.E., Chien J.C.W., Karasz F.E., Lillya C.P. 'Electrically conducting derivative of poly(p-phenylene vinylene)' Polymer Vol. 20, 1441-1443 (1979)

142 Manecke G. 'On some organic semiconducting polymers' 24th Int. Cong. Pure Appl. Chem. 1, 155-176 (1973)

143 Koßmehl G. 'Semiconductive conjugated polymers' Ber. Bunsenges. Phys. Chem. Vol. 83, 417-426 (1979)

144 Wnek G.W., Capistran J., Chien J.C.W., Dickinson L.C., Gable R., Gooding R., Gourley K., Karasz F.E., Lillya C.P., Yao K.D. 'Studies in conducting polymers' Polymer Sci. and Tech. Vol. 15, 183-208 (1981)

145 Makarova N.N., et. al. 'Stereoregular polyorganocyclosiloxanes-soluble liquid crystal polymers with a wide range of mesomorphic state' Otkrytiya. Izobret. Vol. 44, 74-75 (1984)

146 Curtis D.M., Thanedar S., Elsheik M. 'Stereoregular silicones from ring-opening polymerisations of cyclotrisiloxanes' Polym. Prepr. (Am. Chem. Soc., Div. Polym. Chem.) Vol. 25, 224 (1984)